

COULOMB EXCITATION DATA ANALYSIS CODES; G O S I A 2008

T. Czosnyka^{a,b*}, D. Cline^{a,d}, C.Y. Wu^a, A.B. Hayes^{a,d}, P. Napiorkowski^{b,d}, N. Warr^{c,d}

^aDepartment of Physics and Astronomy, University of Rochester

^bHeavy-Ion Laboratory, University of Warsaw

^cInstitut für Kernphysik, Universität zu Köln

^dGosia Steering Committee

April 17, 2009

Abstract

This Gosia User Manual describes the Gosia suite of Coulomb excitation codes that were developed at Rochester in 1980 by T. Czosnyka, D. Cline and C.Y. Wu. The manual has been upgraded to apply to the 20080630.x version of the codes that include significant upgrades both in capability and coding that has been implemented by the Gosia User Steering Committee.

The wealth of Coulomb excitation data collected using present day experimental techniques makes feasible a model independent determination of almost all E1, E2, E3, M1, and M2 matrix elements connecting low-lying collective nuclear levels populated by electromagnetic excitation. A semiclassical coupled-channel Coulomb excitation least-squares search code, GOSIA, has been developed to analyze the large sets of experimental data required to unambiguously determine the many electromagnetic matrix elements involved in heavy-ion induced Coulomb excitation. Up to 999 electromagnetic matrix elements, coupling up to 100 levels, can be fitted to reproduce simultaneously several thousand data from up to 50 independent experiments. Fast semi-analytic approximation of the coupled-channels system of differential equations describing electromagnetic excitation is used to achieve computational speed required for such a task. This manual describes the theory underlying the model-independent determination of electromagnetic matrix elements from Coulomb excitation data, plus detailed input instructions for operation of GOSIA. In addition to the primary search code GOSIA, specialized versions of GOSIA plus an associated rotational invariant code SIGMA are described. These include GOSIA2 which allows simultaneous normalization of projectile and target Coulomb excitation which is useful for Coulomb excitation of weak radioactive beams. PAWEL is designed for cases where the initial state is isomeric. SIGMA evaluates the rotational invariants derived using the complete set of measured E2 matrix elements; these determine the intrinsic frame quadrupole shape parameters for low-lying states. The completeness and extent of information on electromagnetic structure adds a new dimension to the study of collectivity in nuclei.



*Deceased

Contents

0	DEDICATION	5
1	INTRODUCTION	6
1.1	Gosia suite of Coulomb excitation codes	6
1.2	A brief history of Gosia	7
1.3	New features in Gosia 2008	9
1.4	Gosia Users Manual	11
2	COULOMB EXCITATION AND GAMMA DECAY OF EXCITED NUCLEI	12
2.1	Safe bombarding energy:	12
2.2	Semiclassical Theory of Coulomb Excitation and its Applicability	12
2.3	Gamma Decay Following Electromagnetic Excitation	20
2.3.1	Nuclear Deorientation Effect	22
2.3.2	Relativistic Angular Distribution Correction	24
2.3.3	Gamma Detector Solid Angle Attenuation Factors	26
2.3.4	Internal Conversion	27
2.4	Kinematics for inelastic scattering	28
2.4.1	Velocities:	28
2.4.2	Angles:	29
2.4.3	Solid angles:	30
2.4.4	Gosia kinematics assumption:	30
2.5	Sources of Systematic Error	30
3	APPROXIMATE EVALUATION OF EXCITATION AMPLITUDES	33
4	NUMERICAL METHODS	38
4.1	Coulomb Excitation Amplitudes and Statistical Tensors	39
4.2	Approximate Evaluation of the Coulomb excitation Amplitudes	42
4.3	Calculation of the γ -ray Yields	43
4.4	Integration over the Projectile scattering Angle and the Energy Loss in a Target - Correction of Experimental γ -ray Yields	45
4.5	Minimization	48
4.5.1	Definition of the Least-square Statistic	48
4.5.2	Normalization Constants	49
4.5.3	Internal Correction Coefficients	50
4.5.4	Steepest Descent Minimization	51
4.5.5	Gradient + Derivative Minimization	52
4.5.6	Quadratization of the S Statistic by Redefinition of the Variables	54
4.5.7	Selection of the Parameters for Minimization	55
4.5.8	Sensitivity Maps	56
4.6	Estimation of Errors of the Fitted matrix Elements	57
4.6.1	Derivation of the Error Estimation Method	57
4.6.2	Numerical Estimation of Errors	60
4.7	Identification of Erroneous Data Points	61
5	INPUT INSTRUCTIONS FOR THE COMPUTER CODE GOSIA	63
5.1	ORGANIZATION	63
5.1.1	INPUT FORMATS	63
5.1.2	SUMMARY OF AVAILABLE OPTIONS	63
5.2	OP,BRIC (BRICC)	68
5.3	CONT (CONTROL)	69
5.4	OP,CORR (CORRECT)	76
5.5	OP,COUL (COULEX)	77

5.6	OP,ERRO	(ERRORS)	78
5.7	OP,EXIT	(EXIT)	80
5.8	EXPT	(Mandatory suboption of OP,COUL and OP,GOSI)	81
5.9	OP,FILE	(FILES)	83
5.10	OP,GDET	(GE DETECTORS)	84
5.11	OP,GOSI	(GOSIA)	85
5.12	OP,INTG	(INTEGRATE)	86
	5.12.1	NORMAL INPUT TO OP,INTG	86
	5.12.2	CIRCULAR DETECTOR OPTION	89
	5.12.3	SUMMARY OF INPUT TO OP,INTG - NORMAL INPUT	90
	5.12.4	SUMMARY OF INPUT TO OP,INTG - CIRCULAR DETECTOR OPTION	90
	5.12.5	ABSOLUTE COINCIDENT γ -RAY YIELDS	91
5.13	LEVE	(LEVELS)	93
5.14	OP,MAP	(MAP)	94
5.15	ME	(OP,COUL)	95
5.16	ME	(OP,GOSI)	98
5.17	OP,MINI	(MINIMIZE)	102
5.18	OP,POIN	(POINT CALCULATION)	105
5.19	OP,RAND	(RANDOM ME)	106
5.20	OP,RAW	(RAW UNCORRECTED γ YIELDS)	107
5.21	OP,RE,A	(RELEASE,A)	109
5.22	OP,RE,C	(RELEASE,C)	109
5.23	OP,RE,F	(RELEASE,F)	109
5.24	OP,REST	(RESTART)	110
5.25	OP,SELE	(SELECT)	111
5.26	OP,SIXJ	(SIXJ SYMBOL)	112
5.27	OP,STAR	(START)	113
5.28	OP,THEO	(COLLECTIVE MODEL ME)	114
5.29	OP,TITL	(TITLE)	117
5.30	OP,TROU	(TROUBLE)	118
5.31	OP,YIEL	(YIELDS)	119
5.32	INPUT OF EXPERIMENTAL γ -RAY YIELDS FROM COULOMB EXCITATION		126
6	QUADRUPOLE ROTATION INVARIANTS - PROGRAM SIGMA		128
6.1	FORMULATION OF THE E2 ROTATIONAL INVARIANT METHOD		128
6.2	PROGRAM SIGMA		132
	6.2.1	COMPUTATION OF THE INVARIANTS	132
	6.2.2	ESTIMATION OF ERRORS IN SIGMA	133
	6.2.3	INPUT INSTRUCTIONS	135
7	FILE ASSIGNMENTS		137
7.1	FILE ASSIGNMENTS IN GOSIA		137
7.2	FILE ASSIGNMENTS IN SIGMA		139
7.3	FILE ASSIGNMENTS IN SELECT		139
7.4	EXAMPLES OF INPUT FILES AND FILE ASSIGNMENTS FOR TYPICAL JOBS		140
	7.4.1	COULOMB EXCITATION AMPLITUDES	140
	7.4.2	CREATION OF THE GE DETECTORS FILE	141
	7.4.3	CALCULATION OF THE γ YIELDS BY POINT APPROXIMATION	141
	7.4.4	CALCULATION OF THE INTEGRATED γ YIELDS AND GENERATION OF A "CORRECTED" EXPERIMENTAL YIELDS FILE	142
	7.4.5	CALCULATION OF THE q PARAMETER MAP	142
	7.4.6	MINIMIZATION RUN - INITIAL STAGE	143
	7.4.7	MINIMIZATION - FINAL STAGE	144
	7.4.8	SELECT - CORRELATION MATRIX GENERATION	145

7.4.9	DIAGONAL ERROR CALCULATION	145
7.4.10	CALCULATION OF THE CORRELATED ERRORS	146
7.4.11	6-j SYMBOLS TABLE	147
8	SIMULTANEOUS COULOMB EXCITATION: PROGRAM GOSIA2	148
8.1	INPUT INSTRUCTIONS	149
9	COULOMB EXCITATION OF ISOMERIC STATES: PROGRAM PAWEL	156
10	MINIMIZATION BY SIMULATED ANNEALING	157
10.1	The Development of Simulated Annealing	157
10.2	Implementation of SA in GOSIA	159
10.3	Input parameters for OP,ANNL	161
11	LEARNING GOSIA	163
11.1	Compiling GOSIA 2008	163
11.2	Learning to Write Gosia Inputs	164
11.3	Tutorial 1: Gosia basic flow sequence	165
11.3.1	Simulation	165
11.3.2	Fitting Matrix Elements to Gamma-Ray Yield Data	169
11.4	Tutorial 2: A Fit to Many Matrix Elements	174
11.5	Annotated GOSIA input gldemo.inp	179
11.6	Annotated output from a chi-squared (OP,MINI) fit	188
11.7	Annotated excerpt from a Coulomb excitation yield calculation (OP,INTG)	194
11.8	Accuracy and speed of calculations	196
11.9	Troubleshooting GOSIA inputs	196
12	GAMMA DETECTION EFFICIENCY CODE: GREMLIN	199
12.1	Option 1: EFFICIENCY CALIBRATION	199
12.2	Option 2: INTENSITY CALCULATION	202
13	GOSIA 2008 RELEASE NOTES	204
13.1	Chronology of Major Changes to GOSIA1: 2007 - present	205
13.2	Chronology of Major Changes to GOSIA2: 2007 - present	207
13.3	Chronology of Major Changes to GOSIA: 1980 - 2006	208
14	GOSIA MANUAL: RECENT UPDATES	210

0 DEDICATION



Tomasz Czosnyka 1952 - 2006

This GOSIA manual is dedicated to Tomasz Czosnyka who played a pivotal role in the development of the GOSIA code. Tomasz was a brilliant scientist with tremendous drive, dedication and effectiveness. His work led to pioneering advances in the field of Coulomb excitation. His Ph.D. thesis developed sophisticated techniques that solved a problem that many in the field claimed was impossible when started in 1979. This important development now forms the foundation of modern multiple Coulomb excitation that will continue to play a major role in nuclear physics research at the new radioactive beam facilities now in operation or under construction. Tomasz was a generous, thoughtful friend and colleague with a warm, casual style, and a great sense of humor. Even though Tomasz is no longer with us in person, he is with us in spirit and we continue to hold him in much esteem and affection. The legacy of his achievements in nuclear science will endure for a long time. {Douglas Cline}

1 INTRODUCTION

1.1 Gosia suite of Coulomb excitation codes

Coulomb excitation, which is excitation of nuclear states caused solely by the electromagnetic field acting between the colliding nuclei, is a powerful probe of collective nuclear structure [ALD56, ALD66, ALD75]. The main advantage of Coulomb excitation lies in the fact that, unlike nuclear reactions, the interaction can be described by the well-established theory of the electromagnetic interaction allowing nuclear structure to be studied in a model-independent way. Excitation via the short-ranged nuclear interaction is negligible for bombarding energies well below the Coulomb barrier, whereas the long-ranged electromagnetic interaction still gives rise to a considerable Coulomb excitation. Coulomb excitation is the preeminent probe of collective degrees of freedom in nuclear structure in that it selectively populates collective states with cross sections that are a direct measure of the electromagnetic matrix elements.

The recognition of Coulomb excitation as a method of studying collective motion in nuclei dates back to the early 1950's [ALD56]. Coulomb excitation with light-ion beams was exploited extensively to measure the reduced excitation probabilities and quadrupole moments of the lowest excited states. Experiments performed using light-ion beams can be interpreted relatively easily because first- and second order perturbation theory are applicable since only one and two step excitation processes need to be taken into account (see e.g. the extensive discussion of the perturbation approach in [ALD75]). The situation changes dramatically for multiple Coulomb excitation that results when heavy-ion beams are employed. Multiple Coulomb excitation populates many excited states (up to spin, $40\hbar$ in strongly deformed nuclei) providing sensitivity to a large body of electromagnetic matrix elements but unfortunately perturbation methods are no longer viable. Review papers by Cline [CLI86] and de Boer [BOE84] contain a short summaries of the early multiple Coulomb excitation work, complete with extensive lists of references.

A semiclassical theory of multiple Coulomb excitation was developed in 1956 [ALD56]. The first semiclassical multiple Coulomb excitation computer program COULEX was developed by Winther and de Boer in 1965 [WIN65]. The code COULEX provided the first opportunity to calculate quantitatively multiple Coulomb excitation amplitudes using an assumed set of the reduced electromagnetic matrix elements. This code greatly expanded the exploitation of the powerful Coulomb excitation technique to determine electromagnetic matrix elements in nuclear structure. However, the ultimate goal of a model-independent extraction of the electromagnetic structure parameters (reduced matrix elements) from the heavy-ion experiments was not viable until development, in 1980, of the code GOSIA described in this manual. The main difficulty for making a model-independent analysis lies in the large number of reduced matrix elements influencing heavy-ion excitation. More than a hundred matrix elements can contribute significantly to Coulomb excitation when using heavy beams to excite strongly deformed nuclei. There are two major tasks to making a model-independent analysis of multiple Coulomb excitation data. The first task is to overdetermine the problem by collecting enough experimental data, this requires measurements for a wide dynamic range of Coulomb excitation strength. The second task is to extract the many unknown matrix elements from this overdetermined data set.

The need to collect Coulomb excitation data for a wide dynamic range of Coulomb excitation interaction strength, has led to development of experimental methods to record deexcitation γ -rays in coincidence with scattered ions over a wide range of particle scattering angle. The efficiency of data collection has been very much enhanced by the development of 4π arrays of Compton-suppressed Ge detectors, such as Gammasphere, and large solid-angle, position-sensitive, parallel-plate avalanche detectors that provide mass and scattering angle resolution for detection of both scattered ions in kinematic coincidence. The particle detector allows event-by-event kinematic reconstruction to correct the considerable Doppler shifts of observed γ -ray energies, dramatically improving the quality of the γ -ray spectra. Ref. [SIM97] gives technical details of the Rochester designed charged particle detection CHICO, that has been used extensively with Gammasphere for Coulomb excitation studies since 1995.

Initially multiple Coulomb excitation data were analysed by comparing the data with the predictions obtained using the code COULEX coupled to a program like CEGRY [CLI74] to evaluate the γ -deexcitation. The sets of matrix elements required as input data to COULEX were taken from model predictions and the conclusions were drawn based on the quality of the agreement obtained. However, the results of such a model-dependent analyses were not conclusive, primarily due to the unknown sensitivity of the experimental

data to assumed matrix elements and in some cases have proven to be incorrect. A model-independent analysis of multiple Coulomb excitation data, using the formalism employed by COULEX, is not practical taking into consideration the numerical effort necessary for such a task using even the capability of the newest generation computers. To overcome this problem it is necessary to construct simple approximations to the Coulomb excitation formalism, accurate enough to determine a search strategy in a multidimensional space of the matrix elements parametrizing both excitation and decay processes. The development of such an approximation became the basis of the Rochester Coulomb excitation data analysis least-squares search program, GOSIA, presented in this report. GOSIA was developed at the Nuclear Structure Research Laboratory of the University of Rochester during 1980[CZO83] and was subsequently expanded and improved on the basis of experience gained by the Rochester-Warsaw-Uppsala based Coulomb excitation collaboration.

GOSIA is an experiment-oriented program. Although providing the possibility of running theoretical calculations (i.e. evaluation of excitation amplitudes and γ -decay yields for a given set of the matrix elements) it is primarily designed to perform a fit of the matrix elements to reproduce the large amount of experimental data. These data not only include the deexcitation γ -yields observed in a number of independent Coulomb excitation experiments, but also available spectroscopic information, such as branching ratios, E2/M1 mixing ratios, nuclear level lifetimes and previously measured E2 matrix elements. This combined information allows determination of the full set of matrix elements for an investigated nucleus together with a realistic estimate of the errors of the fitted matrix elements. Finally, using the associated quadrupole rotational invariants code, SIGMA, it is possible, on a basis of the results obtained with GOSIA, to evaluate, in a model-independent way[CLI72, CLI86] the expectation values and the statistical distribution of the E2 moments in the intrinsic frame, providing a clear insight into the collective properties of the nuclear states. Advances in heavy-ion accelerator facilities coupled with significantly more powerful γ -ray and heavy-ion detector systems has led to a significant increase in the size and complexity of the nuclear systems being studied. Fortunately, this growth in difficulty has been matched by a comparable advance in computer technology allowing the code GOSIA to handle the increasingly more complicated systems being analyzed since its inception in 1980.

The code GOSIA is available free for use by anyone. However, all users must reference GOSIA[CZO83] in publications based on use of this code. Changes in the author list and/or in the name of the code are possible only with the written approval of the authors. Errors and modifications should be communicated to the authors. The code has been used extensively since 1980 and appears to be trouble free. Since the code GOSIA is complicated, with extensively overlaid coding, users are strongly recommended to seek advice before attempting to make modifications. The goal is to maintain one freely available current version of GOSIA for all users in order to minimize fragmentation of effort and to ensure a robust, accurate code.

1.2 A brief history of Gosia

1965 - 1979:

The genesis of Gosia dates back to 1965 when multiple Coulomb excitation blossomed due to the advent of heavy-ion accelerators plus the high-resolution Ge γ -ray detector, coupled with development in 1965 of the Winther-de Boer semiclassical Coulomb excitation code COULEX [WIN65]. Between 1966 and 1978, Cline and coworkers used heavy-ion beams from the newly commissioned Rochester MP tandem accelerator facility plus the code COULEX to measure static quadrupole moments of the first excited 2^+ states via Coulomb excitation [CLI69a, LES70, GER70a, GER70b, LES72, TOW72, CLI73, TOW73, TOW75] This work employed the particle γ -ray coincidence technique which necessitated the development at Rochester of the γ -ray deexcitation code CEGRY[CLI74] that used the statistical tensors calculated by COULEX to predict the subsequent γ -ray decay properties.

Much higher Z beams became available with the commissioning of the SuperHILAC at Berkeley in 1975, and the UNILAC at GSI in 1976 which greatly advanced the field of multiple Coulomb excitation. Starting in 1975 Cline, plus coworkers at Rochester, became heavily involved in studies of multiple Coulomb excitation using heavy-ion beams from the SuperHILAC and the Rochester MP tandem. This work involved close collaboration with the Diamond-Stephens group at Berkeley plus Rochester graduate students Ching-Yen Wu (1977-present) and Tomasz Czornyka (1979-1982, 1984-87). In addition Julian Srebrny (1978) from Warsaw and Lennart Hasselgren (1979-80) from Uppsala each spent a year in Rochester working on this research program. This group, plus other collaborators, were involved in multiple Coulomb excitation studies of ^{104}Ru , ^{110}Pd , ^{165}Ho , ^{166}Er , $^{186-192}\text{Os}$, and ^{194}Pt .

In 1971, Cline and Flaum[CLI72] developed the theory of rotational invariants that directly and model-independently relate observed $E2$ properties to the intrinsic frame $E2$ properties. The full potential of this technique was not achievable in 1971 due to the paucity of $E2$ data for the excited states. Multiple Coulomb excitation data appeared to be the only viable way to determine a sufficiently complete $E2$ data set useful for this technique.

1979 - 2006:

Population of each state via heavy-ion induced multiple Coulomb excitation results from excitation via many paths involving many $E\lambda$ matrix elements. This strong-coupling invalidates the use of higher-order perturbation expansion analyses commonly used for light-ion induced Coulomb excitation work. An important question in 1979 was whether it was feasible to unambiguously extract electromagnetic matrix elements from a model-independent analysis of multiple Coulomb excitation data. At that time many in the field argued that achieving a model independent analysis of multiple Coulomb excitation data was not feasible. The first real breakthrough in demonstrating the feasibility of extracting electromagnetic matrix elements from multiple Coulomb excitation data resulted from use of the codes COULEX plus CEGRY in a model-independent analysis of the Coulomb excitation data for ^{110}Pd made at Rochester by Lennart Hasselgren [HAS80]. This tour-de-force analysis produced a solution with scientifically interesting implications and provided the proof of principle that led to the development of GOSIA. Unfortunately there was no practical way to prove the uniqueness of his solution, and the time and effort required to replicate such a manual analysis was impractical. Thus as a thesis project Tomasz Czosnyka was asked to develop a Coulomb excitation least-squares search code based on COULEX plus CEGRY to provide a practical way of analysing multiple Coulomb excitation data. The development of GOSIA proved to be a major undertaking but has been a highly satisfying and successful project.

The first success of GOSIA was that it proved that the matrix element set found by the manual analysis for ^{110}Pd was the correct solution. Dr Bodan Kotlinski [KOT84] made recoil-distance lifetime measurements in ^{110}Pd which also confirmed the correctness of the solution found by both the manual analysis and using GOSIA. In parallel, to the ^{110}Pd work, the thesis work of Ching-Yen Wu[WU83, WU89, WU91, WU96] involved an exhaustive analysis of the W-Os-Pt nuclei that was used extensively to develop and test the GOSIA code.

The success of the above mentioned work achieved two long-sought goals of this group. 1) It proved that multiple Coulomb excitation can be used to model-independently determine signs and magnitudes of fairly complete sets of $E2$ matrix elements. 2) This set of matrix elements was sufficient for an analysis using the model-independent Rotational Invariant technique[CLI72, CLI86] to extract the expectation values of the centroids and widths in the intrinsic frame for the $E2$ properties of low-lying states. 3) The $E2$ rotational invariants provided a powerful probe of collective motion in nuclei in shape-transitional nuclei.

The successful development and exploitation of Gosia stimulated a rapid growth in multiple Coulomb excitation work led by the Rochester, Uppsala, Warsaw groups and later included the Liverpool group. The GSI based groups were doing similar Coulomb excitation work at the UNILAC in parallel with our collaboration leading to development of a separate analysis code [GRE84], but they eventually switched to the use of GOSIA.

GOSIA was modelled on the 1978 version[LEL78, LEL78][BOE84] of the Winther-de Boer code COULEX which extended the code to include multipolarities, $E\lambda$ with $\lambda = 1, 2, 3, 4, 5, 6$ as well as incorporating time-saving updates. The γ -ray deexcitation part of the code is based on the Coulomb excitation γ -ray deexcitation code code CEGRY which was developed at Rochester during 1965-75 by Cline, Lesser and Towsley[CLI74]. Significant contributions to the development and testing of GOSIA have been made by additional collaborators. Dr Alexander Kavka [KAV90] tested and elucidated the validity and impact of the deorientation effect, plus he developed the γ -ray efficiency calibration code GREMLIN.

GOSIA, plus the associated quadrupole rotational-invariants program SIGMA, were developed in 1980. Subsequently three special versions of GOSIA were developed. The first code called GOSIA2 is intended to handle both target and projectile simultaneous excitation with common normalization coefficients. The second special code, called PAWEL, is a special offspring of GOSIA designed to handle cases where a fraction of the nuclei have an excited isomeric state as the initial state. The third code ANNL was developed by Dr Richard Ibbotson[IBB95] and exploits simulated annealing techniques to locate least-squares minima.

Tomasz Czosnyka maintained and updated the coding of the GOSIA suite of codes from their inception until his untimely death in October 2006. The 2006 versions of these codes posted on the Gosia User

Group website, <http://www.pas.rochester.edu/~cline/Gosia/index.html>, are the final versions of the codes as developed and maintained by Tomasz Czosnyka.

2006 - present::

The GOSIA program was written in Fortran 77 and was originally developed to run on a CDC Cyber 175. The available memory limited the the program size to 130,000 (60-bit) words which complicated the code and required extensive overlaying. From inception in 1980, GOSIA ran with high reliability on many powerful computers. However, by the start of the 21st century the Fortran compilers became less forgiving of archaic Fortran77 commands and the mixed 32 bit and 64 bit variables in GOSIA resulting in unreliable executables.

In 2007 Dr Nigel Warr started making extensive improvements to the coding of both Gosia and Gosia 2. He worked in collaboration with Adam Hayes and Doug Cline who tested the codes as well as upgraded the Gosia web page and the Users Manual. These programming improvements in the 2007 version of Gosia have produced more reliable executables and eliminated bugs. The Warsaw group also started work on upgrades to Gosia including development of a new genetic algorithm procedure to speed minimization.

Coordination of future development of Gosia by the user community was recognized as being necessary to forestall splintering of the development effort, to maintain quality assurance, and to handle the growing use of Gosia for Coulomb excitation work at new radioactive plus stable beam facilities. At the Gosia Workshop, held in Warsaw, 8 - 10 April 2008, it was recommended that a Gosia Users Group be formed to assume responsibility to manage maintainance, standards, and quality assurance testing as well as to promote, prioritize, facilitate, and coordinate development of the Gosia suite of codes. Establishment of a Gosia Users Steering Committee was proposed to implement the goals of the User Group. The participants at the Workshop endorsed establishment of the Gosia Users Group and supported appointment of Douglas Cline (Rochester), Adam Hayes (Rochester), Pawel Napiorkowski (Warsaw) and Nigel Warr (Cologne) to the Gosia Steering Committee.

Starting in April 2008 the Gosia Steering Committee embarked on an ambitious program to upgrade the Gosia suite of codes. The first phase upgrade of Gosia involved partitioning the Gosia coding into its separate subroutines to simplify the structure and facilitate future development. The complex intertwined coding of Gosia makes upgrading of the original version of Gosia impractical until partitioning is accomplished. This first phase has resulted in the release of the current 2008 version of Gosia that includes coding modifications made to address the immediate needs of users. These include increasing the dimensions of some arrays and replacing the unreliable Lagrange interpolation procedure with a spline interpolation procedure, incorporating the automatic calculation of internal conversion coefficients, and improving the method for handling of inverse kinematic reactions. An arsenal of test inputs have been generated to use for quality assurance testing of the upgraded versions of Gosia. In addition, an intuitive input generator program is being written to simplify creation and checking of Gosia input files. Planned second phase upgrades include investigating use of genetic algorithm procedure for minimization, allowing input of conversion electron and $p - \gamma - \gamma$ coincidence data as well as allowing fits to user-defined model parameters.

To facilitate communication the Gosia Steering Committee replaced the Rochester Gosia web page with a new one, <http://www.pas.rochester.edu/~cline/Gosia/index.html>, that includes a Users Forum. Communication also will be accomplished by publishing newsletters and the use of email.

1.3 New features in Gosia 2008

The Gosia 2008 suite of codes include significant upgrades both to the functionality and to the coding compared with the 2006 versions developed by Tomasz Czosnyka.

Upgrades in Functionality:

The following have been implemented in both the Gosia and Gosia2 codes.

1) Dimensions:

The number of levels has increased from 75 to 100 while the total number of magnetic substates has been increased from 600 to 1200. The number of electromagnetic matrix elements has increased from 500 to 999. These changes are to accommodate the larger dimension systems encountered in analysis of Coulomb excitation measurements performed using the high-sensitivity new generation detector arrays.

2) Internal conversion coefficients:

The BrIcc internal conversion coefficient database supported by the National Nuclear Data Center has been incorporated in Gosia. This allows direct calculation of the internal conversion coefficients for every transition included in the input significantly reducing the amount of data that needs to be typed into the Gosia input file.

3) Spline interpolation:

A spline interpolation procedure has been implemented to eliminate the persistent problem of wild oscillatory behaviour that occurs when many meshpoints are used with Lagrange interpolation. The cubic spline subroutines SPLINE and SPLINT were taken from "Numerical Recipes in Fortran" [PRE92].

4) Energy and angle meshpoints:

The number of energy and angle meshpoints used in integration have each been increased to 100 to improve the accuracy. This upgrade was made possible by changing from Lagrange to spline interpolation.

5) Error correlation matrix:

The generation of the error correlation matrix has been incorporated in a new OP,SELE (SELECT) routine eliminating the need to run the external program SELECT.

6) Inverse kinematics:

The handling of inverse kinematics has been improved to eliminate problems due to two-valued solutions for projectile scattering angles and the infinite Jacobean at the maximum scattering angle of the scattered projectile. The integration over scattering angle now is done in the centre-of-mass which is single valued.

7) Physical constants:

More accurate physical constants have been used to evaluate constants incorporated in Gosia.

Coding upgrades:

Nigel Warr has implemented the following improvements to the underlying Fortran coding to eliminate bugs and produce more reliable executables.

1) Explicit 64-bit Precision Upgrade:

Previous versions of the GOSIA code did not explicitly specify 64-bit precision; the user was expected to compile the code at the highest machine precision available. The current availability of 64-bit machines and the accuracy problems which arise when relying on 32-bit precision led to the decision to make the 2007 version fully and explicitly 64-bit. Modifying the code to run with 32-bit precision is discouraged. Earlier versions of GOSIA had some portability problems arising from misalignment of common blocks. In GOSIA 2007 the common blocks have been re-ordered so that the 64-bit real variables come before the 32-bit integer variables, in order to eliminate alignment problems.

2) Structure and standards:

The 2007 code has been updated to replace many archaic Fortran functions with their modern counterparts. Sections of the code have been restructured using SPAG (© Polyhedron Software) under the academic license. This included unraveling of loops and goto statements, reordering variables so that declarations and common blocks are together, and indenting the source code to make loops and if statements more obvious. The initialization in the main routine has been slightly restructured, mainly to make it similar to the 2007 version of GOSIA2. Other sections have been restructured and commented for clarity, without altering their function.

3) Bugs fixed:

The subroutine in GOSIA which calculates the rotation functions relies on its memory space for local variables being preserved between calls. This occurred automatically on many older systems (e.g. DEC Alpha, VAX). On some newer machines these variables were being lost, causing unpredictable errors, such as negative values of chi-squared. This has been fixed in the 2007 version.

If the user requests an excessive number of Coulomb excitation calculations requiring high accuracy, GOSIA may find that its allocated memory is insufficient for the number of collision functions required (Chapter 2). Previous versions of GOSIA did not terminate execution according to Fortran standards when this occurred, and execution would continue on some newer platforms. This may cause reports of "NaN" in the output file(s), resulting in read errors later. This bug has been fixed. If GOSIA 2007 finds an insufficient memory condition, it reports the error and terminates the job.

The WRN,X. switch in the CONT section of both OP,GOSI and OP,COUL was unintentionally disabled in the 2007 version. It is restored in the present update.

4) The physical constants in the code were changed to more accurate values.

5) Input format:

Tapes 1 and 2 in the pre-2007 versions have been reassigned to tapes 11 and 12, respectively, in order to make switching between GOSIA and GOSIA2 (the mutual excitation code) easier. This change affects only the default naming of files by GOSIA and the tape 1 and 2 entries to OP,FILE (optional—see below). For example, on a typical Unix-like system, if OP,FILE is not used, the file formerly called “fort.2” will now be called “fort.12” and will contain the best set of matrix elements written at the end of the minimization.

User support

1) Gosia User manual:

The User manual has been expanded and extensively revised to reflect the changes in functionality plus coding that have been made to the Gosia2008 suite of codes.

2) Website support:

A new Gosia website has been developed that includes copies of the codes and the User Manual. The Gosia Forum has been implemented to facilitate communication between users.

3) Gosia newsletter:

A Newsletter will be published periodically to keep the community informed regarding Gosia developments.

1.4 Gosia Users Manual

A comprehensive summary of the Coulomb excitation analysis methods requires knowledge of the algorithms used for this purpose. The effectiveness of data analysis is very much dependent on the ability to select the best ways of using the computer codes, such as GOSIA. Therefore this report is extended beyond the typical program manual to make possible the most efficient utilization of the codes. A short overview of the semiclassical Coulomb excitation formalism and the theory of subsequent decay of the excited nucleus is presented in Chapter 2. The fast Coulomb excitation approximation, which is a basis of GOSIA, GOSIA2, and PAWEL, is described in Chapter 3. Chapter 4 is a presentation of the numerical methods used, while Chapter 5 contains the input instructions. The quadrupole rotational invariants and the description of the associated code SIGMA are contained in Chapter 6. The details of the operations on the permanent files, created and used by GOSIA and SIGMA, are given in Chapter 7. A special version of GOSIA, called GOSIA2, was developed to handle simultaneous Coulomb excitation code with common normalization and is described in Chapter 8. Another special version of GOSIA, called PAWEL, is designed to handle cases where a fraction of the nuclei have as the initial state, an excited isomeric state. The special code ANNLS that uses simulated annealing techniques to locating minima, is described in Chapter 10. Chapter 11 provides a tutorial to introduce the new use to Gosia on how to compile and use the code. Chapter 12 describes the code γ -ray detector efficiency code GREMLIN that can be used to calibrate the γ -ray detection efficiency and correct the measured γ -ray yields for detection efficiency.

2 COULOMB EXCITATION AND GAMMA DECAY OF EXCITED NUCLEI

The semiclassical theory of Coulomb excitation is discussed in the Alder -Winther monograph on the subject [ALD75]. This standard reference presents some alternative approaches to the formal description of electromagnetic excitation. Many of these are valuable for better understanding the nature of the processes in question, but they are not viable practically. Therefore, the following outline of Coulomb excitation theory is limited to the formalism actually used in the code. Particularly, the differences between the semiclassical and the fully quantal descriptions will not be discussed. Perturbation approaches are not useful for multiple Coulomb excitation and thus less attention will be given to such perturbation methods. The presentation of γ -ray deexcitation theory strictly follows the formalism used in GOSIA.

2.1 Safe bombarding energy:

The basic assumption of Coulomb excitation is that the interaction between the scattering ions is purely electromagnetic in origin. This occurs when the ranges of nuclear forces of both interacting nuclei are completely separated in space. A simple but convenient classical formula for estimating the maximum safe bombarding energy in head-on collisions has been given by Cline [CLI69]

$$E_{\max}(MeV) = 1.44 \frac{A_1 + A_2}{A_2} \cdot \frac{Z_1 Z_2}{1.25(A_1^{1/3} + A_2^{1/3}) + 5} \quad (2.1)$$

where index “1“ denotes projectile, “2“ is used for target (this convention will be used repeatedly). This crude classical safe-energy criterion is only applicable to heavy-ion collisions where the semiclassical approximation is valid, that is the wavelength is small compared to the distance of closest approach. This criterion corresponds to a minimum separation between the nuclear surfaces of about 5 fm which is required to ensure that the influence of nuclear excitation is $< 0.1\%$. For light ions a fully quantal code, such as Ptolemy [MA78], is required to estimate the importance of both Coulomb-nuclear interference effects and quantal effects on Coulomb excitation at near-barrier bombarding energies.

2.2 Semiclassical Theory of Coulomb Excitation and its Applicability

Full quantal calculations for scattering and Coulomb excitation become impractical using heavy ions. Fortunately considerable simplification is achieved assuming a semiclassical treatment of two-body kinematics. The semiclassical description of the kinematics is justified if the size of the incoming projectile wavepacket is small compared to the dimensions of its trajectory. The semiclassical approximation can be expressed in terms of the Sommerfeld parameter:

$$\eta = \frac{a2\pi}{2\lambda} = \frac{Z_1 Z_2 e^2}{\hbar v_I} \gg 1 \quad (2.2)$$

here a denotes the classical distance of closest approach in a head-on collision, λ is the wavelength of incoming projectile with initial velocity v_I , $Z_1 e$ and $Z_2 e$ are the charges of the projectile and target respectively. Typically for heavy-ion induced Coulomb excitation, equations 2.1 and 2.2 yield values of η ranging from 50 to 500. Therefore, the validity of a classical description of the scattering kinematics is closely connected to the assumption of non-intervention of the nuclear forces; thus the semiclassical approach is applicable par excellence for all heavy-ion processes when the interaction is purely electromagnetic.

The semiclassical approach is not able to take into account the modification of the trajectory due to the energy transfer. To first order, the effect of energy transfer can be approximated by symmetrization of relevant excitation parameters, i.e. taking an average of these parameters corresponding to perturbed and unperturbed orbits (see below). More accurate determination of energy transfer effects is not possible, since in the classical kinematics picture it is not known at which point of the trajectory that this transfer actually took place. Fortunately, in most cases the excitation energy for pure electromagnetic processes is a very small fraction of the total bombarding energy, so the first-order correction, introduced by a symmetrization procedure, is quite adequate. Further assumptions are made concerning the time separation of excitation and subsequent decay processes. The effective collision time is of the order of 10^{-19} to 10^{-20} sec, which is

orders of magnitude shorter than the mean lifetimes of the nuclear states involved in Coulomb excitation. This allows the excitation and subsequent γ decay to be treated sequentially. Finally, using the expansion of the electromagnetic interaction potential in a multipole series [BOH69] allows a representation of this potential in terms of a sum of three factors: a monopole-monopole interaction, defining the kinematics only; a mutual monopole-multipole interaction and a mutual multipole-multipole interaction. The third term is weak compared to the monopole-multipole term and, within the desired accuracy, can be neglected since it does not interfere with the monopole-multipole terms. This treatment yields a convenient separation of the Schrödinger equation, i.e., the excitation of both projectile and target can be independently expressed as:

$$i\hbar \frac{\delta}{\delta t} |\psi_{1,2}\rangle = (H_{1,2}^o + V_{1,2}(\vec{r}(t))) |\psi_{1,2}\rangle \quad (2.3)$$

where $V_{1,2}(\vec{r}(t))$ stands for monopole-multipole interaction between unexcited nucleus (monopole) and excited nucleus (multipole) - indexed by 1 - or vice versa, indexed by 2. The monopole-monopole interaction determines the time-dependence of the potential by the classical trajectory $\vec{r}(t)$. As can be seen, target and projectile nuclei can be interchanged, therefore the indices 1 and 2 are used only where the distinction is necessary. To solve the time-dependent Schrödinger equation 2.3 we represent $|\psi(\vec{r}, t)\rangle$ as a linear combination of free-nucleus wave functions $\phi(\vec{r})$, taken with time-dependent coefficients of the form:

$$|\psi(\vec{r}, t)\rangle = \sum_n a_n(t) |\Phi_n(\vec{r})\rangle \exp(-iE_n t/\hbar) \quad (2.4)$$

with

$$H^o |\Phi_n\rangle = E_n |\Phi_n\rangle$$

Substituting 2.4 in 2.3 gives:

$$i\hbar \sum_n \frac{da_n(t)}{dt} |\Phi_n(\vec{r})\rangle \exp(-iE_n t/\hbar) = \sum_n a_n(t) V(t) |\Phi_n(\vec{r})\rangle \exp(-iE_n t/\hbar) \quad (2.5)$$

Taking into account orthonormality of the free nucleus wavefunctions $|\Phi_n\rangle$, ($\langle \Phi_k | \Phi_n \rangle = \delta_{kn}$) gives:

$$\frac{da_k(t)}{dt} = -\frac{i}{\hbar} \sum_n a_n(t) \langle \Phi_k | V(t) | \Phi_n \rangle \exp \frac{it}{\hbar} (E_k - E_n) \quad (2.6)$$

The system of differential equations 2.6 defines the complex expansion coefficients $a_k(t)$. Before the collision, the nucleus is assumed to be in the ground state, thus the initial condition (corresponding to $t = -\infty$) can be expressed as $a_k = \delta_{k,0}$, where index O stands for ground state. The nucleus after the collision is then described by the set of excitation amplitudes $a_k(t = \infty)$ defining excitation probabilities where $P_k = a_k a_k^*$, as follows from 2.4. As mentioned above, the interaction potential $V(t)$ can be expanded into a multipole series:

$$V_{1,2}(t) = \sum_{\lambda=1}^{\infty} \sum_{\mu=-\lambda}^{\lambda} \frac{4\pi Z_{2,1} e}{2\lambda + 1} (-1)^\mu S_{\lambda\mu}(t) M_{1,2}(\lambda, -\mu) \quad (2.7)$$

where

$$S_{\lambda\mu}(t) = \frac{Y_{\lambda\mu}(\theta(t), \phi(t))}{[r(t)]^{\lambda+1}} \quad (2.8a)$$

for electric and

$$S_{\lambda\mu}(t) = \frac{1}{c \cdot \lambda} \frac{\frac{d\vec{r}}{dt} \cdot (\vec{r} \times \vec{\nabla})}{[r(t)]^{\lambda+1}} Y_{\lambda\mu}(\theta(t), \phi(t)) \quad (2.8b)$$

for magnetic excitation. Note that $Y_{\lambda\mu}$ denotes standard normalized spherical harmonics. The symbol $M(\lambda, \mu)$ stands for electric and magnetic multipole moments, as defined in [BOH69]:

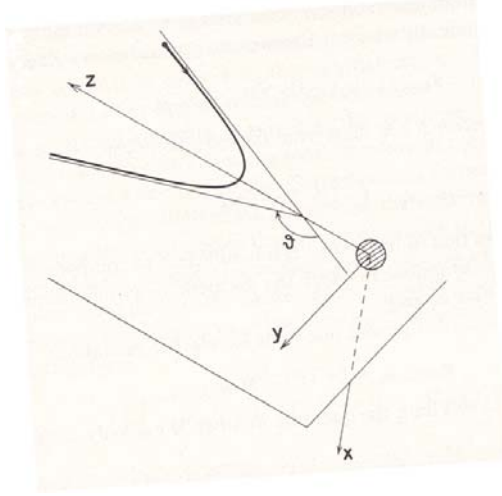


Figure 1: Coordinate system used to evaluate the Coulomb excitation amplitudes. The origin is chosen in the center of mass of the target nucleus. The x -axis is perpendicular to the plane of the orbit, the z -axis is along symmetry axis of the incoming projectile orbit pointing towards the projectile, while the y -axis is chosen such that the y -component of the projectile velocity is positive. The scattering angle θ of the projectile is shown.

$$M(E\lambda, \mu) = \int \rho(\vec{r}) r^\lambda Y_{\lambda\mu}(\theta, \phi) d^3\vec{r} \quad (2.9a)$$

$$M(M\lambda, \mu) = \frac{1}{c(\lambda+1)} \int r^\lambda \vec{j}(\vec{r}) (\vec{r} \times \vec{\nabla}) Y_{\lambda\mu}(\theta, \phi) d^3\vec{r} \quad (2.9b)$$

$\rho(\vec{r})$ and $\vec{j}(\vec{r})$ being spatial charge and current distributions of a free nucleus, respectively. Inserting 2.7 into 2.6 one obtains the parametrization of electromagnetic excitation by the matrix elements of multipole moment operators:

$$\frac{da_k(t)}{dt} = -i \frac{4\pi Z_{1,2} e}{\hbar} \sum_n a_n(t) \exp \frac{it}{\hbar} (E_k - E_n) \sum_{\lambda\mu} (-1)^\mu \cdot S_{\lambda\mu}(t) \langle \Phi_k | M(\lambda, -\mu) | \Phi_n \rangle \quad (2.10)$$

To express the time-dependent functions $S_{\lambda\mu}(t)$ it is convenient to introduce a frame of coordinates with the z -axis along the symmetry axis of the incoming particle trajectory and y -axis in the trajectory plane defined in such a way that the incoming particle velocity component v_y is positive. The x -axis then is defined to form a right-handed cartesian system of coordinates (Fig. 1).

In this system of coordinates, one can describe the relative two-body motion, treated as the classical hyperbolic Kepler solution, introducing two parameters ϵ and ω . The parameter ϵ , called the orbit eccentricity, is expressed by the center-of-mass scattering angle θ_{cm} :

$$\epsilon = \frac{1}{\sin \frac{\theta_{cm}}{2}} \quad (2.11)$$

The dimensionless parameter ω , which replaces time, is given by:

$$t = \frac{a}{v_I} (\epsilon \sinh \omega + \omega) \quad (2.12)$$

where a is half the distance of closest approach for a head-on collision. This parametrization yields the following expression for the length of the radius-vector \vec{r} :

$$r = a(\epsilon \cosh \omega + 1) \quad (2.13)$$

Explicitly, cartesian coordinates are expressed by ϵ and ω as:

$$x = 0$$

$$y = a(\epsilon^2 - 1)^{1/2} \sinh \omega \quad (2.14)$$

$$z = a(\cosh \omega + \epsilon)$$

Note that the closest approach corresponds to $\omega = 0$.

The functions $S(t)$ are replaced by dimensionless ‘‘collision functions’’ $Q(\epsilon, \omega)$:

$$Q_{\lambda, \mu}^E(\epsilon, \omega) = a^\lambda \frac{(2\lambda - 1)!!}{(\lambda - 1)!} \left(\frac{\pi}{2\lambda + 1} \right)^{1/2} r(\omega) S_{\lambda, \mu}^E(t(\omega)) \quad (2.15a)$$

for electric excitations, and

$$Q_{\lambda, \mu}^M(\epsilon, \omega) = \frac{c}{v} a^\lambda \frac{(2\lambda - 1)!!}{(\lambda - 1)!} \left(\frac{\pi}{2\lambda + 1} \right)^{1/2} r(\omega) S_{\lambda, \mu}^M(t(\omega)) \quad (2.15b)$$

for magnetic excitations. The explicit expressions for the collision functions $Q(\epsilon, \omega)$ for $E1$ to $E6$ and $M1$, $M2$ are compiled in Table 2.1.

It is convenient to replace the multipole operator matrix elements $\langle I_s M_s | M(\lambda, \mu) | I_f M_f \rangle$ by reduced matrix elements $\langle I_s || M(\lambda) || I_f \rangle$ using the Wigner-Eckart theorem:

$$\langle I_s M_s | M(\lambda, \mu) | I_f M_f \rangle = (-1)^{I_s - M_s} \begin{pmatrix} I_s & \lambda & I_f \\ -M_s & \mu & M_f \end{pmatrix} \langle I_s || M(\lambda) || I_f \rangle \quad (2.16)$$

It is presumed that the phase convention for the wavefunctions $|I\rangle$ is such, that the reduced matrix elements are real. Insertion of 2.11 through 2.16 into 2.10 yields the final system of differential equations for the excitation amplitudes a_k . The following formulae are given already in a numerical representation of physical constants, corresponding to energies in MeV, reduced electric multipole matrix elements in $eb^{\lambda/2}$ and reduced magnetic multipole matrix elements in $\mu_n b^{(\lambda-1)/2}$, μ_n being the nuclear magneton.

$$\frac{da_k}{d\omega} = -i \sum_{\lambda\mu n} Q_{\lambda\mu}(\epsilon, \omega) \zeta_{kn}^{(\lambda\mu)} \cdot \langle I_k || M(\lambda) || I_n \rangle \cdot \exp(i\xi_{kn}(\epsilon \sinh \omega + \omega)) \cdot a_n(\omega) \quad (2.17a)$$

The one-dimensional indexing of excitation amplitudes a_k involves all magnetic substates of states $|I\rangle$, which from a point of view of a theory of electromagnetic excitation are treated as independent states. The adiabaticity parameters ξ_{kn} , which represent the ratio of a measure of the collision time and the natural nuclear period for a transition, are given by:

$$\xi_{kn} = \frac{Z_1 Z_2 \sqrt{A_1}}{6.34977} ((E_p - sE_k)^{-1/2} - (E_p - sE_n)^{-1/2}) \quad (2.17b)$$

$$s = (1 + A_1/A_2)$$

E_p being the bombarding energy. The above is valid for target excitation, while for projectile excitation indices 1 and 2 are to be interchanged. The adiabaticity parameters have been symmetrized with respect to initial and final velocities in a manner that does not violate unitarity and time reversal invariance.

The same convention is valid for the coupling parameters $\zeta_{kn}^{(\lambda\mu)}$ given by:

$$\zeta_{kn}^{(\lambda\mu)} = (2\lambda + 1)^{1/2} (-1)^{I_n - M_n} \begin{pmatrix} I_n & \lambda & I_k \\ -M_n & \mu & M_k \end{pmatrix} \psi_{kn} \quad (2.17c)$$

with

$$\psi_{kn} = C_{\lambda}^{E(M)} \frac{Z_1 \sqrt{A_1}}{(sZ_1 Z_2)^{\lambda}} \{(E_p - sE_k)(E_p - sE_n)\}^{(2\lambda-1)/4} \quad (2.17d)$$

where the numerical coefficients $C_{\lambda}^E(M)$ are different for electric and magnetic excitation and are given explicitly as:

$$C_{\lambda}^E = 1.116547 \cdot (13.889122)^{\lambda} \cdot \frac{(\lambda-1)!}{(2\lambda+1)!!} \quad (2.17e)$$

$$C_{\lambda}^M = (v/c)C_{\lambda}^E/95.0981942$$

As pointed out in Ref. [ALD75], Appendix J, the dipole polarization effect can be approximately accounted for by modifying the collision functions corresponding to $E2$ type of excitation:

$$Q_{2\mu}(\epsilon, \omega) \longrightarrow Q_{2\mu}(\epsilon, \omega) \cdot \left(1 - z \frac{a}{r}\right) \quad (2.18a)$$

where

$$z = d \cdot \frac{E_p A_2}{Z_2^2 (1 + A_1/A_2)} \quad (2.18b)$$

d being an adjustable empirical $E1$ polarization strength. A widely accepted value of $d = 0.005$ if the bombarding energy E_p is in MeV. Equation 2.13 gives that $\frac{a}{r}$ can be written as:

$$\frac{a}{r} = \frac{1}{\epsilon \cosh \omega + 1}, \quad (2.18c)$$

The useful symmetry properties of $Q_{\lambda\mu}$ are the following:

$$Q_{\lambda\mu}(\epsilon, -\omega) = Q_{\lambda\mu}^*(\epsilon, \omega) \quad (2.19)$$

and, for electric excitation:

$$Q_{\lambda\mu}(\epsilon, \omega) = Q_{\lambda-\mu}(\epsilon, \omega) \quad (2.20)$$

$$Q_{\lambda\mu}(\epsilon, \omega) = (-1)^{\mu} Q_{\lambda\mu}(\epsilon, \omega)$$

while for magnetic excitation:

$$Q_{\lambda\mu}(\epsilon, \omega) = -Q_{\lambda-\mu}(\epsilon, \omega) \quad (2.21)$$

$$Q_{\lambda\mu}(\epsilon, -\omega) = (-1)^{\mu+1} Q_{\lambda\mu}(\epsilon, \omega)$$

It should be noted that, in the coordinate system used here (Fig. 1), for backscattering ($\theta_{cm} = 180^\circ; \epsilon = 1$) all electric Q^E values with $\mu \neq 0$ vanish, as well as all magnetic Q^M values; therefore the magnetic quantum number is conserved. This is physically understandable, since the process along the z -axis cannot change the magnetic quantum number. The conservation of magnetic quantum number, exactly true for backscattering, is approximately valid for an arbitrary scattering angle due to the dominance of electric collision functions with $\mu = 0$. The backscattering is important experimentally, providing the closest possible approach of the nuclei taking part in the excitation process and therefore providing the maximum excitation probability available from Coulomb excitation.

The coefficients ζ , which define coupling of the nuclear states, are dependent on Z, A and energy of the projectile. It is interesting to see the effect of using various beams on a given target, assuming the maximum safe bombarding energy of the projectile given by 2.2. Neglecting symmetrization, one gets from 2.2 and 2.17c:

$$\zeta \sim \left(\frac{Z_1 A_1 d}{s Z_2}\right)^{1/2} \left(\frac{1.44}{d}\right)^{\lambda} \quad (2.22)$$

where

$$d = 1.25 \left(A_1^{1/3} + A_2^{1/3} \right) + 5$$

and s is given by 2.17b.

It can be seen, taking into account the correlation of A_1 and Z_1 , that the coupling coefficients ζ are almost directly proportional to the charge number of a projectile. Consequently, going from lighter to heavier beams leads to excitation of a growing number of levels, while the number of matrix elements influencing the process increases even faster.

The product $\xi\epsilon$ relates the collision time to the natural time period for a nuclear transition. Appreciable excitation of nuclear levels is most probable when the relative oscillation of their eigenfunctions is slow on the scale of the effective collision time. That is, when the Fourier transform of the electromagnetic impulse has significant probability at the transition energy. This implies that the Coulomb excitation cross sections generally increase with decreasing adiabaticity ξ . Taking into account that the excitation energy is small compared to the bombarding energy, expressed in MeV, and expanding 2.17b in a series, yields the approximation:

$$\xi_{kn} \sim \frac{Z_1 Z_2 A_1^{\frac{1}{2}}}{12.65} \frac{E_n - E_k}{E_p \sqrt{E_p}} \quad (2.23)$$

Coulomb excitation is most probable for small transition energy differences in contrast to the deexcitation process, that is, the adiabaticity limits Coulomb excitation to a band of states within about an MeV above the yrast sequence. Increasing the bombarding energy of the projectile enhances the Coulomb excitation not only because of increased coupling parameters ζ but also because of decreased values of ξ .

A convenient way to visualize the excitation process is to introduce so-called orbital integrals $R(\epsilon, \xi)$, defined as:

$$R_{\lambda\mu}(\epsilon, \xi) = \int_{-\infty}^{\infty} Q_{\lambda\mu}(\epsilon, \omega) \exp(i\xi(\epsilon \sinh \omega + \omega)) d\omega \quad (2.24)$$

The orbital integrals R directly determine the excitation amplitudes, provided that the first-order perturbation approach is applicable. Generally, the formal solution of 2.17a can be expressed by an infinite integral series as:

$$\begin{aligned} \bar{a}(\omega = \infty) = & \bar{a}_o + \left\{ \int_{-\infty}^{\infty} A(\omega_o) d\omega_o \right\} \bar{a}_o + \left\{ \int_{-\infty}^{\infty} A(\omega_1) d\omega_1 \int_{-\infty}^{\omega_1} A(\omega_o) d\omega_o \right\} \bar{a}_o + \\ & \dots + \left\{ \int_{-\infty}^{\infty} A(\omega_n) d\omega_n \int_{-\infty}^{\omega_n} A(\omega_{n-1}) d\omega_{n-1} \dots \int_{-\infty}^{\omega_1} A(\omega_o) d\omega_o \right\} \bar{a}_o + \dots \end{aligned} \quad (2.25)$$

where \bar{a} stands for the vector of the amplitudes and $A(\omega)$ is the right-handside matrix operator of 2.17a. The initial vector \bar{a}_o has the ground state amplitude equal to one, all other components vanish. Each term of 2.25 corresponds to given order excitation, i.e., connects a number of matrix elements equal to the number of integrations. Assuming a weak interaction, the first-order perturbation theory expresses the excitation amplitudes of the states k directly coupled to the groundstate as the linear term of 2.25:

$$a_k = \sum_{\lambda} \zeta_{ko}^{(\lambda\mu)} \cdot R_{\lambda\mu}(\epsilon, \xi_{ko}) \langle I_k || M(\lambda) || I_o \rangle \quad (2.26)$$

$$\mu = M_o - M_k$$

where the index “0“ denotes the ground state. Note that 2.26 (and more general 2.17) is valid for a fixed polarization of a ground state, thus for non-zero ground state spin one must average the excitation amplitudes over all possible magnetic substates of the ground state. This explicitly means:

$$a_k = \frac{1}{(2I_o + 1)^{1/2}} \sum_{m_o} a_k(m_o) \quad (2.27)$$

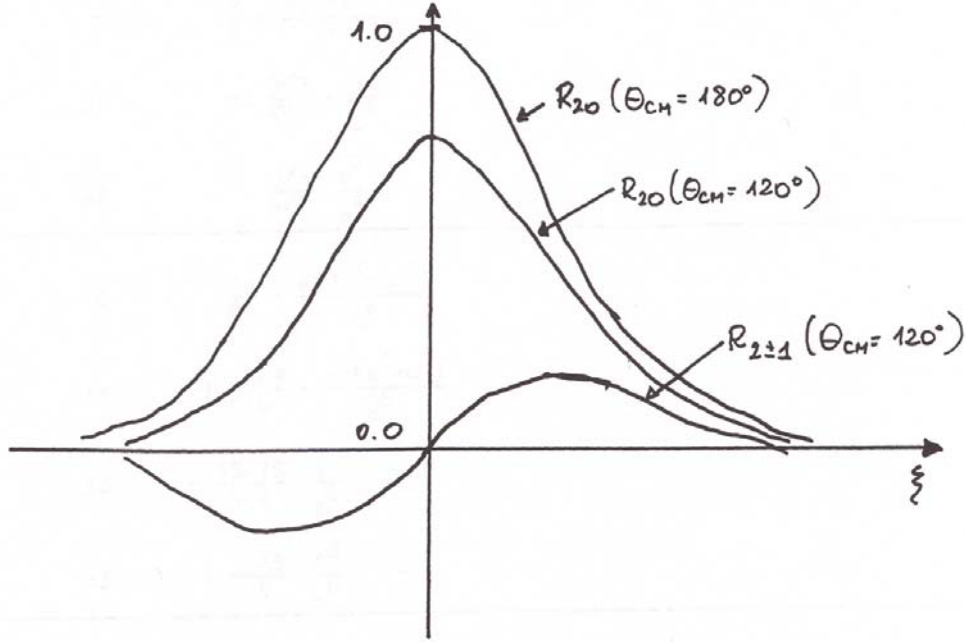


Figure 2: The orbital integrals R_{20} and $R_{2\pm 1}$

and

$$P_k = a_k a_k^* \quad (2.28)$$

where $a_k(m_0)$ denotes the excitation probability of state k with ground state polarization m_0 .

The formula 2.26 has been used extensively to determine reduced excitation probabilities:

$$B(\lambda, I_k \rightarrow I_f) = \frac{1}{2I_k + 1} \langle I || M(\lambda) || I_f \rangle^2 \quad (2.29)$$

for all cases in which the one-step excitation assumption can apply. In addition to their direct applicability to weak Coulomb excitation processes, the orbital integrals R give some general idea about the relationships between different modes of excitation. As an example, Fig. 2 shows the quadrupole orbital integrals R_{20} and $R_{2\pm 1}$ as functions of ξ for $\theta_{cm} = 180^\circ$ and $\theta_{cm} = 120^\circ$. Note that R_{20} is a maximum and $R_{2\pm 1}$ vanishes when $\theta_{cm} = 180^\circ$ while $\theta_{cm} = 120^\circ$ is the optimum scattering angle for $\Delta m = \pm 1$ excitation.

The applicability of first and second order perturbation theories is limited to light-ion induced Coulomb excitation, or for heavy-ion beams, to beam energies far below the safe bombarding energy. In the case of a typical multiple Coulomb excitation experiment, the system of differential equations 2.17 must be solved numerically. It is, for example, estimated that the excitation probability of the first excited 2^+ of ^{248}Cm bombarded with a 641 MeV ^{136}Xe beam is still sensitive to the excitation modes involving 30^{th} order products of the reduced matrix elements. This proves that the perturbation-type simplifications are generally not feasible. An efficient fast approximation to the Coulomb excitation problem is presented in Chapter 3.

Table 2.1a
Electric Collision Functions $Q_{\lambda\mu}^E(\epsilon, \omega)$
 $a = \cosh \omega + \epsilon$ $b = \epsilon \cosh \omega + 1$ $c = \sqrt{(\epsilon^2 - 1) \sinh \omega}$

λ	μ	$Q_{\lambda\mu}^E(\epsilon, \omega)$
1	0	$\frac{1}{2} \cdot \frac{a}{b^2}$
1	± 1	$-i \cdot \frac{1}{2\sqrt{2}} \cdot \frac{c}{b^2}$
2	0	$\frac{3}{4} \cdot \frac{2a^2 - c^2}{b^4}$
2	± 1	$-i \cdot \frac{3\sqrt{3}}{2\sqrt{2}} \cdot \frac{ac}{b^4}$
2	± 2	$-\frac{3\sqrt{3}}{4\sqrt{2}} \cdot \frac{c^2}{b^4}$
3	0	$\frac{15}{8} \cdot \frac{a(2a^2 - 3c^2)}{b^6}$
3	± 1	$-i \cdot \frac{15\sqrt{3}}{16} \cdot \frac{c(4a^2 - c^2)}{b^6}$
3	± 2	$-\frac{15\sqrt{15}}{8\sqrt{2}} \cdot \frac{ac^2}{b^6}$
3	± 3	$i \cdot \frac{15\sqrt{5}}{16} \cdot \frac{c^3}{b^6}$
4	0	$\frac{35}{32} \cdot \frac{8a^4 - 24a^2c^2 + 3c^4}{b^8}$
4	± 1	$-i \cdot \frac{35\sqrt{5}}{16} \cdot \frac{ac(4a^2 - 3c^2)}{b^8}$
4	± 2	$-\frac{35\sqrt{5}}{16\sqrt{2}} \cdot \frac{c^2(6a^2 - c^2)}{b^8}$
4	± 3	$i \cdot \frac{35\sqrt{35}}{16} \cdot \frac{ac^3}{b^8}$
4	± 4	$\frac{35\sqrt{35}}{32\sqrt{2}} \cdot \frac{c^4}{b^8}$
5	0	$\frac{3\sqrt{5}}{256} \cdot \frac{a[-14a^2(a^2 + 9c^2) + 30a^4]}{b^{10}}$
5	± 1	$-i \cdot \frac{315\sqrt{30}}{256} \cdot \frac{c^2a(-21c^2 + 8a^2)}{b^{10}}$
5	± 2	$-\frac{315\sqrt{210}}{128} \cdot \frac{c^2a(-3c^2 + 2a^2)}{b^{10}}$
5	± 3	$i \cdot \frac{315\sqrt{35}}{256} \cdot \frac{c^3(9a^2 - b^2)}{b^{10}}$
5	± 4	$\frac{945\sqrt{70}}{256} \cdot \frac{c^4a}{b^{10}}$
5	± 5	$-i \cdot \frac{945\sqrt{7}}{256} \cdot \frac{c^5}{b^{10}}$
6	0	$\frac{963}{256} \cdot \frac{21a^2[-a^2(11c^2 + 4b^2) + 5b^4] - 5b^6}{b^{12}}$
6	± 1	$\frac{693\sqrt{42}}{512} \cdot \frac{ac[3a^2(-11c^2 + b^2) + 5b^4]}{b^{12}}$
6	± 2	$-\frac{693\sqrt{105}}{512} \cdot \frac{c^2[3a^2(-11c^2 + 5b^2) + b^4]}{b^{12}}$
6	± 3	$-i \cdot \frac{693\sqrt{105}}{256} \cdot \frac{ac^3(-11c^2 + 8b^2)}{b^{12}}$
6	± 4	$\frac{2679\sqrt{14}}{512} \cdot \frac{c^4(11a^2 - b^2)}{b^{12}}$
6	± 5	$-i \cdot \frac{2079\sqrt{77}}{256} \cdot \frac{ac^5}{b^{12}}$
6	± 6	$-\frac{693\sqrt{231}}{512} \cdot \frac{c^6}{b^{12}}$

Table 2.1b
Magnetic Collision Functions $Q_{\lambda\mu}^M(\epsilon, \omega)$

λ	μ	$Q_{\lambda\mu}^M(\epsilon, \omega)$
1	0	0
1	± 1	$\mp \frac{\sqrt{2}}{4} \cdot \frac{\sqrt{(\epsilon^2 - 1)}}{b^2}$
2	0	0
2	± 1	$\mp \frac{3\sqrt{6}}{16} \cdot \sqrt{(\epsilon^2 - 1)} \cdot \frac{a}{b^4}$
2	± 2	$-i \frac{3\sqrt{6}}{16} \cdot \sqrt{(\epsilon^2 - 1)} \cdot \frac{c}{b^4}$

2.3 Gamma Decay Following Electromagnetic Excitation

The decay of a Coulomb-excited nucleus can be treated as completely separated in time from the excitation process. The initial condition for the decay can be described by a statistical tensor, expressing the state of polarization of the decaying level:

$$\rho_{k\chi}(I) = (2I+1)^{1/2} \sum_{MM'} (-1)^{I-m'} \begin{pmatrix} I & k & I \\ -M' & \chi & M \end{pmatrix} a_{IM'}^* a_{IM} \quad (2.30)$$

where we explicitly denote excitation amplitude of a substate $|IM\rangle$ with two-dimensional indexing. Averaging 2.30 over all possible polarizations of a ground state gives:

$$\rho_{k\chi}(I) = \frac{(2I+1)^{1/2}}{2I_o+1} \sum_{M_o MM'} (-1)^{I-m'} \begin{pmatrix} I & k & I \\ -M' & \chi & M \end{pmatrix} a_{IM'}^*(M_o) a_{IM}(M_o) \quad (2.31)$$

where:

$$\rho_{00}(I) = P_I \quad (2.32)$$

In an arbitrary coordinate frame with the origin at the decaying nucleus the angular distribution of gamma radiation can be expressed as:

$$\frac{d^2\sigma}{d\Omega_p d\Omega_\gamma} = \sigma_R(\theta_p) \frac{1}{2\gamma(I_1)\sqrt{\pi}} \sum_{\substack{k \text{ even} \\ \chi}} \rho_{k\chi}^*(I_1) \sum_{\lambda\lambda'} \delta_\lambda \delta_{\lambda'}^* F_k(\lambda\lambda' I_2 I_1) Y_{k\chi}(\theta_\gamma, \phi_\gamma) \quad (2.33)$$

Here $\sigma_R(\theta_p)$ denotes the scattering angle dependent Rutherford cross-section, $F_k(\lambda\lambda', I_2 I_1)$ are the $\gamma - \gamma$ correlation coefficients (as defined, e.g., in FRA65), $Y_{k\chi}(\theta_\gamma, \phi_\gamma)$ are normalized spherical harmonics. The quantities δ_λ are the $I_1 \rightarrow I_2$ transition amplitudes for multipolarity λ , related to the emission probability $\gamma(I_1)$ by:

$$\gamma(I_1) = \sum_{\lambda n} |\delta_\lambda(I_1 \rightarrow I_n)|^2 \quad (2.34)$$

An explicit form of $F_k(\lambda\lambda', I_2 I_1)$ can be expressed in terms of Wigner's $3-j$ and $6-j$ symbols

$$F_k(\lambda\lambda', I_2 I_1) = (-1)^{I_1+I_2-1} [(2k+1)(2I_1+1)(2\lambda+1)(2\lambda'+1)]^{1/2} \begin{pmatrix} \lambda & \lambda' & k \\ 1 & -1 & 0 \end{pmatrix} \left\{ \begin{matrix} \lambda & \lambda' & k \\ I_1 & I_1 & I_2 \end{matrix} \right\} \quad (2.35)$$

while $\delta_\lambda(1 \rightarrow 2)$ is given by:

$$\delta_\lambda(1 \rightarrow 2) = i^{n(\lambda)} \frac{1}{(2\lambda+1)!! \hbar^{\lambda+1}} \left(\frac{8\pi(\lambda+1)}{\lambda} \right)^{1/2} \left(\frac{E_\gamma}{c} \right)^{\lambda+1/2} \frac{\langle I_2 || E(M)\lambda || I_1 \rangle}{(2I_1+1)^{1/2}} \quad (2.36)$$

where

$$n(\lambda) = \begin{cases} \lambda & \text{for E}\lambda \text{ transition} \\ \lambda+1 & \text{for M}\lambda \text{ transition} \end{cases}$$

Note that the transition amplitude for an electric monopole transition, δ_0 , is defined by equation 2.71.

The coordinate system used for evaluation of excitation probabilities is no longer convenient to determine angular distributions of gamma radiation, as it is not fixed with respect to the laboratory frame. Therefore, it is useful to define the z -axis along the beam direction with the x -axis in the plane of orbit in such a way, that the x -component of the impact parameter is positive. The y -axis is then defined to form a right-handed system (Fig. 2.3).

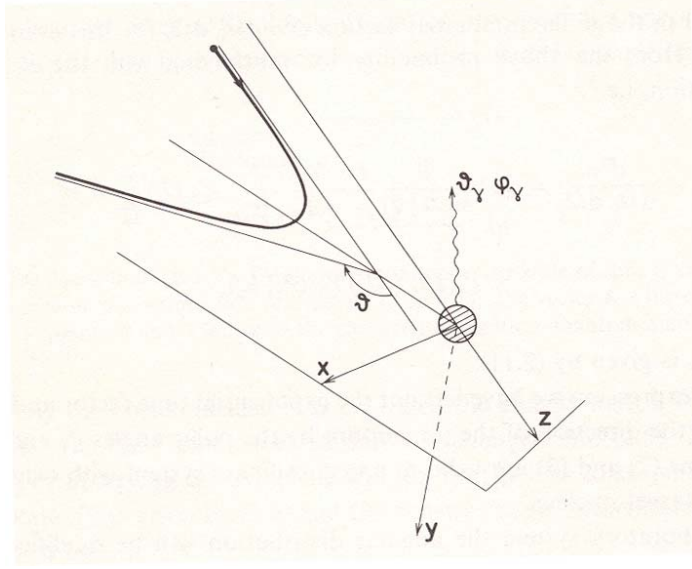


Figure 3: The coordinate system used to describe the γ -decay of a Coulomb-excited nucleus. The z -axis is chosen along the incoming beam direction, the x -axis is in the plane of the orbit such that the x -component of the velocity is positive. A γ -decay in the direction $\theta_\gamma, \varphi_\gamma$ is indicated.

The statistical tensors $\rho_{k\chi}$ in the new coordinate frame are obtained by rotation with Euler angles $(\frac{\pi}{2}, \frac{(\pi+\theta)}{2}, \pi)$:

$$\rho_{k\chi} \rightarrow \sum_{\chi'} \rho_{k\chi'} D_{\chi'\chi}^k \left(\frac{\pi}{2}, \frac{\pi+\theta}{2}, \pi \right) \quad (2.37)$$

the rotation functions $D_{\chi\chi'}^k(\alpha, \beta, \gamma)$ being defined according to [BOH69]:

$$D_{\chi\chi'}^k(\alpha, \beta, \gamma) = e^{i\chi\alpha} d_{\chi\chi'}^k(\beta) e^{i\chi'\gamma} \quad (2.38)$$

with

$$d_{\chi\chi'}^k(\beta) = \left[\frac{(k+\chi')!(k-\chi)!}{(k+\chi)!(k-\chi')} \right]^{1/2} \cdot \sum_m \binom{k+\chi}{k-\chi'-m} \binom{k-\chi}{m} (-1)^{k-\chi'-m} \left[\cos \frac{\beta}{2} \right]^{2m+\chi+\chi'} \left[\sin \frac{\beta}{2} \right]^{2k-2m-\chi-\chi'} \quad (2.39)$$

Inserting 2.38 and 2.39 into 2.37 gives:

$$\rho_{k\chi} \rightarrow (-1)^\chi \cdot \sum_{\chi'} i^{\chi'} d_{\chi'\chi}^k \left(\frac{\pi+\theta}{2} \right) \rho_{k\chi'} \quad (2.40)$$

A complete description of the γ -decay also must involve correction for the depolarization of the excited levels due to the hyperfine interaction, i.e. the interaction between the stripped electron shells and the nucleus. This effect can be taken into account by introducing the k -dependent attenuation coefficients, G_k , multiplying the statistical tensors (this approach is described in Section 2.2.1). The attenuation of the angular distribution due to the hyperfine interactions is usually significant in case of thin-target experiments, while all the G_k 's equal unity if the decaying nucleus has been stopped in the target prior to the γ decay. The basic formula 2.33 can be expressed in terms of the decay statistical tensors, $R_{k\chi}$, which include the hyperfine interaction effects:

$$\frac{d^2\sigma}{d\Omega_p d\Omega_\gamma} = \sigma_R(\theta_p) \sum_{k_X} R_{k_X}(I, I_f) Y_{k_X}(\theta_\gamma, \phi_\gamma) \quad (2.41)$$

where :

$$R_{k_X}(I, I_f) = \frac{1}{2\gamma(I)\sqrt{\pi}} G_k \rho_{k_X} \sum_{\lambda\lambda'} \delta_\lambda \delta_{\lambda'}^* F_k(\lambda\lambda, I_f I) \quad (2.42)$$

is the decay statistical tensor describing the mixed electric and magnetic transition from a state I to a state I_f . The Coulomb excitation statistical tensors are purely real for even values of k in the frame of coordinates introduced above, thus $\rho_{k_X} = \rho_{k_X}^*$. Moreover, taking into account the selection rules for electromagnetic transitions, it is easily seen that the products $\delta_\lambda \delta_{\lambda'}^*$ also are real. Consequently, the decay statistical tensors are purely real.

The above formulas describe γ -decay of a level fed directly and exclusively by Coulomb excitation. With multiple excitation, however, significant feeding from the decay of higher-lying levels must be taken into account. The related modification of the statistical tensors can be expressed as:

$$R_{k_X}(I, I_f) \longrightarrow R_{k_X}(I, I_f) + \sum_n R_{k_X}(I_n, I) H_k(I, I_n) \quad (2.43)$$

where the summation extends over all levels I_n directly feeding level I . The explicit formula for the H_k coefficients is:

$$H_k(I, I_n) = \frac{[(2I+1)(2I_n+1)]^{1/2}}{\gamma(I)} \sum_\lambda (-1)^{I+I_n+\lambda+k} |\delta_\lambda|^2 (1+c(\lambda)) \left\{ \begin{array}{ccc} I & I & k \\ I_n & I_n & \lambda \end{array} \right\} \quad (2.44)$$

where $c(\lambda)$ is the internal conversion coefficient for the $I_n \rightarrow I$ transition. Note that for an electric monopole transition $c(0) = 0$. Formula 2.44 is used to sequentially modify the deexcitation statistical tensors, starting from the highest levels having non-negligible population. This operation transforms the deexcitation statistical tensors, which are inserted into 2.41 to give the unperturbed angular distributions following Coulomb excitation.

In addition, it is necessary to take into account experiment-related perturbations, namely the effects of the detection methods and relativistic corrections due to in-flight decay. These effects can be significant when using thin targets and heavy ion beams. An overview of the methods used in GOSIA to account for experimental perturbations is presented in the following subsections.

2.3.1 Nuclear Deorientation Effect

In typical Coulomb excitation experiments, both the projectile and target particles recoil into vacuum in highly excited ionic states which subsequently decay to a ground state. The fluctuating atomic hyperfine fields cause the depolarization of the nuclear states; this effect is known as the nuclear deorientation effect. This in turn causes an attenuation of the angular distribution of the γ -rays which can be taken into account by introducing the spin and lifetime dependent attenuation coefficients G_k , multiplying the decay statistical tensors. The Abragam and Pound theory [ABR53] has been used extensively to describe nuclear deorientation and has proven to work well in cases where the particles recoil into high-pressure gas. However, significant discrepancies from the Abragam and Pound model were detected for recoil into vacuum. Therefore GOSIA uses a modified version of the two-state deorientation model ([BOS77], [BRE77]), which seems to correlate well with existing data despite the far-reaching simplification enforced by the complexity of the problem. [KAV89]

Within the framework of the two-state model, the electrons may either belong to a ‘‘fluctuating’’ state, during which the excited electronic structure of the atom decays to the atomic ground state, or to a ‘‘static’’ state, corresponding to an equilibrium atomic ground-state configuration. The excitation and decay of stripped electron shells is a complicated stochastic process making it difficult to describe exactly, therefore it is assumed that all atomic processes taking place in the fluctuating state are purely random. The rate of transition from the fluctuating to static state, Λ^* , is an adjustable parameter of the model. The time-dependent deorientation coefficients $G_k(t)$ then are given by :

$$G_k(t) = e^{-\Lambda^* t} G_k^{(fluct.)}(t) + \int_0^t \Lambda^* G_k^{(fluct.)}(t') \cdot e^{-\Lambda^* t'} G_k^{(stat.)}(t-t') dt' \quad (2.45)$$

The references [BOS77], [BRE77], plus references therein, provide the details of the derivation.

The static-state attenuation factor $G_k^{(stat.)}$ is expressed as

$$G_k^{(stat.)} = \langle \alpha_k \rangle + (1 - \langle \alpha_k \rangle) e^{-\Gamma t} \quad (2.46)$$

with $\langle \alpha_k \rangle$ given by:

$$\langle \alpha_k \rangle = \sum_i p(J_i) \cdot \sum_{F_i F'_i} \frac{(2F_i + 1)(2F'_i + 1)}{2J_i + 1} \left\{ \begin{matrix} F_i & F'_i & k \\ I & I & J_i \end{matrix} \right\}^2 \quad (2.47)$$

where F_i is the vector sum of the nuclear spin I and the electronic spin J_i which is the ground state spin of the deexcited atom, i.e. the ground state spin of an atom with the charge number equal to the charge number of the investigated nucleus minus the number of stripped electrons. The standard Nikolayev-Dmitriev stripping formula [NIK68] is used to determine the atomic charge states and the corresponding atomic ground state spins J_i . The term $p(J_i)$ in [2.47] is the discrete distribution of electronic angular momenta J_i . which is evaluated by defining a parameter h :

$$h = \frac{1}{1 + \left(\frac{0.012008c}{v} Z^{0.45} \right)^{5/3}}$$

which includes the best-fit constants given by [NIK68]. Then the Gaussian charge state distribution is taken to be centered around Q_o given by

$$Q_o = Z \cdot (h)^{0.6} \quad (2.48)$$

with a Gaussian width σ_Q given by

$$\sigma_Q = (Q_o(1-h))^{1/2}$$

In equation 2.46, Γ has the meaning of the width of the Larmor frequency distribution resulting from the assumption of many ionic ground states, as well as many long-lived excited atomic states, involved in the static part of the interaction. This distribution is assumed to be Lorentzian, with Γ treated as an adjustable parameter of the model.

The fluctuating-state attenuation factor $G^{(fluct.)}(t)$ is given by:

$$G^{fluct}(t) = (1 - \lambda_k \tau_c) \exp(-\lambda_k t) \quad (2.49)$$

where τ_c is the mean time between random reorientations of the fluctuating hyperfine field and:

$$\lambda_k = \frac{1 - \langle \alpha_k \rangle}{\tau_c} \left(1 - \exp \left(\frac{-\langle \omega^2 \rangle \tau_c^2}{1 - \langle \alpha_k \rangle} \right) \right) \quad (2.50)$$

with $\langle \omega^2 \rangle$ being the average Larmor frequency in the fluctuating state field:

$$\langle \omega^2 \rangle = \frac{1}{3} k(k+1) \sum_{J_i} p(J_i) \frac{a^2(J_i)}{\hbar^2} J_i(J_i+1) \quad (2.51)$$

Practically, averaging over the fluctuating state atomic spins J_i in 2.51 is not possible since the spin distribution is not known. One must therefore use the single mean value of J_i , treated as one more model parameter. The parameter $a(J_i)$ is defined as:

$$a(J_i) = \mu_n g \frac{\overline{H}}{J_i} \quad (2.52)$$

where μ_n is the nuclear magneton and g stands for the gyromagnetic factor. The mean magnetic field \overline{H} in the fluctuating state is approximated as:

$$\overline{H} = KZ \left(\frac{v}{c}\right)^x \quad (2.53)$$

with both K and x being adjustable parameters best fit to data. [GOL77].

Formula 2.49 is valid only for t much larger than τ_c . Taking into account that τ_c is of the order of a few picoseconds, which is the order of a typical lifetime of the collective nuclear levels, and that the time-integral attenuation coefficients are required, we have to introduce a correction to 2.49 in the time range of τ_c . Since $G^{(fluct.)}(t)$ also can be derived for $t \rightarrow 0$, it is practical to introduce an interpolating function between time ranges $t \rightarrow 0$ and t much greater than τ_c , being chosen as a linear combination of two exponential time-decay functions in order to keep the mathematics at a minimum. This procedure yields for the time-integral coefficients G_k :

$$G_k = \lambda_I \int_0^\infty G_k(t) \exp(-\lambda_I t) dt = G_k^{BS} \left[1 + \frac{\lambda_k \tau_I (r - 2p^2 \tau_I \tau_c)}{(r + p\tau_I)(r + 2p\tau_I)} \right] \quad (2.54)$$

where:

$$G^{BS} = \frac{1}{r} \left[1 + \Lambda^* \tau_I \left(\frac{1 + \langle \alpha_k \rangle^{\Gamma\tau} I}{1 + \Gamma\tau_I} \right) \right] \quad (2.55)$$

is an original formula from [BOS77], $\tau_I = 1/\lambda_I$ is the mean lifetime of a nuclear state, while r and p are given by:

$$r = (\Lambda^* + \lambda_k) \tau_I + 1 \quad (2.56)$$

$$p = \frac{(9\lambda_k^2 + 8\lambda_k \tau_c (\langle \omega^2 \rangle - \lambda_k^2))^{1/2} - 3\lambda_k}{4\lambda_k \tau_c} \quad (2.57)$$

The correction to the original model in most cases does not exceed 10% and is easily evaluated since no additional parameters have been introduced. The recommended parameters of the nuclear deorientation model are listed in section 5.3, in the description of the VAC switch of the CONT suboption of GOSIA.

Kavka[KVA89] analysed deorientation data collected as a by-product of Coulomb excitation studies of 9 nuclei. He found that the above two-state model reproduces the data well. As a consequence, GOSIA uses the Two-state model to account for the deorientation effect until a more refined model of the deorientation effect becomes available.

2.3.2 Relativistic Angular Distribution Correction

The coordinate system used to evaluate the angular distribution of the decay γ -rays, having the γ -axis coincident with the laboratory-fixed beam direction, can easily be translated to the fixed laboratory system just by proper definition of the ϕ angle, taking care of the rotation of the $x - y$ plane, dependent on the recoil velocity direction. This is true as long as the relativistic effects can be neglected and the transformation from the decaying-nucleus-centered system to the laboratory system can be treated as Galilean. However, this assumption does not hold for heavy-beam, thin-target experiments. In this case the recoil velocity can reach up to 10% of the velocity of light, so that the transformation from the decaying nucleus centered system of coordinates to the laboratory system should be Lorentzian. The first order description of this effect is given in [ALD75] while an alternate approach, based on second-order Lorentz transformation of decay statistical tensors is presented in [LES71] and is actually used in GOSIA, fitting well the deexcitation formalism employed by the code. Denoting $\beta = \frac{v_{recoil}}{c}$, and using RN for the recoiling nucleus centered system with the z -axis defined by the recoil direction, and LAB for the laboratory-fixed system, then to second order in β the relativistic transformation can be expressed in the form:

$$\frac{dW^{LAB}(\theta, \phi)}{d\Omega_\gamma} = \left\{ (1 - \beta^2) + \beta U + \frac{1}{2} \beta^2 V \right\} \frac{dW^{RN}(\theta, \phi)}{d\Omega_\gamma} \quad (2.58)$$

where the angular distribution in the recoil nucleus system is written as:

$$\frac{dW^{RN}(\theta, \phi)}{d\Omega_\gamma} = \sum_{k_\chi \text{ even}} a_{k_\chi} Y_{k_\chi}(\theta, \phi) \quad (2.59)$$

which is basically a short form of equation 2.33. It is assumed that the statistical tensors ρ_{k_χ} in the recoil nucleus frame, given by equation 2.33, have been modified to account for the γ -ray feeding from above as well as the deorientation effect. A rotational transformation of the a_{k_χ} tensor into the RN system is done using rotation matrices $D_{\chi\chi'}^k$ defined in equation 2.38. Operators U and V are defined as [LES71]:

$$U = T + 2\cos(\theta) \quad (2.60)$$

$$V = T^2 + 4\cos(\theta) \cdot T + 6\cos^2(\theta) \quad (2.61)$$

where:

$$T = \frac{1}{2}[\sin(\theta)e^{-i\phi}L_+ - \sin(\theta)e^{i\phi}L_-] \quad (2.62)$$

Table 2.2
Relativistic transformation of the angular distribution coefficients b_{k_χ}

Odd k			Even k		
k	χ	b_{k_χ}	k	χ	b_{k_χ}
1	0	$\frac{2}{\sqrt{3}}a_{00} + \frac{2}{\sqrt{15}}a_{20}$	2	0	$\frac{2}{\sqrt{5}}a_{00} - \frac{10}{7}a_{20} + \frac{12}{7\sqrt{5}}a_{40}$
1	1	$-\frac{1}{\sqrt{5}}a_{21}$	2	1	$-\frac{17}{14}a_{21} + \frac{2\sqrt{6}}{7}a_{41}$
3	0	$\frac{12}{\sqrt{35}}a_{20} - \frac{4}{\sqrt{7}}a_{40}$	2	2	$-\frac{4}{7}a_{22} + \frac{2\sqrt{3}}{7}a_{42}$
3	1	$\frac{8\sqrt{2}}{\sqrt{35}}a_{21} - \sqrt{\frac{15}{7}}a_{41}$	4	0	$\frac{8\sqrt{5}}{7}a_{20} - \frac{380}{77}a_{40} + \frac{100}{11\sqrt{13}}a_{60}$
3	2	$\frac{4}{\sqrt{7}}a_{22} - \frac{2\sqrt{3}}{\sqrt{7}}a_{42}$	4	1	$\frac{20\sqrt{6}}{21}a_{21} - \frac{723}{154}a_{41} + \frac{20\sqrt{70}}{11\sqrt{39}}a_{61}$
3	3	$-a_{43}$	4	2	$\frac{20\sqrt{3}}{21}a_{22} - \frac{306}{77}a_{42} + \frac{40\sqrt{14}}{11\sqrt{39}}a_{62}$
5	0	$\frac{10}{\sqrt{11}}a_{40} - \frac{30}{\sqrt{143}}a_{60}$	4	3	$-\frac{61}{22}a_{43} + \frac{40\sqrt{3}}{11\sqrt{13}}a_{63}$
5	1	$\frac{4\sqrt{6}}{\sqrt{11}}a_{41} - \frac{5\sqrt{35}}{\sqrt{143}}a_{61}$	4	4	$-\frac{12}{11}a_{44} + \frac{20\sqrt{5}}{11\sqrt{13}}a_{64}$
5	2	$\frac{2\sqrt{21}}{\sqrt{11}}a_{42} - \frac{20\sqrt{2}}{\sqrt{143}}a_{62}$	6	0	$\frac{210}{11\sqrt{13}}a_{40} - \frac{574}{55}a_{60}$
5	3	$\frac{8}{\sqrt{11}}a_{43} - \frac{15\sqrt{3}}{\sqrt{143}}a_{63}$	6	1	$\frac{14\sqrt{210}}{11\sqrt{13}}a_{41} - \frac{1121}{110}a_{61}$
5	4	$\frac{6}{\sqrt{11}}a_{44} - \frac{10\sqrt{5}}{\sqrt{143}}a_{64}$	6	2	$\frac{28\sqrt{42}}{11\sqrt{13}}a_{42} - \frac{104}{11}a_{62}$
5	5	$-\frac{5}{\sqrt{13}}a_{65}$	6	3	$\frac{84\sqrt{3}}{11\sqrt{13}}a_{43} - \frac{181}{22}a_{63}$
7	0	$\frac{56}{\sqrt{195}}a_{60}$	6	4	$\frac{42\sqrt{5}}{11\sqrt{13}}a_{44} - \frac{358}{55}a_{64}$
7	1	$\frac{32}{\sqrt{65}}a_{61}$	6	5	$-\frac{43}{10}a_{65}$
7	2	$\frac{8\sqrt{3}}{\sqrt{13}}a_{62}$	6	6	$-\frac{8}{5}a_{66}$
7	3	$\frac{16\sqrt{2}}{\sqrt{39}}a_{63}$	8	0	$\frac{672}{5\sqrt{221}}a_{60}$
7	4	$\frac{8\sqrt{11}}{\sqrt{65}}a_{64}$	8	1	$\frac{144\sqrt{21}}{5\sqrt{221}}a_{61}$
7	5	$\frac{16\sqrt{2}}{\sqrt{65}}a_{65}$	8	2	$\frac{36\sqrt{12}}{\sqrt{221}}a_{62}$
7	6	$\frac{8}{\sqrt{15}}a_{66}$	8	3	$\frac{24\sqrt{22}}{\sqrt{221}}a_{63}$
7	7	0	8	4	$\frac{144\sqrt{11}}{5\sqrt{221}}a_{64}$
			8	5	$\frac{72\sqrt{2}}{5\sqrt{17}}a_{65}$
			8	6	$\frac{24\sqrt{7}}{5\sqrt{17}}a_{66}$
			8	7	0
			8	8	0

$b_{k, -\chi} = (-1)^\chi b_{k_\chi}^* = (-1)^\chi b_{k_\chi}$ since b_{k_χ} are real.

L_+ and L_- being the raising and lowering operators for spherical harmonics:

$$L_+ Y_{k\chi} = [(k - \chi)(k + \chi + 1)]^{1/2} Y_{k+1\chi} \quad (2.63)$$

$$L_- Y_{k\chi} = [(k + \chi)(k - \chi + 1)]^{1/2} Y_{k-1\chi} \quad (2.64)$$

The transformation 2.58 changes the even-order spherical harmonics to linear combinations of spherical harmonics. Therefore, the effect of the relativistic transformation 2.58 on the angular distribution of γ -rays can be represented as a modification of $\rho_{k\chi}$ tensors. Ordering the relativistic correction by the powers of β gives:

$$\frac{dW^{LAB}(\theta, \phi)}{d\Omega_\gamma} = \frac{dW^{RN}(\theta, \phi)}{d\Omega_\gamma} + \beta \sum_{\substack{k \\ \text{odd}}} b_{k\chi} Y_{k\chi}(\theta, \phi) + \beta^2 \sum_{\substack{k \\ \text{even}}} b_{k\chi} Y_{k\chi}(\theta, \phi) \quad (2.65)$$

where the $b_{k\chi}$ tensors result from equation 2.58 and are linear combinations of the $a_{k\chi}$ components as given in table 2.2. The result of equation 2.65 can be represented as modified statistical tensors and rotated back to the laboratory frame of coordinates with z along the beam direction. It should be noted that due to the relativistic correction, terms involving odd- k spherical harmonics are introduced and the maximum k value is increased by 2. Table 2.2 has been evaluated for multipolarities up to $\lambda = 3$, i.e. $k \leq 6$ in the recoil nucleus frame leading to $k \leq 8$ in the laboratory frame. Higher multipoles than $\lambda = 3$ would have lifetimes that are much longer than the time of flight of the recoiling nuclei and thus are stopped before the γ -ray decay. The relativistic correction formalism [LES71] presented above results in an elegant modification of the decay statistical tensors and is used to the full extent in GOSIA despite the minor importance of some of the correction terms involved.

2.3.3 Gamma Detector Solid Angle Attenuation Factors

Discussing the angular distribution of the γ -rays we have been so far concerned only with a well-defined direction of observation, given by the pair of angles $(\theta_\gamma, \phi_\gamma)$. To reproduce an experiment one must, however, take into account the finite size of the γ detectors as well as the γ -ray absorption mechanism. A practical method to account for these effects has been described by Krane ([KRA72] and references therein). This method is applicable for the coaxial germanium detector, almost exclusively used in the type of the experiments used for Coulomb excitation studies. The method of Krane introduces γ energy-dependent attenuation factors, $Q_k(E_\gamma)$, multiplying the final decay statistical tensors, defined as:

$$Q_k(E_\gamma) = \frac{J_k(E_\gamma)}{J_O(E_\gamma)} \quad (2.66)$$

where:

$$J_k(E_\gamma) = \int_0^{\alpha_{\max}} P_k(\cos \alpha) K(\alpha) (1 - \exp(-\tau(E_\gamma)x(\alpha))) \sin(\alpha) d\alpha \quad (2.67)$$

and α is the angle between the detector symmetry axis and the γ -ray direction, τ is an energy-dependent absorption coefficient of the active germanium layer and x stands for the angle-dependent path length in the detector. P_k are standard Legendre polynomials, while the function $K(\alpha)$ can be introduced to account for the effect of the γ -ray passing through the inactive, p-type core of the detector as well as the absorbers in front of a detector, commonly used to attenuate X-rays. The function $K(\alpha)$ can be written as:

$$K(\alpha) = \exp - \left(\sum_i \tau_i(E_\gamma) x_i(\alpha) \right) \quad (2.68)$$

where the summation extends over various absorbers and the p-core. The Q_k factors, resulting from 2.66, have to be evaluated numerically. In order not to repeat this procedure for every γ energy of interest, it is practical to fit a simple analytic function describing the energy dependence, as discussed in section 4.

To reproduce the experiment one should, in addition to the effects discussed in previous sections, include the integration of 2.33 over the particle detection solid angle and, at least for the long-lived states, include the correction due to in-flight decay, i.e. the time-dependent change in the angular position and the solid angle of a detector as seen by the decaying nucleus. These effects are treated numerically in GOSIA, the algorithms used being presented in Chapter 4.

2.3.4 Internal Conversion

The electromagnetic radiation field for a nuclear transition can lead to the ejection of a bound atomic electron, or the creation of an electron-positron pair if the transition energy exceeds $2m_e c^2$. The total internal conversion coefficient $c(\lambda)$ is defined as the ratio of the internal conversion decay probability to corresponding γ -ray decay probability

$$c(\lambda) = \frac{\Gamma_{ic}}{\Gamma_\gamma} \quad (2.69)$$

where the total internal conversion coefficient is the sum of internal conversion for all atomic shells plus internal pair conversion. Internal conversion opens additional decay paths populating a given state by unobserved cascade feeding from above. Fortunately the total decay width for any transition is increased by just a multiplicative factor times the γ -ray decay probability. That is,

$$\Gamma(I, I_f)_{total} = \Gamma(I, I_f)_\gamma (1 + c(\lambda)) \quad (2.70)$$

which is easy to handle using the concept of a conversion coefficient as illustrated by equation 2.44.

Electric monopole, $E(0)$, transitions are forbidden by single-photon decay, but they can decay by emission of an internally converted electron or by internal pair creation. Double photon decay is an allowed higher-order process that is 10^3 to 10^4 times weaker than $E(0)$ internal conversion and thus can be neglected. The concept of an $E0$ conversion coefficient is not useful since $\Gamma(E0)_\gamma = 0$. The $E(0)$ internal conversion transition probability is defined as

$$\Gamma(E0) = (\delta_0)^2 = \left[\frac{\langle I_f | M(E0) | I \rangle}{eR^2} \right]^2 (\Omega_{ic} + \Omega_\pi) \quad (2.71)$$

where Ω_{ic} and Ω_π are the electronic factors defined by Church and Weneser[CHU56] and are in units of s^{-1} . The other terms are the $E0$ matrix element, $\langle I_f | M(E0) | I \rangle$, the electron charge e , and nuclear radius which is taken to be $R = 1.2A^{1/3} fm$. The first term in equation 2.71 often is expressed in terms of the dimensionless parameter

$$\rho(E0) \equiv \frac{\langle I_f | M(E0) | I \rangle}{eR^2} \quad (2.72)$$

The electric monopole conversion term can be included in the cascade feeding equation 2.44 by including $\lambda = 0$ in the summation with the conversion coefficient $c(0) = 0$.

The National Nuclear Data Center, NNDC, at Brookhaven maintains an Evaluated Nuclear Structure Data File, ENSDF, that includes a new internal conversion coefficient database, called BrIcc[KIB08]. This database integrates a number of tabulations of internal conversion electron coefficients, ICC, and electron-positron pair conversion coefficients, IPC, as well as $\Omega(E0)$ electronic factors for $E(0)$ conversion. The user has the choice of selecting the ICC tables based on Dirac-Fock calculations, which use the "Frozen orbital" approximation, to take into account the effect of atomic vacancies created in the conversion process. The other possible option is to use ICC tables based on the no-hole approximation. The tables do not take into account the partial ionization and the influence of the highly excited atomic shells of the excited nuclear ion recoiling in vacuum. The recoil velocities encountered in heavy-ion Coulomb excitation, when performed at safe bombarding energy, produce only partial ionization and the decay times for the inner-bound atomic shells are three to four orders of magnitude shorter than the lifetimes of nuclear states for which internal conversion is important. Consequently the reduction of the internal conversion coefficients due to partial ionization and excitation of the atomic shells is expected to be small. The database tabulates coefficients calculated for all atomic shells, for transition energies between 1 – 6000keV, and for atomic numbers $5 < Z < 110$.

Gosia can be told to use the BrIcc database to determine the internal conversion coefficients for every transition for which a matrix element has been included in the Gosia input. Interpolation between tabulated

coefficients versus transition energy is performed using a cubic spline on a log-log basis separately for each atomic shell from $1keV$ above the threshold energy to $6000keV$. The individual atomic shell conversion coefficients are assumed to be zero below the threshold energy. The total conversion coefficient is obtained by summing all atomic shells. This approach avoids interpolation problems due to the discontinuities at the atomic binding energies for the total conversion coefficient.

The monotonic dependence on energy of the ICC coefficients can be significantly perturbed by atomic threshold and resonance effects in the region within the first keV above the threshold energy[LEE81]. Thus the BrIcc tables do not provide values within $1keV$ immediately above the threshold for the atomic shell involved. Gosia assumes that the conversion coefficient for that atomic shell is constant between threshold and threshold plus $1keV$. The BrIcc routine in Gosia gives a warning if any transition energy falls within $1keV$ above an atomic shell threshold to give the user the option to correct the ICC value provided by BrIcc.

2.4 Kinematics for inelastic scattering

This section reproduces the formulae [ALD75] necessary for handling inelastic scattering. Consider the centre-of-mass to laboratory transformation shown in Fig 4 reproduced from [ALD75]. Initially the target is assumed to be at rest and the projectile velocity is given by

$$v_i = \sqrt{\frac{2E_P}{m_P}}$$

where E_P is the incident bombarding energy.

2.4.1 Velocities:

The initial velocities in the lab frame are taken to be

$$\begin{aligned} w_P &= v_i \\ w_T &= 0 \end{aligned} \quad \text{(Initial Lab velocities)}$$

The final velocities in the lab frame after the inelastic collision are

$$\begin{aligned} w'_P \\ w'_T \end{aligned} \quad \text{(Final Lab velocities)}$$

In the centre of mass coordinate system the initial velocities are

$$\begin{aligned} u_P &= v_i \frac{m_T}{m_P + m_T} \\ u_T &= v_i \frac{m_P}{m_P + m_T} \end{aligned} \quad (2.73)$$

The final centre of mass velocities after the inelastic collision are

$$\begin{aligned} u'_P &= \frac{m_T}{m_P + m_T} \sqrt{\frac{2}{m_P} \check{E}} \\ u'_T &= \frac{m_P}{m_P + m_T} \sqrt{\frac{2}{m_P} \check{E}} \end{aligned} \quad (2.74)$$

Here the final kinetic energy is

$$\check{E} = E_P - \Delta E \left(1 + \frac{m_P}{m_T}\right) \quad (2.75)$$

and ΔE is the excitation energy of the excited state.

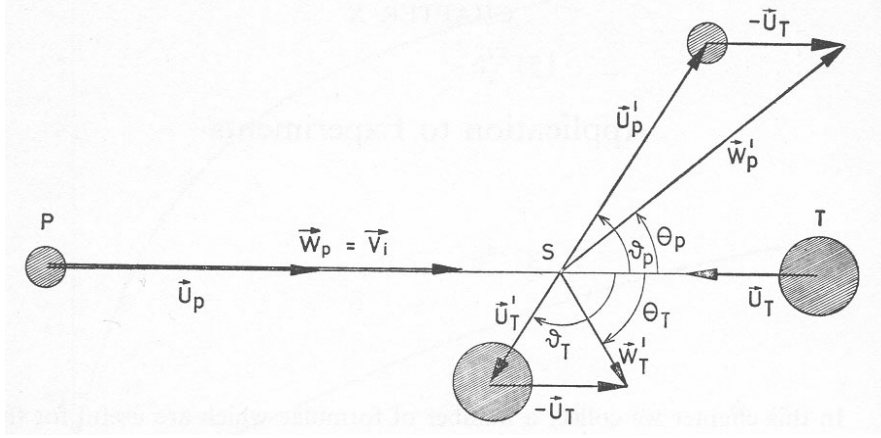


Figure 4: The velocities of the target and projectile before and after the collision. The velocities in the centre-of-mass system are denoted by \mathbf{u} and \mathbf{u}' respectively, while the velocities in the laboratory system are denoted by \mathbf{w} and \mathbf{w}' respectively. The indices P and T refer to projectile and target. [ALD66]

2.4.2 Angles:

The angles of the scattered recoils are written as

$$\begin{aligned} \theta_P & & \text{(Initial laboratory angles)} \\ \theta_T & \end{aligned}$$

and

$$\begin{aligned} \vartheta_P &= \vartheta & \text{(Final CM angles)} \\ \vartheta_T &= \pi - \vartheta \end{aligned}$$

where ϑ is the centre of mass scattering angle.

The angle relations between the lab and CM frames are connected by

$$\frac{\sin(\vartheta_P - \theta_P)}{\sin \theta_P} = \frac{m_P}{m_T} \sqrt{\frac{E_P}{\tilde{E}}} \equiv \tau \quad (2.76)$$

That is;

$$\tau = \frac{m_P}{m_T} \frac{1}{\sqrt{1 - \frac{\Delta E}{E_P} \left(1 + \frac{m_P}{m_T}\right)}} \quad (2.77)$$

Equation 2.76 can be rewritten as

$$\tan \theta_P = \frac{\sin \vartheta_P}{\cos \vartheta_P + \tau} \quad (2.78)$$

Note that for inverse kinematics $\tau > 1$ leading to a maximum scattering angle for the projectile given by

$$\sin \theta_{\max} = \frac{1}{\tau} \quad \text{(Maximum lab scattering angle for inverse kinematics)}$$

Another useful relation from equation 2.76 gives the centre of mass scattering angle in terms of the laboratory scattering angle.

$$\vartheta_P = \sin^{-1}(\tau \sin \theta_P) + \theta_P \quad (2.79)$$

This gives the difference in angle between the lab scattering angle and the centre of mass scattering angle. Be careful with this relation since ϑ_P is two-valued for inverse kinematics corresponding to the two possible signs for the solution.

The angle relations between the lab and centre-of-mass for the recoiling target nucleus are connected by

$$\frac{\sin(\vartheta_T - \theta_T)}{\sin \theta_T} = \sqrt{\frac{E_P}{\check{E}}} \equiv \bar{\tau} \quad (2.80)$$

Note that $\bar{\tau}$ is always larger than or equal to unity. For elastic scattering $\bar{\tau} = 1$ which gives that

$$\theta_T = \frac{1}{2}(\pi - \vartheta) \quad (\text{Recoil angle for elastic scattering})$$

For the target recoil equation 2.81 can be rewritten as

$$\tan \theta_T = \frac{\sin \vartheta_T}{\cos \vartheta_T + \bar{\tau}} \quad (\text{Target lab to CM angle conversion})$$

2.4.3 Solid angles:

The lab solid angles for the scattered projectile and target are taken to be $d\omega_P$ and $d\omega_T$ respectively, while the centre of mass solid angles are $d\Omega_P$ and $d\Omega_T$ respectively. The Jacobian relating the solid angles is

$$\frac{d\omega_P}{d\Omega_P} = \left(\frac{\sin \theta_P}{\sin \vartheta_P} \right)^2 |\cos(\vartheta_P - \theta_P)| \quad (2.81)$$

$$\frac{d\omega_T}{d\Omega_T} = \left(\frac{\sin \theta_T}{\sin \vartheta_T} \right)^2 |\cos(\vartheta_T - \theta_T)| \quad (2.82)$$

Recoil energies:

The laboratory recoil energies after the collision are given by

$$E'_P = \left(\frac{m_T}{m_P + m_T} \right)^2 (1 + \tau^2 + 2\tau \cos \vartheta_P) \check{E} \quad (2.83)$$

$$E'_T = \frac{m_T m_P}{(m_P + m_T)^2} (1 + \bar{\tau}^2 + 2\bar{\tau} \cos \vartheta_T) \check{E} \quad (2.84)$$

2.4.4 Gosia kinematics assumption:

The transformation between the laboratory and centre-of-mass angles are both excitation energy ΔE and beam energy E_P dependent; that is τ is a function of $\frac{\Delta E}{E_P}$ as shown in equation 2.78. For a given laboratory scattering angle the dependence of corresponding centre-of-mass scattering angle on excitation energy is small. For example it corresponds to a 0.035° shift in angle for a 1 MeV change in excitation energy for a 760 MeV beam of ^{178}Hf bombarding a ^{208}Pb target. However, this shift can be larger if a thick target leads to a large change in the beam energy. For simplicity Gosia makes the kinematic transformation for any beam energy assuming that the final state of the excited nucleus is the state specified by the *NCM* input in sub option *CONT*. The default value is *NCM* = 2 which usually corresponds to the first excited state.

2.5 Sources of Systematic Error

The following sources of systematic errors could influence the results extracted using Gosia for analysis of Coulomb excitation data..

a) Coulomb-nuclear interference

The basic assumption of Coulomb excitation is that the interaction is purely electromagnetic. It is crucial to know the maximum bombarding energy consistent with this assumption since multiple excitation of the highest spin members of collective bands requires use of the maximum allowed bombarding energies. Experimental data on the influence of Coulomb-nuclear interference effects on measurements of excited state static quadrupole moments provided an estimate of the maximum bombarding energy at which the influence of nuclear excitation can be neglected. These data suggest that for heavy ions the influence on the cross

sections is $< 0.1\%$ [CLI69a][CLI69b] if the classical distance of closest approach of the Rutherford trajectory for a head-on collision exceeds $[1.25(A_p^{1/3} + A_T^{1/3}) + 5]fm$. This classical safe bombarding energy criterion of Cline is only applicable if the semiclassical approximation is valid, and corresponds to bombarding energies below 4.5 MeV per nucleon for ^{208}Pb ions decreasing to less than 4.1 MeV per nucleon for ^{40}Ar ions. Coupled-channel Born Approximation codes, such as PTOLEMY[MA78, RH80], must be used for a more reliable estimate of the influence of Coulomb-nuclear interference for collisions involving nuclei lighter than ^{16}O . A comparison [KAV90] of PTOLEMY calculations with GOSIA predictions for Coulomb excitation of ^{76}Se by ^{208}Pb showed that at a bombarding energy 7% above the above safe bombarding-energy criterion resulted in destructive interference ranging in magnitude from 2% for the first 2^+ state to 10% for the weakly excited second 2^+ state.

b) Quantal Corrections

The accuracy of the semiclassical approximation improves with increase of the Sommerfeld parameter η defined in equation 2.1. The use of energy-symmetrized orbits in the semiclassical calculations partially corrects for deficiencies in the semiclassical approximation. The remaining quantal correction to the calculated cross sections are of the order of $1/\eta$ for large η . Typically η ranges from 50 to 500 for heavy-ion induced Coulomb excitation. Full quantal calculations by Kavka[KAV90] show that semiclassical calculations differ from full quantal predictions by typically 3%, with some values as much as 10% off. These agree with the predictions of Tolsma [TOL79] for the case of ^{238}U excited by 385 MeV ^{84}Kr ions. However, analysis of heavy-ion induced Coulomb excitation data typically involves a comparison of the deexcitation gamma-ray yields which tends to cancel part of this error[KAV90, STA82].

c) Corrections to the Rutherford orbit

The Coulomb excitation probability is sensitive to the exact distance of closest approach of the classical Rutherford trajectory both for states involving large adiabaticity excitation, and also for many-step multiple Coulomb excitation. The distance of closest approach is proportional to the bombarding energy, thus it is important to have an accurate knowledge of the absolute bombarding energy of the incident beam and a good measure of the energy loss in the target. Most accelerator facilities quote the bombarding energy to many significant digits, but it behoves the experimenter to ascertain what absolute reference was used to calibrate the absolute beam energy.

The classical Rutherford trajectory is perturbed slightly by atomic screening, vacuum polarization and relativistic effects. These effects slightly change the distance of closest approach which can be taken into account by making a small change in the bombarding energy used in the Gosia calculations. Since these effects are small, and tend to cancel, the net correction to the bombarding energy typically is $< 0.3\%$ which is unimportant for most experiments[ALD75, KAV90]

d) Virtual excitation of unobserved states

It is important to include explicitly, in the coupled-channel calculations, all states in the yrast domain that are likely to influence the results significantly. Unobserved states with excitation probabilities exceeding 0.1% can have measurable interference effects on the calculated population of observed states. Also the truncation of the coupled equations results in errors in the calculated cross section for the uppermost state in any collective band. Thus it is necessary to extend all collective bands by adding at least two buffer states beyond what is observed to ensure that virtual excitation and coupled-channel truncation effects are taken into account. The virtual excitation effects are reasonably insensitive to the exact excitation energies assumed for these unobserved states.

Moderate strength matrix elements coupling two nearly degenerate states can lead to appreciable effects even though there is no observable γ -ray deexcitation between them. Experience has shown that, in most nuclei, virtual excitation effects due to low-lying states can be estimated reliably and thus do not significantly add to the uncertainties in the final results.

Virtual excitation of the giant $E1$ resonance can decrease the population of high-spin states by up to 12% [CLI86]. Fortunately this can be estimated reliably by adding a polarization term to the interaction which is incorporated in GOSIA [ALD75].

e) Mutual excitation

Both the target and projectile can be excited simultaneously influencing the cross sections for Coulomb excitation of a given state. Normally one of the two interacting nuclei is chosen to be a closed-shell nucleus, such as ^{208}Pb , to minimize such mutual excitation effects. Fortunately the multipole-multipole interaction term does not interfere with either monopole-multipole term, thus the corrections are small even for cases

when mutual excitation is appreciable. For example, for the case of ^{76}Se excited by ^{48}Ti the predicted mutual excitation changes the ^{76}Se cross sections by only 0.7%. [KAV90]

f) Gamma-ray angular distributions

The hyperfine interaction of the excited nuclei recoiling in vacuum, that is the deorientation effect, contributes the largest uncertainty in predicting the angular distributions of the deexcitation γ -rays. The magnitude of the deorientation effect depends sensitively of the lifetimes of the deexciting states. Use of best-fit global parameters, within the framework of the Brenn and Spehl two-state model of the hyperfine interaction, has been shown to give a reasonable prediction of the deorientation effect [BOS77, BRE77]. Fortunately the uncertainty in our knowledge of the deorientation effect usually contributes less than a 2% error in the final extracted matrix elements, in part because the many γ -ray detectors used in modern γ -ray detector arrays average over the γ -ray angular distribution.

The assumption of cylindrical symmetry in evaluating the attenuation factors Q_λ , used to account for the finite size of the γ -ray detectors, is not applicable for clover-detector geometry used by some Ge detector arrays. However, use of the cylindrical symmetry assumption in general will introduce errors that are smaller than the uncertainties inherent in predicting the hyperfine interactions.

States having lifetimes in the nanosecond range can decay while displaced significantly from the target spot due to the recoil. In most cases the first-order correction for this effect available in Gosia is adequate to correct for this displacement.

g) Absolute normalization of cross sections

Comparison with the well-known Rutherford cross section for elastic scattering can be used to determine absolute Coulomb excitation cross sections. Although this approach is easy using the magnetic spectrometer technique [CLI69a], it is difficult when the higher sensitivity particle- γ coincidence method is employed for heavy-ion Coulomb excitation work [CLI86]. The γ -ray detection efficiency typically is measured to an accuracy of $\approx 5\%$ using well-known γ -ray sources. However, it is necessary to take into account the coincidence detection efficiency which can be significantly reduced due to dead time and pile up rejection. An extreme example is the Coulomb excitation of the ^{242}Am isomeric target where the target activity resulted in a coincidence detection efficiency that was reduced by about 20% due to dead time and pile-up rejection [HAY07].

Comparison of target-excitation with projectile-excitation γ -ray yields provides a simple approach for measuring relative $B(E\lambda)$ values in Coulomb excitation work. Another approach, that is applicable to strongly-deformed nuclei, is to normalize the measured deexcitation γ -ray yields to transitions at the bottom of the ground band which are populated predominantly by cascade feeding and thus are insensitive to the assumed matrix elements.

h) Rotational Invariants

Sufficient states must be included when evaluating the rotational invariants to ensure complete summing of the appropriate strength for the state of interest [CLI72, CLI86]. Agreement between the identities for different intermediate spin coupling provide one measure to ensure adequate completeness of the summations. Another is to ensure that an appropriate number of all multiphonon steps have been included. For example, the expectation values of Q^2 and $Q^3 \cos 3\delta$ involve summing strength to states having a change in oscillator number of $-1 \leq \Delta n \leq +1$. For invariants involving Q^4 it is necessary to sum over $-2 \leq \Delta n \leq +2$, while for the Q^6 invariants it is necessary to sum over $-3 \leq \Delta n \leq +3$. For conventional multiple Coulomb excitation this implies that $E2$ centroids can be evaluated for excited states up to one less than the highest observed complete oscillator shell, while the ground state is the only state for which a viable measure of the variance is achievable.

3 APPROXIMATE EVALUATION OF EXCITATION AMPLITUDES

Numerical integration of the system of differential equations 2.17, defining the excitation process, requires most of the computational effort needed to reproduce the experiment. Usually this takes 90 – 95% of the total computer time for each evaluation of the γ -yields following Coulomb excitation. Therefore, it is essential to replace the exact Coulomb excitation formalism by a fast and sufficiently accurate approximation in order to enable iterative fitting of matrix elements. To construct such an approximation, it is advantageous to consider only the couplings $\Delta m = 0$ and $\Delta m = \pm 1$ (as pointed out in Chapter 2, the strength of the interaction rapidly decreases with Δm) and magnetic excitation is negligible. Denoting the ω -dependence of the right-hand side operator of 2.17a by $f_{lm}(\omega)$ allows the system of differential equations 2.17a to be written as:

$$\frac{da_k}{d\omega} = \sum_{lmn} \zeta_{kn}^{(lm)} \cdot M_{kn}^{(1)} \cdot f_{lm}(\omega) a_n(\omega) \quad (3.1)$$

where $f_{lm}(\omega)$ is explicitly given is:

$$f_{lm}(\omega) = -iQ_{lm}(\omega) \exp[i\xi_{kn}(\varepsilon \sinh \omega + \omega)] \quad (3.2)$$

where

$$M_{kn}^{(1)} = \langle k || E(M)\lambda || n \rangle$$

For both $m = 0$ and $m = \pm 1$ the function $f_{lm}(\omega)$ can be expressed as a sum of two components, one antisymmetric in ω and real, the other symmetric in ω and imaginary:

$$f_{lm}(\omega) = f_{lm}^a(\omega) + i f_{lm}^s(\omega) \quad (3.3)$$

These properties of the $f(\omega)$ function assure the unitarity of the right hand side operator of 3.1. Significant simplifications of the Coulomb excitation formalism can be achieved by replacing the ω -dependent functions by constant effective interaction strengths extended only over finite ranges of ω . For the most important $\Delta m = 0$ couplings $f_{lm}^s(\omega)$ is localized around $\omega = 0$, while $f_{lm}^a(\omega)$ is negligible anywhere except the vicinity of $\pm\omega_0$, ω_0 being case-dependent. Following this observation, one can approximate the total interaction by assuming the effective, constant interaction strengths covering three regions completely separated in ω ; that is, an antisymmetric part, extended over a finite ω range around some value of $\omega = -\omega_0$, a symmetric part around $\omega = 0$, and the reflection of the antisymmetric part around $\omega = \omega_0$, as schematically presented in figure 5.

The $\Delta m = \pm 1$ couplings can be treated in a similar way, although the separation of symmetric and antisymmetric components in ω is not as pronounced in this case. Nevertheless, taking into account the weakness of these couplings and their second-order importance, it is not worthwhile to construct a more accurate approximation.

According to the above model, the system of differential equations describing the Coulomb excitation can be represented as three independent equations of the form:

$$\begin{aligned} \frac{d\bar{a}}{d\omega} &= A_1^* \bar{a}(\omega); & \bar{a}_o &= \bar{a}(-\infty) & -\omega_1 &\leq \omega \leq (-2\omega_o + \omega_1) \\ \frac{d\bar{a}}{d\omega} &= iA_2^* \bar{a}(\omega); & \bar{a}_o &= \bar{a}(-2\omega_o + \omega_1); & (-2\omega_o + \omega_1) &< \omega \leq (2\omega_o - \omega_1) \\ \frac{d\bar{a}}{d\omega} &= -A_1^* \bar{a}(\omega); & \bar{a}_o &= \bar{a}(2\omega_o - \omega_1); & (2\omega_o - \omega_1) &< \omega \leq \omega_1 \end{aligned} \quad (3.4)$$

where the matrix operators A^* result from replacing the functions f_{lm} of equation 3.2 with effective constants over specified ranges. The sequential set of equations 3.4 has an obvious solution:

$$\bar{a}(\infty) = \exp(-A_1) \exp(-A_2) \exp(A_1) \bar{a}(-\infty) \quad (3.5)$$

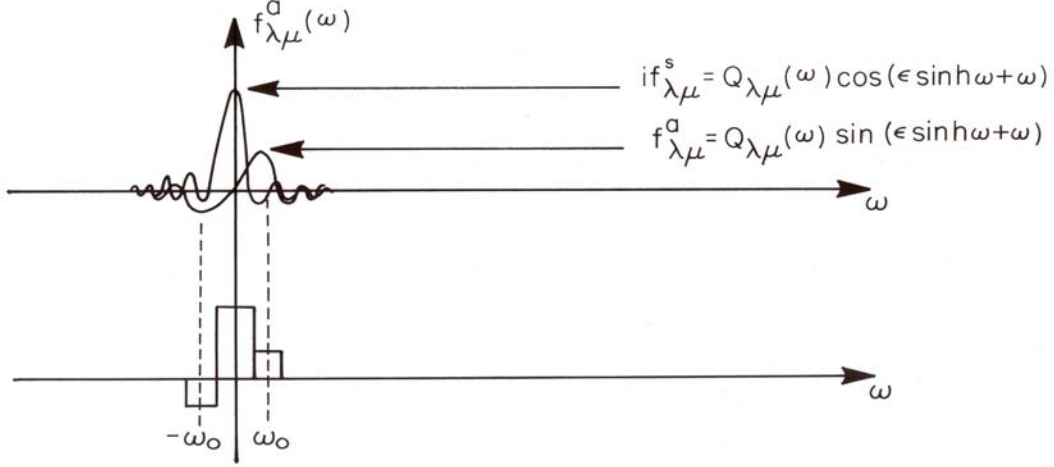


Figure 5: Actual and approximate Coulomb interaction strength functions.

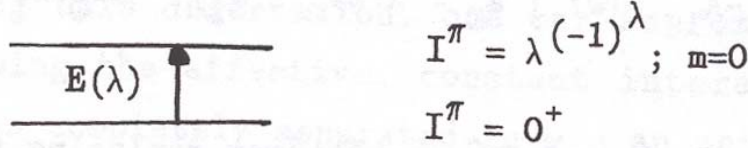


Figure 6: Two-level system

where the matrix operators A correspond to A^* in equation 3.4, differing only by appropriate scaling to eliminate the independent variable ranges from the final formula. The A matrices are purely real and fulfill the symmetry conditions:

$$A_{1ki} = -A_{1ik} \quad (3.6)$$

$$A_{2ki} = A_{2ik}$$

The relations 3.6, resulting from the symmetry properties of the reduced matrix elements and coupling coefficients ζ , assure the conservation of total excitation probability. The matrix elements of A can be explicitly written as:

$$A_{ik} = M_{ik}^{(\lambda)} \cdot \zeta_{ik}^{(\lambda m)} \cdot q_a^{(\lambda m)} \quad (3.7)$$

$$A_{2ik} = M_{ik}^{(\lambda)} \cdot \zeta_{ik}^{(\lambda m)} \cdot q_s^{(\lambda m)}$$

where $q_a^{(\lambda m)}$ and $q_s^{(\lambda m)}$ are effective strength parameters, replacing $f_{\lambda m}^{(a)}(\omega)$ and $f_{\lambda m}^{(s)}(\omega)$, respectively. These parameters are functions of ϵ and ξ , thus for a given experiment one needs to determine them as functions of ξ only, the eccentricity ϵ assumed constant.

The most flexible way of obtaining the q parameters is to extract them from the exact excitation calculation for a two-level system. Let us consider the simple case shown in figure 6:

with the reduced matrix element M connecting both levels. For this case, the A matrices are explicitly given as:

$$A_1 = \begin{pmatrix} 0 & -q_a^{(\lambda_0)} M\zeta \\ q_a^{(\lambda_0)} M\zeta & 0 \end{pmatrix} \quad (3.8)$$

$$A_2 = \begin{pmatrix} 0 & -q_s^{(\lambda_0)} M\zeta \\ q_s^{(\lambda_0)} M\zeta & 0 \end{pmatrix}$$

and, according to 3.5:

$$a(0^+) = \cos(q_s^{(\lambda_0)} M\zeta) + i \sin(q_s^{(\lambda_0)} M\zeta) \cdot \sin(2q_a^{(\lambda_0)} M\zeta) \quad (3.9)$$

$$a(I^\pi) = -i \sin(q_s^{(\lambda_0)} M\zeta) \cdot \cos(2q_a^{(\lambda_0)} M\zeta)$$

The above yields:

$$q_s^{(\lambda_0)} = \frac{\text{Arccos}(\text{Re } a(0^+))}{M\zeta} \quad (3.10)$$

$$q_a^{(\lambda_0)} = -\text{arctg} \left(\frac{\text{Im } a(0^+)}{\text{Im } a(I^\pi)} \right) / 2M\zeta$$

Using 3.10 it is possible to extract q parameters substituting the excitation amplitudes resulting from the exact calculation, i.e. the solution of 2.17. A similar procedure can be applied to find the q parameters corresponding to $\Delta m = \pm 1$ coupling.

The appropriate formula 3.5 works best in cases where the range of ξ -parameters is not excessively wide. This practically assures good performance in all cases of multiple Coulomb excitation, since, as discussed in Chapter 2, small values of ξ are required to produce significant multiple excitation. To demonstrate the reliability of the semianalytic approximation, let us consider a test case in which we simulate the Coulomb excitation of a $Z = 46$, $A = 110$ nucleus by a 200 MeV ^{58}Ni beam. The target nucleus is described by the level and coupling scheme (of course having nothing to do with the real ^{110}Pd) shown in Figure 7. The level energy differences all are assumed to be equal to 0.5 MeV. All reduced $E2$ matrix elements are given in units of $e.b.$

Comparison between the exact solution of Eq. 2.17 and the approximate solution using 3.5 is as follows:

Excitation amplitude (population)

Levels	Equation 2.17	Equation 3.5
0^+	.494 + .018i (.244)	.499 - .145i (.265)
2^+	.134 + .139i (.032)	.161 + .096i (.035)
4^+	-.205 + .391i (.194)	-.186 + .407i (.200)
6^+	-.176 + .388i (.145)	-.192 + .312i (.134)
2^+	.276 + .266i (.119)	.284 + .157i (.105)
4^+	-.482 - .165i (.260)	-.445 - .236i (.254)

The A matrix approximation is generally more than adequate to calculate derivatives of level populations with respect to the matrix elements, using internal correction factors (see chapter 4) to account for differences between the approximate and the exact approach. It also provides a useful tool to investigate (at least qualitatively) the Coulomb excitation process. As an example, let us consider the influence of the quadrupole moment for the two-level system shown in Figure 8 and discussed extensively in the Alder-Winther monograph [ALD75].

To simplify the notation, let us denote:

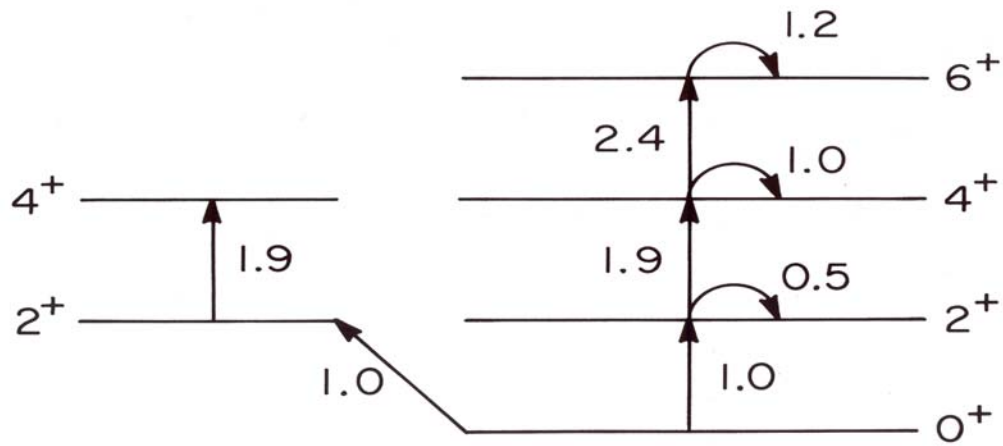


Figure 7: Model Coulomb excitation case for 200 MeV ^{56}Ni beam on $Z=46$, $A=110$ nucleus.

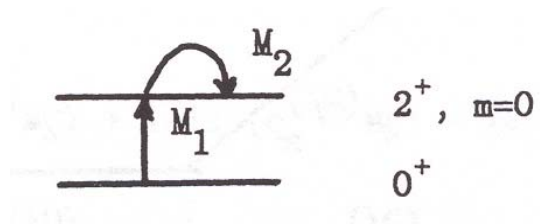


Figure 8: Reorientation effect for the two-level system

$$\begin{aligned}
q_s^{(20)}(0^+ \rightarrow 2^+) \cdot M_1 \zeta_{0+2^+}^{(20)} &= q \\
q_a^{(20)}(0^+ \rightarrow 2^+) \cdot M_1 \zeta_{0+2^+}^{(20)} &= q_1 \\
q_s^{(20)}(2^+ \rightarrow 2^+) \cdot M_2 \zeta_{2+2^+}^{(20)} &= Q
\end{aligned} \tag{3.11}$$

Note that there is no antisymmetric component of the interaction for the quadrupole moment, since $\zeta = 0$.

The A matrices can then be written as:

$$\begin{aligned}
A_1 &= \begin{pmatrix} 0 & -q_1 \\ q_1 & 0 \end{pmatrix} \\
A_2 &= \begin{pmatrix} 0 & q \\ q & Q \end{pmatrix}
\end{aligned} \tag{3.12}$$

yielding:

$$\begin{aligned}
\exp(\pm A_1) &= \begin{pmatrix} \cos q_1 & \mp \sin q_1 \\ \pm \sin q_1 & \cos q_1 \end{pmatrix} \\
\exp(-iA_2) &= e^{iQ/2} \begin{pmatrix} \cos p - \frac{1}{2}i\frac{Q}{p} \sin p & -\frac{iq}{p} \sin p \\ -\frac{iq}{p} \sin p & \cos p + \frac{1}{2}i\frac{Q}{p} \sin p \end{pmatrix}
\end{aligned} \tag{3.13}$$

where

$$p = \frac{1}{2}(Q^2 + 4q^2)^{1/2}$$

Using 3.5 gives:

$$a_{2^+} = \frac{1}{2} i e^{iQ/2} \frac{\sin p}{p} (Q \sin 2q_1 - 2q \cos 2q_1) \tag{3.14}$$

which results in an excitation probability:

$$P_{2^+} = \frac{1}{4} \frac{\sin^2 p}{p^2} (Q \sin 2q_1 - 2q \cos 2q_1)^2 \tag{3.15}$$

The formula 3.15 is a generalization of the second-order perturbation theory result. Taking into account only the lowest order terms in q , q_1 , q_1 and Q gives:

$$P_{2^+} \approx q^2 \left(1 - Q \cdot \frac{q_1}{q}\right)^2 \tag{3.16}$$

as predicted by second-order perturbation theory. It should be observed, that the influence of the quadrupole moment is significant only if the ratio of antisymmetric to symmetric q parameters is high, which physically corresponds to a large value of ξ . As can be seen from 3.14, the primary effect of the static moment is rotation of the complex excitation amplitude, due to the $\exp(iQ/2)$ factor. This allows rather accurate measurements of static moments in cases of interfering paths of excitation, i.e., when a state is excited in a comparable way via two or more sequences of couplings. In this situation the phases that the partial excitation amplitudes are summed are of primary importance.

In general, 3.10 is only a semianalytical formula, since for complex cases, exponents of the A matrices must be evaluated numerically. Nevertheless, numerical determination of $\exp(A)$ operators is much faster than the integration of a system of differential equations. Application of the A matrix approximation for fitting of matrix elements to reproduce experimental data will be discussed in some more detail in Chapter 4. It is worth observing that the truncation of Taylor series approximating the $\exp(A)$ operators provides a way to generate perturbation theory of a given order, thus being useful for investigating weak excitation processes.

4 NUMERICAL METHODS

The code GOSIA is designed to perform various functions defined by user-specified sequence of options. In the simplest mode, GOSIA can be used to calculate the excitation probabilities, population of the levels and γ -decay statistical tensors, equation 2.30, thus providing an equivalent of the code COULEX. Activating the γ -decay module of the code extends this type of calculation to obtain the γ yields for a single value of bombarding energy and scattering angle, as well as performing integration over specified ranges of the bombarding energy (due to the projectile energy loss in a target) and projectile scattering angle to reproduce real experimental conditions. These calculations require an input set of matrix elements treated as fixed data. The main purpose of GOSIA is, however, to fit the electromagnetic matrix elements to reproduce available experimental data. GOSIA can handle simultaneously experimental γ yields (up to 48000) observed in 50 independent experiments. Additional data, i.e. branching ratios (max. 50), lifetimes of the nuclear levels (max. 10), $E2/M1$ mixing ratios (max. 20) and previously measured $E\lambda$ matrix elements (max. 30) also may be included. All these data, and their experimental uncertainties, are used to construct a least-squares statistic, usually called χ^2 or penalty function. The minimum of this statistic, treated as a function of matrix elements, defines the solution, while its distribution in the vicinity of the minimum determines the errors of fitted matrix elements. In the present version of the code, the investigated nucleus is described by a maximum of 100 energy levels, with the number of magnetic substates not exceeding 1200. The levels may be coupled with up to 999 matrix elements ($E1$ through $E6$ and $M1$, $M2$), any number of them allowed to be declared as the variables to be fitted.

As mentioned before, direct use of the full Coulomb excitation formalism to perform the minimization is out of the question due to the computer time necessary for repeated calculations. The minimization can be accelerated using the approximation presented in Chapter 3. A significant amount of time also can be saved if the recoil-velocity correction (2.2.2) is neglected. The effect of both replacing the full excitation formalism by the matrix approximation and neglecting the relativistic correction is only weakly dependent on the matrix elements, therefore it is feasible to introduce the “correction factors“, that account for the differences between full and approximate calculations which are assumed to be independent of the fitted matrix elements. The minimization can be performed using only the fast, approximate formalism, with correction factors refreshed by running the full calculation periodically. In addition, the Coulomb excitation approximation is applied only to $\Delta m = 0$ and $\Delta m = \pm 1$ couplings, thus an effect of truncation of the number of magnetic substates being taken into account is also included in the correction factors, since this is not strongly dependent on the actual set of matrix elements.

Further acceleration of the fitting procedure is made possible by replacing the integration over experiment-dependent scattering angle and bombarding energy ranges with a single calculation of the Coulomb excitation induced γ yields assuming the mean values of the scattering angle and bombarding energy. This approximation also is not explicitly dependent on the fitted matrix elements, thus the difference between the integration procedure and the result of using the mean values of bombarding energy and scattering angle can be accounted for by introducing another set of correction factors, treated as constants. Actually, it is convenient to apply this correction to the experimental yields, i.e. to rescale the experimental data according to the comparison of integrated and “mean“ yields. This is done initially using a starting set of matrix elements and the resulting “corrected experimental yields“ are subsequently used as the experimental values for fitting (this procedure is presented in detail in Section 4.4). Thus, the fitting of matrix elements is performed using two levels of iteration - first, external, is to replace the experimental ranges of bombarding energy and scattering angle with the average values of these parameters, while second, internal, is the actual minimization of the least-squares statistic. After the convergence at the internal level is achieved, one should recalculate the correction to the experimental yields with the current set of matrix elements and repeat the minimization. Usually, for thin targets and a not excessively wide range of scattering angles, the second repetition of external iteration already yields negligible changes in the matrix elements found by the minimization. It has been checked, that even if no particle coincidences were required, only 2-3 recalculations on the external level were necessary despite the integration over the full solid angle.

Estimation of the errors of fitted matrix elements is a final step for the Coulomb excitation data analysis. This rather complicated procedure is discussed in Section 4.6. A Gosia subroutine OP,SELE (SELECT) has been written to reduce the considerable computational effort required for this task using the information obtained during minimization. This information, preprocessed by OP,SELE, is fed back to GOSIA. Option-

ally, the results of minimization and error runs can be used to evaluate quadrupole sum rules by a separate code SIGMA (Chapter 6).

The extraction of the matrix elements from experimental data requires many runs of GOSIA. During these runs, GOSIA creates and updates a number of disk files, containing the data needed to resume the analysis or to execute OP,SELE or SIGMA codes. The details of permanent file manipulation are presented in Chapter 7.

Relatively modest central memory requirements of GOSIA (about 1.5MB) are due to the sharing of the same memory locations by different variables when various options are executed and to replacing the straightforward multidimensional arrays (such as e.g. matrix elements) with catalogued vectors and associated logical modules. The description of the code given in this chapter therefore will not attempt to account for its internal organization, which is heavily dependent on the sequence of options executed and, in general, of no interest to the user. Instead, it will concentrate on the algorithms used and the logic employed in GOSIA. The basic knowledge of the algorithms is essential since the best methods of using the code are strongly case-dependent, so much freedom is left to the user to choose the most efficient configurations according to the current needs.

All three codes- GOSIA, SIGMA and SELECT- are written in the standard FORTRAN77 to make their implementation on various machines as easy as possible. The necessary modifications should only involve the output FORMAT statements, which are subject to some restrictions on different systems. Full 64 bit accuracy is strongly recommended since the results can be untrustworthy when run using 32 bit accuracy.

4.1 Coulomb Excitation Amplitudes and Statistical Tensors

The state of a Coulomb excited nucleus is fully described by the set of excitation amplitudes, $a_{IM}(M_0)$, defined by the solution of Eq. 2.17a at $\omega = \infty$, or, approximately, by the matrix expansion Eq. 3.5, used for minimization and error estimation. To set up the system of coupled-channel differential equations 2.17a it is necessary first to define the level scheme of an excited nucleus. Certainly, from a practical point of view, the level scheme should be truncated according to the experimental conditions in such a way that reasonable accuracy of the excitation amplitudes of the observed states is obtained with a minimum of the levels included in the calculation. As a rule of thumb, two levels above the highest observed state in each collective band should be taken into account to reproduce a given experiment reliably. Truncation of the level scheme at the last observed level leads to an overestimation of the excitation probability of this level due to the structure of the coupled-channels system 2.17a, while including additional levels above, even if their position is only approximately known, eliminates this effect.

The solution to the coupled-channels system 2.17a should, in principle, involve all magnetic substates of a given state $|I \rangle$, treated as independent states within a framework of the Coulomb excitation formalism. However, due to the approximate conservation of the magnetic quantum number in the coordinate system used to evaluate the Coulomb excitation amplitudes (as discussed in Chapter 2) it is practical to limit the number of the magnetic substates taken into account for each polarization of the ground state, M_0 . In any case, the excitation process follows the “main excitation path“, defined as a set of magnetic substates having the magnetic quantum number equal to M_0 , the remaining magnetic substates being of less and less importance as the difference between their magnetic quantum number and M_0 increases. The relative influence of the excitation of magnetic substates outside the main excitation path is experiment-dependent, therefore GOSIA allows the user to define the number of magnetic substates to be taken into account separately for each experiment. This choice should be based on the requested accuracy related to the quality of the experimental data, keeping in mind that reasonable truncation of the number of the magnetic substates involved in Coulomb excitation calculations directly reduces the size of the coupled channels problem to be solved.

The integration of the coupled differential equations 2.17a should be in theory carried over the infinite range of ω , which, practically, must be replaced with a finite range wide enough to assure the desired accuracy of the numerical solution. To relate the effect of truncating the ω -range to the maximum relative error of the absolute values of the excitation amplitudes, a_c , the following criterion is used to check that the integration of the collision functions is sufficiently accurate:

$$\frac{1}{4} \frac{\int_{-\infty}^{\infty} Q_{\lambda 0}(\epsilon = 1, \omega) d\omega - \int_{-\omega^{\max}}^{\omega^{\max}} Q_{\lambda 0}(\epsilon = 1, \omega) d\omega}{\int_{-\infty}^{\infty} Q_{\lambda 0}(\epsilon = 1, \omega) d\omega} \leq a_c \quad (4.1)$$

where, as a worst case, the backscattering geometry ($\epsilon = 1$) is taken into account, thus $\Delta m \neq 0$ couplings vanish for electric excitations. There is no magnetic excitation for backscattering, as discussed in Chapter 2, moreover, the magnetic excitation is weak enough to be neglected at the excitation stage for any scattering angle, therefore only electric excitation is considered in this criterion. The factor 1/4 is introduced in equation 4.1 to account for the further decrease of the importance of the excitation taking place at large $|\omega|$ due to the high-frequency oscillation introduced by the exponential term of equation 2.17a. Using the normalization property of the collision functions:

$$\int_{-\infty}^{\infty} Q_{\lambda \mu}(\epsilon = 1, \omega) d\omega = 1 \quad (4.2)$$

and the asymptotic, pure exponential form of collision functions for large $|\omega|$ one finally gets:

$$\omega^{\max} \geq \alpha_{\lambda} - \frac{1}{\lambda} \ln a_c \quad (4.3)$$

where the values of α_{λ} can be found from the asymptotic form of the collision functions and are given in the table below, together with the resulting ω^{\max} assuming $a_c = 10^{-5}$ which is the default value in GOSIA

Table 4.1

multipolarity	α_{λ}	ω^{\max} for $a_c = 10^{-5}$
E1/M2	-.693	10.82
E2/M3	.203	5.96
E3	.536	4.37
E4	.716	3.59
E5	.829	3.13
E6	.962	2.88

The range of integration over ω corresponding to a given accuracy level decreases with multipolarity, as can be seen in Table 4.1. Following this observation, the coupling between energy levels corresponding to a given multipolarity is included in GOSIA only within the integration range assigned to this multipolarity, which is a time-saving feature in cases many multipolarities have to be included. For $M\lambda$ couplings, neglected so far, the integration ranges have been set according to:

$$\omega^{\max}(M\lambda) = \omega^{\max}(E(\lambda + 1)) \quad (4.4)$$

The actual integration of the coupled-channel system of differential equations 2.17a is performed in GOSIA using the Adams-Moulton predictor-corrector method. According to this algorithm, first the predicted solution \bar{a} at $\omega + 4\Delta\omega$, based on a knowledge of the solution at $\omega + 3\Delta\omega$ and the derivatives \bar{a}' at four points, ω , $\omega + \Delta\omega$, $\omega + 2\Delta\omega$ and $\omega + 3\Delta\omega$ is found using:

$$\bar{a}(\omega + 4\Delta\omega) = \bar{a}(\omega + 3\Delta\omega) + \frac{\Delta\omega}{24} \{55\bar{a}'(\omega + 3\Delta\omega) - 59\bar{a}'(\omega + \Delta\omega) + 37\bar{a}'(\omega + \Delta\omega) - 9\bar{a}'(\omega)\} \quad (4.5)$$

and then corrected by:

$$\bar{a}(\omega + 4\Delta\omega) = \bar{a}(\omega + 6\Delta\omega) + \frac{\Delta\omega}{24} \{9\bar{a}'(\omega + 4\Delta\omega) + 19\bar{a}'(\omega + 3\Delta\omega) - 5\bar{a}'(\omega + 2\Delta\omega) + \bar{a}'(\omega + \Delta\omega)\} \quad (4.6)$$

where the excitation amplitudes are once again treated as a vector and the prime symbolically denotes the differentiation with respect to ω . The predicted solution is used to obtain the derivatives defined by the right-hand side of 2.17a at $\omega + 4\Delta\omega$, employed to evaluate the corrector 4.6. Step size, $\Delta\omega$, is controlled on a basis of

the comparison of the predicted and corrected solutions. The accuracy test parameter, d , is defined as 1/14 of the absolute value of the maximum difference between the predicted and corrected excitation amplitudes at a current value of ω . The stepsize is then halved if $d > a_c$ or doubled if $d < a_c/50$. This procedure assures the adjustment of the stepsize according to the strength of the interaction and is performed every n steps, n being an adjustable parameter defined by the user ($n = 1$ is used as a default in GOSIA). The Adams-Moulton integration algorithm, with stepsize control, usually is faster than Runge-Kutta type methods, thus it has been employed in GOSIA despite some drawbacks. The most important drawback is when the interaction, defined by the left-hand side of 2.17a, is weak over most of the integration range, peaking only around some value of the independent variable. In this case, the stepsize will be subsequently doubled and can become excessively large when the strong interaction region is reached, consequently, even though the loss of accuracy is detected, the overall accuracy of integration would be irretrievably lost. Note that convergence problems are more likely to occur for high excitation energy transitions, $> 2.5 MeV$ where the large adiabaticity parameter ξ_{kn} in equation 2.17a leads to a rapid oscillation relative to the stepsize $\Delta\omega$. Fortunately for these large adiabaticities the excitation probabilities are well below the experimental sensitivity of current experiments. The loss of accuracy for high adiabaticity transitions can be detected by checking the sum of excitation probabilities provided in the output of GOSIA. The recommended procedure if the sum of probabilities differs significantly from unity, is to switch off the stepsize control for a given experiment using the INT switch of CONT suboption (see V.3) rather than decrease the accuracy parameter a_c . This is due to the fact that GOSIA uses the table of Q_{lm} functions and hyperbolic functions with a tabulation step $\Delta\omega = 0.03$ which defines the minimum stepsize of the integration independent of the accuracy requested, allowing the highest accuracy corresponding to $a_c = 10^{-6}$. Moreover, changing the requested accuracy a_c may not solve the stepsize control problem, but result only in extending the integration range, thus making this problem more likely to occur.

Another drawback of the Adams-Moulton method, compared to the Runge-Kutta algorithms, is that Adams-Moulton algorithm is not self-starting, requiring the initial solutions at four points. This problem can be overcome by employing the Runge-Kutta algorithm to provide the starting values, then switching to the more efficient Adams-Moulton method (note that the same procedure is to be applied when the stepsize is changed, since restarting the integration with different stepsize requires the knowledge of the solution at new independent parameter intervals). The Runge-Kutta integration algorithm is used in the code COULEX to provide the starting solution for both the initialization of the integration and the changes of stepsize. In GOSIA the starting solutions are found using a first-order perturbation approach, valid at large values of ω , using the asymptotic form of the collision functions. It is assumed, that the ground state is connected to at least one excited state with $E1$, $M1$ or $E2$ matrix element. The initial excitation amplitudes then can be found as combinations of trigonometric and integral-trigonometric functions, the latter being evaluated using a rational approximation (given for example in [ABR72]). To fully eliminate switching to the Runge-Kutta algorithm, the new starting values, when changing the stepsize, are evaluated using backward interpolation. This procedure is reliable enough to assure reasonable accuracy while considerably speeding up the integration.

The integration of the system 2.17a in principle should be repeated for each possible polarization of the ground state, M_0 . However, the reflection symmetry in the plane of the orbit in the coordinate system used to evaluate the excitation amplitudes yields:

$$a_{Im}(M_o) = (-1)^{\Delta\pi + I_o - I} a_{I-m}(-M_o) \quad (4.7)$$

where $\Delta\pi = 0$ if there is no parity change between the ground state and a given excited state $|I\rangle$, and $\Delta\pi = 1$ otherwise. Using the symmetry relation 4.7 one only has to solve the coupled-channel system 2.17a for the ground state polarizations $M_0 \geq 0$, the solution of the coupled-channel system for $M_0 \leq 0$ being defined by the relation 4.7. As mentioned before, due to the approximate conservation of the magnetic quantum number in the frame of coordinates used, one practically has to take into account only a limited subset of magnetic substates beyond the main excitation path. This explicitly means that if n magnetic substates have been specified by the user to be included in the Coulomb excitation calculation, then for each excited state, I , and ground state polarization, M_0 , GOSIA will catalog the magnetic substates according to the inequality:

$$\min(I, -M_0 + n) \geq m \geq \max(-I, -M_0 - n) \quad (4.8)$$

which, by virtue of 4.7, defines simultaneously a set of excitation amplitudes obtained with the inverse polarization of the ground state in a range given by:

$$\max(-I, M_0 - n) \leq m \leq \min(I, M_0 + n) \quad (4.9)$$

allowing for the summation of excitation amplitudes to form a statistical tensor defined by 2.31 for $+M_0$ and $-M_0$ at the same time.

A special simplification of the solution of 2.17a occurs for the ground state spin equal to 0 (even-even nuclei). In this case only $m \leq 0$ substates are explicitly included for numerical integration, the values of the excitation amplitudes and their derivatives for $m \geq 0$ are substituted during the integration using 4.7. Therefore, a separate setup of the system of coupled-channels equations 2.17a is constructed by GOSIA for even-even nuclei, resulting in the appreciable increase of the speed of the integration if $I_0 = 0$.

The statistical tensors $\rho_{k\chi}$ are evaluated first according to 2.31 in the coordinate system used to calculate the excitation amplitudes, then rotated to a new system, more convenient to describe the γ -deexcitation, as discussed in Chapter 2. This transformation is done using the rotation matrices according to 2.40. Rotated statistical tensors are treated as an interface between the Coulomb excitation and γ -deexcitation modules of the code, providing the complete information needed to calculate the γ -decay. These tensors can be calculated either using the full Coulomb excitation formalism or using the fast matrix approximation.

4.2 Approximate Evaluation of the Coulomb excitation Amplitudes

The matrix approximation, equation 3.5, is used in GOSIA to evaluate the Coulomb excitation amplitudes within the minimization and error estimation modules. The level and matrix element scheme used for this procedure is identical to that employed for the full calculation, as presented in 4.1, with two exceptions. First, the number of magnetic substates taken into account beyond the main excitation path, n , can only assume values of 0 or 1. Second, only $E1$ through $E6$ multipolarities are used to construct the matrix approximation. The only additional information needed is the knowledge of the effective strength parameters, q_a and q_s , as introduced in the formula 3.7. The effective strength parameters depend on the experimental conditions as well as on the energy difference of the levels coupled by a given matrix element, and thus, in principle, should be assigned to every matrix element independently for each experiment. However, from a point of view of the memory requirements, this approach is not feasible, therefore it has been chosen to create the maps of q parameters at discrete ξ points for every experiment and to obtain the actual parameters using linear interpolation. The q parameters should be independent of the coupling strength ζ (2.17c) if the model were perfect, but practically some weak ζ dependence is still present. A significant improvement of the matrix approximation accuracy can thus be obtained by including the first-order ζ -dependence correction for the prevailing $\Delta m = 0$ couplings, which is equivalent to define the q -parameters as:

$$q(\Delta m = 0; \xi, \zeta) = a(\xi)M\zeta + b(\xi) \quad (4.10)$$

where M symbolically stands for a matrix element associated with a given coupling. The q parameters for $\Delta m = \pm 1$ couplings are still treated as functions of ξ only, the possible improvement of the approximation introduced by the ζ -dependent correction being negligible because of the weakness of these couplings.

The map of the q parameters is generated and stored when a separate option (5.14) is executed and read if either the minimization command (5.17) or the error estimation command (5.6) is encountered. For each experiment, GOSIA establishes the ranges of ξ and ζ according to the level scheme (the maximum decay energy defines the maximum value of ξ) and the specified limits of the matrix elements (5.16) which determine the maximum value of ζ . The q parameters are extracted following the method discussed in Chapter 3 (3.10) using the two-level system described using preset values of ζ and ξ . For each ξ meshpoint, fifty values of ζ , covering the whole range, are used to fit the coefficients a and b (4.10) by the usual linear regression ($\Delta m = 0$ only). Ten ξ meshpoints are used for all multipolarities, thus the map consists of ten pairs (a, b) for each multipolarity and experiment for both q_a and q_s corresponding to $\Delta m = 0$ couplings while the $\Delta m = \pm 1$ are treated as ζ -independent, therefore only the b coefficients are computed and stored.

The q parameters map, once generated, should not be recalculated unless the ranges of ξ or ζ were changed by including additional levels or couplings resulting in a higher maximum decay energy or by expanding the limits of the matrix elements. It is always recommended to keep these ranges at a reasonable

minimum, especially the range of ξ . This can be achieved by eliminating couplings between levels having no influence on both excitation and deexcitation, but creating high-energy decays. As a rule, the matrix approximation reliability improves with decreasing values of ξ , thus by narrowing its range one usually obtains faster convergence of the minimization.

The approximate excitation amplitudes are computed according to the formula 3.5, with A matrices defined by 3.7. An algorithm:

$$\begin{aligned}\bar{a}_p^{(0)} &= \bar{a}^{(0)} \\ \bar{a}_p^{(n+1)} &= \frac{1}{n+1} A \bar{a}_p^{(n)} \\ \bar{a}^{(n+1)} &= \bar{a}^{(n)} + \bar{a}_p^{(n+1)}\end{aligned}\tag{4.11}$$

equivalent to the Taylor series expansion, is used to evaluate iteratively the product of the matrix exponentials acting on the initial amplitude vector $\bar{a}=\bar{a}(\omega=-\infty)$. The convergence of this procedure is controlled by monitoring the sum of excitation probabilities and the evaluation of matrix exponentials is truncated if this sum differs from unity by less than user-specified accuracy. In some cases, the summation 4.11 may not converge within the requested accuracy due to the computer-dependent roundoff error propagation. This usually happens when the matrix elements of the A operators are large. To overcome this problem it may be necessary to logically subdivide the matrix operators using the identity:

$$\exp(A)\bar{a} = \exp\left(\frac{A}{2}\right)\exp\left(\frac{A}{2}\right)\bar{a}\tag{4.12}$$

which is done by GOSIA automatically, with the message:

EXP(A) EXPANSION FAILURE- EXP. N NEW SUBDIVISION(L,K)

issued, specifying experiment number N and number of times K the subdivision of either A_1 or A_2 operator ($L = 1$ or 2) was performed. Usually a single subdivision is sufficient to assure the default accuracy 10^{-5} for any Coulomb excitation experiment, thus more subdivisions probably points to unreasonable values of the matrix elements.

The matrix operators used for the fast approximation are sparse and are never stored as matrices. Instead, the expansion 4.11 is performed using the fact that non-zero elements of these operators correspond to the matrix elements as follows from 3.7, therefore the catalog of the matrix elements is used to avoid dummy multiplications. The resulting excitation amplitudes then are used to calculate the statistical tensors exactly like the solution of the full Coulomb excitation coupled channel calculation.

4.3 Calculation of the γ -ray Yields

The Coulomb excitation statistical tensors rotated into the coordinate frame, having the z -axis along the incoming beam direction and the x -axis in the scattering plane (Fig. 3), are the interface between the excitation and deexcitation modules of GOSIA. The deexcitation module, activated automatically if OP,YIEL (m) is encountered in the input stream, first establishes the decay scheme, common for all the experiments defined. The γ -decays are ordered ‘‘chronologically’’, i.e. from the highest to the lowest to take into account the effect of feeding. This has nothing to do with the user-defined sequence of the observed γ yields, which can be defined arbitrarily and will be assigned by the code to the proper decays on a basis of the initial and final state indices provided by the user in an experimental yields file (5.32). The initialization of the decay module involves the calculation of the $F_k(\lambda\lambda I_f I)$ coefficients for each decay (see Eq. 2.35) which are dependent neither on the matrix elements nor on the experimental conditions and can be stored to avoid recalculating them for each experiment and for each set of the matrix elements during the minimization. The same holds for the decay amplitudes, δ_λ , divided by the appropriate matrix elements (see Eq. 2.36). The evaluation of the γ yields then is first compared to the Coulomb excitation calculation, involving, for different experiments and matrix element sets, only the recalculation of the deorientation effect and the transformation of the Coulomb excitation statistical tensors to the decay statistical tensors, $R_{k\chi}$, including the feeding from above (2.43). The tensors $R_{k\chi}$ are calculated in the system of coordinates originating in

the decaying nucleus, as defined by Fig. 3, thus one has to transform them to the laboratory-fixed system. As long as the distance traveled by the decaying nucleus is negligible, this transformation consists of the relativistic velocity correction, outlined in Section 2.2.2. It should be noted, that this transformation is time-consuming and it is not performed when calculating the gradients used during minimization, its effect is absorbed into internal correction coefficients (4.5.3). Finally, using the symmetry properties of the decay tensors and the spherical harmonics, the double differential cross sections for the γ decay from a state I to a state I_f can be written in the purely real form as:

$$\frac{d^2\sigma(I \rightarrow I_f)}{d\Omega_p d\Omega_\gamma} = \sigma_R(\theta_p) \sum_{\substack{k \\ \chi \geq 0}} R_{k\chi}(I, I_f; \theta_p) P_{k\chi}(\theta_\gamma) (2 \cos \chi (\phi_p - \phi_\gamma) - \delta_{\chi 0}) \quad (4.13)$$

where $P_{k\chi}$ stands for the Legendre spherical function. It should be noted that Eq. 4.13 is given in the laboratory system of coordinates, differing from the scattering plane oriented system by the definition of the ϕ angle. The ϕ angle in the laboratory-fixed system of coordinates is given by the difference between the particle ϕ angle and the γ -ray ϕ angle, therefore the user-defined frame of coordinates is only restricted to have an origin corresponding to the position of the target and the z -axis along the beam direction, with the x and y axes defined arbitrarily. As long as all the angles are consistently given in the same frame of coordinates, then the definition of the angular distribution is unique.

The double-differential cross section, defined by 4.13, describes the angular distribution of γ rays assuming that the direction of observation is well-defined, i.e. the detector used can be treated as a point detector. The finite size of a γ detector results in the attenuation of the angular distribution, which can be taken into account by introducing the attenuation coefficients, Q_k , transforming the decay statistical tensors, $R_{k\chi}$, according to:

$$R_{k\chi} \rightarrow R_{k\chi} Q_k \quad (4.14)$$

The attenuation coefficients Q_k are generally dependent on the geometry of the γ detector, the γ -ray energy and the materials used for the γ -ray detection. It is assumed, that the decay γ -rays were detected using coaxial Germanium detectors, optionally equipped with a set of absorbers frequently used to attenuate unwanted X-rays and low energy γ -rays. Typically, such detectors are used to study discrete γ -ray spectroscopy. It is assumed that the Ge detectors have a symmetry axes that is aligned with the target, and the procedure outlined in Section 2.2.3 is used to evaluate the Q_k factors in GOSIA. The absorption coefficients data for Ge and most commonly used absorber materials - Al, Fe, Cu, Cd/Sn, Ta and Pb - are built into the code. The Q_k attenuation factors are γ -energy dependent, thus, as a compromise between the extensive storage and the necessity of recalculating them during each step of minimization or error calculation, a two-parameter fit of the γ -energy dependence is performed in a separate step and only the fitted parameters are stored on a permanent file read in by GOSIA prior to the first γ decay calculation. The fitted formula, which describes well the γ -energy dependence, is taken to be:

$$Q_k(E_\gamma) = \frac{C_2 Q_k(E_0) + C_1 (E_\gamma - E_0)^2}{C_2 + (E_\gamma - E_0)^2} \quad (4.15)$$

where $E_0 = 50 \text{ keV}$ with no graded absorbers or only a combination of Al, C, and Fe specified and $E_0 = 80, 100, \text{ or } 150 \text{ keV}$ if the Cd/Sn, Ta or Pb layers were employed as absorbers, respectively. The shift in “zero“ energy is intended to provide a smooth dependence above the highest absorption cutoff point. It is assumed, that the γ transitions of energies below the highest cutoff point are of no interest, therefore no attempt is made to fit this region. $Q_k(E_0)$ in 4.15 stands for the attenuation coefficient for the “zero“ energy calculated according to the prescription of 2.2.3., while C_1 and C_2 are fitted to reproduce the energy dependence obtained using this formalism.

To reproduce the experimentally observed γ -ray intensities for a given beam energy and scattering angle θ_p the double-differential cross sections, as defined by 4.13 including the γ -ray detector solid angle attenuation factors (4.14), should be integrated over the ϕ angle range defining the particle detector shape for this scattering angle (note that from a point of view of the Coulomb excitation, an independent experiment is defined only by the scattering angle and the bombarding energy for the same beam). Also, the solid angle factor, $\sin(\theta)$, where θ is the projectile or target laboratory scattering angle, dependent on which particle

has been detected, should be taken into account. The γ -ray decay intensities, referred to as “yields“, are therefore defined in GOSIA as:

$$Y((I \rightarrow I_f), \theta_p, E) = \sin(\theta_p) \int_{\phi_p} \frac{d^2\sigma(I \rightarrow I_f)}{d\Omega_\gamma d\Omega_p} d\phi_p \quad (4.16)$$

where the integrand is given by equation 4.13. The integration over the ϕ angle is trivial since the ϕ -dependence is analytical, described only by a single cosine function, as seen from equation 4.13. According to the input units requested by GOSIA (Section 5) the yields will be calculated in units of $mb/srad/rad$ (i.e. millibarns per steradian of the γ -ray solid angle per radian of the particle scattering angle). This holds for the γ yields calculated using OP,POIN (5.18). The reproduction of the experimentally observed yields should, however, involve the integration over the particle scattering angle including the beam energy loss in the target, thus the fully integrated yields, obtained using OP,INTG, have a different meaning, as described in Section 4.4.

So far, we have neglected the effect of the geometric displacement of the origin of the system of coordinates due to in-flight decay, i.e. it is assumed that all observed decays originate at the center of a target, thus the relativistic velocity correction is the only one needed to transform the nucleus-centered system to the laboratory-fixed system. This approximation is adequate as long as the mean lifetimes of the decaying states are in the subnanosecond range. For the cases involving longer-lived states, GOSIA provides an optional first-order treatment to correct for the geometric displacement. To treat this effect rigorously, one has to take into account both the change of the angles of the γ detectors, as seen by the decaying nucleus, and the change of the solid angles subtended by the detectors. For a given direction of the recoil the observed yield of the decay of a state having the decay constant λ can be written as:

$$Y = \lambda \int_0^\infty \exp(-\lambda t) \cdot S(t)Y(t)dt \quad (4.17)$$

where $S(t)$ denotes the time dependence of the solid angle factor, while $Y(t)$ stands for the time dependence of the “point“ angular distribution. To the lowest order, the product $S(t)Y(t)$ is expressed as:

$$S(t)Y(t) \approx Y(0) + pt \quad (4.18)$$

where p stands for the time derivative of this product taken at $t = 0$ (note that $S(0) = 1$, thus $S(0)Y(0) = Y(0)$). Inserting 4.18 into 4.17 and using the displacement distance, s , as an independent variable instead of time we finally obtain for mean lifetime τ :

$$Y = Y(0) + \tau p \quad (4.19)$$

where p is calculated numerically using a second set of yields evaluated in a point shifted by s in the recoil direction, i.e.:

$$p = \frac{S(s)Y(s) - Y(0)}{s} \quad (4.20)$$

where $S(s)$, is calculated assuming that the the displacement is small compared to the distance to the detector, r_0 ;

$$S(s) = \frac{r_0^2}{(\bar{r}_0 - \bar{s})^2} \quad (4.21)$$

The displacement correction requires the γ yields to be calculated twice for each evaluation, thus should be requested only when necessary to avoid slowing down the execution.

4.4 Integration over the Projectile scattering Angle and the Energy Loss in a Target - Correction of Experimental γ -ray Yields

The γ -decay formalism presented in Section 4.3 has so far assumed that the projectile scattering angle, θ_p , and the bombarding energy, E^L , are constant for a given experiment. An exact reproduction of the experimentally observed γ yields requires the integration over a finite scattering angle range and over the range of bombarding energies resulting from the projectile energy loss in a target.

For inverse kinematics, where $\frac{m_P}{m_T} > 1$, the projectile laboratory scattering angle is two valued and the Jacobean for the laboratory to centre-of-mass transformation is infinite at the maximum scattering θ_{\max} where

$$\sin \theta_{\max} = \frac{1}{\tau} \quad (\text{Maximum lab scattering angle for inverse kinematics})$$

and τ is given by equation 2.77. As a consequence, it is difficult to interpolate between laboratory scattering angle meshpoints needed to integrate over projectile scattering angle in the laboratory frame. This problem is avoided by performing the angle integration in the centre-of-mass scattering angle frame which is single valued and for which the angular dependence of the cross section is well behaved.

Rewriting equation 4.13 in the centre-of-mass frame gives

$$\frac{d^2\sigma(I \rightarrow I_f)}{d\Omega_p^{CM} d\Omega_\gamma} = \sigma_R^{CM}(\vartheta_p^{CM}) \sum_{\substack{k \\ \chi \geq 0}} R_{k\chi}(I, I_f; \vartheta_p^{CM}) P_{k\chi}(\theta_\gamma) (2 \cos \chi (\phi_p - \phi_\gamma) - \delta_{\chi 0}) \quad (4.22)$$

To integrate in the centre-of-mass system requires changing equation 4.16 to give the centre-of-mass "point" yields in terms of the the centre-of-mass angle ϑ_p^{CM} and laboratory frame bombarding energy, E^L ;

$$Y((I \rightarrow I_f), \vartheta_p^{CM}, E^L)_{CM} = \sin(\vartheta_p^{CM}) \int_{\phi_p} \frac{d^2\sigma(I \rightarrow I_f)}{d\Omega_p^{CM} d\Omega_\gamma} d\phi_p \quad (4.23)$$

Note that both the Rutherford cross section and the solid angle factor, $\sin\theta_p$, are already included in the definition of the "point" yields, as well as integration over the detected particle ϕ angle.

Using the centre-of-mass definition of the "point" yields (4.23), the angle-integrated yields at beam energy E given by:

$$Y_i((I \rightarrow I_f), E^L) = \int_{\vartheta_{p,lower}^{CM}}^{\vartheta_{p,upper}^{CM}} Y((I \rightarrow I_f), \vartheta_p^{CM}, E^L) d\vartheta_p^{CM} \quad (4.24)$$

The centre-of-mass angular limits are $\vartheta_{p,lower}^{CM}$ and $\vartheta_{p,upper}^{CM}$. Note that performing the angle integration of the centre-of-mass yields between two centre-of-mass angles is identical to integrating the corresponding laboratory frame yields as a function of laboratory scattering angle between corresponding angular limits in the laboratory frame.

Integrating the angle-integrated yields through the thickness of the target gives the total integrated yield $Y_i(I \rightarrow I_f)$

$$Y_i(I \rightarrow I_f) = \int_{E_{\min}^L}^{E_{\max}^L} \frac{Y_i((I \rightarrow I_f), E^L)}{\left(\frac{dE}{dx}\right)} dE^L \quad (4.25)$$

The $Y_i(I \rightarrow I_f)$ are the γ -ray yields that are fit to the experimental yields.

In some experiments the absolute integrated γ -particle yields are normalized to the Rutherford scattering yield. Thus the elastic scattering yield also is evaluated by integrating over the centre-of-mass "point" elastic yields

$$Y_{Elastic}(\vartheta_p^{CM}, E) = \sin(\vartheta_p^{CM}) \int_{\phi_p} \sigma_R(\vartheta_p^{CM}) d\phi_p \quad (4.26)$$

Integrating these over centre-of-mass scattering angle gives

$$Y_{Elastic}(E^L) = \int_{\vartheta_{p,lower}^{CM}}^{\vartheta_{p,upper}^{CM}} Y_{Elastic}(\vartheta_p^{CM}, E^L) d\vartheta_p^{CM} \quad (4.27)$$

Integration over energy loss in the target gives

$$Y_{Elastic} = \int_{E_{\min}^L}^{E_{\max}^L} \frac{Y_{Elastic}(E^L)}{\left(\frac{dE}{dx}\right)} dE^L \quad (4.28)$$

This is the elastic yield used for absolute normalization. Note that dead time, pileup rejection, and pulse-height dependence of the time resolution can lead to substantial loss of $p - \gamma$ coincidence efficiency.

The electronic stopping powers, dE/dx , in units of $MeV/(mg/cm^2)$, are defined by a user-specified table assuming common energy meshpoints for all experiments. The actual values of the stopping powers are obtained using spline interpolation. The double integral is then evaluated numerically using the discrete Simpson method. GOSIA performs the integration in two separate steps - first, the full Coulomb excitation coupled-channel calculation is done at each of the user-specified (θ_p, E) meshpoints to evaluate the “point“ γ -yields, next, the actual numerical integration is performed according to the user-defined stepsizes in both dimensions. The “point“ yields at the (θ_p, E) points as required by the fixed subdivisions are evaluated from the meshpoint values by logarithmic scale interpolation using the cubic spline subroutines SPLINE and SPLINT [PRE92]. The $\theta_p - E$ mesh is limited to a maximum of 100×100 points, while up to 100 steps in angle and 100 steps in energy can be defined for subdivisions in the integration. Do not use Lagrangian interpolation since it usually diverges with more than 20 mesh points for either θ_p or E . Subdivision of the calculated mesh improves the accuracy of integration, since spline interpolation provides the information of the order dependence on the number of meshpoints, while the Simpson method is a fixed second-order algorithm. In addition, in cases for which the $\phi_p(\theta_p)$ dependence is complicated, such as for the large area particle detectors where kinematic and mechanical constraints may create complicated shapes, the user may optionally choose to input this dependence at the subdivision meshpoints. The interpolation is then performed between the values divided by ϕ_p ranges to assure continuity, then the user-given dependence is used to estimate the yields at the subdivision meshpoints. The calculation of yields at the meshpoints requires the full coupled-channel Coulomb excitation calculation which is time-consuming. Consequently, one should balance the number of meshpoints needed with the required accuracy.

The integrated yields are calculated in units of mb/sterad times the target thickness (mg/cm^2), which for thick targets, could be assumed to be the projectile range in the target.

The integration module of GOSIA is almost exclusively used in conjunction with the correction module, invoked by the OP,CORR command (5.4), used to transform the actual experimentally-observed yields to the ones to which the subsequent fit of the matrix elements will be made. This operation is done to avoid the time-consuming integration while fitting the matrix elements and is treated as an external level of iteration. An effect of the finite scattering angle and bombarding energy ranges as compared to the “point“ values of the yields is not explicitly dependent on the matrix elements, thus the fit can be done to the “point“ values and then the integration/correction procedure can be repeated and the fit refined until the convergence is achieved. Usually no more than two integration/correction steps are necessary to obtain the final solution, even in case of the experiments performed without the particle- γ coincidences, covering the full particle solid angle. The correction module of GOSIA uses both the integrated yields and the “point“ yields calculated at the mean scattering angle and bombarding energy, as defined in the EXPT (5.8) input, to transform the actual experimental yields according to:

$$Y_{\text{exp}}^c(I \rightarrow I_f) = Y_{\text{exp}}(I \rightarrow I_f) \frac{Y_{\text{point}}(I \rightarrow I_f)}{Y_{\text{int}}(I \rightarrow I_f)} \quad (4.29)$$

where the superscript “c“ stands for the “corrected“ value.

To offset the numerical factor resulting from the energy-loss integration the lowermost yield observed in a γ -detector labeled as #1 for the first experiment defined in the EXPT input is renormalized in such a way that the corrected and actually observed yield are equal. This can be done because the knowledge of the absolute cross-section is not required by GOSIA, therefore, no matter how the relative cross-sections for the various experiments are defined, there is always at least one arbitrary normalization factor for the whole set of experiments. This normalization factor is fitted by GOSIA together with the matrix elements, as discussed in the following section (4.5). The renormalization procedure results in the “corrected“ yields being as close as possible to the original values if the same target has been used for the whole set of the experiments analyzed, thus the energy-loss factor in the integration procedure is similar for the whole set of the experiments. However, one should be aware of the fact, that the correction factors may differ significantly for different experiments, thus the corrected yields, normalized to a user-specified transition, always given in the GOSIA output, should be used to confirm that the result is reasonable rather than absolute values.

4.5 Minimization

The minimization, i.e. fitting the matrix elements to the experimental data by finding a minimum of the least-squares statistic is the most time-consuming stage of Coulomb excitation analysis. A simultaneous fit of a large number of unknown parameters (matrix elements) having in general very different influences on the data, is a complex task, which, to whatever extent algorithmized, still can be slowed down or speeded up dependent on the way it is performed. GOSIA allows much freedom for the user to define a preferred strategy of the minimization. A proper use of the steering parameters of the minimization procedure can significantly improve the efficiency of fitting dependent on the case analyzed - in short, it still takes a physicist to get the results! The following overview of the fitting methods used by GOSIA is intended to provide some ideas about how to use them in the most efficient way.

4.5.1 Definition of the Least-square Statistic

A set of the matrix elements best reproducing the experimental data is found by requesting the minimum of the least-squares statistic, $S(\bar{M})$. The matrix elements will be treated as a vector ordered according to the user-defined sequence. The statistic S is in fact a usual χ^2 -type function, except for the normalization to the number of data points rather than the number of degrees of freedom which cannot be defined due to a very different sensitivity of the excitation/deexcitation process to various matrix elements, as discussed in more detail in Section 4.6. The statistic S , called CHISQ in the output from GOSIA, is explicitly given by:

$$S(\bar{M}) = \frac{1}{N} \left(S_y + S_1 + \sum_i w_i S_i \right) \quad (4.30)$$

where N is the total number of data points (including experimental yields, branching ratios, lifetimes, mixing ratios and known E2 matrix elements) and S_y , S_1 and S_i are the components resulting from various subsets of the data, as defined below. Symbol w_i stands for the weight ascribed to a given subset of data.

The contribution S_y to the total S function from the measured γ -yields following the Coulomb excitation, is defined as:

$$S_y = \sum_{I_e I_d} w_{I_e I_d} \sum_{k(I_e, I_d)} \frac{1}{\sigma_k^2} (C_{I_e I_d} Y_k^c - Y_k^e)^2 \quad (4.31)$$

where the summations extend over all experiments (I_e), γ -detectors (I_d) and experiment- as well as detector-dependent observed γ -yields, indexed by k . The weights ascribed to the various subsets of data ($w_{I_e I_d}$) can be chosen independently for each experiment and γ -detector, facilitating the handling of data during the minimization (particularly, some subsets can be excluded by using a zero weight without modifying the input data). The superscript “c” denotes calculated yields, while the superscript “e” stands for experimental data, with σ_k being the experimental errors. The coefficients $C_{I_e I_d}$ are the normalization factors, connecting calculated and experimental yields (see 4.5.2).

The next term S_1 of equation 4.30 is an “observation limit” term, intended to prevent the minimization procedure from finding physically unreasonable solutions producing γ -ray transitions which should be, but have not been, observed. An experiment and detector dependent observation upper limit, $u(I_e, I_d)$ is introduced, which is the ratio of the lowest observable intensity to that of the user-specified normalization transition (see 5.31). S_1 is defined as:

$$S_1 = \sum_j \left(\frac{Y_j^c(I_e, I_d)}{Y_n^c(I_e, I_d)} - u(I_e, I) \right)^2 \cdot \frac{1}{u^2(I_e, I_d)} \quad (4.32)$$

the summation extending over the calculated γ transitions not defined as experimentally observed and covering the whole set of the experiments and γ -detectors defined, provided that the upper limit has been exceeded for a given transition. The terms added to S_1 are not counted as data points, thus the normalization factor N is not increased to avoid the situation in which the fit could be improved by creating unreasonable transition intensities at the expense of the normalization factor.

The remaining terms of 4.24 account for the spectroscopic data available, namely branching ratios, mean lifetimes, $E2/M1$ mixing ratios and known E2 matrix elements. Each S_i term can be written as:

$$S_i = \sum_{n_i} (d_{n_i}^c - d_{n_i}^e)^2 \cdot \frac{1}{\sigma_{n_i}^2} \quad (4.33)$$

where the summation extends over all the spectroscopic data included in the input to GOSIA, d and σ being the data points and their errors, respectively. In case of the known E2 matrix elements, the absolute values of the transitional matrix elements are used (since usually only the B(E2) values are known), while the diagonal matrix elements are taken including the sign. The user-defined weights, w_i , common for a given group of data, once again provide an easy way of manipulating the spectroscopic information according to the current needs without modifying the input.

The least-squares statistic S is used to determine a set of the matrix elements fitted to the experimental data as well as to ascribe the errors of the fitted matrix elements, which are defined by the shape of the S hypersurface in the space of the matrix elements (see Section 4.6).

4.5.2 Normalization Constants

To relate the calculated and experimental yields it is necessary to introduce the normalization constants, treated as an additional set of parameters (it is assumed that the experiments are conducted without total flux measurement, which would provide the required normalization). An alternate approach would be to fit the yields normalized to the intensity of a specified transition. Such an approach, however, has severe drawbacks, namely the increased uncertainties to be ascribed to the data, elimination of one data point for each γ detector and, last but not least, a danger of obtaining a wrong result if, for some reason, the transition chosen for the normalization was incorrect (being, for example, an unresolved doublet with an unknown component).

The number of the unknown normalization constants can be reduced appreciably by using the fixed relative γ -ray detector efficiencies, known from the measured γ -ray detector efficiency calibration, after correction for the γ -energy dependence. This reduces the number of fitted normalization constants to one per experiment, instead of one per γ detector. A further reduction is possible if a set of experiments resulted from dividing the data, acquired during a single physical run, into scattering angle slices, as in the case of experiments conducted using position-sensitive particle detectors. By monitoring the singles (i.e. the events for which the detection of the γ -ray is not required) one obtains the relative normalization for various scattering angle slices, which includes the Rutherford cross section, the solid angle factor and the particle detector efficiency. GOSIA provides an option to “couple“ such sets of experiments by including the relative normalization of various experiments in the relative normalization of the γ detectors. The relative normalization between the experiments should be given as the ratio of singles divided by the mean particle ϕ and θ ranges for an appropriate slice. As an example, let us consider a “physical“ experiment, conducted using a position-sensitive particle detector and three γ -ray detectors. The full range of the scattering angle was logically divided into two slices, subtending the mean ranges $(\Delta\theta_1, \Delta\phi_1)$ and $(\Delta\theta_2, \Delta\phi_2)$, respectively. Assuming that monitoring the singles yielded N_1 events for “logical“ experiment 1, and N_2 events for “logical“ experiment 2, one can find the relative normalization of experiment 2 with respect to experiment 1 as:

$$C(2 : 1) = \frac{N_2 \Delta\phi_1 \Delta\theta_1}{N_1 \Delta\phi_2 \Delta\theta_2} \quad (4.34)$$

Assuming the intensities of a calibration peak in three γ detectors used were I_1, I_2 and I_3 , respectively, one can finally specify the relative normalization of these detectors for both coupled experiments as:

$$I_1, I_2, I_3 \quad (\text{Experiment 1})$$

$$C(2 : 1)I_1, C(2 : 1)I_2, C(2 : 1)I_3 \quad (\text{Experiment 2})$$

Note that all six values can be arbitrarily rescaled, because of the remaining single absolute normalization factor to be fitted by the code. For example all six can be divided by I_1 to have unity for the first γ -ray detector in experiment 1, the remaining values then being relative to this detector. Finally, GOSIA provides the possibility of treating all the γ -ray detectors as independent, in which case the user-specified normalization constants become redundant, since the fit is done to each γ detector independently.

The fitted absolute normalization constants are found by requesting that:

$$\sum_k (CC_k Y_k^c - Y_k^e)^2 / \sigma_k^2 = \min \quad (4.35)$$

where the summation extends over all yields belonging to the subsets of data coupled by the relative normalization constants, C_k . Equation 4.35 leads to:

$$C = \frac{\sum_k C_k Y_k^c Y_k^e / \sigma_k^2}{\sum_k C_k^2 (Y_k^c)^2 / \sigma_k^2} \quad (4.36)$$

The procedure of finding the normalization constants for all the coupled subsets of data is repeated in GOSIA each time the S function is evaluated, which means that the changes in normalization constants are included on the same basis as the changes of the matrix elements while searching for the minimum of S and the errors of resulting matrix elements.

4.5.3 Internal Correction Coefficients

Replacing the coupled-channel Coulomb excitation calculation by the semianalytic approximation (see Chapter 3 and Section 4.2) makes it possible to speed up the calculations so that the fitting of the matrix elements becomes feasible. Both the minimization procedure and the error evaluation procedure normally use the approximate excitation calculation mode. To improve the accuracy of this approximation (involving for excitation, the replacement of the coupled-channel calculation by the fast approximation as well as simultaneous truncation of the number of magnetic substates taken into account, and, for deexcitation, neglect of the time-consuming relativistic coordinate system transformation plus integration over scattering solid angle) the internal correction factors, correcting the effect of the approximations made, are introduced according to:

$$c_k = \frac{Y_k^c(\text{full})}{Y_k^c(\text{appr.})} \quad (4.37)$$

The correction factors c_k , calculated and stored for all experimentally observed γ -ray transitions, multiply the approximate values of the γ -ray yields. A multiplicative correction factor has been chosen to assure that the correction factors remain relatively constant (i.e. independent of the matrix elements) in the vicinity of a set of matrix elements used to evaluate them. As could be expected, the discrepancy between full and approximate calculations is most prominent for the uppermost levels, due to error propagation. The excitation probability of the uppermost levels, however, depends mostly on a single product of squares of matrix elements connecting these levels to the ground state. It is observed that in such a case the correction factors depend little on the actual values of the matrix elements, no matter how much the correction factors differ from unity.

The internal correction factors translate the γ -ray yields resulting from the approximate calculation to the ones resulting from the full calculation for a fixed set of the matrix elements. However, since the dependence of the correction factors on matrix elements is weak, it can be assumed that the correction is valid locally in the neighbourhood of the point of origin, understood as the set of matrix elements used to evaluate the correction factors. The correction factors should be refreshed in the course of minimization dependent on how much the current set of matrix elements has changed compared to the point of origin. To decide when to recalculate the internal correction factors GOSIA uses an S -function decrease criterion, i.e. the correction factors are refreshed every time the value of S drops by an user-specified factor compared to its value at which the last recalculation took place. This minimizes time-consuming recalculations of the correction factors while still far from minimum (by requesting the recalculation only when the value of S has dropped significantly) and to gradually increase the accuracy by changing the S -drop criterion while approaching the final solution.

The internal correction factors are not evaluated for unobserved γ -ray transitions, thus it is possible that, if the cumulative error due to the approximations used is significant, some of the calculated unobserved transitions may exceed the upper limits given by the user, contributing to the least-squares statistic S . GOSIA issues a warning pointing out all the γ -ray transitions (resulting from the approximate calculation)

that exceed the upper limits. The comparison of the calculated and experimental yields, given by default following the completion of the minimization and obtained using the full calculation, allows detection of transitions that are significantly too strong due to the deficiency in the approximation used. Then it is recommended that such transitions be included as experimentally observed data, with large errors ascribed, to force the code to include them in the correction factors table.

4.5.4 Steepest Descent Minimization

Choice of the minimization strategy is dependent on specific characteristics of the function to be minimized. While it is possible generally to tailor the strategy for the case where the function to be minimized can be expressed analytically, the multidimensional search for a minimum of a function that can only be evaluated numerically - which is a case of the multiple Coulomb excitation analysis - cannot be fully algorithmized to provide a universal optimum strategy. Thus the minimization procedure should leave much room for user intervention, based on both intuition and understanding of the processes being analyzed. The most commonly used minimization strategies - simplex, variable metric and gradient algorithms- perform better or worse dependent on the case. In our case, the simplex-type methods are not useable, because the exact calculation is replaced by the fast approximation. Correction factors, only valid locally, are introduced, thus the construction of a simplex involving points far from the matrix element set used for evaluating the correction factors, is not reliable. In turn, the variable metric method, based on an exact solution of the second-order approximation to the S function, is efficient only if the second-order approximation is justified within a wide range of the parameters, which is usually not true for the Coulomb excitation analysis. In addition, the variable metric method requires that a second derivative matrix is calculated and stored, thus extending both the computing time and the central memory requirements to perform a single step of minimization without much improvement compared to the steepest descent method, discussed below if the function is far from quadratic. Considering the above, the gradient methods are the only approach suitable for fitting large sets of matrix elements to the Coulomb excitation data. GOSIA offers two gradient-type methods which can be chosen by the user dependent on the case being analyzed - a simple steepest descent minimization, outlined below, and a gradient+derivative method, described in Section 4.5.5. A version that uses the annealing technique has been developed for special applications [IBB95]

The steepest descent method is one of the most commonly used methods of minimization based on the local behaviour of the function to be minimized. Assuming local validity of a first-order Taylor expansion around the central set of arguments, \bar{x}_0 , any function can be approximated as:

$$f(\bar{x}) = f(\bar{x}_0) + \bar{\nabla}_0 \Delta \bar{x} + \dots \quad (4.38)$$

with $\bar{\nabla}_0$ being a gradient, i.e. a vector of derivatives calculated at the point \bar{x}_0 , explicitly defined as:

$$\bar{\nabla}_{0,i} = \frac{\delta f}{\delta x_i} \quad (4.39)$$

The steepest descent method is based on a simple observation that the local decrease of the function to be minimized, f , is maximized if the change of the vector of the parameters, $\Delta \bar{x}$, is antiparallel to the gradient. As long as a minimized function is not multivalued and does not have saddle points, a simple iteration scheme:

$$\bar{x} \rightarrow \bar{x} - h \bar{\nabla} \quad (4.40)$$

provides a safe and efficient way to minimize a function using the gradient evaluated at each successive point \bar{x} . The stepsize, h , must be found by performing one-dimensional minimization along the direction antiparallel to the gradient. Assuming the locally quadratic behaviour of the function f , the value of h is expressed by:

$$h = \frac{\bar{\nabla}^2}{\bar{\nabla} J \bar{\nabla}} \quad (4.41)$$

where J is the matrix of second derivatives of f with respect to \bar{x} i.e.:

$$J_{ik} = \frac{\delta^2 f}{\delta x_i \delta x_k} \quad (4.42)$$

However, estimation of the stepsize according to equation 4.41 is out of question, since the second-derivative matrix is never calculated in GOSIA and, moreover, the assumption of local quadraticity is in general not valid. Instead, an iterative procedure is used to find a minimum along the direction defined by the gradient, based on a well known Newton-Raphson algorithm for finding the zeros of arbitrary functions. A search for a minimum of a function is equivalent to finding a zero of its first derivative with respect to the stepsize h , according to the second-order iterative scheme:

$$h \rightarrow h - \frac{\frac{\delta f}{\delta h}}{\frac{\delta^2 f}{\delta h^2}} \quad (4.43)$$

which can be repeated until the requested convergence is achieved, unless the second derivative of f with respect to h is negative, which implies that the quadratic approximation cannot be applied even locally. In such a case, the minimized function is sampled stepwise until the Newton-Raphson method becomes applicable when close enough to the minimum along the direction of the gradient. One-dimensional minimization is stopped when the absolute value of the difference between two subsequent vectors of parameters is less than the user-specified convergence criterion.

The gradients in GOSIA are evaluated numerically, using the forward-difference formula or, optionally, the forward-backward approximation. While the forward difference formula

$$\frac{\delta f}{\delta x_i} = \frac{f(x_1, x_2, \dots, x_i + h, \dots) - f(x_1, x_2, \dots, x_i, \dots)}{h} \quad (4.44)$$

requires only one calculation of the minimized function per parameter, in addition to the evaluation of the central value $f(x_1, x_2, \dots, x_n)$, the forward-backward formula

$$\frac{\delta f}{\delta x_i} = \frac{f(x_1, x_2, \dots, x_i + h, \dots) - f(x_1, x_2, \dots, x_i - h, \dots)}{2h} \quad (4.45)$$

requires two calculations of the minimized function per parameter. The forward-backward formula then should be requested only in the vicinity of the minimum, where the accuracy of the numerical calculations starts to play an important role.

4.5.5 Gradient + Derivative Minimization

The steepest descent minimization is efficient if a minimized function is smooth in the space of parameters, but it exhibits considerable drawbacks when dealing with functions having sharp “valleys“ superimposed on smooth surfaces. Such valleys are created by strong correlations of two or more parameters. In the case of Coulomb excitation analysis, the valleys are introduced mainly by including accurate spectroscopic data, especially the branching ratios, which fix the ratio of two transitional matrix elements. Note, that even if the branching ratio is not introduced as an additional data point, the valley still will be present in the yield component of the least-squares statistic S if both transitions depopulating a given state are observed. To demonstrate this deficiency of the simple steepest descent method, let us consider a model situation in which a two-parameter function $f(x, y) = x^2 + (x - y)^2$ is minimized, starting from a point $x = y$. The term $(x - y)^2$ creates a diagonal valley leading to the minimum point $(0, 0)$. Using the analytic gradient and the stepsize given by 4.41, it is seen that the minimization using the steepest descent method will follow a path shown in the figure instead of following the diagonal.

To facilitate handling of the two-dimensional valleys, introduced by the spectroscopic data, GOSIA offers a gradient+derivative method, designed to force the minimization procedure to follow the two-dimensional valleys, at the same time introducing the second-order information without calculating the second order matrix (4.42), thus speeding up the minimization even if the minimized function has a smooth surface. Generally, to minimize a locally parabolic function:

$$f(\bar{x}) = f(\bar{x}_0) + \bar{\nabla}_0 \Delta \bar{x} + \frac{1}{2} \Delta \bar{x} J \Delta \bar{x} \quad (4.46)$$

one can look for the best direction for a search expressed as a linear combination of an arbitrary number of vectors, \bar{P}_i , not necessarily orthogonal, but only linearly independent. This is equivalent to requesting that:

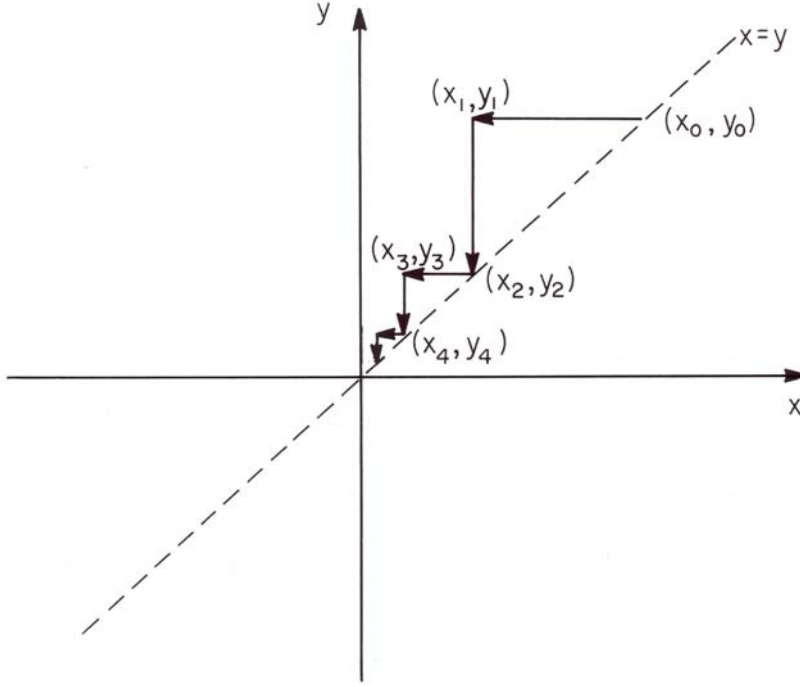


Figure 9: Simple steepest descent minimization of the function $f(x, y) = x^2 + (x - y)^2$

$$f\left(\bar{x}_0 - \sum_i \alpha_i \bar{P}_i\right) = \min \quad (4.47)$$

with respect to the coefficients α_i . Merging 4.46 and 4.47 we get:

$$f(\bar{x}_0) - \sum_i \alpha_i (\bar{\nabla}_0 \cdot \bar{P}_i) + \frac{1}{2} \sum_{ij} \alpha_i \alpha_j \bar{P}_i \bar{J}_j \bar{P}_j = \min \quad (4.48)$$

which can be written in the vector form as:

$$f(\bar{x}_0) - \bar{\alpha} \cdot \bar{\beta} + \frac{1}{2} \bar{\alpha} R \bar{\alpha} = \min \quad (4.49)$$

with a set of coefficients α_i treated as a vector $\bar{\alpha}$ and with:

$$\beta_i = \bar{\nabla}_0 \cdot \bar{P}_i \quad (4.50)$$

$$R_{ij} = \bar{P}_i \bar{J}_j \bar{P}_j$$

The matrix R is symmetric following the symmetry of J , thus the solution for the vector $\bar{\alpha}$ is given by:

$$\bar{\alpha} = R^{-1} \bar{\beta} \quad (4.51)$$

The gradient+derivative minimization algorithm uses two directions - the gradient, defining a direction of steepest descent, and a derivative of the gradient with respect to the displacement along its direction:

$$\bar{D} = \lim_{h \rightarrow 0} \frac{\bar{\nabla}(\bar{x}_0 + h \bar{\nabla}_0) - \bar{\nabla}_0}{h} \quad (4.52)$$

It can be shown that as long as the quadratic approximation 4.48 is valid:

$$\bar{D} = J\bar{\nabla}_0 \quad (4.53)$$

Using the identity resulting from the symmetry of J :

$$\bar{\nabla}_0 J^2 \bar{\nabla}_0 = (J\bar{\nabla}_0)^2 \quad (4.54)$$

gives:

$$R = \begin{vmatrix} \bar{\nabla}_0 \bar{D} & \bar{D}^2 \\ \bar{D}^2 & \bar{D} J \bar{D} \end{vmatrix} \quad (4.55)$$

where all terms, except R_{22} , are known. By sampling the minimized function this missing term can be expressed as:

$$\bar{D} J \bar{D} = \frac{2}{h^2} [f(\bar{x}_0 + h\bar{D}) - f(\bar{x}_0) - h\bar{\nabla}_0 \cdot \bar{D}] \quad (4.56)$$

The coefficients α_1 and α_2 , resulting from the solution of 4.51, can be rescaled arbitrarily, since we are only interested in the direction of search, the stepsize being found by the one-dimensional minimization procedure outlined in a previous section. A most convenient representation of a direction of search $\bar{\nabla}$, renormalized to avoid numerical overflows, is given by:

$$\bar{\nabla} = \left(\frac{\bar{D} J \bar{D}}{|\bar{D}|^3} - \frac{\bar{\nabla}_0 \cdot \bar{D}}{|\bar{\nabla}_0|^2 |\bar{D}|} \right) \bar{\nabla}_0 + \frac{1}{|\bar{D}|} \left(\frac{(\bar{\nabla}_0 \bar{D})^2}{|\bar{\nabla}_0|^2 |\bar{D}|^2} - 1 \right) \bar{D} \quad (4.57)$$

Although primarily designed to accommodate the narrow valleys superimposed on the least-squares statistic by the spectroscopic data, the gradient+derivative method usually gives much better results than the simple steepest descent, providing faster fitting despite the necessity of calculating two sets of derivatives per step of minimization. Since two linearly independent vectors define a two-dimensional space, the gradient+derivative method is very suitable to deal with the decoupled correlated pairs of matrix elements (note that, as could be expected, the solution of the model case discussed above then is found in a single step of minimization).

4.5.6 Quadraticization of the S Statistic by Redefinition of the Variables

The minimization methods outlined in previous subsections are built on the assumption that the minimized function can be described locally by the first or second order approximation, therefore their efficiency is strongly dependent on the extent to which this assumption is justified. Generally, the Coulomb excitation data analysis problem cannot be parametrized in such a way that the least-squares statistic S (4.32) becomes strictly a quadratic function. Some hints as how to improve the efficiency of minimization come, however, from considering extreme cases, most important of which is a perturbation-type process, characterized by direct dependence of the excitation probabilities on the product of squares of the matrix elements directly connecting a given level to the ground state. Assuming a cascade-like decay with negligible feeding from above and negligible branching, the γ -decay intensities are expected to be proportional to the product of squares of the level-dependent subsets of transitional matrix elements, thus the γ -yields part of the S statistic can be expressed as a quadratic function of the logarithms of γ -ray yields versus the logarithms of the matrix elements (note that the same holds for the spectroscopic data, although the signs of the $E2/M1$ mixing ratios and known $E2$ matrix elements are to be disregarded). While expressing the dependent variables in a logarithmic scale is straightforward, the same operation for the matrix elements would mean enforcing a sign identical to that of the initial guess. To avoid this problem, the logarithmic transformation of the matrix elements is only taken to first order of Taylor expansion, resulting in the actual minimization still performed in the matrix elements space with the direction of search being modified. To derive such an approach, let us consider the modification of a single matrix element, M , having an initial value of M_0 , during a single step of minimization. A transformation to the logarithmic scale yields the transformed derivative of a minimized function f with respect to M :

$$\frac{\delta f}{\delta \ln M} = |M_0| \frac{\delta f}{\delta M} \quad (4.58)$$

which, using the steepest descent method, gives a new value of M according to:

$$\ln |M| = \ln |M_0| - h |M_0| \frac{\delta f}{\delta M} \quad (4.59)$$

Expanding $\ln |M|$ into a Taylor series around M_0 and retaining only the first order term gives:

$$M = M_0 - h M_0^2 \frac{\delta f}{\delta M} \quad (4.60)$$

which defines the modified direction of the search. When the gradient+ derivative method is used, both vectors must be combined according to equation 4.58 and multiplied by $|M_0|$ to obtain the transformed direction of the search.

A scale change of the matrix elements is, in principle, mainly justified if the logarithmic scale is simultaneously used for the dependent variables (γ -ray yields etc.). However, even if the dependent variables are not transformed, the change of scale for the matrix elements, resulting in relative, rather than absolute, variations, can improve the efficiency of the minimization. A typical situation in which fitting the relative changes is efficient is the one when a strong dependence on a small matrix element determines the stepsize, h , common for a whole set, thus inhibiting the modification of much larger matrix elements if the absolute changes are used. Using the relative changes, however, one brings the sensitivity to all matrix elements to a common range, thus improving the simultaneous fit.

The minimum of a logarithmically transformed S function does not, in general, coincide with the minimum of the original least-squares statistic. The minimization procedure uses only the direction of search resulting from the transformation of the dependent variables, if requested, still monitoring the original S statistic. The transformation of the dependent variables therefore should be switched off when the current solution is close to the minimum of S .

4.5.7 Selection of the Parameters for Minimization

The gradient-type minimization, as used in GOSIA, tends to vary the parameters according to their influence on the least-squares statistic S . It is easily understandable, since the most efficient decrease of S primarily is obtained by varying the parameters displaying the strongest influence, measured by the current magnitude of the respective components of a gradient. With the stepsize, h , being common for the whole set of parameters, it is clear that unless the strong dependences are already fitted (which results in reduction of their derivatives) the weak dependences practically will not be activated. This is a serious concern in Coulomb excitation analysis, since the sensitivity of the S function to different matrix elements can vary by orders of magnitude. The attempt to perform the minimization using a full set of the matrix elements usually means that most of them will come into play only after some number of steps of minimization but all the necessary derivatives are to be calculated from a very beginning, enormously increasing the time spent on computation without any significant improvement compared to the much faster minimization performed initially for only a subset of matrix elements. To speed up the process of fitting, GOSIA offers a wide range of both user-defined and automatic ways of reducing a number of parameters according to the current status of the minimization. The user may decide first to fix some of the matrix elements included in the initial setup, but found to have no influence on the processes analyzed. Secondly, the user may specify a subset of the matrix elements to be varied during a current run overriding the selection made initially. The selection of the free variables for a current run also can be made by the minimization procedure itself, based on the magnitudes of the absolute values of the gradient components evaluated during a first step of the minimization compared to the user-specified limit. The direction of the search vector, being either a gradient or a gradient+derivative vector, is always normalized to unity, allowing the user to define the limit below which the matrix elements will be locked for a current run if the absolute values of the respective derivatives are below this limit. In addition, some precautions are taken against purely numerical effects, most notably against the situation in which numerical deficiency in evaluating the derivative causes a spurious result. The minimization procedure in GOSIA stops if either of three user-defined conditions is fulfilled: first, the value of the S function has dropped below the

user-specified limit; second, the user-specified number of steps has been exceeded; third, the user-given convergence limit has been achieved, i.e. the difference between two subsequent set of matrix elements (taken as a length of the difference vector) is less than this limit. The first two conditions fulfilled terminate a current run, while, after the convergence limit has been hit, the minimization is resumed if it was specified to lock a given number of the matrix elements influencing the S function to the greatest extent to allow the weaker dependences to be fitted (the details of the usage of the user-defined steering parameters are given in Chapter 5). To further reduce the numerical deficiency, GOSIA monitors the directions of two subsequent search vectors and fixes the matrix element having the largest gradient component if two subsequent directions are almost parallel, which usually signifies that a spurious result of the numerical differentiation of S with respect to this matrix element inhibits the fitting of the less pronounced dependences. A warning message is issued if this action was taken.

An additional reduction of the free variables can be done by coupling of the matrix elements, i.e. fixing the ratios of a number of them relative to one “master“ matrix element. This feature is useful if the experimental data available do not allow for a fully model-independent analysis, therefore some model assumptions have to be introduced to overdetermine the problem being investigated. The “coupled“ matrix elements will retain their ratios, as defined by the initial setup during the fitting, a whole “coupled“ set is treated as a single variable.

Finally, GOSIA requires that the matrix elements are varied only within user-specified limits, reflecting the physically acceptable ranges. The matrix elements are not allowed to exceed those limits, neither during the minimization nor the error calculation.

4.5.8 Sensitivity Maps

As a byproduct of the minimization, GOSIA provides optional information concerning the influence of the matrix elements on both the γ -ray yields and excitation probabilities. The compilation of those maps is, however, time-consuming and should be requested only when necessary. The yield sensitivity parameters, α_{ki}^y , define the sensitivity of the calculated γ -ray yield k with respect to the matrix element i as:

$$\alpha_{ki}^y = \frac{\delta \ln Y_k}{\delta \ln |M_i|} = \frac{M_i \delta Y_k}{Y_k \delta M_i} \quad (4.61)$$

The excitation probability sensitivity parameters, α_{ki}^p , are expressed similarly, the yields being replaced by the excitation probabilities. The code allows the six most pronounced dependences to be selected for each experimentally observed yield for the printout, while a number of the matrix elements for which the most important probability sensitivity parameters are printed out can be selected by the user.

By definition, the sensitivity parameters provide (to the first order) a relationship between the relative change of the excitation probabilities, p , (or the calculated γ -ray yields) and the relative change of the matrix elements according to:

$$\frac{\Delta p_k}{p_k} = \alpha_{ki}^p \frac{\Delta M_i}{M_i} \quad (4.62)$$

thus supplying locally valid information on the dependence of experimental data on matrix elements. An identical relationship holds for the yield sensitivity parameters, although the code calculates them only for the γ detector labeled as #1 for each experiment, thus the angular distribution of the γ rays, affected for example by the mixing ratios, is not accounted for fully. It is suggested that a γ -ray detector yielding the most complete and accurate yields should be defined as the first one in the description of an experiment to ensure that the yield sensitivity maps are calculated for all the yields observed.

The sensitivity parameters are not strongly dependent on the actual matrix elements, therefore the sensitivity maps can be treated as an indication of the features of the excitation/deexcitation process at any stage of minimization. As an extreme case, it should be noted that if the lowest-order perturbation theory applies, i.e. the excitation probability of a given state is proportional to the product of the squares of matrix elements connecting this state with the ground state, then the probability sensitivity parameter will equal 2 for all such matrix elements and will vanish for all others, no matter what the actual values are. The same holds for the yield sensitivity parameters, provided that the γ -ray decay follows a simple cascade with no

branching (the feeding from above can be neglected as a consequence of assuming the applicability of the lowest-order perturbation approach).

The sensitivity maps provide useful information that can be used during fitting to define the current sets of correlated matrix elements to be varied, to check to what extent the different sets of experimental data are independent and, finally, to ascertain which matrix elements included in the initial setup have a significant influence on the processes analyzed. The data obtained during the compilation of the yield sensitivity map also are used to generate the correlation matrix, selecting the subsets of matrix elements that are strongly correlated for the error estimation (see Section 4.6). It should be noted, however, that the compilation of the sensitivity maps is time-consuming, thus it should be requested only periodically when needed. The sensitivity maps also are helpful when planning an experiment, in which case a set of simulated γ -ray yields can be used as experimental data for a dummy minimization run (simulated yields can be created by GOSIA using OP,POIN - see 5.18). A comparison of the sensitivity parameters for different (existing or planned) experiments give an indication to what extent the additional sets of data provide qualitatively new information.

4.6 Estimation of Errors of the Fitted matrix Elements

The most commonly used methods of estimating the errors of fitted parameters (in our case the matrix elements) resulting from a least-squares minimization, are derived using the assumptions that do not necessarily apply to Coulomb excitation analyses. Usually, the errors of the fitted parameters are evaluated either, using the curvature matrix, or by requesting an increase of the least-squares statistic dependent on the number of degrees of freedom and the value of this statistic at the minimum. An approach based on the second-order approximation is not applicable because this approximation is in general not valid even in the vicinity of the fitted set of matrix elements, not to mention the problems resulting from the so-called “nuisance parameters“, i.e. parameters that can be introduced formally, but have no influence on the observed processes. The inclusion of such parameters prohibits a straightforward inversion of the second-derivative matrix. Moreover, the curvature matrix approximation assumes that the fit is perfect, i.e. the gradient at the solution point vanishes, thus only the second-order term describes the behavior of the least-squares statistic. Practically, however, we have to assume that a fitting procedure must be stopped at some point even though a number of the matrix elements that have a weak influence on the Coulomb excitation process, are far from their best values. This is not important from the point of view of extracting the information contained in the experimental data but can considerably disturb the error estimation of the significant dependences when the second-order approximation is used.

The unavoidable presence of the nuisance parameters also prohibits the error estimation procedures based on the assumption that the least-squares statistic should obey the χ^2 distribution with a given number of degrees of freedom. It should be noted that the concept of the number of degrees of freedom is implicitly based on the assumption that all the parameters are of about equal significance, which is obviously not true in the case of Coulomb excitation since the sensitivity of the observed γ yields to the various matrix elements differs by the orders of magnitude. This is illustrated by noticing that to describe a given experiment one can arbitrarily add any number of unobserved levels connected by any number of the matrix elements having no influence on either the Coulomb excitation or the γ deexcitation, thus arbitrarily changing the number of parameters and, consequently, the number of degrees of freedom. Finally, any procedure based on the number of degrees of freedom will result in ascribing the errors of the fitted matrix elements according to the subjective feeling as to what is a valid parameter of the theory and what is not. The error estimation formalism used in GOSIA, described in subsequent sections, has been derived without employing either the local quadratic approximation or the concept of the degrees of freedom to provide a reliable (however in general non-analytic) method of calculating the errors of the fitted parameters.

4.6.1 Derivation of the Error Estimation Method

Let us assume that a set of observables, Y_k , measured with known and fixed experimental errors, σ_k , is used to determine the values of a set of parameters, x_i . We also assume that the observables are related to the parameters by an error-free functional dependence, i.e. that if the experiments were error-free each experimental point Y_k could be exactly reproduced as:

$$Y_k = f_k(\bar{x}) \quad (4.63)$$

where f_k stands for the functional description of the k -th observed data point using a given set of parameters, represented as a vector. However, since we have to assume the experimental uncertainties, we can only determine the parameters by requesting that the least-squares statistic (as defined by 4.30) is minimized with respect to the set of parameters. In other words, the assumption that a set of n parameters is sufficient to reproduce N experimental observables ($N \geq n$), is equivalent to assuming that only certain values of observed data forming an n -dimensional hypersurface in the space of observables are allowed, and the fact that the measured set of observables does not correspond exactly to any set of parameters is due only to experimental errors. From this point of view the extraction of the parameters based on a set of observables reduces to determining which point on a hypersurface of the “allowed“ experimental values (referred to as a “solution locus“) corresponds to the measured values. While the assignment of the closest point on a solution locus defines a “best“ set of parameters (as shown below), the distribution of the probability that different points belonging to the solution locus actually represents the set of observables defines the errors ascribed to the parameters. It can be shown that both the “best“ set of the parameters and the errors of the parameters can be found by examining the least-squares statistic if the “perfect theory“ approach is assumed. Such an approach, actually employed in GOSIA, is presented below.

To simplify the notation, it is convenient to introduce the normalized observables, y_k , defined as:

$$y_k = \frac{Y_k}{\sigma_k} \quad (4.64)$$

and to assume that the functional dependence also includes the normalization relative to the fixed experimental errors σ_k . Treating both the set of normalized observables and the set of normalized functional dependences as vectors, allows a compact definition of the unnormalized least-squares statistic, χ^2 , as:

$$\chi^2 = [\bar{f}(\bar{x}) - \bar{y}]^2 \quad (4.65)$$

where we have used a symbol χ^2 to distinguish the unnormalized statistic from the normalized statistic S , as defined by Eq. 4.30. Assuming that the normalized observables, y_i , are independent and normally distributed (the width of the distribution is equal to unity, as a result of the normalization to the known experimental errors) one finds that the probability of the observed set \bar{y} is an experiment-distorted reflection of a “true“ set \bar{y}' which is proportional to:

$$P(\bar{y}') \approx \exp\left(-\frac{1}{2}(\bar{y} - \bar{y}')^2\right) \quad (4.66)$$

An assumption of the “perfect“ theory allows only the “true“ sets of experimental data which can be described by the functional dependence ϕ , belonging to the solution locus. Therefore only the sets \bar{y}' which can be expressed as:

$$\bar{y}' = \bar{f}(\bar{x}) \quad (4.67)$$

are to be taken into account. Substituting 4.67 into 4.66 gives:

$$P(\bar{f}(\bar{x})) \approx \exp\left(-\frac{1}{2}\chi^2\right) \quad (4.68)$$

Note that in this “geometrical“ picture, χ^2 has the meaning of the square of the distance from the observed set of data to a point belonging to the solution locus, thus the least-squares minimization is equivalent to finding a point on the solution locus closest to the experimentally observed set of data. Such a point has the highest probability of reflecting an error-free measurement, as long as the assumption of a perfect theory is in effect. Eq. 4.68 gives the probability that the observed set of data corresponds to a given point on the solution locus per element of volume of the solution locus. Thus the transition to a probability of a given set of parameters per unit of volume in the parameter space requires the density function, given by:

$$\rho(\bar{x}) = \frac{dV}{dx_1 dx_2 \dots dx_n} \quad (4.69)$$

is used, with dV standing for the volume element of the solution locus as a function of the parameters x_i . The probability distribution in the parameter space can be subsequently written as:

$$\frac{dP(\bar{x})}{dx_1 dx_2 \dots dx_n} = C \rho(\bar{x}) \exp\left(-\frac{1}{2} \chi^2(\bar{x})\right) \quad (4.70)$$

with a normalization constant C resulting from the condition that the integral of the probability distribution over the whole parameter space is equal to unity. Eq. 4.70 defines the probability distribution of simultaneous assignment of a whole set of parameters. Practically, however, we are interested in ascribing the errors to individual parameters, therefore we have to reconstruct the one-dimensional probability distributions corresponding to individual parameters. Such a distribution for parameter i , with no assumptions made as to the “true“ values of the remaining parameters, will be given by:

$$\frac{dP(x_i)}{dx_i} = \int \frac{dP(\bar{x})}{dx_1 dx_2 \dots dx_n} dx_1 dx_2 \dots dx_{i-1} dx_{i+1} \dots dx_n \quad (4.71)$$

$Y_i(I \rightarrow I_f)$ the integration extending over all allowed values of the parameters except of the parameter i . Using equation 4.71 the error bars of a given parameter can be found by requesting that the probability that the “true“ value of this parameter (evaluated by integrating the distribution 4.71) is contained within the error bars and is equal to an adopted confidence limit of 68.3%; this corresponds to the confidence level for a standard deviation with the Gaussian distribution. Since, neither the minimum is perfect, nor the symmetry of χ^2 around the minimum is assumed, it is reasonable to define upper and lower error limits independently. This is explicitly given by requesting that:

$$\frac{\int_{x_i}^{x_i + \delta x_i} \frac{dP(x_i)}{dx_i} dx_i}{\int_{x_i}^{x_i(\max)} \frac{dP(x_i)}{dx_i} dx_i} = 0.683 \quad (4.72)$$

where δx_i stands for the upper error limit, while $x_i(\max)$ denotes the maximum allowed value of x_i . A similar formula is used to determine the lower error limit with the maximum allowed value of x_i replaced by the minimum allowed value of this parameter.

Until now the derivation of the error estimation formalism has rigorously followed the initial assumptions. The error estimation using equation 4.72 is, however, not practical when dealing with a multidimensional parameter space and non-analytic description of the functional dependence used to relate the parameters to the observed data. First, it is technically impossible to evaluate the density function, $\rho(\bar{x})$, if the analytic functional dependence is not known, as in the case of the multiple Coulomb excitation. It can be argued that if the parametrization of the processes observed is reasonable, the density function should be dependent only weakly on the actual set of parameters compared to the dependence of the χ^2 function (otherwise, the parametrization would be unstable). Assuming that the χ^2 exponent in equation 4.72 drops sharply in the vicinity of the error limit, while no drastic change of the density function takes place, one can take for granted that within a reasonable accuracy, the effect of weighting the Gaussian distribution with the density function can be safely neglected. Second, it is easily seen that the reconstruction of the one-dimensional probability distribution according to Eq. 4.71 is not feasible if the analytic form of the functional dependence is not known. Therefore it is necessary to adopt a “worst case“ approach, i.e. to use an approximation yielding overestimated error bars but allowing a reduction of the multidimensional problem to a one-dimensional one without performing the numerical integration in the multidimensional space. To construct such an approach we introduce a concept of a “maximum correlation curve“ defined as a curve in the parameter space for which an effect of varying a given parameter is, to the greatest extent, balanced by the changes of the correlated parameters to minimize an overall change of the χ^2 function. Introducing the above approximations, the error criterion 4.72 can be rewritten as:

$$\frac{\int_{x_i}^{x_i + \delta x_i} \exp\left(-\frac{1}{2}\chi^2(x_i)dl(\bar{x})\right)}{\int_{x_i}^{x_i(\max)} \exp\left(-\frac{1}{2}\chi^2(x_i)dl(\bar{x})\right)} = 0.683 \quad (4.73)$$

where l stands for the “maximum correlation“ path and the probability distribution is treated as a function of the i -th parameter only; the dependence on other correlated parameters being defined by the path of integration, l . This simplification results in overestimation of the error bars, corresponding to the confidence limit of at least 68.3%.

The error estimation formalism, presented above, fits well the needs of Coulomb excitation analysis. It is not sensitive to the redundant parameters, which will simply display no influence on the χ^2 statistic. It allows introduction of physical limits for the matrix elements just by normalizing the probability distribution to its integral between those limits (note that in case of insignificant matrix elements, this will yield the errors of 68.3% of the full range - GOSIA issues a warning if the integration is stopped on the limit before the criterion 4.73 was fulfilled). Finally, note that neither the purely quadratic behaviour of χ^2 nor the perfect minimum are explicitly assumed.

4.6.2 Numerical Estimation of Errors

The error estimation in GOSIA is performed in two separate steps. First, the “diagonal“ errors, i.e. the errors of individual matrix elements with all the others kept fixed, are found. This part of the error calculation is relatively fast and thus has been separated from the “full“, or correlated, error estimation. The calculation itself consists of a straightforward numerical solution of equation 4.73, the fourth-order Runge-Kutta integration method is used to numerically evaluate the integrals involved. The probability distribution is renormalized to its value at the central set of matrix elements to avoid under- and overflows, i.e. $\Delta\chi^2$ is used instead of χ^2 . As mentioned above, the diagonal error calculation is not very time-consuming, therefore it also can be used to speed up minimization provided that the strong influences were already fitted. Running the diagonal errors allows detection of the matrix elements that still are far from their best values judging from the pronounced asymmetries of the error bars. In addition, GOSIA notifies the user every time a better value of the statistic S has been found. This information can be used to “manually“ predict a better solution without performing a time-consuming minimization of the weak dependences. Also, in some cases, the improvement of χ^2 found during the error calculation can be so large that the Gaussian distribution associated with the error estimation cannot be handled due to the machine-dependent overflow of the exponential involved. GOSIA detects such situations using a user-defined capacity of the computer, allowing to indicate which subsets of the matrix elements are to be refitted to improve the minimum.

The diagonal error calculation is usually repeated a few times until the minimum of the least-squares statistic S is found to be satisfactory from the point of view of individual matrix elements. The following “full“ error calculation differs from the diagonal error calculation only by applying Eq. 4.73 along the predicted path of maximum correlation. Although, in general, this path is a curve in the space of the parameters, we are forced, for practical reasons, to approximate it by a straight line. To make this approximation as reliable as possible, the information resulting from the diagonal error calculation is used by GOSIA to determine the way the probability distribution is sampled. An estimate of the diagonal error for a given matrix element is first used to evaluate an appropriate stepsize for the Runge-Kutta integration algorithm. Since the influence of a given matrix element is not a priori known, a common stepsize is used for the diagonal error estimation. This approach is subsequently refined by adjusting the stepsize for each matrix element individually during the full error calculation based on the diagonal error range. It may, in some cases, cause a slight decrease of the error range if there is no significant correlation and the stepsize assumed for the diagonal error calculation has not correctly taken into account the sensitivity of the χ^2 statistic to a given matrix element. The diagonal error bars also are used to define how the maximum correlation curve is approximated by a straight line in the space of the parameters. This operation is performed by assuming that the matrix element, for which the correlated error is estimated, is varied to the value corresponding to its central value \pm an appropriate diagonal error and fixed at this value, while the one-step gradient minimization of the remaining matrix

elements is done to find the correlation axis. The maximum correlation direction is then defined as a vector difference of the resulting set of the matrix elements and the central point. In this way, a correlation curve is approximated at a range consistent with the order of magnitude of the final error. However, it should be noted that performing the one-step gradient minimization to find the correlation axis is very time-consuming if all the matrix elements are taken into account. Moreover, since the gradient method will only affect the values of the matrix elements strongly correlated with the one investigated, the calculation of the derivatives with respect to all others is simply redundant and does not yield any improvement in predicting the correlation axis. To speed up the full error calculation, GOSIA offers a mechanism for reducing the number of matrix elements being taken into account, by predicting the subsets of mutually correlated matrix elements. This requires that at a final stage of minimization, the yield sensitivity map is compiled and the full set of the sensitivity parameters α_{ki}^y (4.61) is stored in a permanent file. A subroutine, OP,SELE, (SELECT), uses the map of the sensitivity parameters to predict the correlation. Each two matrix elements are correlated if they affect the same data points, thus, for each matrix element M_l the correlation with a matrix element M_k can be measured by:

$$c_{lk} = \sum_i |\alpha_{ki}^y \alpha_{li}^y| \quad (4.74)$$

the summation extending over all observed γ -ray yields. The absolute values are taken to prevent the neglect of the correlation due to coincidental cancellation of opposite sign terms. For each matrix element, indexed by the row index l , OP,SELE identifies those matrix elements M_k having values of c_{lk} greater than 10% of the maximum value of c_{lk} in this row. As a result, OP,SELE produces a binary matrix whose elements are either 0, if no strong correlation was predicted, or 1. The matrix elements explicitly correlated by the spectroscopic data are assumed to be correlated by definition. The correlation matrix then is used during the full error calculation to fix the matrix elements for which the correlation was not predicted when searching for the correlation axis.

GOSIA issues messages if lower values of the S statistic have been found. The set of the matrix elements producing an overall best value of S is stored on a permanent file, which could be used eventually to improve the minimization as a starting guess. However, it should be remembered that the uncorrected fast approximation used during the error estimation can be a source of inaccuracies, thus the small changes in the S statistic usually can be disregarded.

4.7 Identification of Erroneous Data Points

Fitting a large set of parameters, as in the case of Coulomb excitation analyses, one must be aware of the possible existence of local minima, which can cause the fitting procedure to be trapped in an erroneous solution. While there is no general method of distinguishing a local minimum from a global one, some judgement is still possible based on the value of the normalized least-squares statistic S and the comparison of experimental and fitted data. A local minimum could be created artificially by including erroneous pieces of data, such as incorrectly assigned γ yields, or, even if there were no mistakes in the data, could result from the local dependence on the parameters. The information provided by GOSIA during the minimization and error estimation usually is sufficient to determine whether the solution is acceptable. To further facilitate the identification of the local solutions, GOSIA is equipped with a “troubleshooting“ module, designed to detect inconsistencies within the data set. This module uses the information obtained at a current stage of minimization concerning the dependence of the observed γ yields on matrix elements. Only the γ yields observed in the detectors labeled #1 for each experiment are used, as a result of the convention that the γ detector providing the most complete and reliable set of data should be defined as the first one. The troubleshooting routine first calculates the normalized S statistic disregarding the other γ detectors and the spectroscopic data, assuming the independent, code-calculated normalization, thus overriding the user-specified normalization constants. A large difference between a value of S calculated this way, and the value resulting from the minimization, points to either a wrong relative normalization or a problem with reproduction of the γ -ray angular distribution, which may be due to the errors in assigning the angular positions of the γ detectors (inconsistencies within the spectroscopic data are easy to notice by comparing the calculated and experimental values). A next step is to select the experimental γ yields data, which locally inhibit minimization with respect to the individual matrix elements. Keeping in mind the gradient

method used for the minimization, it is easily seen that a “perfectly consistent“ set of data used to form a least-squares statistic, which can be written in the form:

$$\chi^2 = \sum_i \delta_i^2 \tag{4.75}$$

is characterized by the fact, that all individual components of the derivative with respect to a given matrix element M_k

$$\frac{\partial \chi^2}{\partial M_k} = 2 \sum_i \delta_i \frac{\partial \delta_i}{\partial M_k} \tag{4.76}$$

should be of the same sign. This means that the overall direction found to improve the minimum with respect to this matrix element is the same as resulting from the separate pieces of data. Inconsistent pieces of data may, in turn, produce large terms of opposite sign, which consequently causes a small value of the derivative due to cancellation. In such situation a given matrix element will not be varied. As a measure of this effect we introduce a parameter r_k , defined for each matrix element M_k as:

$$r_k = \log \frac{\sum_i \left| \delta_i \frac{\partial \delta_i}{\partial M_k} \right|}{\left| \sum_i \delta_i \frac{\partial \delta_i}{\partial M_k} \right|} \tag{4.77}$$

This parameter equals 0 if all the terms summed are of the same sign and becomes large when the cancellation effect is dominant. The numerator of 4.77 can be treated as an indication of the influence of a given matrix element M_k (the “strength“ of this matrix element) and is listed in the output of the troubleshooting routine separately. The routine further selects the data points having the largest positive and negative contributions to the derivative for all the matrix elements for which calculated r_k exceeds an user-specified limit. This information may be helpful to pinpoint erroneous data points, e.g. missassigned γ transitions. Sometimes, mostly for weakly overdetermined cases, local minima and saddle points may occur even if all the data are correct. The information provided by the troubleshooting module then can be used to modify the setup of the matrix elements to be fitted or to temporarily switch off some γ yield data to allow the minimization procedure to find a way out of such an erroneous solution.

5 INPUT INSTRUCTIONS FOR THE COMPUTER CODE GOSIA

5.1 ORGANIZATION

Input, execution and control of the code GOSIA is achieved by specifying a given sequence of option commands. These option commands are activated using the input format `OP,—` where `—` designates the four-character alphanumeric name of the option command. Some options are used for input or selection of input needed for specific tasks, while other options execute appropriate modules of the code.

The code GOSIA can operate in either of two mutually exclusive modes. The first, activated by the option `OP,COUL`, performs the calculation of Coulomb excitation probabilities and γ -ray yields for a fixed set of the matrix elements. No fitting of matrix elements to experimental data is performed if `OP,COUL` has been selected. The other mode, activated by the command `OP,GOSI`, should be used if a least-squares fit of matrix elements to experimental data is desired. The user is free to use any other option commands in conjunction with either the `OP,COUL` or the `OP,GOSI` commands consistent with an obvious logic. For example, the code cannot calculate Coulomb excitation amplitudes if the level scheme is not defined, also it cannot execute the fit-related commands if `OP,COUL` has been selected. The input to the option commands `OP,COUL` and `OP,GOSI` contains suboptions for which the prefix `OP,` is not appended to the name. The suboptions must occur in a logical order to ensure that the required information has been input as illustrated in section 7.4 of this user manual.

5.1.1 INPUT FORMATS

As a rule the input should be given in free format mode (`READ*`). This implies that the number of entries should correspond to the number of variables in the respective read list, different entries being separated by either a comma or a space. Floating-point values can be given as integers (the decimal point is not required and the conversion is automatic). Integers may not be given as floating point numbers. Blanks are not equivalent to zeros, unlike fixed-field formats, therefore zeros must be typed in explicitly. Some exceptions to this general input format will be stressed in the descriptions of various options. A wrong sequence of input entries is usually detected when a number is encountered instead of an expected alphanumeric option code. In this case a message `UNRECOGNIZED OPTION —` is issued and the job aborted (`—` designates an unrecognized string). This means that the sequence of the input entries is wrong somewhere between the last recognized option command and the entry reprinted.

5.1.2 SUMMARY OF AVAILABLE OPTIONS

A summary of all available options is given below. Detailed descriptions of each option and suboption command are given in alphabetical order in the subsection of this chapter listed next to the name of each option. Details of the file manipulation procedures are given in Chapter 7. The names of the option commands are truncated to four characters. Full, self-explanatory names are given in parentheses in the following description.

`OP,BRIC` (BRICC) (5.2):

Activates calculation of the internal conversion coefficients for all transitions included in the matrix element file.

`CONT` (CONTROL) (5.3):

Suboption of `OP,COUL` and `OP,GOSI` which is used to control and select various optional features of the code for both execution and output. This option can be omitted in which case default parameters will be used.

OP,CORR (CORRECT) (5.4):

Execution option to modify the experimental data to correct for the difference between the integrated yield calculations and the point values used for calculation of the Coulomb excitation cross sections and γ -ray yields, as described in detail in 4.4.

OP,COUL (COULEX) (5.5):

Activates the simple excitation/deexcitation mode. No fit of matrix elements to the data is made with this option in contrast to OP,GOSI. Consequently, the appreciable input required for the fit procedure can be skipped. OP,COUL contains the following suboptions:

LEVE
(Section 5.13)
ME
(Section 5.15)
EXPT
Section 5.8)
CONT
(Section 5.3)

OP,ERRO (ERRORS) (5.6):

Activates the error estimation module of the code. Also, it can be used to test the goodness of the solution, as discussed in detail in Chapter 8.

OP,EXIT (EXIT) (5.7):

Terminates the job and causes the final output to be compiled.

EXPT (EXPERIMENT) (5.8):

Suboption of OP,COUL and OP,GOSI which is used to input the experimental conditions for each of the experiments to be analyzed.

OP,FILE (FILES) (5.9):

Optionally allows to declare permanent files to be attached to the job in the input rather than in the job control stream.

OP,GDET (GE DETECTORS) (5.10):

Creates the files that contain the data needed to calculate the solid angle attenuation factors (2.2.3). Output files should be attached to the job when OP,YIEL is encountered.

OP,GOSI (GOSIA) (5.11):

This alternative option to OP,COUL is used when a fit of matrix elements is to be made to Coulomb excitation data. The suboptions for this option are the same as for OP,COUL (however, note that the input to ME differs from that used for OP,COUL):

LEVE

(Section 5.13)

ME

(Section 5.16)

EXPT

(Section 5.8)

CONT

(Section 5.3)

OP,INTG (INTEGRATE) (5.12):

Execution option used to integrate the deexcitation γ -ray yields, resulting from Coulomb excitation, over energy loss of the incident beam in the target and over the solid angles of the particle detectors.

LEVE (LEVELS) (5.13):

Suboption of OP,COUL and OP,GOSI which is used to read in and catalog the level scheme of the investigated nucleus.

OP,MAP (MAP) (5.14):

Causes the q-parameter maps (4.2) to be calculated and stored on a permanent file.

ME (MATRIX ELEMENTS OP,COUL Version) (5.15)

Suboption of OP,COUL which is used to input and catalog the matrix elements.

ME (MATRIX ELEMENTS OP,GOSI Version) (5.16)

Suboption of OP,GOSI which is used to establish the matrix element setup for fitting.

OP,MINI (MINIMIZE) (5.17):

Executes the least-squares fit of the matrix elements to the experimental data.

OP,POIN (POINT) (5.18):

Execution option to calculate the Coulomb excitation and deexcitation γ -ray yields at fixed scattering angle and bombarding energy.

OP,RAND (RANDOM) (5.19):

Used to overwrite a given set of matrix elements by a set of random values lying within specified limits.

OP,RAW (RAW DATA) (5.20):

Used to input data necessary if efficiency-uncorrected (raw) γ yields and/or yields resulting from summing several γ spectra are to be used as experimental data.

OP,RE,A (RELEASE A) (5.21):

Releases all matrix elements previously fixed and voids all coupling of matrix elements for the current minimization run.

OP,RE,C (RELEASE C) (5.22):

Releases all previously fixed matrix elements but preserves couplings.

OP,RE,F (RELEASE F) (5.23): Voids coupling of matrix elements while retaining fixed ones.

OP,REST (RESTART) (5.24):

Causes the program to use, as a starting point, a set of matrix elements stored on disk by a previous calculation in place of the set given as input.

OP,SELE (SELECT) (5.25):

Creates the correlation matrix for use by OP,ERRO

OP,SIXJ (SIX-j SYMBOL) (5.26):

Creates a table of Wigner 6-j symbols used by the sum rules code SIGMA (Chapter 6). OP,SIXJ is case-independent, thus it can be executed without defining the level and matrix elements scheme. It can also be inserted anywhere in the input sequence.

OP,STAR (START) (5.27):

Execution option to calculate only the Coulomb excitation amplitudes and cross sections, not the γ -ray yields. This comprises a subset and consequently an alternative to OP,POIN. This option can be used with either OP,COUL or OP,GOSI.

OP,THEO (COLLECTIVE MODEL ME) (5.28):

Generates matrix elements according to the geometrical model following the Bohr-Mottleson prescription.

OP,TITL (TITLE) (5.29):

Reads in the user-given title to be reprinted as a header of the output (maximum 80 alphanumeric characters). Can be repeated if more than one line is needed.

OP,TROU (TROUBLE) (5.30):

Performs an analysis at the local minimum to pinpoint erroneous experimental data. This option must be inserted immediately before OP,EXIT.

OP,YIEL (YIELDS) (5.31):

Used for input of data required if it is necessary to calculate the γ -ray deexcitation of the Coulomb excited nucleus. OP,YIEL is mandatory if OP,GOSI has been selected, in which case it is also used to specify additional spectroscopic information, i.e. branching ratios, mixing ratios, lifetimes and known $E2$ matrix elements, as well as relative γ detector efficiencies and upper limits of the unobserved transitions. The experimental deexcitation yields are supposed to reside on a separate permanent file attached to the job.

INPUT OF EXPERIMENTAL γ -RAY YIELDS (5.32)

Section 5.31 describes the structure of the file containing the experimental γ -ray yields from Coulomb excitation.

5.2 OP,BRIC (BRICC)

This option uses the National Nuclear Data Center database, BrIcc, to calculate the internal conversion coefficients for all E1, E2, E3, M1, and M2 matrix elements included in the OP,COUL, or OP,GOSI input files. In order that the matrix elements included in the calculation are defined, the OP,BRIC must follow either OP,COUL or OP,GOSI. A Gosia subroutine CONV generates all needed internal conversion coefficients in a table of the ICC values for each multipolarity for each transition.

Two lines of data occur after the OP,BRIC. input command. The first is the filename of the BrIcc index file, and the second is the filename of the BrIcc.icc file. That is, the input looks like:

```
OP,BRIC
/usr/local/bricc-22/BrIccFOV22.idx
/usr/local/bricc-22/BrIccFOV22.icc
```

(Two BrIcc files have been installed in /usr/local/bricc-22. They can of course go elsewhere and the user may wish to use the "no hole" version of the ICC tabulation, or, in the future, a later version than V22).

The BrIcc command will generate a file on unit 29. You can set a filename in the usual way with OP,FILE. Unit 29 will contain a table with the following information for each transition matrix element.

ENERGY ICC(E1) ICC(E2) ICC(E3) ICC(M1) ICC(M2)

This table will also be output to unit 22, the main output file if PRT, option 18,1 is set (the default) in sub-option CONT.

If the GOSIA input file already contains internal conversion data in OP,YIEL, it is simple to turn on or off the use of OP,BRIC by changing the sign of N1 to negative in OP,YIEL. No other changes need to be made to the input. The user-input internal conversion data can be restored by changing the sign of N1 to positive to restore compatibility to older GOSIA versions and removing the OP,BRIC option. In this case, the current version of GOSIA will interpolate the ICC data from the user-supplied data as in older versions, except that the cubic spline method now replaces the Lagrange method. Note that the use of the older spline interpolation of the BrIcc tables can be unreliable near the K, L edges and can give unreliable values between meshpoints. The newer OP,BRIC approach gives much more reliable results since since interpolation is done separately for each multipole eliminating the need to interpolate across K,L edges etc.

If a new input is being written for the current version of GOSIA, implement OP,BRIC as above, and enter a dummy sequence for internal conversion data as follows. (This is designed to preserve backward compatibility for older input files.) Enter the following records in OP,YIEL.

```
N1, N2
E1, E2, E3, ...EN1
as
-1, 0
0.010
```

Since $N2 = 0$, Gosia will expect no input (0 records) for I1, CC1(I1), CC2(I1)..., and these fields must be omitted. Gosia will read all necessary internal conversion data from unit 29, rather than interpolating. The 0.010 is a dummy record.

If the level scheme or the transition multipoles are changed, it is necessary to re-run the input with OP,BRIC to generate a new set of coefficients for new energies or added transitions. OP,BRIC can be removed for subsequent runs, which is useful if the user desires to change one or more ICCs in unit 29 manually.

5.3 CONT (CONTROL)

This suboption of either OP,GOSI or OP,COUL is used to override default settings of the job performance controls and to specify optional features of the program. CONT can be omitted if the default settings of the control parameters are satisfactory. CONT can be used anywhere in the OP,COUL and OP,GOSI input stream, usually as the last suboption specified. The input format is as follows:

CONT

.

Input control parameters needed for the job.

.

END, Marks the end of the CONT input. End must be followed by a blank line

The control switches are specified by a three-character alphanumeric string followed by a comma and, in some cases, by a floating point number X (as a convention, X will be used as the initial symbol for floating point entries while symbols beginning with I are specified to be integer). Even if X has obviously the meaning of an integer it should be entered as a floating point number, the conversion being done by the code. Some of the switches require additional input. The available control switches are as follows:

.....

ACC,X. Sets the accuracy parameter used as an internal check of the Adams-Moulton routine to 10^{-X} . The default value is $X = 5$. The step-size is either doubled or halved depending on whether the maximum deviation is less than $0.02x10^{-X}$ or greater than 10^{-X} . Do not use too large a value of X , as it slows down the calculation considerably with little increase in accuracy for X much larger than 6. Instead use the switch INT, to achieve maximum accuracy. See 4.1 for details.

.....

ACP,X. Sets the convergence test parameter for the $exp(A)$ expansion (4.2) to 10^{-X} . Default value is $X = 5$.

.....

CCF, This switch overrides OP,MINI or OP,ERRO commands and causes GOSIA to terminate execution after calculating and storing the internal correction factors. This allows splitting the minimization or error estimation jobs, which can be helpful when using unreliable or overloaded computer systems.

.....

CRF, This option causes GOSIA to read in the internal correction factors from file TAPE1 instead of recalculating them. This is a valuable time saver for restarting the minimization and error calculations using the OP,REST command. The internal correction factors are stored on TAPE1 automatically when calculated by the code.

.....

CRD,X. This switch defines which experiments use circular particle detectors. CRD, simplifies the input to OP,INTG. The additional input is as follows:

IE(1) The indices, according to the input sequence to EXPT, of those X experiments

IE(2) involving circular detectors. Note that the axial symmetry option in the EXPT input should be used rather than CRD, if the circular detector is symmetric with respect to the z (i.e. beam) axis.

IE(X)

.....

DIP,X. Sets the $E1$ dipole polarization parameter to $X/1000$. (See 2.18). Default value is 5.

.....
END, Mandatory CONT flag marking the end of CONT input. Must be followed by a blank line
.....

FIX, This switch provides the easiest way to override the matrix elements setup specified by the ME input. When FIX, is encountered all matrix elements are fixed and only those specified by subsequent input are released for minimization or error estimation. Further input required:

IM The number of matrix elements to be released.
I(1), Indices of the matrix elements to be released (defined by the sequence
I(2) of the ME input).
.
.
I(IM)

Using FIX, it is easy to reduce the number of free matrix elements without modifying the ME input.
.....

FMI, Fast minimization switch. Causes the code to terminate the job immediately after the OP,MINI step was completed, without compiling the final output. FMI, provides substantial time saving when the final output is not needed since the compilation of the final OP,MINI output involves a full Coulomb excitation calculation. The remainder of the input, including the repeated OP,MINI commands is ignored if the FMI, switch has been selected. FMI, cannot be used when the SEL, switch is set.
.....

INR, Independent normalization switch. Overrides the relative normalization of γ detectors and different experiments as specified in OP,YIEL input. With the INR, switch set, the code will calculate the best normalization factors (i.e. the ones providing the minimum value of χ^2 for a given set of elements) for each single γ detector independently.
.....

INT,X.

IE₁,IS, Overrides the default step size check parameter, IS, of the Adams-Moulton integration routine for specified experiments. The step size check is made every IS steps,
.
.
.
.
IE_X, IS_X with a resultant possible change in integration stepsize. The default value is IS = 1, thus the stepsize may be adjusted after each complete integration step. Setting IS = 1000 effectively switches off the stepsize control since 1000 steps exceeds the range of integration (according to 4.1), forcing the code to retain maximum accuracy.

X has the meaning of the number of experiments for which the default is to be altered. Additional input consists of X records, IE_n being the experiment number and IS_n the accuracy control parameter for this experiment. The experiments are numbered according to the sequence of the EXPT input, thus this control switch only can be used after the suboption EXPT definition.
.....

LCK, This switch allows fixing a series of matrix elements without modifying the initial setup, e.g. it can be used to keep the matrix elements belonging to a given multipolarity fixed during minimization. It requires further input as follows:

I,I1 Ranges of matrix elements to be fixed.
I,I1
 .
0,0 Two zeros end input

.....
NCM,X. Causes the kinematics calculation to be performed assuming the final state of the excited nucleus is the state with user- given index equal to *X*. Default value is 2.0. The states of an excited nucleus are numbered according to the sequence of the LEVE input.

.....
PIN,X. The PIN option is used when the charged particle detector comprises an array of small PIN diodes. *X* is the number of experiments. This is followed by

I,I1 *I* is the experiment number and *I1* is the number of PIN diodes for that experiment
 .
 There should be *X* such records
I,I1

This should be followed by labelling these experiments as circular detector type using CRD. Small area square PIN diodes can be approximated as equivalent circular detectors; this is accurate enough and saves defining the complicated orientation of the squares in space.

For the example of 2 experiments, each employing 30 PIN diodes, the input sequence should be:

```

CONT
PIN,2.
1,30
2,30
CRD,2.
1
2

```

Note that under OP.INTG the detectors should be defined according to the circular detector input - in this case there will be 2×30 double records. That is, the circular detector input requires two lines for each detector. OP,INTG then will perform a summation over the whole set of PIN diodes. The PIN switch tells the code that a specified experiment involves not a single detector but a number of them.

.....
PRT, This overwrites the default options specifying the printout. It requires additional input as follows:

I,I1 *I* is the print option code and *I1* is the user-specified setting
I,I1
 .
0,0 The **0,0** ends the input of the print options.

The following table lists all the available codes

CODE	DEFAULT VALUE	OTHER VALUES	CONSEQUENCES OF OPTION
1	1	0 -1	Print out level scheme, input matrix elements and kinematics (1). 0 inhibits such printouts, while -1 can be used to suppress kinematics only. When 0 is selected, the sequence: <pre> CONT PRT, 1,0 0,0 END,</pre> should be inserted before the LEVE and ME suboptions of either OP,COUL or OP,GOSI to set an appropriate flag.
2	1	0	Reprint of experimental γ yields to be fitted (1). 0 suppresses this printout.
3	1	0	Prints out experimental branching ratios and a comparison of experimental and calculated values (1). 0 inhibits this printout.
4	-2	0 or any positive integer	Prints out the yield sensitivity (α_γ parameters) map (see 4.5) after every $I1$ number of minimization steps if $I1$ is positive. Note that compilation of this yields sensitivity map is time consuming since it requires the calculation of derivatives with respect to all matrix elements. Consequently, it should be compiled only when necessary. $I1 = 2$ causes the compilation of this map when the OP,EXIT command is encountered after at least one execution of the OP,MINI command. $I1 = 0$ specifies no compilation or printout of this sensitivity map.
5	11111	Any positive integer	Prints out the value of χ^2/N , where N is the number of data points, after every specified $I1$ number of minimization steps. If $I1 = 1$ then χ^2/N will be printed after every step.
6	11111	Any positive integer	Printout of the gradient will occur every $I1$ minimization steps. Default value effectively inhibits this printout.
7	0	1	Specifies printout of excitation amplitudes and population when OP,EXIT is encountered after at least one OP,MINI command (1). $I1 = 0$ specifies no such printout.
8	1	0	$I1 = 1$ specifies a comparison of experimental and calculated yields. $I1 = 0$ specifies no such printout. This table will not be compiled if FMI, switch was used, even if $I1 = 1$.
9	1		Unused - free to be assigned.
10	1	0	$I1 = 1$ specifies printout of the kinematics for each integration meshpoint. $I1 = 0$ inhibits such printout.

CODE	DEFAULT VALUES	OTHER VALUES	CONSEQUENCES OF OPTION
11	1	0	$I1 = 1$ specifies printout of the γ yields for each integration mesh-point. $I1 = 0$ inhibits such printout.
12	1	0	$I1 = 1$ specifies printout of the q -parameter maps. $I1 = 0$ inhibits such printout.
13	1	0	$I1=1$ specifies printout of the normalization constants as defined by equation 4.28. $I1 = 0$ inhibits such printout.
14	1	0	$I1 = 1$ specifies printout of the deorientation effect attenuation coefficients. $I1 = 0$ inhibits such printout. At least one minimization step using OP,MINI or an OP,GOSI calculation is required to print the deorientation coefficients G_K . In the output file, they are labelled "vacuum depolarization coefficients."
15	1	0	$I1 = 1$ specifies printout of the mean lifetimes. $I1 = 0$ inhibits such printout.
16	0	1	$I1 = 1$ causes all possible calculated yields to be printed in the tables comparing the experimental and calculated yields. $I1 = 0$ causes the printout of the experimental and calculated yields only for the observed transitions and unobserved transitions for which the calculated values exceed the upper limits specified in the OP,YIEL input.
17	0	Any positive integer	Causes printout of the probability sensitivity maps (the α_p parameters defined in 4.5). $I1$ specifies the number of matrix elements having the largest influence to be printed for each level with the corresponding α_p values.
18	0	1	Causes the printout of the interpolated internal conversion coefficients. $I1=0$ inhibits this printout.
19	0	1	$I1 = 1$ causes the printout of the excitation amplitudes when executing commands other than OP,STAR (e.g. OP,INTG).
20	0	1	$I1 = 1$ causes the printout of the efficiency-uncorrected yields and respective efficiencies if OP,RAW is used. This output is produced on TAPE23. Note that the γ -ray energies printed out are Doppler-shifted, according to the user given geometry and calculated kinematics modified energies are used to calculate the detection efficiencies.

.....

SEL, Creates file (TAPE18) containing the information needed by the program SELECT to generate the correlation matrix used for the error calculation - see the description of OP,MINI and OP,ERRO. This switch is only active when OP,MINI is executed with a default setting of the print parameter 4 (see the description of the print parameters defined by the PRT, switch above).

.....

SKP,X This causes the code to skip X selected experiments during the minimization procedure, i.e., the code does not take into account the selected experiments. This switch can be quite useful since

often a subset of the experiments is sensitive only to a subset of matrix elements. The SKP,X switch requires additional input:

I(1) The indices of experiments to be skipped (experiments
I(2) are numbered according to the sequence in which
 · they appear in the EXPT input)
 ·
 ·
I(X)

SMR, This control switch causes the input file for the SIGMA program (See Section 6) to be generated when OP,ERRO is executed. This switch is ignored if OP,ERRO is not executed.

SPL,X. This control switch with $X = 1$ causes the use of the cubic spline routine SPLINE plus SPLINT[PRE92] instead of the default lagrange interpolation for integration of yields over particle energy, θ_{mesh} .

TEN, Causes GOSIA to write the statistical tensors in the system of coordinates defined by Fig. 3 on TAPE17 when either OP,STAR or OP,POIN is executed. The tensors written are the pure Coulomb excitation tensors, as defined by 2.30, and can subsequently be used by external programs to examine the γ -decay process (e.g. to study the deorientation effect). The structure of the statistical tensors file is described in Chapter 7.

VAC, This switch is used when it is desired to change the default parameters used to evaluate the vacuum deorientation effect (2.2.1). It requires the following additional input:

I,X(I): where $I = 1, 2, \dots, 7$ specifies the parameter to be overwritten, $X(I)$ being the new value. Two zeros end this input. The

parameters are defined as in 2.53 . The index value I is as follows:

I	$X(I)$	Default value
1	J_1	3
2	Γ	$0.02(ps^{-1})$
3	Λ^*	$0.0345(ps^{-1})$
4	τ_c	$3.5(ps)$
5	g	Z/A
6	K	6.10^{-6}
7	x	0.6

A common g factor is assumed for all nuclear levels. Note that $g = Z/A$ often is a poor estimate. The known g factors of the lowest states can be used to give a better estimate.

Since the lifetimes are given in picoseconds the field strength parameter K is 10^{-12} times the true value in gauss (the default values corresponds to 6.10^6 gauss). Note that OP,EXPT must occur in the input file before the CONT option VAC, otherwise OP,EXPT will overwrite the values set by VAC.

The deorientation effect can be switched off (if, for example, the influence of deorientation on the result is to be tested) by specifying:

VAC,
 3, 0.
 6, 0.
 0, 0.

.....

WRN,X. This switch causes a warning message to be printed with the comparison of experimental and calculated yields for those yields for which the experimental and calculated values differ by more than X standard deviations. The default setting is $X = 3$.

5.4 OP,CORR (CORRECT)

This execution-only option requires no input other than the command itself. It uses the file of original experimental yields (see Section 5-30), read from TAPE3, and writes on TAPE4 a set of yields which have been modified to correct for the difference between the yields calculated using full integration and the yields calculated using “mean“ values of the bombarding energy and scattering angle for each experiment (see Equation 4.23). The modified (corrected) experimental yields, on TAPE4, then are used as data for the minimization and error estimation procedures. The OP,INTG and OP,CORR commands must be run as one job with the OP,CORR command following OP,INTG in the sequence of option commands. The values of the mean energy and scattering angle used for the point calculations are those specified for each experiment in the EXPT input.

Note that NTAP (specifying the file containing the experimental yields in OP,YIEL) must equal 3 when using the OP,CORR command (i.e. the file containing the original uncorrected experimental yields must be TAPE3).

5.5 OP,COUL (COULEX)

This option is used to calculate the Coulomb excitation cross sections and yields of deexcitation γ -rays when no fitting of matrix elements to data is required. This option essentially is a truncated version of OP,GOSI which it replaces when fitting of matrix elements to data is not desired. The advantage of OP,COUL over the alternate OP,GOSI is that the considerable input of data required for the fitting procedure can be omitted. The OP,COUL command is used to input the information defining the nucleus studied and the experiments for which the Coulomb excitation calculations are to be performed. The OP,COUL command should occur immediately following OP,TITL since the input to OP,COUL is used by almost all modules of the program. The input to OP,COUL comprises four different sub-options:

- LEVE** Read and establish the level scheme of the investigated nucleus. See Section 5.13.
- ME** Read and catalog the matrix elements. See Section 5.15. Note that this sub-option input differs from that of the version used with OP,GOSI.
- EXPT** Input of experimental parameters. See Section 5.8.
- CONT** Used to control and select various optional features of the program for both execution and output. This suboption can be omitted in which case default parameters of the code will be used. See Section 5.3. A blank record is necessary to terminate the input to OP,COUL

5.6 OP,ERRO (ERRORS)

The module of GOSIA activated by OP,ERRO is designed primarily for estimating the error bars to be assigned to the set of matrix elements corresponding to the minimum value of χ^2 . However, this option also can be helpful in checking the existence of better solutions by providing a relatively fast way of scanning the χ^2 hypersurface. Error estimation is performed in two separate stages. First, the “diagonal“, or uncorrelated errors are found, next, the diagonal errors are used in the estimate of the “overall“, or correlated errors. This procedure is described in detail in Section 4.6. Section 7.4.10 shows the correct location of OP,ERRO in the input stream.

The input to OP,ERRO is as follows:

```
OP,ERRO
IDF, MS, MEND, IREP, IFC, RMAX
```

where:

IDF Mode flag. $IDF = 0$ sets diagonal error calculation mode, $IDF = 1$ causes overall error estimation.

MS,MEND The range of matrix elements indices for which error estimation is to be performed, i.e. the calculation will be carried out for matrix elements with indices fulfilling $MS \leq INDEX \leq MEND$. MS can also be entered as 0 or -1 . $MS = 0$ implies that the calculation will be performed for all matrix elements (excluding fixed ones - see below), thus providing a short form of specifying the full range. $MS = -1$ can be used only for “overall“ error calculation ($IDF = 1$). This allows the user to select an arbitrary set of the matrix elements defined by additional input required only if $MS = -1$. In this case the input to OP, ERRO is as follows:

```
OP, ERRO
1, -1, 0, IREP, IFC, RMAX
MS1, MEND1
.
.
MSn, MENDn
0, 0
```

where MS_i and $MEND_i$ define the range of matrix elements indices similarly to MS and $MEND$ when both are positive. $MS_i = MEND_i$ selects a single matrix element. Two zeros terminate this portion of input. This feature allows repeating the overall error estimation for a subset of matrix elements or to include the matrix elements that previously have been skipped without modifying the ME setup. A given value of $MEND$ is redundant if $MS = 0$ or $MS = -1$ has been selected.

IREP Repetition flag, assuming values of 0, 1 or 2. $IREP = 0$ implies a new calculation, i.e. no previously stored errors are read in and the error file will be created. Obviously, $IREP = 0$ should be used in conjunction with $IDF = 0$ for a first calculation of the diagonal errors. $IREP = 1$ causes previously stored errors to be read in and used for the continuation of the error estimation. The errors are stored on file TAPE15, which is updated during each execution of OP,ERRO. $IREP = 2$ means that the sum-rules file, TAPE3, has already been created during a previous “overall“ errors calculation and causes the code to read it in and update it during the current run. The CONT switch SMR, should be set for both creation and update of TAPE3. Note that in this case the experimental yields must reside on TAPE4 to avoid a multiple definition of the input/output files. TAPE3 is created with $IREP=1$ and updated with $IREP = 2$ only if SMR, was specified. $IREP = 2$ reduces to $IREP = 1$ if the SMR, switch was not encountered. Both TAPE15 and TAPE3 are required by the sum-rules code SIGMA - see Section 6.2.2. The proper combination of MS,MEND and IREP makes it possible to split the time-consuming error estimation into several runs which is important when running GOSIA on heavily loaded or unreliable computers. Note that in OP,YIEL NTAP must equal 4.

IFC : $IFC = 0$ specifies that the correlation matrix is to be used to reduce the number of matrix elements taken into account to calculate the correlated errors (see Section 4.6). The correlation matrix is created by the external program SELECT. To prepare the input information for SELECT it is necessary to execute OP,MINI with CONT switch SEL, and the default value of the print parameter 4, i.e. 4, -2. This should be done at a final stage of minimization prior to the error calculation. The information for SELECT is written by GOSIA on TAPE18 which should be attached to SELECT also as TAPE18. No other input is necessary. The output from SELECT is written on TAPE10 and should be attached to the OP,ERRO job as TAPE18. $IFC = 1$ implies that the correlation matrix will not be used. In this case it is not necessary to create and attach TAPE18. It is however strongly recommended that $IFC = 1$ be used only for small cases with all matrix elements of similar significance. Otherwise, selecting $IFC = 1$ will dramatically increase the execution time with no effect on the result. IFC is redundant if $IDF = 0$.

RMAX The largest floating point number available on a given computer. RMAX is used to prevent possible overflows during the scan of a probability distribution (see 4.6).

Note: Fixed matrix elements will not be varied during the error calculation. Matrix elements cannot be coupled when OP,ERRO is executed. Use release options (OP,RE,A and OP,RE,F) to remove couplings and unwanted fixing of matrix elements introduced in the ME setup.

N.B. Do not re-run the correlated error calculation without first re-running the diagonal error. Doing so will cause Gosia to over-estimate the errors because the output of the first stage (which should be the diagonal errors) is used to make an initial guess at the correlated error limits. Running OP,ERRO repeatedly to calculate correlated errors without repeating the diagonal error will approximately double the correlated error estimate each time.

5.7 OP,EXIT (EXIT)

This option causes the code to terminate the execution and to compile the final printout as specified by the CONT PRT, print options. OP,EXIT may be inserted anywhere in the input stream and the execution will terminate after the completion of the last executable OP,— command encountered before OP,EXIT. The remainder of the input stream will be ignored, thus OP,EXIT allows to execute various modules of the code without removing the irrelevant portions of the input. No additional input is required.

5.8 EXPT (Mandatory suboption of OP,COUL and OP,GOSI)

This suboption provides input of the experimental conditions used for the various experiments to be analyzed. The experiments are defined by mean values of projectile energy and scattering angle, which are used for “point“ excitation/deexcitation calculations. The realistic approach must include integration of γ -ray yields over finite ranges of bombarding energy and scattering angles. This feature is provided by OP,INTG which should be used to reproduce observed γ yields. As described in Chapter 4, GOSIA uses “point“ energy and scattering angles to execute all modules except for the integration module activated by OP,INTG. The options OP,INTG and OP,CORR are used to convert experimental γ yields to “point“ values. Mean values of bombarding energy and scattering angle used by OP,CORR are the ones given in the EXPT input. EXPT should follow LEVE in OP,GOSI or OP,COUL.

The input to EXPT is as follows:

```
EXPT
NEXP,Z1,A1
±Zn,±An,Ep,±θLAB, Mc,Ma, IAX,φ1,φ2,IKIN,LN
.
.
```

There needs to be NEXP records equal to the number of experiments. The experiments will be numbered by the code according to the sequence of these records from 1 to NEXP. A detailed explanation of entries is given below.

NEXP The number of experiments defined in the input. Each experiment corresponds to a particular combination of bombarding energy, scattering angle, experimental detector arrangement and (Z, A) of the nucleus exciting the nucleus being investigated. ($NEXP \leq 50$).

Z₁ Charge number of the investigated nucleus (Integer format).

A₁ Mass (in units of amu) of the investigated nucleus.

Z_n Charge number of the uninvestigated nucleus. A positive value signifies target excitation, i.e., $Z_n = Z_{projectile}$. A negative value signifies projectile excitation, i.e., $Z_n = Z_{target}$ (Integer format).

A_n Mass (in the units of amu) of the uninvestigated nucleus. A_n will thus correspond to the projectile mass if Z_n is positive and target mass if Z_n is negative. A negative sign appended to A_n signifies that this is a “thick“ target experiment, that is, the beam is completely stopped in the target. This latter option has the time saving feature of switching off some irrelevant calculations such as the deorientation effect and recoil velocity correction.

E_P The mean projectile bombarding energy, in the laboratory frame of reference, to be used for calculating the Coulomb excitation yields for the particular experiment. Input in units of MeV.

θ_{LAB} The mean scattering angle must be positive if the projectile is detected. A negative sign should be given with the true value of the projectile scattering angle if the recoiling target nucleus has been detected to ensure the selection of the proper kinematics. Note that by definition θ_{LAB} is always positive, the sign being only used by the code to set appropriate flags.

M_C Controls the number of magnetic substates to be included in the full Coulomb excitation calculations. For a given ground state polarization M_o , the magnetic substates in the range $(M_o - M_c, M_o + M_c)$ will be included for each level. Note that the sum total of magnetic substates for all levels must not exceed 1200. The code takes care of the obvious limitations in magnetic substates set by the spins of the states. $M_c = 0$ corresponds to the conservation of magnetic quantum number as occurs for backscattering.

M_A Controls the number of magnetic substates to be included in the approximate Coulomb excitation calculation. The meaning of M_A is the same as for M_C , namely magnetic substates in the range $(M_o - M_a, M_o + M_a)$ will be included for all states for a given ground state polarization M_o . The only allowed values of M_a are 0 or 1.

IAX The axial symmetry flag which can take values of 0 or 1 only. Zero defines axial symmetry of the particle detector, in which case further input is simplified and the calculations are speeded up. Unity implies that axial symmetry is not assumed.

ϕ_1, ϕ_2 The azimuthal angular limits of the particle detector (in degrees). The coordinate system used has the z axis in the direction of the incoming beam. The x and y axes can be defined in any convenient way provided that the angles of all detectors are given relative to the same coordinate system. Note that ϕ_2 must be larger than ϕ_1 .

IKIN The kinematics flag which can take values of 0, and 1, only. *IKIN* specifies which of the two-valued kinematic solutions to choose for detection of scattered projectiles in experiments involving inverse kinematics. *IKIN* is redundant if $A_{Projectile} < A_{Target}$. The possible choices are given below.

IKIN The centre-of-mass scattering angles chosen corresponding to laboratory angles θ

0 This selects the backward angle ϑ^{CM}

1 This selects the forward angle ϑ^{CM}

LN Normalization constant control which specifies that the given experiment has a normalization constant coupled to that for experiment *LN*. The normalization constant is the factor normalizing the calculated yields to the experimental for a given experiment (See the description of the input YNRM in OP,YIEL, Section (5.30). Experiments are numbered according to the sequence of records read in under EXPT. Therefore, if *LN* is equal to the record number defining a particular experiment then an independent normalization is assumed. If *LN* does not equal the record number defining a given experiment then the program requires a user-given relative normalization between the current experiment and experiment *LN* which is input using the OP,YIEL command. This input is useful for experiments where several scattering angles are measured simultaneously and therefore the relative normalization for the different scattering angles is known for this common experiment. The code will fit one absolute normalization constant to the coupled experiments.

As an example consider two experiments to study ^{72}Ge . One experiment involves Coulomb excitation of a ^{72}Ge target by a 50 MeV ^{16}O beam studied at a laboratory scattering angle of 160° using an annular particle detector. The second experiment involves projectile excitation of a 170 MeV ^{72}Ge beam on a ^{208}Pb target studied at a scattering angle of 150° by a particle detector subtending an azimuthal ϕ range from -30° to 30° . The sample input is as follows:

EXPT

2,32,72

8,16,50,160,3,1,0,0,0,1

82,208,170,150,3,1,1,-30,30,0,2

Three magnetic substates are included for the full Coulomb excitation calculation and one magnetic substate for the approximate calculations for both experiments. Experiment 1 was done using an axially symmetric geometry, therefore ϕ_1 and ϕ_2 are redundant. Independent normalization of both experiments is desired; therefore, the *LN* indices correspond to the experiment record numbers. In both cases $A_{Projectile} < A_{Target}$, thus *IKIN* is redundant.

5.9 OP,FILE (FILES)

This option allows to define the permanent files necessary for a current job in the GOSIA input rather than in an external job control stream. The use of OP,FILE is optional, but when used it should be the first command in the input stream, so the full output goes to the user-defined file. The input to OP,FILE is as follows:

OP,FILE

I1,I2,I3

NAME

.

.

0,0,0

where:

I1 - Unit number (TAPE number). $I1 = 22$ is the output file.

I2 - Status indicator. $I2 = 1$ indicates STATUS=OLD, $I2 = 2$ implies STATUS=NEW, while $I2 = 3$ corresponds to STATUS=UNKNOWN.

I3 - $I3 = 1$ to indicate formatted file, $I3 = 2$ means unformatted (binary) file. All files used by GOSIA are formatted, except of TAPE1 (internal correction coefficients file) which should be declared as unformatted.

NAME - user-assigned filename.

5.10 OP,GDET (GE DETECTORS)

This option is used to create a file (TAPE9) which contains the data needed to reproduce the γ -energy dependence of the solid angle attenuation factors for the coaxial Ge or detectors (see Section 2.2.3). For each γ detector a calculation following the formalism presented in Section 2.2.3 is carried out at several γ -energy meshpoints, then the energy dependence is fitted using a rational approximation according to Eq. 4.15. The fitted coefficients stored on TAPE9 are automatically read in when OP,YIEL or OP,INTG is encountered. This means that OP,GDET should be executed once before the execution of either OP,YIEL or OP,INTG. Section 7.4.2 shows the location of OP,GDET in the input stream.

The input to OP,GDET is as follows:

NPD A number of physically different γ detectors being used for a whole set of experiments defined in EXPT. The physically identical detectors are understood as the ones having an identical crystal geometry and being placed at the same distance from the target. In addition, if graded absorbers were used, the physically identical detectors are assumed to be equipped with the same sets of graded absorbers. (NPD<50) NPD should be given with a minus sign pre-pended if OP,RAW is to be used, i.e. if any of the experiments defined contains not efficiency-corrected spectra. In this case an additional file, TAPE8, is created. TAPE8 contains the absorber information, needed to reproduce the efficiency curves - see OP,RAW (IV.20).

r, R, L, d

I₁, I₂...I₇ Specifies the geometry and the graded absorbers setup for each of the physically different detectors. This sequence should be repeated NPD times. All entries are given in centimeters. The entries are defined as follows:

r The radius of the inactive p-core (the inner radius of a crystal)

R The radius of the active n-core (the outer radius of a crystal).

L The length of a crystal.

d The distance from a target to the face of a crystal.

I₁.....I₇ The thicknesses of the commonly used graded absorber materials, with the subscripts 1 through 7 corresponding to Al, C, Fe, Cu,Ag/Cd/Sn, Ta and Pb, respectively. The absorption coefficients for these materials are defined in GOSIA, for the energy meshpoints used, as internal data. It should be noted that if Ta or Pb absorber layers were used it is assumed that the γ transitions having an energy below the cutoff of the absorption curve are of no interest, therefore the energy-dependence fit is made only using a subset of meshpoints corresponding to the γ energies above 60 keV if Cd/Sn layer was employed, above 80 keV if a Ta layer was employed and above 100 keV if a Pb layer was employed. It is also assumed that the symmetry axis of the crystal is aligned with the center of the target. Moreover, the effect of the in-flight decay, which changes the geometry as seen by a decaying nucleus, is not taken into account for the estimation of the solid angle attenuation factors. The significance of this correction is in all cases far below the level of the experimental accuracy.

The printout for OP,GDET lists *NPD*, *d* (centimeters), and E_0 . This is followed by a table with 3 columns and 8 rows which list $Q_k(E_0)$, C_1 , and C_2 respectively for $k = 1, 2, 3, 4, 5, 6, 7, 8$. These values are defined by equation 4.15. All $Q_k(E)$ are zero when a 4π γ -ray detector is used. The $Q_k(E)$ can be set to zero by setting all the entries in the $Q_k(E_0)$ and C_1 columns to zero in the file on TAPE9.

5.11 OP,GOSI (GOSIA)

This alternate option to OP,COUL is used when fitting matrix elements to Coulomb excitation data. The OP,GOSI command is used to input the information defining the nucleus studied and the Coulomb excitation experiments to be used in the least-squares fit procedure. The OP,GOSI command shall occur immediately following OP,TITL since the input to OP,GOSI is used by almost all the other option commands of this program. OP,GOSI requires the same input sequence of suboptions as OP,COUL, the only difference being that a different version of ME is used. That is, the input comprises the following four suboptions:

LEVE Read and establish the level scheme of the investigated (LEVELS) nucleus. See Section 5.13.

ME Read and catalog the matrix elements. See section 5.16. Important: note that the input to ME under OP,GOSI differs from the version used for OP,COUL.

EXPT Input of experimental parameters. See Section 5.8.

CONT Used to control and select various optional features of (CONTROL) the program for both execution and output. This option can be omitted in which case default parameters of the code will be used. See section 5.3.

A blank record is necessary to terminate the input to OP,GOSI.

5.12 OP,INTG (INTEGRATE)

This command produces the most accurate calculation of the yields of deexcitation γ -rays following Coulomb excitation to be used for realistic comparison with experimental data. This option includes integration over solid angle of the particle detectors, energy loss in the target as well as full correction for the recoil velocity of the deexciting nucleus and the deorientation effect. This option also integrates the Rutherford scattering over the particle detectors and energy loss in the target in order to use as an absolute normalization.

OP,INTG comprises two distinct stages. The first stage calculates the yields of deexcitation γ -rays integrated over azimuthal angle ϕ for each energy and centre-of-mass scattering angle meshpoint. This calculation of the meshpoint yields should be repeated for each experiment according to the order that the experiments appear in the EXPT input. GOSIA stores the calculated meshpoint yields as internal files. The second stage uses the data stored in these internal files to integrate over bombarding energy and the range of scattering angles subtended by the particle detectors which is performed by interpolating between the γ yields calculated at each meshpoint. It is permitted to integrate over any arbitrary (θ, ϕ) shape for the particle detector including the case of several (≤ 4) ϕ ranges for each θ value. An option is included to simplify integration over circular detectors because of the frequent use of such a geometry. The input for the circular detector is a slightly modified subset of the normal input.

It is strongly recommended that the *SPL, X*. option in CONT be set to *SPL, 1*.

in order to select use of the cubic spline interpolation procedure. For more than 20 mesh points the Lagrange interpolation approaches is unreliable since it diverges.

Note that *OP, GOSI* including its four suboptions, plus *OP, YIEL*, must occur in the input file prior to *OP, INTG* in order to provide the input necessary to run *OP, INTG*.

The full input to OP,INTG is described below followed by the input for the circular detector option. Since the input to OP,INTG is long, a summary of the input is given at the end of this section to serve as a quick reference. Section 7.4.4 shows the correct location of OP,INTG in the input stream.

5.12.1 NORMAL INPUT TO OP,INTG

The input sequence is as follows:

OP,INTG

$NE, \pm NT, E_{\min}, E_{\max}, \theta_{\min}, \theta_{\max}$

where:

NE The total number of energy meshpoints at which full Coulomb excitation calculations will be performed ($NE \leq 100$).

NT The total number of θ^{CM} meshpoints at which the full Coulomb excitation calculations will be performed, ($NT \leq 100$). Negative value of NT specifies that the $\Delta\phi$ data specifying the shape of the detector will be entered by the user to improve the accuracy for complicated θ, ϕ , shapes. (see below) Note that the code takes NT equally-spaced meshpoints in the centre-of-mass system between the centre-of-mass limiting angles.

E_{\min}, E_{\max} The minimum and maximum bombarding energies (in MeV) between which the integration is to be performed.

$\theta_{\min}, \theta_{\max}$ The minimum and maximum angles (in degrees) between which the integration is to be performed. Note, θ angles are always positive and correspond to laboratory scattering angles of the detected particle, that is, the angle of the scattered projectile if it is detected and the angle of the recoiling target nucleus if it is detected. The above input string is modified if the circular detector flag CRD in CONT is activated for this experiment, as described later.

$\theta_{\min}^1, \theta_{\max}^1, \theta_{\min}^2, \theta_{\max}^2$ Where $\theta_{\min}^1, \theta_{\max}^1$ are the limits for the forward centre-of-mass angular range and $\theta_{\min}^2, \theta_{\max}^2$ are the limits for the backward centre-of-mass angular range.

E₁, E₂, ... E_{NE} Energy meshpoints at which the exact Coulomb excitation calculations are performed (MeV). These must exceed or at least equal the range over which the integration is to be performed to obtain reliable spline interpolation.

θ₁, θ₂, ... θ_{NT} Projectile scattering angles (degrees) in the laboratory frame, used as meshpoints to define the ϕ angular shape of the particle detector boundaries. Note, if the target is detected then the projectile scattering angle corresponding to the detected recoiling target angle must be input with a negative sign to set the flag specifying the target nucleus detected. The input angles must correspond to the detected particle angular range which exceeds or at least equals the range of angles subtended by the detector to obtain reliable spline interpolation. Do not input these angles for the circular detector option.

NFI The number of ϕ ranges for each θ_i meshpoint needed to describe the $\theta(\phi)$ dependence. Omit *NFI* input if either the circular detector option or axial symmetry is specified.

φ₁, φ₂, ... *NFI* pairs of ϕ angles describing the ϕ range for given θ_i . Omit ϕ input if either the circular detector option or axial symmetry is specified.

The above two records must be input for each θ meshpoint specified. *NFI* should not exceed 4. In most cases *NFI* = 1, then the pair of ϕ angles simply specifies the lower and upper limits for a given θ meshpoint. However, for some geometries, such as for rectangular shaped detectors, it is necessary to include more than one ϕ range for some θ values. For example, a rectangular detector placed with its normal at 45° to the incident beam has (θ, ϕ) contours shown in Figure 10:

This ends the input required to calculate the γ -ray yields integrated over azimuthal angle ϕ at the specified set of meshpoints. This part of input must be repeated for all experiments defined in EXPT.

The second stage of the input is required for the integration and once again has to be entered for all experiments:

NP Number of stopping powers to be input, $3 \leq NP \leq 20$. If *NP* = 0 then the stopping power table is taken from the previous experiment and the following input of energy and dE/dx values can be omitted for this case. This is useful where experiments differ only with regard to range of scattering angles or bombarding energies.

E₁, E₂, ... E_{NP} The energy meshpoints (in MeV) at which values of the stopping power are to be input.

$\left(\frac{dE}{dx}\right)_1 \dots \left(\frac{dE}{dx}\right)_{NP}$ Stopping powers in units of $MeV/(mg/cm^2)$. Interpolation between the energy meshpoints of the stopping power table is performed during integration. Consequently it is important to ensure that the range of energy meshpoints of the stopping power table exceed the range of energies over which the integration is to be performed.

NI1, ±NI2 The number of equal subdivisions of energy (*NI1*) and projectile scattering angle (*NI2*) used for integration. $NI1 \leq 100, |NI2| \leq 100$. The cubic spline interpolation subroutines SPLINE, SPLINT [PRE92] are used to interpolate between the (E_i, θ_i) meshpoints at which the full Coulomb excitation calculations of the deexcitation γ -ray yields were performed (See Section 4.4). The rapid angle dependence of the Rutherford scattering cross section at forward angles can cause problems with interpolation for the elastic channel if insufficient angle meshpoints are used. Always use many integration subdivisions which has little impact on the speed of the program since the full Coulomb excitation calculations are performed only at the meshpoints, not at the integration points, and interpolation is fast. *NI1* should be even and not exceed 100 while *NI2* must not exceed 100. If odd

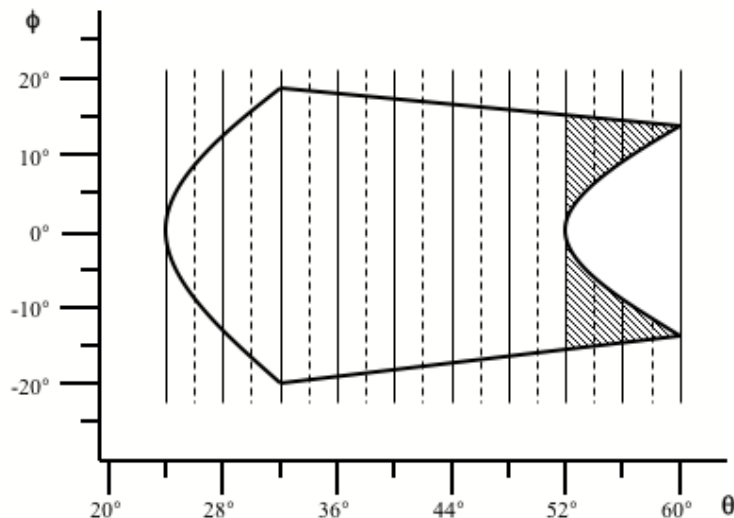


Figure 10: A rectangular particle detector has a non-azimuthally symmetric shape in the θ, ϕ space of projectile scattering angle. This shape must be defined by entering a number (NFI) of azimuthal angular ranges. In the hatched region, $NFI = 2$ ranges must be entered specifying the two active regions. The solid lines represent θ meshpoints, while the dashed lines indicate θ subdivisions. The rapid variation in active ϕ range in the hatched region necessitates input of the active ranges of $\Delta\phi$ at each subdivision specifying each of the two active detection regions shown hatched.

values are given the program increases them to the next larger even number. However, the $\Delta\phi$ input will be confused if $NI2$ is negative and odd. Important: $NI2$ can be negative and must be negative if NT is specified to be negative. Conversely, $NI2$ must be positive if NT is positive. If $NI2$ is negative then the following input must be provided:

$\Delta\phi_1, \Delta\phi_2, \dots, \Delta\phi_{|NI2|+1}$ where $\Delta\phi_i$ is the total range of ϕ (in degrees) for each equal subdivision of projectile scattering angle as illustrated in Figure 10. That is, $\Delta\phi_i$ equals the sum of all ϕ ranges for a given subdivision θ value if the azimuthal angular range also is subdivided into non-contiguous regions. The $\Delta\phi$ values correspond to equal divisions of projectile scattering angle from θ_{\min} to θ_{\max} rather than equal subdivisions of the meshpoints as in the normal input for $NI2 > 0$. Note that there is an important difference in how the interpolation over scattering angle is performed depending on whether NT and $NI2$ are both positive or both negative. For the positive sign the program interpolates between the calculated yields at each θ meshpoint. This produces excellent results if the ϕ dependence of the particle detector is a smooth function of projectile scattering angle, θ . The negative sign option should be used if the ϕ dependence is more complicated or if ϕ changes rapidly with θ . When the negative sign is used the program stores for each meshpoint the calculated yields per unit angle of azimuthal range, i.e., the calculated yields divided by the total ϕ range specified at that angle for the exact calculation. The program then interpolates these yields per unit of ϕ between the meshpoints. These interpolated values then are multiplied by the appropriate $\Delta\phi$ for each subdivision meshpoint prior to integration. Note that the code uses $NI2$ equal subdivisions of projectile scattering angles. This is not the same as equal division of geometric angle of the detector if the recoiling target nucleus is detected.

The following sample input segment goes with Figure 10. It shows the input of the absolute azimuthal angles under NFI , which are entered if the azimuthal symmetry flag was turned off in sub-option `EXPT`. It also shows the entry of total azimuthal angular ranges when NT and $NI2$ are set to negative values.

OP,INTG	
5,-10,634,650,24.0,60.0	NE,NT,E _{min} ,E _{max} , θ_{min} , θ_{max}
634,638,642,646,650	E ₁ ,E ₂ ,E ₃ ,E ₄ ,E ₅
24.,28.,32.,36.,40.,44.,48.,52.,56.,60.	
1	NFI
-2.0,2.0	$\phi_1\phi_2$
1	NFI
-12.5,12.5	$\phi_1\phi_2$
1	
-18.75,18.75	etc.
1	
-18.0,18.0	
1	
-17.5,17.5	
1	
-17.0,17.0	
1	
-16.0,16.0	
2	
-15.0,-2.0,2.0,15.0	
2	
-14.5,-9.0,9.0,14.5	
2	
-13.75,-13.0,13.0,13.75	
4	NP
625,635,645,655	E ₁ ,E ₂ ,E ₃ ,E _{NP}
32.395,32.401,32.404,32.404	(dE/dx) ₁ ,...
10,-18	NI1,-NI2
4.,16.25,24.5,31.25,37.5,36.9,36.25,35.6,35,34.1,33.25,	
32.6,31.9,29.2,26.5,18.5,11.2,5.7,1.5	

The last two lines contain the $NI2 + 1 = 19$ values of $\Delta\phi$ for $\theta = 20.0^\circ$ to 60.0° . These correspond to the θ values $20.0^\circ, 22.0^\circ, 24.^\circ, \dots$ in Figure 10.

The circular detector option (CONT CRD,) incorporates a feature to calculate automatically the azimuthal angular range $\Delta\phi$ at each subdivision of scattering angle θ . Consequently, do not input $\Delta\phi$ values when using the circular detector option.

The integration-related portion of the input must be repeated for each experiment defined in EXPT.

It is recommended to use as small a number of meshpoints as possible because the full Coulomb excitation calculations performed at the meshpoints are time-consuming. In many cases the required accuracy can be achieved by requesting a large number of subdivisions between the meshpoints, the values in subdivision points being found by fast interpolation.

5.12.2 CIRCULAR DETECTOR OPTION

The input for a given experiment differs slightly if the circular detector option is selected. This option is activated by the flag CRD, in the CONT suboption of either OP,COUL or OP,GOSI. For such experiments the input to OP,INTG is as follows:

NE,NT,E_{min},E_{max}, θ , ϕ , $\theta_{1/2}$ In this case θ and ϕ are the angular coordinates of the center of a circular particle detector subtending the half-angle $\theta_{1/2}$. The remaining entries are identical to the ones described in the previous section.

$\mathbf{E}_1, \mathbf{E}_2, \dots, \mathbf{E}_{NE}$ The energy meshpoints for the full Coulomb excitation calculation, analogous to those described in the previous section.

The above input is used in the first stage, that is, in the meshpoint calculation. When using arrays of PIN diodes follow the instructions described in the instructions in CONT; switch PIN. The input of the second stage, that is, the integration section, should look as follows:

NP Number of stopping powers to be input.

$\mathbf{E}_1, \mathbf{E}_2, \dots, \mathbf{E}_{NP}$ Energy meshpoints for the stopping powers in MeV.

$(dE/dx)_1, \dots, (dE/dx)_{NP}$ The values of the stopping powers, analogous to the normal input. If $NP = 0$ the values of this table will be those from the previous experiment.

NI1, NI2 Number of subdivisions of energy ($NI1$) and projectile scattering angle ($NI2$) used during the integration. Both shall be even numbers and shall not exceed 100 and 50 respectively.

5.12.3 SUMMARY OF INPUT TO OP,INTG - NORMAL INPUT

OP,INTG

$NE, NT, E_{\min}, E_{\max}, \theta_{\min}, \theta_{\max}$

E_1, E_2, \dots, E_{NE}

$\pm\theta_1, \pm\theta_2, \dots, \pm\theta_{NT}$

NFI

$\phi_1, \phi_2, \dots, \phi_{2NFI-1}, \phi_{2NFI}$

This portion of input is to be entered for each experiment defined in EXPT, unless the axial symmetry or circular detector option have been used.

NP

E_1, E_2, \dots, E_{NP}

$(dE/dx)_1, (dE/dx)_2, \dots, (dE/dx)_{NP}$

$NI1, \pm NI2$

$\Delta\phi_1, \Delta\phi_2, \dots, \Delta\phi_{|NI2|+1}$

This portion of the input again must be given for each experiment.

5.12.4 SUMMARY OF INPUT TO OP,INTG - CIRCULAR DETECTOR OPTION

OP,INTG

$NE, NT, E_{\min}, E_{\max}, \theta, \phi, \theta_{1/2}$

E_1, E_2, \dots, E_{NE}

This input should be defined in the part of the input related to the calculation of the meshpoints. The remainder, listed below, should be included in the integration-related section.

NP

E_1, E_2, \dots, E_{NP}

$(dE/dx)_1, (dE/dx)_2, \dots, (dE/dx)_{NP}$

$NI1, NI2$

5.12.5 ABSOLUTE COINCIDENT γ -RAY YIELDS

Note that OP.INTG evaluates the integrated coincident γ -ray yield for transition $I \rightarrow I_f$ that is defined by equations 4.22-4.25. That is:

$$\frac{d^2\sigma(I \rightarrow I_f)}{d\Omega_p^{CM} d\Omega_\gamma} = \sigma_R^{CM}(\vartheta_p^{CM}) \sum_{\substack{k \\ \chi \geq 0}} R_{k\chi}(I, I_f; \vartheta_p^{CM}) P_{k\chi}(\theta_\gamma) (2 \cos \chi (\phi_p - \phi_\gamma) - \delta_{\chi 0}) \quad (4.22)$$

The integration over scattering angle is performed in the centre-of-mass system. The "point" yields at centre-of-mass angle ϑ_p^{CM} and laboratory frame bombarding energy, E^L mesh points are given by

$$Y((I \rightarrow I_f), \vartheta_p^{CM}, E^L)_{CM} = \sin(\vartheta_p^{CM}) \int_{\phi_p} \frac{d^2\sigma(I \rightarrow I_f)}{d\Omega_p^{CM} d\Omega_\gamma} d\phi_p \quad (4.23)$$

Note that both the Rutherford cross section and the solid angle factor, $\sin\theta_p$, are already included in the definition of the "point" yields, as well as integration over the detected particle ϕ angle.

Using the centre-of-mass definition of the "point" yields (4.23), the angle-integrated yields at beam energy E are given by, $Y_i((I \rightarrow I_f), E^L)$, where:

$$Y_i((I \rightarrow I_f), E^L) = \int_{\vartheta_{p,lower}^{CM}}^{\vartheta_{p,upper}^{CM}} Y((I \rightarrow I_f), \vartheta_p^{CM}, E^L) d\theta_p^{CM} \quad (4.24)$$

The centre-of-mass angular limits are $\vartheta_{p,lower}^{CM}$ and $\vartheta_{p,upper}^{CM}$. Note that performing the angle integration of the centre-of-mass yields between two centre-of-mass angles is identical to integrating the corresponding laboratory frame yields as a function of laboratory scattering angle between corresponding angular limits in the laboratory frame.

Integrating the angle-integrated yields through the thickness of the target gives the total integrated yield $Y_i(I \rightarrow I_f)$

$$Y_i(I \rightarrow I_f) = \int_{E_{min}^L}^{E_{max}^L} \frac{Y_i((I \rightarrow I_f), E^L)}{\left(\frac{dE}{dx}\right)} dE^L \quad (4.25)$$

The $Y_i(I \rightarrow I_f)$ are the γ -ray yields that are fit to the experimental yields.

Note that $Y(I \rightarrow I_f)$ includes the Rutherford cross section, the $\sin(\theta_p)$ term, the target thickness, integration over the θ_p, ϕ_p for the detected coincident particles, the deorientation effect and γ -detector Q_K attenuation coefficients. Note that OP,INT does not include the detection efficiencies per unit solid angle for charged particle and γ -rays, ε_p and ε_γ .

The total number of coincident γ -rays detected then is given by

$$\text{Detected } p - \gamma \text{ coincident events } N_i = 10^{-30} \cdot \left[\frac{Q}{qe} \right] \cdot \left[\frac{N_A}{A} \right] \cdot Y(I \rightarrow I_f) \cdot \varepsilon_p \cdot \varepsilon_\gamma \cdot \Delta\Omega_\gamma$$

where:

Q is the integrated beam charge [C]

\hat{q} the average charges state of the beam
 e the proton charge [$1.602 \times 10^{-19}C$]
 N_A Avogadro number ($6.022 \times 10^{23}Atoms/mol$)
 A target mass number (gm/mol)
 $\frac{dE}{dx}$ energy loss in target in [$\frac{MeV}{mg/cm^2}$]
 $Y(I \rightarrow I_f)$ OP.INT output in [$mb \cdot mg/cm^2/sr$]

ε_p particle detection efficiency which normally is perfect, that is, $\varepsilon_p = 1$ regardless of solid angle covered by the integration in OP,INTG.

ε_γ γ -ray detection efficiency per unit solid angle $\Delta\Omega_\gamma$. That is, for a perfect blackbody γ -ray detector of solid angle $\Delta\Omega_\gamma$ the $\varepsilon_\gamma = 1$. Note that for a 4π array like Gammasphere the product $\varepsilon_\gamma \cdot \Delta\Omega_\gamma \approx 0.09$ at 1.33 MeV.

In some experiments the absolute integrated γ -particle yields are normalized to the Rutherford scattering yield. Thus the elastic scattering yield also is evaluated by integrating over the centre-of-mass "point" elastic yields

$$Y_{Elastic}(\vartheta_p^{CM}, E) = \sin(\vartheta_p^{CM}) \int_{\phi_p} \sigma_R(\vartheta_p^{CM}) d\phi_p \quad (4.26)$$

Integrating these over centre-of-mass scattering angle gives

$$Y_{Elastic}(E^L) = \int_{\vartheta_{p,lower}^{CM}}^{\vartheta_{p,upper}^{CM}} Y_{Elastic}(\vartheta_p^{CM}, E^L) d\theta_p^{CM} \quad (4.27)$$

Integration over energy loss in the target gives

$$Y_{Elastic} = \int_{E_{min}^L}^{E_{max}^L} \frac{Y_{Elastic}(E^L)}{\left(\frac{dE}{dx}\right)} dE^L \quad (4.28)$$

This is the elastic yield used for absolute normalization.

The total number of elastically scattered event detected then is given by

$$\text{Detected elastic events } N_{elastic} = 10^{-30} \cdot \left[\frac{Q}{\hat{q}e} \right] \cdot \left[\frac{N_A}{A} \right] \cdot Y_{elastic} \cdot \varepsilon_p$$

Thus the ratio of $p - \gamma$ events to elastic events is given by

$$\frac{\text{Detected } p - \gamma \text{ coincident events } N_i}{\text{Detected elastic events } N_{elastic}} = \frac{Y(I \rightarrow I_f) \cdot \varepsilon_\gamma \cdot \Delta\Omega_\gamma}{Y_{elastic}}$$

Note that the efficiency factor ε_γ must include the $p - \gamma$ coincidence efficiency factor to account for dead time, pileup rejection, and pulse-height dependence of the time resolution.

EXAMPLE:

During a complete experiment 1.71×10^{15} ^{136}Xe ions bombarded a ^{178}Hf target of areal density $\rho \cdot dx = 0.50mg/cm^2$ and $A = 178g/mol$. A GOSIA integration over the CHICO charged particle detector plus target thickness produces $Y_{14^+}(14^+ \rightarrow 12^+) = 9.65mb \cdot mg/cm^2/sr$ for the $626keV$ $14^+ \rightarrow 12^+$ ground-band transition. The particle detection efficiency $\varepsilon_p = 1$ and γ -ray detection efficiency of Gammasphere for this $626keV$ transition is $\varepsilon_\gamma \cdot \Delta\Omega_\gamma = 0.14$. Thus the total number of detected events is

$$\begin{aligned}
 N_{14^+} &= 10^{-30} \cdot 1.71 \times 10^{15} \cdot \left[\frac{6.02 \times 10^{23}}{178} \right] \cdot 9.65 \cdot 1 \cdot 0.14 \\
 &= 7.8 \times 10^6 \text{ detected events}
 \end{aligned}$$

5.13 LEVE (LEVELS)

Mandatory suboption of both OP,COUL and OP,GOSI. This suboption is used to define the level scheme of the investigated nucleus. Each level of the investigated nucleus is defined by a single record. LEVE should immediately precede ME in the input stream. Currently up to 100 levels are allowed.

Note that it is essential to add in each band at least one level above the last level observed because the solution of a coupled channels system give erroneous values for the uppermost state in each band. Moreover, if the experimental sensitivity is poor it is possible that virtual excitation will play a major role. In this case it is recommended that two levels be added above the last observed level in each band.

The input is as follows:

LEVE

I₁, IP₁, S₁, E₁ Each record describes one level, the number of records

I₂, IP₂, S₂, E₂ being equal to the number of levels of the investigated

I₃, IP₃, S₃, E₃ nucleus to be included in the calculations.

.

.

0, 0, 0, 0 Terminates input to LEVE.

I Is a user-given state number. Each nuclear level will be referred to in the code by its *I* value. By convention, index of the ground state must be 1.

IP Can be given values of ± 1 . Positive parity is designated by +1 and negative parity by -1.

S Is a floating point number specifying the spin quantum number of the state.

E Is a floating point number specifying the excitation energy of the state in MeV.

The input to LEVE is terminated by four zeros.

5.14 OP,MAP (MAP)

This execution option causes the calculation and storage of the maps of the q-parameters (see Section 4.2). Maps for $\Delta m = \pm 1$ transitions will be calculated only if the inclusion of the magnetic substates was requested for the approximate calculations by setting $M_A = 1$ in the input to EXPT. The maps will be read correctly if the input to EXPT is subsequently changed to $M_A = 0$. However, the maps will be read incorrectly if OP,MAP was executed with $M_A = 0$ and subsequently M_A was changed to 1. The maps are stored on TAPE7 and read from TAPE7. Both minimization and error calculation require that TAPE7 is attached to the job if OP,MAP was not executed during the same run.

No input other than the command is required for OP,MAP. Section 7.4.5 shows the correct location of OP,MAP in the input stream.

5.15 ME (OP,COUL)

Mandatory suboption of OP,COUL

This suboption of OP,COUL is used to input and catalog the matrix elements. The suboption LEVE must immediately precede ME since the catalog of matrix elements is performed using the level scheme and state indices assigned using the LEVE command. Up to 999 matrix elements are allowed.

The input is as follows:

ME

$\lambda, 0, 0$ Specify multipolarity λ .

INDEX1, INDEX2, ME List of matrix elements for multipolarity λ .

INDEX1, INDEX2, ME

INDEX1, INDEX2, ME

.

.

$\lambda_1, 0, 0$ Specify multipolarity λ_1

INDEX1, INDEX2, ME List of matrix elements for multipolarity λ_1

INDEX1, INDEX2, ME

INDEX1, INDEX2, ME

.

.

.

0, 0, 0 Terminates ME input.

The matrix elements for each multipolarity are given separately. The set of matrix elements for a given multipolarity is preceded by a single record defining the multipolarity λ , i.e.

$$\lambda, 0, 0$$

where $\lambda = 1$ through 6 for $E1$ through $E6$ respectively while $\lambda = 7$ for $M1$ and $\lambda = 8$ for $M2$. The ME data sets for each multipolarity must appear in increasing order for $\lambda = 1$ through $\lambda = 8$. Unused multiplicarities can be skipped in the input. The matrix elements for each multipolarity are read in as:

INDEX1, INDEX2, ME INDEX# is the user given state number as defined in the LEVE input

ME = < INDEX2 || E(M) λ || INDEX1 > i.e., the reduced multipole matrix element defined by equation 2.16

Note that the definition of reduced matrix element does not include the i^λ term for the $E\lambda$ matrix elements used in the original Winther-deBoer semiclassical Coulomb excitation code (WI66). The $E\lambda$ matrix elements are given in units of $e.barns^{\lambda/2}$ i.e., $e(10^{-28}m^2)^{\lambda/2}$. The $M\lambda$ matrix elements are given in units of $\mu_n barns^{(\lambda-1)/2}$. Within a given multipolarity, only matrix elements in the upper triangle, i.e. $INDEX2 \geq INDEX1$, should be given. Matrix elements in the lower triangle are set by the program. Within a given multipolarity both $INDEX1$ and $INDEX2$ columns must appear in increasing order (odometer ordering). The header of the next multipolarity ends input for a given multipolarity. A single record of 3 zeros ends the input to ME.

RESTRICTIONS:

Note that the sequence of matrix elements is uniquely set by the input conventions. An error message will be printed and the job aborted if any of the following restrictions are violated.

- a. Multipolarities must appear in order from lowest to highest starting with $E\lambda$ and then $M\lambda$.
- b. Matrix elements must belong to the upper triangle, i.e., $INDEX2 \geq INDEX1$.
- c. $INDEX$ values must be in increasing order, i.e. odometer order.

MATRIX ELEMENT PHASES:

Note that the phase of a wavefunction is arbitrary. However, to facilitate comparison with models it is best to fix the relative phases of states. Choosing one matrix element between two states to be positive couples the relative phases of the wavefunctions of these two states to be the same. Then the phases of any other matrix elements coupling these two states, relative to the phase of the positive one, are observables. Consequently for typical collective bands it is convenient to choose the primary $\Delta I = 2, E2$ transitions in the band to have a positive phase locking the state wavefunctions of the band to have the same phase. In addition the phase of one strong matrix element connecting two separate collective bands locks the relative phase between these collective bands.

When entering matrix elements in the upper triangle be careful to enter the correct phase remembering that time reversal invariance relates the time-reversed matrix elements by

$$\langle J_1 || T^\lambda || J_2 \rangle = (-)^{J_1 - J_2 - \lambda} \langle J_2 || T^\lambda || J_1 \rangle$$

Thus the phase of the matrix elements in the lower triangle is related to the upper triangle phase by the $(-)^{J_1 - J_2 - \lambda}$ phase term. Similar care must be taken comparing the observed relative phases with model predictions.

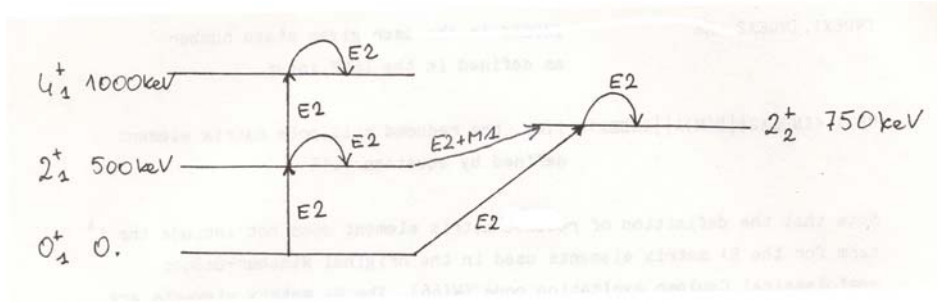


Figure 11: Model system having 4 states with $E2$ and $M1$ coupling. The $2_1^+ - 2_2^+$ coupling is assumed to be of mixed $M1$ and $E2$ character.

EXAMPLE:

An example of the use of the suboptions LEVE and ME for a OP,COUL calculation is given below. Consider the definition for the following nuclear level scheme shown in the figure.

OP,TITL

Example of definition of nucleus

OP,COUL

LEVE

1, 1, 0, 0 - Ground state is given index "1".

2, 1, 2, 0.500

3, 1, 4, 1.000

4, 1, 2, 0.750

0, 0, 0, 0 - Ends LEVE input.

ME

2, 0, 0 E2 - matrix elements. All E2 matrix elements

1, 2, 1.0 equal to 1.0 e.barns.

1, 4, 1.0

2, 2, 1.0 INDEX1 and INDEX2 - in increasing order.

2, 3, 1.0

2, 4, 1.0

3, 3, 1.0

4, 4, 1.0

7, 0, 0 - Terminates input for E2. Starts input for

2, 4, 1 M1 - matrix element equal to 1mN.

0, 0, 0 End ME input.

5.16 ME (OP,GOSI)

Mandatory suboption of OP,GOSI

This suboption of OP,GOSI is used both to input and to catalog the starting set of matrix elements as well as to set constraints on the variation of these matrix elements for the least-squares search procedure. The suboption LEVE must immediately precede ME since the catalog of the matrix elements is performed using the level scheme and state indices assigned using the LEVE command. Up to 999 matrix elements are allowed.

Although similar in many respects, the input to the OP,GOSI version of ME is more extensive than that required by the OP,COUL version of ME (Section 5-15). The OP,GOSI version of ME differs from the OP,COUL version in the following respects:

- (a) Restrictions are placed on the range over which each matrix element is allowed to vary during the least-squares search procedure. These restrictions are used to prevent the code from finding unphysical solutions. Moreover, these restrictions limit the range of coupling coefficients ζ over which the ζ -dependence of the q -parameters is fitted.
- (b) Specifications are given defining which matrix elements are to be treated as free variables, and which are to be kept fixed or varied conserving a preset coupling with other matrix elements. This allows a reduction in the number of unknowns by using other knowledge such as lifetime, branching ratio or multiple mixing-ratio data to restrict the number of free parameters used in the least-squares search. Note that lifetimes, branching ratios, multiple mixing ratios and $E2$ matrix elements also can be included explicitly in the data set used for the least-squares search (See OP,YIEL, Section 5-29). Restrictions on matrix elements can be overridden by the OP,RE,A, OP,RE,C and OP,RE,F options or, conversely, additional restrictions can be imposed using the FIX or LCK command of the suboption CONT without changing the ME input file. Input from the OP,GOSI version of ME requires a five-entry record.

A summary of the input format is as follows:

ME

$\lambda_1 0, 0, 0, 0$ Specify multipolarity.

INDEX1, \pm INDEX2, ME, R_1, R_2 List of matrix elements for multipolarity λ_1 plus lower (R_1) and upper (R_2) limits.

.

.

$\lambda_2, 0, 0, 0, 0$ Specify multipolarity.

INDEX1, \pm INDEX2, ME, R_1, R_2 List matrix elements for multipolarity λ_2 .

.

.

$0, 0, 0, 0, 0$ - Terminates input.

Matrix elements for each multipolarity are input as a set preceded by a single record defining the multipolarity, i.e., $\lambda, 0, 0, 0, 0$ where $\lambda = 1$ through 6 from $E1$ through $E6$ respectively, while $\lambda = 7$ for $M1$ and $\lambda = 8$ for $M2$.

Matrix elements are input as:

INDEX1, \pm INDEX2, ME, R_1, R_2 INDEX# is the user-given state number as defined in the LEVE input.

ME = < **INDEX2** || **E(M)** λ || **INDEX1** > The multipole matrix element defined by equation 2.16. It is given in units of e.barns^{1/2} for $E\lambda$ matrix elements and μ_N .barns^{(1-1)/2} for $M\lambda$ matrix elements. The sign assigned **INDEX2** plays no role in the definition of the matrix element. A negative sign signifies coupled matrix elements as discussed below.

The lower and upper limits, respectively, between which the given matrix element **ME** is allowed to vary. Obviously $R_2 > R_1$. Equality of R_1 and R_2 implies that this given matrix element is kept fixed at the value **ME**. Note that in this case, i.e., $R_1 = R_2$, R_1 need not be equal to the **ME**. For example record 1, 2, 0.5, 2, 2 is equivalent to 1, 2, 0.5, 0.5, 0.5

Fixing matrix elements as in the first example is recommended because of two features of the code. First, when an **OP,RE** command is used the limits of fixed matrix elements are set as $R_2 = |R_2|$ and $R_1 = -|R_1|$. If fixing is done as in the second example the matrix element will be allowed to vary only in one direction, i.e., between ± 0.5 . Secondly, when fitting the q -parameters, the ζ -ranges are set according to the actual limits R_1, R_2 . If fixed matrix elements are released at a later stage during the analysis, then there is less risk of incorrect extrapolation if the approach used in the first example is employed rather than later extending the limits without recalculating the q -parameter maps. Note that neither R_1 nor R_2 should be exactly zero, use a small number instead.

A negative sign assigned to **INDEX2** specifies that the matrix element defined by the pair of indices **INDEX1**, **INDEX2** is not a free variable but is a coupled one. In this case R_1 and R_2 are no longer upper and lower limits but the pair of indices of the matrix element to which this matrix element is coupled. The code automatically assigns upper and lower limits to the coupled matrix elements using the upper and lower limits given to the one to which it is coupled while preserving the ratio of the initial values of the coupled matrix elements. These upper and lower limits calculated by the code are used by the code if this coupling is subsequently released. The ratio of coupled matrix elements set by the initial values is preserved in the least squares search if the coupling is not released.]

As an example consider the pair of matrix elements:

1, 2, 2.0, -4, 4
 2, -3, 1., 1, 2

The second statement signifies that the matrix element connecting state 2 to 3 is coupled to the matrix element connecting states 1 and 2 in the ratio:

$$\frac{M(2+3)}{M(1+2)} = +0.5$$

This ratio will be preserved in the least squares search if this coupling is not released. Limits (R_1, R_2) of -2, +2 will be assigned by the code to the matrix element connecting states 2 and 3. These limits are useful if the coupling of these matrix elements is subsequently released.

The convention of coupling matrix elements already described is valid only within a single multipolarity. The coupling of matrix elements belonging to different multiplicities is performed by using $100\lambda + R_2$ as input for the index R_2 of the "slave" matrix element where λ is the multipolarity of the master matrix element. The convention that $\lambda = 7$ for $M1$ and $\lambda = 8$ for $M2$ is still valid.

An important restriction is that there can be only one "master" matrix element with a number of slaves coupled to it if a group of matrix elements are specified to be mutually related. For example, a valid sequence is

1, 2, 2., -4, 4 E2 set of matrix elements
 2, -3, 2., 1, 2
 .
 2, -3, 0.5, 1, 202 M1 set of matrix elements

This describes the coupling of both the $M1$ and $E2$ matrix elements of the $2 \rightarrow 3$ transition to the $E2$ matrix element connecting states 1 and 2. The $E2$ matrix element connecting states 1 and 2 will be treated as a variable, any changes of this matrix element will cause appropriate changes in both the $M1$ and $E2$ matrix elements connecting states 2 and 3.

An invalid sequence is

```
1, 2, 2., -4, 4      E2 matrix elements
2, -3, 1., 1, 2
.
2, -3, .5, 2, 203   M1 matrix elements
.
```

This is invalid because it couples the $M1$ matrix element to the $E2$ matrix element $2 - 3$ which already is a “slave“. Coupling of a set of matrix elements to a fixed one is allowed, it will simply fix the whole set. Nevertheless, it is not allowed to fix the master matrix element using $R_1 = R_2$ of a sign opposite to the matrix element.

For example use of the statement:

```
1, 2, 2.0, -4, -4      will cause a flip of the signs of all matrix elements coupled to the above matrix element.
The correct statement is:
```

```
1, 2, 2.0, 4, 4      Note it is useful to reiterate that it is not necessary to change the ME input in order to alter
constraints etc. in the fitting of matrix elements. The commands OP,RE,A; OP,RE,C; and OP,RE,F
can override some constraints introduced by the ME setup, while the FIX and LCK commands of
suboption CONT allow addition of new constraints.
```

RESTRICTIONS

Failure to comply with the following restrictions may cause erroneous results or an error message will be printed and the job aborted:

- (a) Multipolarities must appear in order from lowest to highest starting with $E\lambda$ then $M\lambda$.
- (b) Matrix elements must belong to the upper triangle, i.e. $INDEX1 < INDEX2$.
- (c) $INDEX$ values must be in increasing order, i.e. odometer ordering.
- (d) The limits $R_2 > R_1$ must be obeyed.
- (e) Neither R_1 nor R_2 should be exactly zero.
- (f) Do not set $R_1 = R_2$ with a sign opposite to the matrix element if couplings are made to other matrix elements.

MATRIX ELEMENT PHASES:

Note that the phase of a wavefunction is arbitrary. However, to facilitate comparison with models it is best to fix the relative phases of states. Choosing one matrix element between two states to be positive couples the relative phases of the wavefunctions of these two states to be the same. Then the phases of any other matrix elements coupling these two states, relative to the phase of the positive one, are observables. Consequently for typical collective bands it is convenient to choose the primary $\Delta I = 2$, $E2$ transitions in the band to have a positive phase locking the state wavefunctions of the band to have the same phase. In addition the phase of one strong matrix element connecting two separate collective bands locks the relative phase between these collective bands.

When entering matrix elements in the upper triangle be careful to enter the correct phase remembering that time reversal invariance relates the time-reversed matrix elements by

$$\langle J_1 \| T^\lambda \| J_2 \rangle = (-)^{J_1 - J_2 - \lambda} \langle J_2 \| T^\lambda \| J_1 \rangle$$

Thus the phase of the matrix elements in the lower triangle is related to the upper triangle phase by the $(-)^{J_1 - J_2 - \lambda}$ phase term. Similar care must be taken comparing the observed relative phases with model predictions.

EXAMPLE:

To illustrate a typical input consider the example discussed in the previous section, but here used under the OP,GOSI command. Let us assume that the number of experimental data is insufficient to perform a completely model-independent analysis. Then some model is used to couple all the diagonal quadrupole matrix elements to the $0_1^+ - 2_1^+$ transition matrix element. In addition, the E2/M1 mixing ratio for the $2_2^+ - 2_2^+$ transition is fixed. The sample input then will be as follows:

```

OP,TITL
NUCLEUS DEFINITION FOR OP,GOSI
OP,GOSI
LEVE
1,1,0,0          ground state is given index 1
2,1,2,0.500
3,1,4,1.00
4,1,2,0.750
0,0,0,0          ends LEVE input
ME
2,0,0,0,0       E2 header
1,2,1.,-2,2     free variable
1,4,1.,-2,2     free variable
2,-2,1.,1,2     coupled to 1V2
2,3,1,-3,3     free variable
2,4,1.,01,5     free variable
3,-3,1,1,2     coupled to 1V2
4,-4,1,1,2     coupled to 1V2
7,0,0,0,0       ends E2 input, starts M1 input
2,-4,1,2,204    coupled to 2V4 E2
0,0,0,0,0       ends ME input

```

In this example there are only four variables, i.e. the $1 \rightarrow 2$, $2 \rightarrow 3$, $1 \rightarrow 4$ and $2 \rightarrow 4$ E2 matrix elements. All the diagonal matrix elements are kept equal to the E2 matrix element connecting $1 \rightarrow 2$, the same holds for the $2 \rightarrow 4$ M1 matrix element which is equal to the $2 \rightarrow 4$ E2 matrix element.

5.17 OP,MINI (MINIMIZE)

This command causes execution of the least-squares fitting of matrix elements to the experimental data. Refer to Section 4.5 for an explanation of the procedures used for the least-square search. The starting set of matrix elements used by OP,MINI depends on the other option commands specified. If OP,RAND is specified then OP,MINI uses the set of random numbers generated by OP,RAND as the set of starting matrix elements. If OP,REST is specified, then the starting set of matrix elements is read from TAPE2. If neither OP,RAND nor OP,REST are specified then the matrix elements input using the suboption ME are used as a starting set. Completion of an OP,MINI command causes the set of matrix elements resulting from minimization to be written onto TAPE2. This current set can be used as a new starting point for continued minimization.

The OP,MINI command provides various switches to allow those matrix elements satisfying certain criteria to be locked during the current minimization procedure. This reduction of the number of free variables can greatly speed up the minimization procedure. The FIX command in the suboption CONT provides another mechanism for fixing matrix elements (see Section 5.3). Sections 7.4.6 and 7.4.7 show the correct location of OP,MINI in the input stream.

The input to OP,MINI comprises the title plus one record, i.e.

OP,MINI

IMODE,NPTL,CHILIM,CONV,TEST,LOCKF,NLOCK,IFBL,LOCKS,DLOCK

where:

IMODE Mode selector. IMODE should be defined as a four-digit number $IJKL$ where:

I = 1 or 2

$I = 1$ specifies that the fast approximation will be used to calculate both S (Eq.4.24) and its partial derivatives.

$I = 2$ implies that S will be calculated using the full Coulomb excitation formalism while its derivatives still will be estimated using the fast approximation.

Use of $I = 1$ is recommended for almost all applications. The time required to complete the minimization step using $I = 2$ is about an order of magnitude greater than when using $I = 1$. The use of $I = 2$ should be reserved for small cases or for cases requiring extreme accuracy in locating the minimum. The TEST switch, described below, provides a more efficient way of retaining high accuracy than using $I = 2$.

J = 0 or 1

$J = 0$ selects the simple steepest descent minimization while $J = 1$ selects the gradient and gradient derivative method (see Section 4.5).

K = 0 or 1

$K = 0$ implies that the absolute changes in matrix elements will be used to improve the minimum while $K = 1$ requests the use of the relative changes. To first order $K = 1$ corresponds to using the logarithms of matrix elements as independent variables instead of the matrix elements themselves, as when $K = 0$.

L = 0 or 1

$L = 0$ specifies that the experimental yields, branching ratios etc. will be used as dependent variables to construct the S function while $L = 1$ requests that a logarithmic scale will be used for dependent variables.

There are no restrictions concerning the selection of the above switches and any combination can be used. Proper selection of IMODE can speed up the minimization procedure appreciably and is case-dependent

NPTL The maximum number of steps of minimization allowed.

CHILIM The S criterion to stop minimization. That is, the minimization terminates if $S < CHILIM$.

CONV The convergence criterion to stop minimization when $|\bar{M}_{i+1} - \bar{M}_i| < CONV$ where \bar{M}_i denotes the vector of matrix elements at the i -th step of minimization. This convergence criterion also is used by the iterative search for the minimum along the gradient direction. This iterative procedure is stopped when the absolute difference between two subsequent iterations is less than CONV. Minimization may be resumed after the CONV criterion is fulfilled if $LOCKF = 1$ (see below). Note: any of the above three criteria, namely NPTL, CHILIM and CONV, stops minimization if fulfilled. The LOCKF switch resumes minimization only when the calculation was terminated because convergence was achieved. A reasonable value for CONV is 10^{-4} .

TEST Specifies recalculation of the internal correction factors every time S drops by a factor of TEST. In the limit $TEST \leq 1$ the internal correction coefficients will be calculated at each step of minimization which corrects for the discrepancy between the value of S calculated using the fast approximation and S coming from the full formalism. Note that this is faster than using $I = 2$ since only one full calculation is required per step for $TEST \leq 1$ whereas each sampling of the minimized function during the one-dimensional search along the gradient direction will require a full Coulex calculation using the $I = 2$ option.

LOCKF Can equal 0 or 1. $LOCKF = 0$ implies that minimization will be terminated if the convergence limit CONV is satisfied. $LOCKF = 1$ causes the program to fix the $NLOCK$ matrix elements having the most significant S derivatives. This switch provides a different subspace of matrix elements, this can be useful when trapped in a local minimum or when the matrix elements having weak influence on S should be allowed to vary. As described in Section 4.5, GOSIA will lock the matrix element having the most significant S derivative if the search directions in two consecutive steps are close to being parallel, even if $LOCKF = 0$.

NLOCK The number of matrix elements having the largest derivatives of S to be locked if $LOCKF = 1$ and the convergence limit CONV is satisfied. See LOCKF.

IFBL May equal 0 or 1. If $IFBFL = 0$ then the derivatives are calculated using only the forward difference method whereas $IFBFL = 1$ causes the forward-backward difference method to be used for calculation of the derivatives. The $IFBPL = 1$ option is justified only in the vicinity of the minimum when the forward difference method may produce spurious results since the $IFBFL = 1$ option is a factor of two slower than the $IFBFL = 0$ option.

LOCKS May equal 0 or 1. If $LOCKS = 1$ then the code fixes, at the first stage of minimization, all matrix elements M_i for which the absolute value of the partial derivative of S with respect to M_i is less than DLOCKS (the gradient is always normalized to unity), i.e

$$\left| \frac{\delta S}{\delta M_i} \right| < DLOCKS$$

This allows an automatic reduction of the number of variables for which derivatives need to be calculated to only those having a significant influence. LOCKS=0 switches off this option.

DLOCKS Specifies the limit of the derivative below which a matrix element will be fixed if $LOCKS = 1$.

Note that the yields printed in OP.MINI are defined to be

$$Y^{Mini}(I \rightarrow I_f) = \frac{Y^{Point}(I \rightarrow I_f)}{\sigma_R(\theta_p) \cdot \sin(\theta_p)}$$

do not include $\sigma_R(\theta_p) \cdot \sin(\theta_p)$. $Y^{Point}(I \rightarrow I_f)$ is given by equation 4.16. See also section 5.18, OP.POIN

The experimental values are compared to the calculated $Y^{Mini}(I \rightarrow I_f)$ which do include the $\sigma_R(\theta_p) \cdot \sin(\theta_p)$ term. Thus these missing terms in $Y^{Mini}(I \rightarrow I_f)$ are absorbed into the normalization constants for each experiment.

5.18 OP,POIN (POINT CALCULATION)

This option command causes execution of a calculation of the γ -ray yields for one scattering angle and one bombarding energy as specified for each experiment in EXPT. OP,POIN can be used to simulate 'corrected' experimental γ yields. In this mode OP,POIN also generates a 'corrected experimental yields file' on TAPE4, which can be used subsequently for simulating the real experiments (e.g. to analyze the influence of the matrix elements on the supposedly observed yields). Note: when executing OP,POIN one should set the experimental yields file selector (NTAP in OP,YIEL input) to 0 - see 5.29. Section 7.4.3 shows the correct location of OP,POIN in the input stream.

The input to OP,POIN is as follows:

OP, POIN

IFL, YLIM $IFL = 0$ specifies the normal calculation, $IFL = 1$ the 'simulation' calculation. $YLIM$ is redundant if $IFL = 0$, whereas if $IFL = 1$ it specifies that all transitions whose yield divided by the yield of the normalizing transition (defined in OP,YIEL) exceeds $YLIM$ will be treated as 'experimentally observables' and will be included in the TAPE4 file. OP,POIN will also produce a file containing the γ detector efficiency information if OP,RAW was executed and PRT, flag 20 was set to 1 (TAPE23). Note that the decay energies in TAPE23 output are Doppler-shifted.

Note that OP.POIN evaluates the point γ -ray yield in the laboratory frame for transition $I \rightarrow I_f$ that is defined by equation 4.16. That is:

$$Y^{Point}(I \rightarrow I_f) = \sin(\theta_p) \int_{\phi_p} \frac{d^2\sigma(I \rightarrow I_f)}{d\Omega_\gamma d\Omega_p} d\phi_p \quad (4.16)$$

where the integrand is given by

$$\frac{d^2\sigma(I \rightarrow I_f)}{d\Omega_p d\Omega_\gamma} = \sigma_R(\theta_p) \sum_{\substack{k \\ \chi \geq 0}} R_{k\chi}(I, I_f; \theta_p) P_{k\chi}(\theta_\gamma) (2 \cos \chi (\phi_p - \phi_\gamma) - \delta_{\chi 0}) \quad (4.13)$$

Note that $Y^{Point}(I \rightarrow I_f)$ includes the Rutherford cross section, the $\sin(\theta_p)$ term, integration over the projectile ϕ_p angle, the deorientation effect and γ -detector Q_K attenuation coefficients.

The total number of coincident γ -rays detected then is given by

$$Counts = 10^{-27} \cdot \left[\frac{Q}{\hat{q}e} \right] \cdot \left[\frac{N_A}{A} \right] \cdot [\rho dx] \cdot Y^{Point}(I \rightarrow I_f) \cdot \Delta\theta_p \cdot \varepsilon_p \cdot \varepsilon_\gamma \cdot \Delta\Omega_\gamma$$

where:

- Q is the integrated beam charge [C]
- \hat{q} the average charges state of the beam
- e the proton charge [$1.602 \times 10^{-19}C$]
- N_A Avogadro number [$6.022 \times 10^{23}atoms/mol$]
- A Target mass number [g/mol]
- ρdx areal target thickness in [g/cm^2]
- $Y^{Point}(I \rightarrow I_f)$ OP.POIN output in [$\frac{mb}{sr \cdot rad}$]
- $\Delta\theta_p$ Projectile scattering angle range [rad]
- ε_p particle detection efficiency per unit solid angle
- ε_γ γ -ray detector efficiency excluding the geometrical solid angle
- $\Delta\Omega_\gamma$ geometrical solid angle of the γ -ray detector. Note that usually one only knows the product $\varepsilon_\gamma \cdot \Delta\Omega_\gamma$

5.19 OP,RAND (RANDOM ME)

This option generates a set of random matrix elements which replaces the set defined previously for the current job. Each matrix element in the random set is created assuming a uniform distribution of random numbers lying between the limits specified for each matrix element in the input to ME. This option is used to eliminate bias in the analysis and to test the uniqueness of the least-squares fit to a given data set by retrying the minimization starting from a number of sets of random matrix elements. If OP,RAND is used it should immediately precede OP,YIEL.

The input requires only one number:

SEED: A floating-point seed number for the internal random number generator. SEED should be larger than unity and less than 32000. Note that FORTRAN random number generators are reproducible, giving the same sequence of random numbers when called. Therefore SEED should be different for repeated runs, otherwise the results will be identical.

5.20 OP,RAW (RAW UNCORRECTED γ YIELDS)

This option allows defining the γ -intensities for some, or all, experiments as “raw“, i.e. not detector efficiency-corrected. In addition, the raw γ intensities can be summed over a set of γ detectors. This feature is important when analyzing data from multidetector arrays (crystal balls). Spectra from the γ detectors symmetric with respect to the recoil direction, identically Doppler-shifted, can be added to increase statistics and to reduce the number of datasets to be processed (such sets of data will be referred to as “clusters“). GOSIA can handle such data provided that the efficiency calibration of the individual detectors is input. This information should be given using OP,RAW and should be executed if at least one experiment involves raw data or clusters. OP,RAW should immediately follow OP,YIEL (5.31). If OP,RAW is to be used, the first entry of OP,GDET (5.10) should be negative to produce the additional file, TAPE8, required by OP,RAW. Do not use OP,RAW if all γ intensities are efficiency-corrected.

Energy-dependent efficiency calibration for each individual γ detector is assumed to follow the functional form used by the code GREMLIN (see Chapter 12).

The input to OP,RAW is as follows:

IEXP Number of experiment to be labeled as raw (according to the sequence of CONT suboption EXPT).

A1, A2, ..., A8 Logical detector 1

A1, A2, ..., A8 Logical detector 2

.

A1, A2, ..., A8 Parametrization of efficiency curves for all γ detectors used in the experiment *IEXP*. Parameters *A1* through *A8* correspond to $a_0, a_1, a_2, a_3, f, N, b, c$, as defined in GREMLIN. See Chapter 12. Use $f = 0$ to switch off the *F* factor and $c = 0$ to switch off the *W* factor. These sets of parameters should be ordered according to the sequence of “logical“ γ detectors, as defined in OP,YIEL (IV.31) input. The Doppler shift of the γ energies is taken into account when evaluating the detection efficiency

NC Number of clusters.

ID1 Number of γ detectors for cluster #1.

I1, I2...I(ID1) Indices of “logical“ detectors forming cluster #1, according to the sequence defined in OP,YIEL.

.

0 IEXP=0 ends input.

The sequence *ID1...* obviously should be repeated *NC* times to define every cluster, unless *NC* = 0 (no clusters). The whole input is to be defined for every raw experiment. The use of OP,RAW imposes an important constraint on how the experimental γ yields should be ordered in either TAPE3 or TAPE4. The sequence of γ yields data sets should follow the HIGHEST “logical“ detector index within a cluster. Single detectors can be handled as if they were one-detector clusters, without labeling them as clusters.

Example:

Three γ detectors were used and the γ -ray spectra from the detectors labeled 1 and 3 in OP,YIEL assignment were added. In this case there are two clusters, namely composite detector 1 + 3 and single detector 2. The input to OP,RAW should then be as follows:

OP,RAW
1 experiment #1 labeled as raw
A1....A8 for logical detector 1
A1....A8 for logical detector 2
A1....A8 for logical detector 3
1 one cluster
2 two detectors in this cluster
1,3 logical detectors forming this cluster
0 ends OP,RAW input

In this case the experimental γ yields from detector 2 should precede these from the 1 + 3 cluster (highest logical detector index for the data from detector 2 is 2, while for 1 + 3 cluster it is 3).

5.21 OP,RE,A (RELEASE,A)

This option voids all coupling of matrix elements and releases fixed ones. As described in ME (Section 5.16) matrix elements are fixed by specifying identical upper and lower limits $R1 = R2$. When a fixed matrix element is released these upper and lower limits are set equal to $-|R2|$ and $|R2|$, respectively. Consequently, it is useful to use $|R1| = |R2| > |ME|$ when fixing matrix elements to ensure that the released matrix element can be varied within an appropriate range.

5.22 OP,RE,C (RELEASE,C)

This option releases fixed matrix elements but retains the couplings of matrix elements. No additional input is required. As described in 5.16 and 5.21, when fixed matrix elements are released the upper and lower limits are set equal to $|R2|$ and $-|R2|$, respectively.

5.23 OP,RE,F (RELEASE,F)

This option voids the coupling of matrix elements but retains the fixing of matrix elements. No additional input is required. As described in section 5.16, the upper and lower limits assigned to a coupled matrix element on its release are calculated from the corresponding limits assigned to the master matrix element using the ratio of initial values of the coupled matrix elements.

Note that if OP,RE is used it should immediately precede OP,ERRO or OP,MINI to function correctly.

5.24 OP,REST (RESTART)

This option causes a set of matrix elements to be read from file TAPE2 which then replaces the set defined by the input to ME for the current job. This option enables continuation of a minimization or performing most other operation using the latest set of matrix elements instead of the one appearing in the ME setup. Note that each OP,MINI command causes its final set of matrix elements to be written on file TAPE2. If OP,REST is used it should immediately follow OP,YIEL.

OP,REST provides the possibility to manually overwrite some of the matrix elements stored on TAPE2 for the current job. This feature can be the useful time-saver when, for example, better estimates of some matrix elements have been found during a preliminary diagonal errors calculation. The input to OP,REST should be given as:

OP,REST

I_1, V_1 Index of the matrix element (according to the sequence of ME)

I_2, V_2 to be overwritten (I) and its new value (V).

.

0,0 Two zeros terminate input.

Example:

OP,REST

0,0 This sequence leaves the values stored on TAPE2 unchanged.

5.25 OP,SELE (SELECT)

This option creates the correlation matrix for use in Op,ERRO. To prepare the input information for SELECT it is necessary to execute OP,MINI with CONT switch SEL, and the default value of the print parameter 4, i.e. 4, -2. This should be done at a final stage of minimization prior to the error calculation. The information for SELECT is written by GOSIA on TAPE18 which should be attached to SELECT also as TAPE18. No other input is necessary. The output from SELECT is written on TAPE10 and should be attached to the OP,ERRO job as TAPE18. $IFC = 1$ implies that the correlation matrix will not be used. In this case it is not necessary to create and attach TAPE18. It is however strongly recommended that $IFC = 1$ be used only for small cases with all matrix elements of similar significance. Otherwise, selecting $IFC = 1$ will dramatically increase the execution time with no effect on the result. IFC is redundant if $IDF = 0$.

5.26 OP,SIXJ (SIXJ SYMBOL)

This stand-alone option creates a 6- j table to be used by the quadrupole sum-rules program SIGMA (see Chapter 6). OP,SIXJ is not related to an investigated nucleus, thus it can be inserted anywhere in the input stream, even as the only option command. The output is written to a file TAPE14. No further input is required.

Note: The execution of OP,SIXJ will cause GOSIA to stop the job after the 6 – j symbol table has been written. The remainder of the input will be ignored.

5.27 OP,STAR (START)

Execution command to calculate Coulomb excitation amplitudes and probabilities, not the γ -ray yields, at the energy and scattering angles specified in the EXPT input. This comprises a subset and consequently an alternative to OP,POIN. The OP,STAR requires no input.

Note that OP,STAR is (besides the OP,SIXJ and OP,GDET commands) the only executable option which does not require the γ -ray deexcitation related information provided using OP,YIEL and thus can immediately follow OP,COUL or OP,GOSI commands.

5.28 OP,THEO (COLLECTIVE MODEL ME)

Coulomb excitation is the preeminent probe of collective modes in nuclear structure. Consequently frequently it is convenient to calculate Coulomb excitation cross sections assuming a set of matrix elements related by a collective model. OP,THEO generates matrix elements according to the geometrical model following Bohr-Mottelson prescription (General Structure of Matrix Elements, paragraph 4-3d in Nuclear Structure) (BOH69).

OP, THEO generates only the matrix specified in the ME input and writes them to the REST file. Therefore it should be used after OP, COUL or OP, GOSI, but before OP, REST command is executed. Fixing, coupling and releasing of the matrix elements is controlled by the ME and CONT commands, the only function of OP,THEO being to create numerical values and write them to the restart file. This allows making model-dependent analyses by specifying the coupling scheme, generating a set of matrix elements and, keeping the values coupled, performing the minimization, thus effectively fitting only geometrical intrinsic moments which can greatly reduce the number of fitted variables. To define the OP,THEO input the user must divide the levels specified in the LEVE input into bands of definite values of K quantum number. The first entry under OP, THEO is the number of bands, which, as an input-saver feature, can be given as a negative integer, in which case the remainder of the input to OP, THEO will be ignored and the contents of the restart file not affected. This is helpful if some matrix elements are added or removed using ME option - OP, THEO then can be easily reactivated.

OP,THEO input is divided into two loops. The first one is the definition of the bands and the levels ascribed to be band members. As usual, LEVE-defined state indices are used to identify the levels. The second loop is the multipolarity loop, which should exhaust all couplings defined in the ME input. Here for each band-to-band coupling (band indices being either identical for inband matrix elements or different for interband matrix elements) one should specify relevant intrinsic moments for a given multipolarity. In general there are three intrinsic moments that could be involved. For in-band or equal- K interband transitions only one of them, marked $Q1$ is relevant. For non-equal K values generally two moments with the projections equal to the sum and difference of K 's are required ($Q1$ and $Q2$), unless one of the K 's is zero, when again only $Q1$ is needed. For the K -forbidden transitions a three parameter Mikhailov formula is used. Thus, in general, three Q -values are to be input for each band-to-band coupling. Note that $Q3$ - a decoupling parameter - is irrelevant if none of the K -values assumes the value of $1/2$ and $Q2$ is irrelevant for in-band transitions and for K -allowed, one $K = 0$ interband couplings. Nevertheless, three numbers are required for each band-to-band coupling.

The specification of multiplicities follows the general convention of GOSIA - $E1$ through $E6$ are labeled just by 1 through 6, while $M1$ is labeled as 7 and $M2$ as 8. Definition of bands and multiplicities should exhaust all couplings included in ME scheme. It is important that calculated matrix elements fit within the user-specified limits.

The structure of the input to OP, THEO is:

NBANDS Number of user-defined bands. If negative OP,THEO is ignored

K,NLEV Band definition - K of a band, number of levels in band #1

N1,N2,.....,NNLEV Indices of levels forming band #1

.

. The above two records should be repeated NBANDS times to define all bands

.

λ_1 Start of multipolarity loop - first multipolarity

NB_i,NB_j Band indices

Q1, Q2, Q3 Intrinsic moments

. The above sequence should be repeated until all possible

· in- and interband couplings for the first multipolarity are exhausted
·
0,0 Ends first multipolarity definition
 λ_2 Second multipolarity
NB_i, NB_j
Q1, Q2, Q3
·
·
·
0,0 Ends second multipolarity definition
·
·
·
0 Ends multipolarity loop and the input to OP, THEO

Example:

Assume an even-even nucleus X with two bands - a ground state band and a gamma-vibrational band.
The LEVE and ME setup is as follows:

LEVE
1,1,0,0
2,1,.2,2 Levels 1,2,3 form the ground-state band, while 4,5,6 form the gamma band
3,1,4,.5
4,1,2,.7
5,1,3,1.1
6,1,4,1.5
0,0,0,0
ME
2,0,0,0,0
1,2,1,-2,2
1,4,1,-2,2
2,2,1,-2,2
2,3,1,-2,2
2,5,1,-2,2
2,6,1,-2,2
3,3,1,-2,2
3,5,1,-2,2
3,6,1,-2,2
4,4,1,-2,2
4,5,1,-2,2
4,6,1,-2,2
5,6,1,-2,2
6,6,1,-2,2
7,0,0,0,0
2,4,1,-2,2

2,5,1,-2,2
3,5,1,-2,2
3,6,1,-2,2

Matrix elements on the restart file can be generated by OP, THEO using the following sequence:

```
OP, THEO
2          Two bands
0,3       K of the gsb, # of levels
1,2,3     Level list for the gsb
2,3       K of the gamma band, # of levels
4,5,6     Level list for the gamma band
2         Multipolarity E2
1,1       In-band, gsb
1,0,0     Q1, two zeros irrelevant
1,2       Interband E2
1,1,0     Q1,Q2- Mikhailov formula, none of the K's=1/2, so Q3 irrelevant
2,2       In-band, gamma band
1,0,0     In-band Q1, Q2 and Q3 irrelevant
0,0       Ends E2 loop
7         M1 loop
1,2       Interband M1
1,1,0     Q1 and Q2 for Mikhailov formula
2,2       In-band M1
1,0,0     Q1 for in-band transitions
0,0       Ends M1 loop
0         Ends multipolarity loop and OP, THEO input
```

As a result, the restart file will be created overriding the values of matrix elements as given in ME input. If the first entry, NBANDS, is changed to -2 OP, THEO will become inactive.

5.29 OP,TITL (TITLE)

This option requires one input record consisting of up to 80 alphanumeric characters. This string is reprinted as a run title. OP,TITL should appear as the first option command, or follow OP,FILE command if used, since execution is immediate. Otherwise, the title will not appear as a header of the output. OP,TITL can be skipped. If more than one title line is wanted this command can be repeated as many times as desired.

5.30 OP,TROU (TROUBLE)

This troubleshooting option can be used to pinpoint erroneous experimental data and to check if the minimization is trapped in a local minimum. As described in detail in section 4.7, this module analyzes the contribution to χ^2 of the deexcitation γ -ray yields to ascertain if there is an inconsistency in the data. The parameter r_k defined in equation 4.71 is a measure of the consistency of the data. That is, it identifies if the current minimum of χ^2 , with respect to a given matrix element, results from cancellation of large and opposite contributions due to inconsistent data or whether all the data are consistent.

The input consists of one record:

NS,RL NS is the number of experimental yields giving the largest positive and negative components of the derivative of χ^2 with respect to a given matrix element to be selected and printed out. This information will appear in the output if for this given matrix element r_k exceeds RL . The χ^2 function is defined by Eq. 4.69.

NOTE:

- 1) OP,TROU must be used with, and immediately follow, OP,MINI. OP,TROU must be the last option before OP,EXIT
- 2) OP,TROU must be used in conjunction with the yields sensitivity map, i.e. print control parameter $IPRM(4)$ in *CONT* (Section 5.3) must assume its default value equal to -2 .
- 3) The OP,TROU analysis will appear at the end of the output file (unit 22).

5.31 OP,YIEL (YIELDS)

This option is mandatory if it is desired to calculate the yields of deexcitation γ -rays following Coulomb excitation. The first part of this option is used to input the internal conversion coefficients and the description of the γ -ray detectors. This first section is used in conjunction with either OP,COUL or OP,GOSI. The second part of this option is used in conjunction with OP,GOSI to input additional information required for the least-squares fitting such as normalization constants, γ -ray branching ratios, lifetimes, $E2/M1$ mixing ratios, and diagonal or transitional E2 matrix element data to be included in the fit. The input to OP,YIEL must be complete and consistent with the option of the code selected. Section 7.4 shows the correct position of OP,YIEL in the input stream for various calculations.

OP,YIEL defines the “logical“ γ detectors, which are referred to everywhere in the input except in OP,GDET. Different logical detectors may be in fact the same “physical“ ones. This distinction allows to reduce the number of experiments defined in all cases where the setup used is symmetric with respect to the beam axis. As an example, let us consider the experiment in which two particle detectors are placed symmetrically about the beam axis at angles (θ, ϕ) and $(\theta, \phi, +\pi)$, respectively. Gamma rays are detected in coincidence with scattered particles in one Ge detector placed at position (θ_g, ϕ_g) , so the scan of event-by-event data yields two γ spectra. A straightforward approach is to define two experiments, differing only by the placement of the Ge detector with respect to the scattered particles. Instead, one can define only one experiment (keeping in mind that the Coulomb excitation depends on θ , but not on ϕ) and two logical detectors, one at (θ_g, ϕ_g) , and another at $(\theta_g, \phi_g + \pi)$. Both are identified as the same “physical“ detector, but different sets of γ yields (both spectra resulting from the scan) are assigned to them. Such a manipulation saves almost 50% of CPU time since evaluation of deexcitation γ yields requires negligible computation time compared to the excitation calculation.

GOSIA allows also to define logical detector clusters (see OP,RAW-5.20), i.e. sets of γ yields which result from summing the raw spectra, therefore the number of experimental data sets is not always equal to the number of logical detectors. Further description will refer to the “logical“ detectors simply as γ detectors, which should be distinguished from either “physical“ detectors or data sets.

Brief resumé of the input to OP,YIEL:

OP, YIEL

IFLAG Assumes the values of 0 or 1. *IFLAG* = 1 means that the correction to the angular distribution of the γ -rays due to a finite distance traveled by the decaying nucleus will be included in the calculation (see Section 4.3). *IFLAG* = 0 switches off this correction.

N1, N2 Number of energies ($N1 \leq 50$) and multiplicities (*N2*) to define the internal conversion coefficients. If *N1* is negative the internal conversion coefficients are taken from the table of values for each transition created by *OP, BRIC*.

E₁, E₂, ..., E_{N1} Energy meshpoints for the internal conversion coefficients (in MeV), common for all multiplicities for the nucleus of interest. The code uses four point interpolation between meshpoints. Note that the large discontinuities in the internal conversion coefficients at the *K* and *L* edges can be taken into account correctly by ensuring that there are at least two mesh points between the transition energy of interest and the nearest discontinuity; that is, so that the four point interpolation does not straddle any discontinuity.

I1 Multiplicity *I1*.

CC(I1, 1)..CC(I1, N1) Internal conversion coefficients for multiplicity *I1* at each energy meshpoint (*N1* entries). Note that internal conversion coefficients can be obtained from the NNDC (US National Nuclear Data center) at <http://www.nndc.bnl.gov/bricc/>.

I2 This sequence should be repeated for all multiplicities defined, i.e. *N2* times.

CC(I2, 1)..CC(I2, N1)

NANG(I)..NANG(NEXP) Number of γ -ray detectors for each of the NEXP experiments. NANG(I) can be entered as its true value with a negative sign, which means that the γ detector setup is identical to that of the previous experiment, for example if the experiments differ only by the scattering angle. In this case the next three records need not be entered.

IP(1)..IP(NANG(I)) Identifies the γ detectors used in a given experiment according to the sequence the “physical“ detectors were defined in the input to OP,GDET (Section 5.10). For example, if $IP(L) = K$, then it is understood that the L -th detector used in the current experiment is the K -th detector defined in the OP,GDET input. This assignment of “physical“ detectors to the “logical“ ones is the only instance the “physical“ detectors are referred to. Everywhere else the γ detectors are the “logical“ detectors.

$\theta_1, \dots, \theta_{NANG(I)}$ θ angles for γ detectors used in experiment I .

$\phi_1, \dots, \phi_{NANG(I)}$ ϕ angles for γ detectors used in experiment I .

The above sequence, starting from the definition of IP should be repeated for each of NEXP experiments defined, except of the experiments for which NANG is negative. The experiments must be ordered according to the sequence they appear in EXPT input.

NS1, NS2 The transition from $NS1$ to $NS2$ to be used as the normalization transition where $NS1$ and $NS2$ are the state indices.

End of input for OP, COUL. The remainder of the input is required only if OP,GOSI was specified.

NDST Number of data sets in experiment 1. Usually equal to NANG(1), unless detector clusters were defined in OP,RAW.

UPL₁...UPL_n Upper limits for all γ detectors used in experiment 1.

YNRM₁....YNRM_n Relative normalization factors of γ detectors used in experiment 1.

The above three records should be repeated for all experiments according to the sequence of EXPT, except for those assigned the negative value of NANG. Subscript $n = NDST$ denotes the number of data sets.

NTAP Specifies file containing experimental yields. NTAP=0 is used when this file is not necessary, e.g. when running OP,STAR or OP,POIN under OP,GOSI. Otherwise NTAP=3 or 4 corresponding to file TAPE3 or TAPE4, respectively. NTAP must equal 3 if OP,CORR is executed and must equal 4 if OP,ERRO is executed.

NBRA, WBRA Number and weight of branching ratios.

I1, I2, I3, I4, B, DB... NBRA records of branching ratios.

· $(I1 \rightarrow I2)/(I3 \rightarrow I4) = B/DB$ where $I_1 \equiv I_3$ and

· where $I1, I2, I3, I4$ are state indices, B is the branching ratio with error DB . Note $I1 = I3$ is the initial state that γ decays and $I2, I4$ are the final states.

NL, WL Number and weight of mean lifetimes.

INDEX, T, DT T/DT is the mean lifetime of level INDEX.

... NL records, lifetimes in picoseconds

NDL, WDL Number and weight of E2/M1 multipole mixing ratios.

IS, IF, DELTA, ERROR $\delta \frac{E2}{M1}(IS \rightarrow IF) = DELTA \pm ERROR$

... NDL records

NAMX, WAMX Number and weight of known EM matrix elements.

LAMBDA, INDEX₁, INDEX₂, ME, DME Repeat NAMX times.

... *LAMBDA* is the multipole, *Eλ* with $\lambda = 1, 2, 3, 4, 5, 6$ and *M1* with *LAMBDA* = 7. *INDEX_n* is the level index. Note the restriction $INDEX_1 \leq INDEX_2$. *ME* is the *Eλ* or *M1* matrix element, in the same units as for the *ME* input, while *DME* is the error, assumed to be symmetrical. In the fit procedure the sign of *ME* is ignored if *INDEX1* is not equal to *INDEX2*.

The input of known electromagnetic matrix element data concludes the input to OP,YIEL.

Extended description of OP,YIEL

IFLAG Determines whether the effect of the finite distance traveled by the decaying nucleus on the γ -ray angular distribution is to be included (*IFLAG* = 1) or not (*IFLAG* = 0). This effect, taken into account as a first-order correction (see Section 4.3), is important only for the long-living states and should not be included in the cases where all the life-times are supposed to be in the subnanosecond range to speed up the calculations. Also, the first-order correction may be inhibited if it is necessary to change the sign of some matrix elements, in which case the lifetimes calculated during the minimization may assume unreasonable values if the matrix elements determining the lifetime of a level happen to be close to zero during the search procedure. In such cases GOSIA will automatically reset *IFLAG* to 0 if *IFLAG* was input as 1. It is recommended to use *IFLAG* = 1 only at the final stage of the minimization, when the signs of the matrix elements are already defined. *IFLAG* = 1 should not be used in conjunction with OP,RAND.

N1, N2 *N1* is the number of energies used as meshpoints for input of the internal conversion coefficients for the nucleus of interest. Energy meshpoints are presumed to be identical for each multipolarity.

- a) For *N1* positive Gosia uses cubic spline interpolation of the input internal conversion coefficients at these meshpoints by four-point interpolation. At least one point below the lowest transition energy and one point above the highest are required for reliable interpolation of internal conversion coefficients. Use a reasonable range of internal conversion coefficients to ensure a reliable interpolation. Check the interpolated values at least once by requesting the print-out of internal conversion coefficients (refer to print controls described in Section 5.3). Note that the Lagrangian four point interpolation used is not able to take into account the discontinuities which may be present at low γ energies due to the *K*, *L*, etc cutoff edges. GOSIA calculates the *K* and *L* edge energies and uses different interpolation functions above the *K* edge, between the *K* and *L* edges, and below the *L* edge to account for the discontinuities in the internal conversion coefficients at these thresholds. Thus it is necessary to include at least three meshpoints below the *L* edge and between the *L* and *K* edges. Since the interpolation uses two points on both sides of the decay energy, make sure that the discontinuity is separated from the closest decay energy by at least two meshpoints. This is important for converted transitions even if the γ -ray branches are not observed.
- b) For *N1* negative the internal conversion coefficients are taken from the table of values for each input matrix element that has been created by *OP, BRIC*.

N2 is the number of multiplicities for which internal conversion coefficients are given. This must be consistent with the number of multiplicities used for the matrix element setup in *ME*.

E₁, E₂, E₃, ... E_{N1} Input of the energies used as meshpoints for the internal conversion coefficients. Units of MeV.

I1 Multipolarity of the internal conversion coefficients. *I1* = 1...6 for *E1*...6 respectively. *I1* = 7 for *M1* and 8 for *M2*.

CC1(I1), CC2(I1), ..CCN1(I1) Internal conversion coefficients for multipolarity *I1* at the energy meshpoints given above. Repeat the multipolarity, *I1*, and internal conversion coefficient records *CC* for all *N2* multiplicities.

NANG(1)...NANG(NEXP) NANG is the number of γ detectors for each experiment. NANG is limited to <200 . In many cases, a series of logically different experiments is in fact performed during one “physical“ run, for example when position-sensitive parallel-plate particle detectors are used, providing the data for a wide range of scattering angles. For this type of experiments the physical setup of the γ detectors remains unchanged, therefore repeating the γ -detector related input would be redundant. To reduce the unnecessary input, one can enter NANG(I) as the true value of the γ detectors used with a negative sign. It will be understood that the γ detector setup is the same as for the previous experiment, in the EXPT input sequence. In this case the next three records should not be input.

IP(1),IP(2)..IP(NANG(I)) The definition of the “physical“ γ detectors used in an experiment I according to the sequence of OP,GDET.

$\theta(1),\theta(2),\dots\theta(NANG(I))$ The angular coordinates (θ,ϕ) in degrees of each γ detector in the same coordinate frame as used for the EXPT input for this experiment.

$\phi(1),\phi(2),\dots\phi(NANG(I))$ The z axis always is in the direction of the incident beam.

N.B. It is recommended that for each experiment the γ -ray detector giving the best quality data be selected as detector number one. This is because only γ -ray detector number one is taken into account for certain features of the code, namely, generation of the yield sensitivity maps, i.e. $(\frac{\partial \ln(YIELDS)}{\partial \ln(ME)})$ and the consistency tests performed by the troubleshooting routine OP,TROU.

The sequence of input records starting from the definition of IP must be repeated for all experiments $I=1,NEXP$ as defined in EXPT input, unless NANG is negative for a given experiment I.

NS1,NS2 The transition from the state with index $NS1$ to the state with $NS2$ is chosen as a normalizing transition. Make sure that the energy of state $NS1$ is higher than that for state $NS2$. The transition is common to all experiments. It is used for setting upper limits of unobserved γ -ray transitions and for printout compiled by OP,POIN.

The input to OP,YIEL required by OP,COUL ends at this point. The remainder of the input is related to the least-squares fitting and needs to be entered only for OP,GOSI. The following three records should be input if $NANG(I)$ is positive.

NDST Number of data sets, equal to the number of γ detectors if no detector clusters were defined in OP,RAW. $NDST \leq 32$, while up to 20 clusters per experiment can be defined.

UPL₁...UPL_n These are the upper limits expressed as a fraction of the normalizing transition, $NS1 \rightarrow NS2$. The number of entries in each record corresponds to the number of data sets for each experiment defined, i.e. $n = NDST$. If the calculated yield of any unobserved γ -ray transition, divided by the yield of the normalizing transition, exceeds UPL , then it is included in the calculation of the least squares summation used for the fit. Otherwise, the unobserved transitions whose calculated yields are below the limit of detection for a particular experiment are not included in the least squares fit procedure. (See Section 4.6).

YNRM₁...YNRM_n $YNRM_i$ is the relative normalization factor for Ge detector i used in experiment $IEXP$. GOSIA does not require the absolute normalization for a given experiment, instead, the code finds the best normalization constant correlating calculated and experimental γ yields. See record LN in section 5.8 $EXPT$.

For each γ detector i used in experiment $IEXP$ the calculated and experimental γ yields are correlated by:

$$Y_i^{\text{exp}} = Y_i^{\text{calc}} * C_i(IEXP)$$

where $C_i(IEXP)$ is the normalization constant for experiment $IEXP$ and detector i . The code fits the common normalization factor for all γ detectors used in a given experiment $IEXP$, $C(IEXP)$, related to the individual γ detectors' normalization factors $C_i(IEXP)$ by:

$$C_i(IEXP) = C(IEXP) * YNRM_i(IEXP)$$

Different experiments may have a known relative normalization, e.g. when different projectile scattering angle slices are defined as experiments. In this case the physical setup, i.e. the location of γ detectors etc. is the same for a whole group of experiments and their relative normalization is set only by the Rutherford cross sections and the efficiencies of the particle detectors for specified scattering angle ranges. The known relative normalization may be used by specifying the proper LN indices in the $EXPT$ input, then the code will use given $YNRM_i(IEXP)$ values to fit the common $C(IEXP)$ value for the whole subgroup of experiments, the definition of $C_i(IEXP)$ for individual γ detectors remaining the same. Note that it is possible to request independent normalization for each individual γ detector by using the $CONT$ switch INR . In this case the $YNRM$ input is redundant. The normalization constants calculated using user-supplied information are printed by the code along with the recommended relative $YNRM$ values calculated independently for each γ detector.

Consider the example of ^{72}Ge discussed in the description of $EXPT$ (see section 5.8). Assume that there are two γ -detectors for each experiment and that a correction needs to be made to the detection efficiency of the second detector. An input of the form:

```

2
0.05,0.10
1,0.7
2
0.02,0.03
1.,0.6

```

means that unobserved transitions will contribute to the least-squares sum when their calculated yield intensities exceed:

EXPT #	γ -Detector #	
1	1	5% of normalization transition
1	2	10% of normalization transition
2	1	2% of normalization transition
2	2	3% of normalization transition

and the normalizations constants are:

EXPT #	γ -Detector #	
1	1	C1 calculated by the code
1	2	0.7 * C1
2	1	C2 calculated by the code
2	2	0.6 * C2

NTAP Specifies the number of the file on which the experimental yields reside. $NTAP$ can have values of 3 or 4 corresponding to TAPE3 or TAPE4. The file of original experimental yields is modified to correct for the difference between full Coulomb excitation calculations, integrated over detector solid angles as well as target thickness, and point calculations at fixed scattering angle and incident energy. This modified file of experimental data is used for the least squares minimization and error estimation in conjunction with point calculations. This correction is performed by the $OP,CORR$ command (see Section 4.4 and Section 5.4) which reads the unmodified experimental yields from file TAPE3 and writes the corrected experimental yields in TAPE4. Consequently, $NTAP$ must equal 3

when OP,CORR is used. The least-squares minimization and error estimation require the corrected yields. In this case, NTAP should be consistent with the file assignment given in the computer control statements preceding this program. *NTAP* must equal 4 when OP,ERRO is executed with the CONT SMR, switch because TAPE3 is then reserved for the output needed by the quadrupole sum-rules program SIGMA. *NTAP* may equal 0 when experimental yields are not required, e.g. when running OP,STAR or OP,POIN under OP,GOSI. *NTAP* = 0 implies that the code will not attempt to find and read in the experimental yields file.

NBRA, WBRA Are the number of experimental branching ratios to be input and weighting factor, respectively. A maximum of 50 branching ratios can be input. If NBRA=0 then no further input of branching ratios is required. The weighting factor, WBRA, is defined for all the branching ratios used in the least-squares summation. Thus, normally WBRA=1.0. It can be helpful, during minimization, to switch off (WBRA=0) or reduce the weight of the branching ratio data to eliminate a problem caused by trapping of the search in the narrow valleys resulting from accurate branching ratio data. For example, branching ratio data can cause the search to be trapped in a solution having the wrong sign for a given matrix element.

If NBRA is not zero then the input is as follows:

I1, I2, I3, I4, B, DB Repeated NBRA times

... where I is the level index specified in the LEVE input. The branching ratio *B* with error *DB* is defined by the ratio of γ -ray intensities:

$$\frac{I1 \rightarrow I2}{I3 \rightarrow I4} = B \pm DB$$

NL, WL Are the number of experimental mean lifetimes to be input and the weighting factor. $NL \leq 50$. If $NL = 0$ then no further lifetime records need to be input. The weighting factor, *WL*, is used for all the lifetime data in the least-squares summation. Normally, $WL = 1$. The weighting factor can be set to a smaller number or zero if it is desired to reduce or switch off, respectively, the influence of the lifetime data.

INDEX, T, DT *NL* records. *INDEX* is the index of the level, specified in the input to LEVE. *T* is the mean lifetime, in picoseconds (10^{-12} secs), of the level.

... Note, it is not the half-life $T_{1/2} = \ln(2) * T$. while *DT* is the error of the mean lifetime in picoseconds.

NDL, WDL Are the number of experimental *E2/M1* mixing ratios to be input and the weighting factor. $NDL \leq 20$. If $NDL = 0$ no further mixing ratio records are required. The weighting factor, *WDL*, is used for all the data points in the least-squares summation. Normally, $WDL = 1.0$. *WDL* can be made smaller or zero to reduce or switch off the influence of the mixing ratio data.

IS, IF, DELTA, ERROR *NDL* records of mixing ratios. *DELTA* is the *E2/M1* mixing ratio for the transition from level *IS* to level *IF*. It is defined as:

$$DELTA = \partial \left(\frac{E2}{M1} \right) = 0.835 E_{\gamma}(MeV) \frac{\langle IF || M(E2) || IS \rangle}{\langle IF || M(M1) || IS \rangle}$$

Note that the phase convention used is that of Krane [KRA70]. See [KRA70] for a discussion of the various phase conventions. *ERROR* is the error in the mixing ratio. Note the error is assumed to be symmetric to assure continuity of the least squares function.

NAMX, WAMX The number of experimental $E\lambda/M\lambda$ matrix elements ($NAMX$) to be input and the weighting factor ($WAMX$). If $NAMX = 0$ no more input is required. The weighting factor, $WAMX$, is common for all the matrix elements used in the least-squares summation. Normally $WAMX = 1.0$. $WAMX$ can be made smaller or zero to reduce or switch off the influence of these additional data, $NAMX \leq 100$

LAMBDA, INDEX₁, INDEX₂, ME, DME Repeat $NAMX$ times.

... $LAMBDA$ is the multipole, $E\lambda$ with $\lambda = 1, 2, 3, 4, 5, 6$ and $M1$ with $LAMBDA = 7$. $INDEX_n$ is the level index. Note the restriction $INDEX_1 \leq INDEX_2$. ME is the $E\lambda$ or $M1$ matrix element, in the same units as for the ME input, while DME is the error, assumed to be symmetrical. In the fit procedure the sign of ME is ignored if $INDEX_1$ is not equal to $INDEX_2$.

The input of known electromagnetic matrix elements concludes the input to $OP, YIEL$. The experimental deexcitation γ -ray yields are input separately as described in Section 5.31.

5.32 INPUT OF EXPERIMENTAL γ -RAY YIELDS FROM COULOMB EXCITATION

The experimental γ -ray yields from the Coulomb excitation experiments should be put in a separate file TAPE3. (See also OP,FILE in section 5.9). GOSIA then creates TAPE4 if OP,CORR is executed.

The structure of the file is as follows:

IEXP, NG, ZP, AP, EP, ND, WT This header record appears before the experimental yields for each experiment and data set.

IEXP This is the experiment number. The experiments must be input in the same order as used for EXPT and OP,YIEL.

NG Number of data sets for experiment IEXP. is equivalent to the OP,YIEL NDST.

ZP Charge number of the projectile.

AP Mass number of the projectile.

EP Bombarding energy of the projectile (MeV).

ND Number of experimental γ -ray yields to be in-put for the specific IEXP and data set.

WT The weighting factor assigned to a given data set (see Eq.3.25). Normally WT=1.0. This weight factor can be made less than one or zero to reduce or switch off respectively the influence of this particular data set.

All the entries of the header, except *WT* and *ND*, are used only for reprint of experimental data, therefore using the values defined in EXPT and OP,YIEL inputs is not strictly required. Nevertheless, it is recommended to enter *IEXP, ZP, AP, EP* and *NG* according to the previous definition to make sure that the sequence of experimental yields is correct.

Each header should be trailed by *ND* records for that particular experiment and data set. The format is:

II, IF, Y, ΔY

where:

II Initial level index.

IF Final level index.

Y, DY The arbitrarily normalized γ -ray yield for transition *II* \rightarrow *IF* with absolute experimental error $\pm\Delta Y$.

For unresolved doublets, consisting of the *II1* \rightarrow *IF1* transition plus the *II2* \rightarrow *IF2* transition, the input format is: $(100 * II1 + II2)$, $(100 * IF1 + IF2)$, $Y_1 + Y_2$, $\Delta(Y_1 + Y_2)$ where:

II1, II2 Are the initial level indices for transition 1 and 2.

IF1, IF2 Are the final level indices for transition 1 and 2.

$Y_1 + Y_2, \Delta(Y_1 + Y_2)$ Is the summed yield of the unresolved transitions *II1* \rightarrow *IF1* and *II2* \rightarrow *IF2* with error $\pm\Delta(Y_1 + Y_2)$.

There are no restrictions regarding the sequence of the experimental data within the single data set. Data sets within an experiment should be ordered according to the highest logical detector index. If no clusters are defined (see OP,RAW) this is equivalent to ordering the data sets according to the sequence of logical detectors defined in OP,YIEL.

Below is an example of an experimental γ -ray yield data file for a ^{20}Na beam at 34 MeV. Experiments 1 and 2 have two physical γ -ray detectors each, while experiment 3 has one. Note that the header is repeated for each detector. The third experiment measured an unresolved doublet of the $7 \rightarrow 6$ and $5 \rightarrow 4$ transitions. The second detector in experiment 2 is weighted 0.5.

```
1,2,11,20,34,2,1.
2,1,634.,6.
3,2,247.,3.
1,2,11,20,34,1,1.
2, 1, 454., 10.
2,2,11,20,34,2,1.
2, 1, 74., 13.
3, 2, 40., 10.
2,2,11,20,34,3,0.5
2, 1, 722., 32.
4, 3, 392., 20.
3, 2, 302., 13.
3,1,11,20,34,1,1.
705, 604, 9.6, 1.1
.
```

6 QUADRUPOLE ROTATION INVARIANTS - PROGRAM SIGMA

The heavy-ion induced Coulomb excitation allows the measurement of essentially full sets of the $E2$ matrix elements for the low-lying states of the nuclei. It is interesting to ascertain to what extent these sets of data can be correlated using only a few collective degrees of freedom. The quadrupole rotational invariants [CLI72, CLI86] have been proven to be a powerful tool for extracting the collective parameters from the wealth of data produced by the Coulomb excitation. This procedure, outlined below, provides a completely model-independent way of determining the $E2$ properties in the rotating collective model frame of reference directly from the experimental $E2$ properties in the laboratory frame without recourse to models. Conversion of the measured $E2$ matrix elements to the quadrupole invariants is performed by the separate code, SIGMA, which uses the information stored by GOSIA on a permanent file during error calculation.

6.1 FORMULATION OF THE E2 ROTATIONAL INVARIANT METHOD

Electromagnetic multipole operators are spherical tensors and thus zero-coupled products of such operators can be formed that are rotationally invariant, i.e., the rotational invariants are identical in any instantaneous intrinsic frame as well as the laboratory frame. Let us, for practical reasons, consider only the $E2$ operator. The instantaneous ‘‘principal’’ frame can be defined in such a way, that:

$$E(2, 0) = Q \cos \delta \quad (6.1)$$

$$E(2, 1) = E(2, -1) = 0$$

$$E(2, 2) = E(2, -2) = (1/\sqrt{2}) \cdot Q \sin \delta$$

where Q and δ are the arbitrary parameters. This parameterization is general completely and model-independent. It is analogous to expressing the radial shape of a quadrupole-deformed object in terms of Bohr’s shape parameters (β, γ) . Using this parameterization the zero-coupled products of the $E2$ operators can be formed in terms of Q and δ , e.g.:

$$[E2 \times E2]^0 = \frac{1}{\sqrt{5}} Q^2 \quad (6.2)$$

$$\left\{ [E2 \times E2]^2 \times E2 \right\}^0 = \frac{\sqrt{2}}{\sqrt{35}} Q^3 \cos 3\delta \quad (6.3)$$

which are the two lowest order products. It is straightforward to form any order product, the limit being set only by practical feasibility. On the other hand, one can evaluate the matrix elements of the $E2$ operators products by recursively using the basic intermediate state expansion:

$$\left\langle s \left| (E2 \times E2)^J \right| r \right\rangle = \frac{(-1)^{I_s + I_r}}{(2I_s + 1)^{1/2}} \sum_t \langle s || E2 || t \rangle \langle t || E2 || r \rangle \left\{ \begin{matrix} 2 & 2 & J \\ I_s & I_r & I_t \end{matrix} \right\} \quad (6.4)$$

which allows the rotational invariants built from Q and δ to be expressed as the sums of the products of the reduced $E2$ matrix elements using the experimental values of these matrix elements.

As an example, an expectation value of Q^2 can be found directly using 6.2 and 6.4:

$$Q^2 = \frac{\sqrt{5}}{(2I_s + 1)^{1/2}} \langle s || (E2 \times E2)^0 || s \rangle = \frac{(-1)^{2I_s} \sqrt{5}}{(2I_s + 1)^{1/2}} \sum_r M_{sr} M_{rs} \left\{ \begin{matrix} 2 & 2 & 0 \\ I_s & I_s & I_r \end{matrix} \right\} \quad (6.5)$$

where the abbreviation for the matrix elements:

$$M_{sr} = \langle s || E2 || r \rangle \quad (6.6)$$

is used. The Wigner’s 6-j symbol $\left\{ \begin{matrix} 2 & 2 & 0 \\ I_s & I_t & I_r \end{matrix} \right\}$ is equal to ([ROT59]):

$$\left\{ \begin{array}{ccc} 2 & 2 & 0 \\ I_s & I_t & I_r \end{array} \right\} = (-1)^{I_s+I_r} \frac{1}{\sqrt{5}} \frac{1}{(2I_s+1)^{1/2}} \delta_{I_s I_t} \quad (6.7)$$

The 6-j symbol, 6.7, appears frequently in the rotational invariants and its simple analytic form makes possible the simplification of the formulas resulting from the intermediate state expansion. The general phase rule for the reduced $E2$ matrix elements M_{rs} can also be used to further simplify 6.5:

$$M_{rs} = (-1)^{J_s-J_r} M_{sr} \quad (6.8)$$

It can be easily seen that by inserting 6.7 and 6.8 into 6.5 gives:

$$Q^2 = \frac{1}{2I_s+1} \sum_r M_{sr}^2 \quad (6.9)$$

A similar evaluation of $Q^3 \cos 3\delta$ yields:

$$Q^3 \cos 3\delta = \mp \frac{\sqrt{35}}{\sqrt{2}} \frac{1}{2I_s+1} \sum_{tu} M_{su} M_{ut} M_{ts} \left\{ \begin{array}{ccc} 2 & 2 & 2 \\ I_s & I_t & I_u \end{array} \right\} \quad (6.10)$$

where a negative sign corresponds to the integral spin system, while a positive sign corresponds to the half-integral spin system.

Higher order rotational invariants can be formed with the different J couplings, involving summation over different sets of the reduced $E2$ matrix elements. This provides an important test for the self-consistency of the $E2$ experimental data, as well as for the convergence of the rotational-invariant sum rules themselves. It is estimated [CL186] that about 90% of the non-energy-weighted $E2$ strength is contained within the low-lying, and thus Coulomb excitation accessible, level structure. The missing strength is primarily due to the giant $E2$ resonance which we have neglected so far. Assuming that this high-lying missing strength can be neglected then the different J couplings should yield the similar results for the rotational invariants. Practically, however, the finite level system used in the analysis and the finite coupling scheme will result in discrepancies between the different J -coupled sum rules for the rotational invariants giving an estimate of the completeness of the data used. The simplest rotational invariant involving the different J coupling is given by the fourth-order product related to the expectation value of Q^4 :

$$\begin{aligned} P^4(J) &= \left\langle s \left| \left\{ (E2 \times E2)^J \times (E2 \times E2)^J \right\}^0 \right| s \right\rangle = \\ &= \frac{(2J+1)^{1/2}}{2I_s+1} \sum_{rtu} M_{st} M_{tr} M_{ru} M_{us} \left\{ \begin{array}{ccc} 2 & 2 & J \\ I_s & I_r & I_t \end{array} \right\} \left\{ \begin{array}{ccc} 2 & 2 & J \\ I_s & I_r & I_u \end{array} \right\} (-1)^{I_s-I_r} \end{aligned} \quad (6.11)$$

Three independent estimates of Q^4 can be evaluated using $P^4(J)$ for $J = 0, 2, 4$ where:

$$Q^4(0) = 5P^4(0) \quad (6.12a)$$

$$Q^4(2) = \frac{7\sqrt{5}}{2} P^4(2) \quad (6.12b)$$

$$Q^4(4) = \frac{35}{6} P^4(4) \quad (6.12c)$$

The above expressions for Q^4 involve summation over the different sets of matrix elements, the selection rules being set by the $6-j$ symbols of 6.11. The expectation values of Q^2 and Q^4 can be used to build the Q^2 -variance defined by:

$$v^2(J) = Q^4(J) - [Q^2]^2 \quad (6.13)$$

having the physical meaning of the square of the softness in Q^2 . The fifth-order product of the rotational invariants gives

$$P^5(J) = \left\langle s \left| \left\{ (E2 \times E2)^J \times [(E2 \times E2)^2 \times E2]^J \right\}^0 \right| s \right\rangle \quad (6.14)$$

which defines $Q^5 \cos 3\delta$. There are three independent sum rules for $J=0, 2, 4$ coupling for this rotational invariant. Making an intermediate state expansion and reducing the resulting $6-j$ symbols with $I_s = 0$ gives:

$$Q^5 \cos 3\delta(J) = \mp C(J) \frac{1}{2I_s + 1} \sum_{rtvw} M_{st} M_{tr} M_{rv} M_{vw} M_{ws} \\ \bullet (-1)^{I_w + I_s} \left\{ \begin{matrix} 2 & 2 & J \\ I_s & I_r & I_t \end{matrix} \right\} \left\{ \begin{matrix} 2 & 2 & J \\ I_s & I_r & I_w \end{matrix} \right\} \left\{ \begin{matrix} 2 & 2 & 2 \\ I_w & I_r & I_v \end{matrix} \right\} \quad (6.15)$$

where $C(0) = 5\frac{\sqrt{35}}{\sqrt{2}}$, $C(2) = C(4) = \frac{35}{2}\frac{\sqrt{35}}{\sqrt{2}}$

and a negative sign should be used for the integral-spin cases, while a positive sign corresponds to the half-integral spin cases.

The sixth order products of $E2$ operators define both the expectation value of Q^6 and the expectation value of $Q^6 \cos 3\delta$. The matrix element:

$$P_0^6(J) = \langle s | \{ [(E2 \times E2)^J \times (E2 \times E2)^J]^0 \times (E2 \times E2)^0 \}^0 | s \rangle \quad (6.16)$$

is related to Q^6 , while the matrix elements:

$$P_1^6(J) = \langle s | \{ [(E2 \times E2)^2 \times E2]^J \times [(E2 \times E2)^2 \times E2]^J \}^0 | s \rangle \quad (6.17)$$

and

$$P_2^6(J) = \langle s | \{ [(E2 \times E2)^2 \times E2]^J \times [E2 \times (E2 \times E2)^2]^J \}^0 | s \rangle \quad (6.18)$$

both define $Q^6 \cos^2 3\delta$. The intermediate coupling scheme 6.16 yields for $J = 0, 2, 4$:

$$Q^6(J) = C(J) \sum_{\substack{rtvwu \\ I_r = I_w}} \frac{1}{2I_r + 1} M_{st} M_{tw} M_{wu} M_{ur} M_{rv} M_{vs} \\ \cdot \left\{ \begin{matrix} 2 & 2 & J \\ I_s & I_w & I_t \end{matrix} \right\} \left\{ \begin{matrix} 2 & 2 & J \\ I_s & I_r & I_v \end{matrix} \right\} (-1)^{I_s - I_u} \quad (6.19)$$

where $C(0) = \frac{5}{2I_s + 1}$; and $C(2) = C(4) = \frac{35}{2(2I_s + 1)}$

Knowing the expectation value of Q^6 one can construct the second statistical moment, the skewness, of Q^2 :

$$s(Q^2)(J) = Q^6(J) - 3Q^4(J)Q^2 + 2(Q^2)^3 \quad (6.20)$$

The evaluation of $P_1^6(J)$ (6.17) and $P_2^6(J)$ (6.18) may involve the $J=0, 2, 3$ and 4 coupling schemes. However, the $J=3$ coupling is insignificant from the point of view of Coulomb excitation since it favors strongly $E2$ matrix elements coupling the states with $\Delta I = \pm 1$ spin difference. These matrix elements are not well defined by Coulomb excitation which is most clearly seen in the case of even-even nuclei where the ground state spin is 0 and the preferable path of excitation involve the $m=0$ magnetic substates for all states. In this case, the 3-j symbol involved in the definition of the coupling parameters ζ_{kn} (2.17c) is:

$$\left(\begin{matrix} I & 2 & I+1 \\ 0 & 0 & 0 \end{matrix} \right) = 0$$

since $j_1 + j_2 + j_3 = (2I + 2) \pm 1$ is odd (see e.g. [ROT59]). This means that the lowest significant coupling is the $\Delta m = \pm 1$ coupling being an order of magnitude weaker than the $\Delta m = 0$ coupling. Applying the first order perturbation theory 2.24, 2.26 one also finds that due to the antisymmetry of $Q_{2,\pm 1}(\omega)$ this mode of excitation is strongly inhibited. As a result, the $E2$ matrix elements connecting the even and odd spin

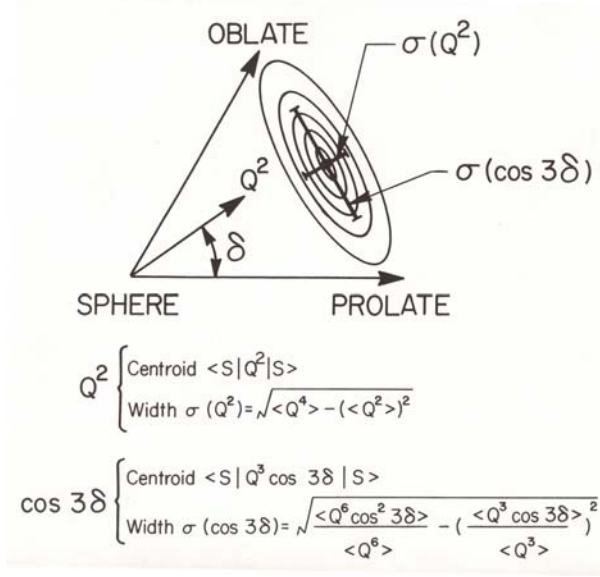


Figure 12: Distribution plot of the parameters Q^2 and δ required to define the E2 properties in the intrinsic frame for a state S . All possible E2 moments are defined by the region $Q \geq 0$ and $0 \leq \delta \leq 60^\circ$.

states are measured with large errors, unless some additional data, most important the branching ratios, are available.

Restricting ourselves to $J = 0, 2$ and 4 couplings we have from 6.17 and 6.18:

$$Q^6 \cos^2 3\delta(0) = \frac{35}{2} P_1^6(0) = \frac{35}{2} P_2^6(0) \quad (6.21)$$

and

$$Q^6 \cos^2 3\delta(J)_{J=2,4} = 35(P_{1,2}^6(4) - \frac{\sqrt{5}}{4} P_{1,2}^6(2)) \quad (6.22)$$

$$\text{with } P_1^6(J) = \frac{5(2J+1)^{1/2}}{2I_s+1} \sum_{rutvw} M_{su} M_{ut} M_{tr} M_{rv} M_{vw} M_{ws}$$

$$\bullet \left\{ \begin{array}{ccc} 2 & 2 & J \\ I_s & I_r & I_t \end{array} \right\} \left\{ \begin{array}{ccc} 2 & 2 & 2 \\ I_s & I_t & I_u \end{array} \right\} \left\{ \begin{array}{ccc} 2 & 2 & J \\ I_s & I_r & I_w \end{array} \right\} \left\{ \begin{array}{ccc} 2 & 2 & 2 \\ I_w & I_r & I_v \end{array} \right\} (-1)^{2I_s+I_t+I_w} \quad (6.23)$$

$$\text{with } P_2^6(J) = \frac{5(2J+1)^{1/2}}{2I_s+1} \sum_{rutvw} M_{su} M_{ut} M_{tr} M_{rv} M_{rw} M_{ws}$$

$$\bullet \left\{ \begin{array}{ccc} 2 & 2 & J \\ I_s & I_r & I_t \end{array} \right\} \left\{ \begin{array}{ccc} 2 & 2 & 2 \\ I_s & I_t & I_u \end{array} \right\} \left\{ \begin{array}{ccc} 2 & 2 & J \\ I_s & I_r & I_v \end{array} \right\} \left\{ \begin{array}{ccc} 2 & 2 & 2 \\ I_s & I_v & I_w \end{array} \right\} (-1)^{I_s+I_r+I_t+I_w} \quad (6.24)$$

6.21 through 6.24 define three independent estimates of $Q^6 \cos^2 3\delta$ - one involving the $J = 0$ coupling, identical for both P_1^6 and P_2^6 and two involving the $J = 2$ and $J = 4$ couplings for P_1^6 and P_2^6 , respectively. Using the value of Q^6 (6.19) the expectation from 6.22, which, combined with the expectation value of $\cos 3\delta$ can be obtained which defines the softness in δ as being given by the square root of the $\cos 3\delta$ variance:

$$v^2(\cos 3\delta) = \langle \cos^2 3\delta \rangle - \langle \cos 3\delta \rangle^2 \quad (6.25)$$

The expectation value of $\cos 3\delta$ can be extracted either from the $Q^3 \cos 3\delta$ invariant or three possible values of $Q^5 \cos 3\delta$ provided that the expectation values of Q^3 and Q^5 are known. These values can be estimated using an interpolation between Q^2 , Q^4 and Q^6 . We use:

$$\langle Q^3 \rangle = \left(\frac{1}{2} ((Q^2)^{1/2} + (Q^4(0))^{1/4}) \right)^3 \quad (6.26)$$

$$\langle Q^5 \rangle = \left(\frac{1}{2} ((Q^4)^{1/4} + (Q^6(0))^{1/6}) \right)^5 \quad (6.27)$$

where the $J = 0$ coupling for Q^4 and Q^6 is used because of the minimum number of the matrix elements involved; this being preferable from a point of view of the completeness of the summation and the error propagation. For the same reason only the expectation value of $\cos 3\delta$ extracted from $Q^3 \cos 3\delta$ is used for the softness in δ .

To summarize, the sum rules derived from the rotational invariants allow measurement of the expectation values of rotational invariants built of Q and δ . Then, as shown in figure 12, it is possible to find the statistical distribution of Q^2 and $\cos 3\delta$ i.e. the first statistical moments related to the softness in both parameters and the second statistical moment, the skewness (in our case calculated for Q^2 only). With various J -couplings which can be used to evaluate the higher-order invariants, the rotational invariance of the sum rules provide the test of the completeness of the data as well as of the self-consistency of the fitted $E2$ matrix elements.

6.2 PROGRAM SIGMA

A separate code, SIGMA, has been written to evaluate the quadrupole rotational invariant sum rules. This program has been designed to use the information created by GOSIA (see 5.3), although it can be used separately to calculate the centroids (i.e., the expectation values) of the rotational invariants only, with no error estimation. The following subsection outlines the algorithms used for the computation of the rotational invariants and resulting statistical distribution of Q and $\cos 3\delta$ and the method employed to estimate the errors of computed values.

6.2.1 COMPUTATION OF THE INVARIANTS

The most efficient way to evaluate the rotational invariants is to use the matrix multiplication formalism having the selection rules for different sum of products superimposed by masking the array of the $E2$ matrix elements with the appropriate $6 - j$ matrices. Let us define (with s being a fixed target state index):

$$\bar{V}_L = \{M_{sr}\} \text{ "left-hand vector"} \quad (6.28a)$$

$$\bar{V}_R = \{M_{sr}\} \text{ "right-hand vector"} \quad (6.28b)$$

$$S_{rv}(J) = \{M_{rv}\} \left\{ \begin{array}{ccc} 2 & 2 & J \\ I_s & I_r & I_v \end{array} \right\} \quad (6.28c)$$

$$S_{rv}^T(J) = \{M_{vr}\} \left\{ \begin{array}{ccc} 2 & 2 & J \\ I_s & I_r & I_v \end{array} \right\} \quad (6.28d)$$

$$T_{rv}(J) = \left(\sum_w M_{rw} M_{wv} \left\{ \begin{array}{ccc} 2 & 2 & J \\ I_r & I_v & I_w \end{array} \right\} \right) \left\{ \begin{array}{ccc} 2 & 2 & 2 \\ I_s & I_r & I_v \end{array} \right\} \quad (6.28e)$$

$$T'_{rv}(J) = \sum_w M_{rw} M_{wv} (-1)^{I_w - I_s} \frac{1}{2I_r + 1} \delta_{I_r I_v} \quad (6.28f)$$

The rotational invariants can be expressed in terms of the operators 6.28 as (if the phase needs to be appended, r stands for the row index and v stands for the column index):

$$Q^2 = \frac{1}{2I_s + 1} \bar{v}_L \bullet \bar{v}_L \quad (6.29a)$$

$$Q^3 \cos 3\delta = \mp \frac{\sqrt{35}}{\sqrt{2}} \frac{1}{2I_s + 1} \bar{v}_L \bullet S(2) \bullet \bar{v}_R \quad (6.29b)$$

$$Q^4(J) = C(J) \bar{v}_L \bullet S^T(J) \bullet [S(J)(-1)^{I_s+3I_r}] \bullet \bar{v}_R \quad (6.29c)$$

$$Q^5 \cos 3\delta(J) = \mp C(J) \bar{v}_L \bullet S^T(J) \bullet T(J) \bullet \bar{v}_L \quad (6.29d)$$

$$Q^6(J) = C(J) \bar{v}_L \bullet S^T(J) \bullet T' \bullet S(J) \bullet \bar{v}_R \quad (6.29e)$$

$$Q^6 \cos^2 3\delta(J) = C(J) \bar{v}_L \bullet [S(2)(-1)^{I_s+I_w}] \bullet S^T(J) \bullet [T(J)(-1)^{I_s+I_w}] \bullet \bar{v}_R \quad (6.29f)$$

$$Q^6 \cos^2 3\delta(J) = C(J) \bar{v}_L \bullet [S(2)(-1)^{I_s+I_r}] \bullet S^T(J) \bullet S(J) \bullet [S(2)(-1)^{I_s+I_w}] \bullet \bar{v}_R \quad (6.29g)$$

where $C(J)$ are the appropriate constants as defined in the previous subsection and the two formulas for $Q^6 \cos 3\delta(J)$ correspond to the coupling schemes 6.17 and 6.18. The invariants are evaluated according to 6.29 from the right side, so that only the matrix-vector multiplications are performed, without any matrix-matrix multiplications.

6.2.2 ESTIMATION OF ERRORS IN SIGMA

The rigorous estimation of the errors of the function of the E2 matrix elements would require the knowledge of all sets of these matrix elements yielding a given value of this functions together with the probability of each such set. Technically it is of course out of question to apply this method to evaluate the errors of the rotational invariants. We are therefore forced to use a crude approximation, which is to assume that the set of the measured matrix elements is contained within an ellipsoidal contour (note that because of the correlation all matrix elements, not only E2, have to be taken into account). This contour is defined by a requested increase of the S statistic (3.24) and its orientation in the space of the matrix elements results from the correlations introduced by a method of measurement. One should be aware that the correlation of the matrix elements introduced by a functional form may be completely different from that resulting from the measurement. As an extreme example it is easily checked that the variance of Q^2 vanishes if there is only one state of a given spin, whatever values of the matrix elements are used. In this case, the error of the variance is zero, no matter what errors are assigned to the matrix elements.

The error contour, defined by the increase of the S statistic (3.24), is approximated by the quadratic formula:

$$\Delta S = \delta = \bar{\nabla}_o \bullet \Delta \bar{M} \bullet J \bullet \Delta \bar{M} \quad (6.30)$$

- - where $\bar{\nabla}_o$ is the gradient taken at the origin, \bar{M}_o , while J is the second derivatives matrix:

$$J_{ik} = \frac{\delta^2 S}{\delta M_i \delta M_k} \quad (6.31)$$

and

$$\Delta \bar{M} = \bar{M} - \bar{M}_o$$

It is easily checked that all points on the contour 6.30 can be parameterized by

$$\Delta \bar{M} = \bar{M} - \bar{M}_o \frac{2\delta \bar{e}}{\bar{\nabla}_o \bar{e} + [(\bar{\nabla}_o \bar{e})^2 + 2\delta \bar{e} J \bar{e}]^{1/2}} \quad (6.32)$$

where \bar{e} is an arbitrary vector. Denoting a given function of matrix elements by $S(\bar{M})$ we have to locate the points \bar{M} on the contour yielding the extremum values of $S(\bar{M})$. Let us consider the function $S(\bar{M})$ which can locally be approximated by the linear expansion in \bar{M} :

$$\Delta_s(\bar{M}) = \nabla_s \bullet (\bar{M} - \bar{M}_s) \quad (6.33)$$

where we expand $S(\bar{M})$ in a vicinity of \bar{M}_2 . To find the extrema of 6.33 on the contour 6.30 we have to find the vectors \bar{e} satisfying:

$$\frac{d}{d\bar{e}} \left(\frac{2\delta \bullet (\bar{\nabla}_s \bullet \bar{e})}{\bar{\nabla}_o \bar{e} + [(\bar{\nabla}_o \bar{e})^2 + 2\delta \bar{e} J \bar{e}]^{1/2}} \right) = 0 \quad (6.34)$$

which yields:

$$\bar{\nabla}_s(2\delta - \bar{\nabla}_o \bar{e}) - \bar{\nabla}_o(\bar{\nabla}_s \bar{e}) - (\bar{\nabla}_s \bar{e}) \bullet \bar{J} e = 0 \quad (6.35)$$

From 6.35 it is clear that the vector \bar{e} must be a linear combination of $J^{-1}\bar{\nabla}_s$ and $J^{-1}\bar{\nabla}_o$. Inserting

$$\bar{e} = \alpha J^{-1}\bar{\nabla}_s + \beta J^{-1}\bar{\nabla}_o \quad (6.36)$$

to 6.35 we get, using the identity

$$\bar{\nabla}_s J^{-1}\bar{\nabla}_o = \bar{\nabla}_o J^{-1}\bar{\nabla}_s \quad (6.37)$$

resulting from the symmetry of J :

$$\alpha = \pm \left(\frac{2\delta + \bar{\nabla}_o J^{-1}\bar{\nabla}_o}{\bar{\nabla}_s J^{-1}\bar{\nabla}_s} \right)^{1/2}; \beta = -1 \quad (6.38)$$

which is valid for any arbitrarily chosen origin \bar{M}_o . However, in our case we can assume that \bar{M}_o , the vector of fitted matrix elements, is a close approximation of the minimum, thus $\bar{\nabla}_o \approx 0$. Neglecting the terms containing $\bar{\nabla}_o$ we finally get:

$$\bar{M} = \bar{M}_o \pm \left(\frac{2\delta}{\bar{\nabla}_s J^{-1}\bar{\nabla}_s} \right)^{1/2} J^{-1}\bar{\nabla}_s \quad (6.39)$$

where a positive sign corresponds to the maximum of 6.33 on the contour 6.30 and a negative sign corresponds to its minimum. This formula gives an exact solution for any linear function of \bar{M}_o . For non-linear functions 6.39 can be used iteratively following the scheme:

$$\begin{aligned} \bar{\nabla}_s^{(0)} = \bar{\nabla}_s(\bar{M}_o) &\implies \bar{M}^{(1)} \\ \bar{\nabla}_s^{(1)} = \bar{\nabla}_s(\bar{M}^{(1)}) &\implies \bar{M}^{(2)} \end{aligned} \quad (6.40)$$

until the convergence is achieved. This procedure is used in SIGMA to estimate the errors of Q^2 , $\cos 3\delta$ and their statistical moments. Because of the fact that the implementation of the rotational-invariant sum rules is only possible for the cases in which virtually all the E2 matrix elements for low lying states are known, implying that the underlying Coulomb excitation problem is well overdetermined, it is reasonable to assume a least-squares statistic increase $\delta=1$. The J matrix is estimated using the gradients computed by GOSIA during the calculation of correlated errors (see 4.6) and stored on a permanent file. Applying the quadratic approximation 6.1 and assuming $\bar{M}_o = \text{minimum}$ (i.e. $\bar{\nabla}_o=0$) one can write:

$$\bar{\nabla}(\bar{M}) = \hat{J}(\bar{M} - \bar{M}_o) \quad (6.41)$$

During the correlated errors calculation GOSIA evaluates the gradients in points \bar{M} for which only one matrix element at the time is perturbed from its central value. This means that $\bar{M} - \bar{M}_o$ has only one non-zero component, thus 5.41 defines k -th column of J if M_k has been perturbed. Two estimates of J_{ki}

are available using positive and negative values of ΔM_k . In addition, J_{ki} can be evaluated using the i -th component of the gradient at perturbed M_k or using the k -th component of the gradient with perturbed M_i . Since the quadratic approximation 6.1 is not fully adequate, the averaging procedure must be used to cancel the difference between various estimates and to preserve the symmetry of J . Furthermore, for the matrix elements M_k for which the full error calculation was not performed only the diagonal element J_{kk} is assumed to be non-zero, i.e., the correlation is neglected. The estimate of J_{kk} in this case results from:

$$\Delta S = 1 = \frac{1}{2} J_{kk} \Delta M_k \quad (6.42)$$

where ΔM_k is the average diagonal error of M_k , i.e., the mean value of the negative and positive deviations.

The method presented above allows to estimate the errors of the collective parameters and their distributions with the reasonable efficiency. However, one must be aware of the scope of the approximations used, which do not allow treating the estimated errors very rigorously, providing only a crude estimate of the determined accuracy the sum rules.

6.2.3 INPUT INSTRUCTIONS

SIGMA reads in the input file, which must be called SIGMA.INP and in addition three permanent files created by GOSIA, referred to in SIGMA as **filename.err** [TAPE11], **filename.smr** [TAPE12] and **sixj.tab** [TAPE3].

The input file selects the mode of calculation and should be given as:

IL

NST

filename.smr corresponding to SIGMA TAPE12
 filename.err corresponding to SIGMA TAPE11
 sixj.tab corresponding to SIGMA TAPE3

I(1)

I(2)

· only if $0 < NST \leq 75$

I(NST)

That is, the input file comprises two switches, three filenames, followed by the list of states for which all errors are to be calculated (NST records) where:

IL may be either 0 or 1. *IL* = 1 will cause the printout of the matrix elements (by their indices) involved in the evaluation of 14 invariants calculated for each state. The invariants are numbered from 1 to 14 according to the sequence they appear in the first column of the output table (see the sample output at the end of this chapter). *IL* = 0 will cause no compilation of this list.

NST selects the mode of error calculation. Three special values of *NST*: *NST* = -1, *NST* = 0 or *NST* = 99 require no further input. *NST* = -1 is used if only the invariants and the resulting statistical moments (given in the second column of the output table) are to be calculated and no error estimation is requested. In this mode SIGMA can be used independently of GOSIA and the information concerning the level scheme and coupling scheme, normally produced by GOSIA, must be provided by the user (see the description of the TAPE files below). *NST* = 0 implies that the error calculation is to be performed only for Q^2 , three values of $v(Q^2)$ and four values of $\cos 3\delta$ for all states, while *NST* = 99 specifies the errors to be estimated for every statistical moment for all states. The reason for this distinction is that the statistical moments based on the sixth-order invariants are usually not meaningful due to the number of the matrix elements involved and the resulting error propagation. Also, calculation of these invariants is most time-consuming. Usually, it is practical to calculate all the errors only for the few lowest-lying states. This can be

achieved using “mixed“ calculation mode, specified by $0 < NST \leq 75$. In this case, NST has the meaning of the number of states for which the “full“ calculation is to be done, while for the remaining states the “fast“ mode, corresponding to $NST = 0$ will be used. In this mode the list of state indices (NST records) must follow.

Note that the errors quoted are the errors of the statistical moments (column 2 of the output table), not of the invariants listed in the first column.

An example is:

```
0
0
nd.smr
nd150.err
sixj.tab
```

Permanent Files:

TAPE11 This file contains the errors of the matrix elements and is written by GOSIA as TAPE15. It is not required if $NST = -1$. Use the filename explicitly in the input, e.g. nd150.err

TAPE3 Contains the table of the 6-j symbols used for the calculation of the invariants. This table can be created by GOSIA with OP,SIXJ (see 5.25). GOSIA writes the table on TAPE14.

TAPE12 This file is written by GOSIA during full error calculation on TAPE3 if the CONT switch SMR, is set. TAPE12 contains the level scheme, the coupling scheme and the set of gradients used to evaluate the J matrix. Use filename explicitly in the input, e.g.nd150.smr. If SIGMA is to be used independently of GOSIA, (i.e., only if $NST = -1$) a part of this file must be prepared by the user. The format of this portion of TAPE12 should be the following:

NS, NME, NI, NF where

```
NS = number of states
NME =number of matrix elements
NI =index of a first E2 matrix element
NF =index of a last E2 matrix element
```

INDEX(1), SPIN(1), ENERGY(1)

- Level scheme
- NS records

INDEX(NS), SPIN(NS), ENERGY(NS)

IME(1), INI(1), INF(1) Coupling scheme. IME is the index of matrix element,

- INI is the index of an initial state
- INF is the index of a final state.
- The GOSIA convention applies to the ordering of the matrix elements (see 5.15).

IME(NME), INI(NME), INF(NME) NME records.

IME(1), ME(1) Values of the matrix elements.

- NME records
-

IME(NME), ME(NME)

0, 0 Two zeros terminate the input.

7 FILE ASSIGNMENTS

The following chapter provides an overview of the file assignments in GOSIA, SIGMA and SELECT. A permanent or temporary file is referred to as TAPE n , where n designates the code-declared file number. An actual name for such a file depends on the operating system of a given computer, for example the CDC/NOS file TAPE1 will be named FOR001 under VAX/VMS. To allow the possibility of examining the contents of the permanent files generated by all three codes a free format FORTRAN write (i.e. *WRITE*($n, *$)) is used. The only exception is the internal correction factors file TAPE1 (seeSection 4.5) which may be frequently updated during the least-squares fit, therefore to speed up the input/output operations the binary format (i.e. *WRITE*(1)) has been chosen instead. The short description of the files being used by GOSIA, SIGMA and SELECT is presented in sections 7.1, 7.2 and 7.3, respectively. The files are classified as input files, i.e. the ones that must be attached to the current job, output files, i.e. the ones that are created by the job and should be saved as permanent files for further use, and internal files, used to transfer the data between some of the modules of GOSIA. The internal files need not be attached to the job or saved after the execution. Both GOSIA and SIGMA require an input file which should be provided by the user in the *READ** format, while no such a file is needed to run SELECT. Section 7.4 provides a series of examples of the typical command sequences together with the lists of the input, output and internal files employed during the execution.

7.1 FILE ASSIGNMENTS IN GOSIA

TAPE3 The function of TAPE3 depends on the command being executed. TAPE3 is the input file of the original, uncorrected experimental γ yields for OP,CORR (the output file of the corrected yields will be written on TAPE4). Note that if OP,CORR is to be executed the OP,YIEL input entry *NTAP* (see Section 5.29) must equal 3. TAPE3 can also be assigned instead of TAPE4 as an input file of the corrected yields for OP,MINI and OP,ERRO, if the value of *NTAP* is 3. To avoid a possible input/output assignment conflict it is, however, recommended to use TAPE4 when executing OP,ERRO, since TAPE3 is reserved as an output file for the code SIGMA if the *CONT* switch *SMR*, is set. In this case TAPE3 is created during a first run of OP,ERRO with *IDF* = 1 and *IREP* = 1 (see Section 5.6) and updated if *IDF* = 1 and *IREP* = 2.

TAPE4 Contains the corrected yields written when OP,CORR is executed. TAPE4 then should be an input file of the experimental yields for both OP,MINI and OP,ERRO with the OP,YIEL entry *NTAP* = 4. As discussed above, TAPE3 can also be assigned for this purpose. TAPE4 is also written when OP,POIN is executed with *IFL* = 1 (see Section 5.18) to create the simulated “experimental“ yields

TAPE7 Contains the maps of the q-parameters to be used by the fast Coulomb excitation calculation (see Section 4.2). TAPE7 is written by OP,MAP and read automatically when either the OP,MINI or OP,ERRO command is encountered. This means that the existing permanent file containing the q-parameter map should be attached to the minimization or error calculation jobs as TAPE7 unless OP,MAP has been executed before during the same run.

TAPE8 Contains the absorption coefficients needed to reproduce γ -ray energy dependence of the detector efficiency. Created if *NPD* in OP,GDET is negative, which is connected to the use of “raw“ spectra as defined by the input to OP,RAW.

TAPE9 Contains the parameters needed to approximately reproduce the γ -energy dependence of the Ge detector solid angle attenuation coefficients Q_k (see Section 4.3). TAPE9 is written when OP,GDET is executed and automatically read in when OP,YIEL is encountered, which implies that TAPE9 should be attached to any job involving the calculation of γ yields.

TAPE11 Contains the internal correction factors (see Section 4.5) created and updated when OP,MINI is executed. TAPE11 is required as an input file if the CONT switch CRF, was selected. CRF, causes GOSIA to read the internal correction factors from TAPE11 instead of calculating them when OP,MINI is encountered. Obviously, TAPE11 is to be saved after a previous run to use the time-saving CRF, switch when resuming the minimization. The internal correction factors are updated (and stored on TAPE11) every time the TEST criterion of the OP,MINI input (5.17) is fulfilled, thus the internal correction coefficients stored on TAPE11 will correspond to the last set of matrix elements for which the update, defined by TEST, was done. In addition, the internal correction coefficients can be calculated using the CONT switch CCF, for a given set of matrix elements. In this case TAPE11 should be saved and defined as an input file for the subsequent run using the CONT CRF, switch.

TAPE12 Contains the set of matrix elements resulting from the last minimization run. TAPE12 is overwritten after completion of each OP,MINI command. The values of the matrix elements stored on TAPE12 can be used instead of those specified in the ME input using the OP,REST command before the selected executable option. An existing permanent file must be assigned to TAPE12 if OP,REST is used.

TAPE14 An output file for OP,SIXJ. Contains the table of Wigner's $6 - j$ symbols to be used by SIGMA. TAPE14 also serves as an internal file when OP,INTG, OP,CORR, OP,TROU or OP,MINI with the calculation of the sensitivity maps (see Section 4.5) are executed.

TAPE15 Contains the current set of errors of the matrix elements calculated by OP,ERRO. TAPE15 is written by OP,ERRO if $IREP = 0$ (see Section 5.6) and read, updated and overwritten if $IREP = 1$. Internal for OP,INTG, OP,CORR and OP,TROU.

TAPE17 An output file for OP,ERRO, containing the best (i.e. yielding the lowest value of x_2) set of matrix elements found during the scan of the x_2 hypersurface (see Section 4.6). Also serves as the output file to write the statistical tensors after Coulomb excitation using the CONT switch TEN, in conjunction with either OP,STAR or OP,POIN (see Section IV.3). The structure of this file, which may be used by external programs to examine the g decay following the Coulomb excitation is as follows:

$$\begin{aligned}
 &N \\
 &\rho_{00} \\
 &\rho_{20}, \rho_{21}, \rho_{22} \\
 &\rho_{40}, \rho_{41}, \rho_{42}, \rho_{43}, \rho_{44} \\
 &\rho_{60}, \rho_{61}, \rho_{62}, \rho_{63}, \rho_{64}, \rho_{65}, \rho_{66}
 \end{aligned}$$

here N is the level index as defined by the sequence of the input to LEVE. The tensors for the ground state $N=1$ are not stored, thus $2 < N < NMAX$ where $NMAX$ is the number of levels included. This sequence is repeated for each experiment according to the sequence of the input to EXPT. Note that because of the symmetry $r_{km} = (-1)^m r_{k,-m}$ only the components with $m > 0$ are stored. TAPE17 is also used as an internal file by OP,TROU and OP,INTG.

TAPE18 An input file for the program SELECT and for OP,ERRO if the correlation matrix is to be used to reduce the number of correlated matrix elements during a full error calculation ($IDF = 1$ and $IFC = 0$ in the OP,ERRO input - see Section 5.6, see also Section 4.6). TAPE18 should be created first using the CONT switch SEL, and the default setting of the print parameter 4 (i.e. -2) while executing OP,MINI. TAPE18 should then be attached to the execution of SELECT, the result being written as TAPE10. The latter file can then be attached to the OP,ERRO job as TAPE18. This is internal for OP,TROU.

TAPE22 Output printer file. Unit 22 is used instead of default FORTRAN unit 6 to avoid merging the output with system messages (e.g. underflow warnings) on some systems. During minimization the current value of CHISQ is also output on TAPE6. Dependent on the system and execution mode it will appear either on the screen or in log file, which usually can be viewed during execution. This helps to decide whether or not interrupt the job if no progress is made.

TAPE23 Lists the Doppler-shifted γ -ray energies and detector efficiencies when OP,POIN is executed in conjunction with OP,RAW.

7.2 FILE ASSIGNMENTS IN SIGMA

SIGMA requires three input TAPE files - TAPE11, TAPE12 and TAPE3. All three files are written by GOSIA. However, if no error estimation of the invariants is desired, it is not necessary to attach TAPE11, and only a part of TAPE12 is needed - see Section 6.2.2 for details. SIGMA produces no output files other than the printer output. The input file assignments are the following:

TAPE11 Contains the errors of the matrix elements, equivalent to the GOSIA output file TAPE15.

TAPE12 Equivalent to the GOSIA output file TAPE3 written during the calculation of the full errors (OP,ERRO with $IDF = 1$ and the CONT switch SMR).

TAPE3 The table of the $6 - j$ symbols created by GOSIA as TAPE14 using OP,SIXJ.

TAPE23 The printer output file.

7.3 FILE ASSIGNMENTS IN SELECT

SELECT requires one input TAPE file, TAPE18, written by GOSIA and no user-given input. The file assignments are as follows:

TAPE6 The printer output file.

TAPE10 Output file, containing the “correlation matrix“, i.e. the square matrix, indexed by the indices of the matrix elements and having the elements either equal to 0 (no correlation detected) or to 1 (correlation detected). This matrix should be attached to the OP,ERRO job when calculating the correlated errors as TAPE18.

TAPE18 Input file, containing the information written by GOSIA also on TAPE18 during the execution of OP,MINI with the CONT switch SEL, set and the print parameter 4 equal to -2.

7.4 EXAMPLES OF INPUT FILES AND FILE ASSIGNMENTS FOR TYPICAL JOBS

This section provides some examples of the file assignments necessary to run typical jobs. The schematic examples of the input streams, ordered according to the usual sequence of the jobs run to analyze a given case, are followed by the list of the input and output files. Details of each section omitted for brevity are marked by dots. The user-given input file and the printer output file (TAPE22 in GOSIA, TAPE23 in SIGMA, TAPE6 in SELECT) are not listed. OP,TITL is always optional and can be skipped. It is also assumed that for all the jobs involving minimization or error calculation (i.e. starting from 7.4.5.) the corrected experimental yields reside on file TAPE4.

7.4.1 COULOMB EXCITATION AMPLITUDES

```
OP,TITL
.
OP,GOSI
LEVE
.
.
ME
.
.
EXPT
.
.
CONT
.
.
END,

OP,STAR
OP,EXIT
```

Input: None
Output: None

Comments: This job can be run with both OP,GOSI and OP,COUL. Adding the CONT switch TEN, will cause creation of the output file TAPE17 (the statistical tensor file).

7.4.2 CREATION OF THE GE DETECTORS FILE

```
OP,TITL
.
OP,GDET
.
OP,EXIT
```

Input: None

Output: TAPE9 (TAPE8)

Comments: The file TAPE9 is needed as input for all jobs involving the calculation of the γ yields. It is not necessary to select OP,COUL or OP,GOSI to run OP,GDET. TAPE8 is necessary only if OP,RAW is to be used.

7.4.3 CALCULATION OF THE γ YIELDS BY POINT APPROXIMATION

```
OP,TITL
.
OP,GOSI
LEVE
.
ME
.
EXPT
.
CONT
(TEN,)
.
END,
OP,YIEL
.
OP,POIN
IFL,YLIM
OP,EXIT
```

Input: TAPE9

Output: TAPE4 if IFL=1, TAPE17 if the CONT switch TEN, is selected.

Comments: This job can be run with either OP,COUL or OP,GOSI. The OP,YIEL entry NTAP must equal 0.

7.4.4 CALCULATION OF THE INTEGRATED γ YIELDS AND GENERATION OF A "CORRECTED" EXPERIMENTAL YIELDS FILE

```
OP,TITL
.
OP,GOSI
LEVE
.
.
ME
.
.
EXPT
.
.
CONT
.
.
END,

OP,YIEL
.
.
OP,INTG
.
.
OP,CORR
OP,EXIT
```

Input: TAPE3,TAPE9
Output: TAPE4

Comments: The OP,YIEL entry NTAP must equal 3 (i.e. the original experimental yields must reside on TAPE3). OP,INTG can be executed without a subsequent OP,CORR, in this case NTAP must equal 0, TAPE3 need not be attached and no output file is written.

7.4.5 CALCULATION OF THE q PARAMETER MAP

```
OP,TITL
.
OP,GOSI
LEVE
.
.
ME
.
.
EXPT
.
```

```
.  
CONT  
. .  
END,  
  
OP,YIEL  
. .  
OP,MAP  
OP,EXIT
```

Input: TAPE4,TAPE9
Output: TAPE7

Comments: The maps of the q-parameters can be calculated without entering the decay-related information contained in the input to OP,YIEL. However, these maps are only needed for the fitting of the matrix elements, so the deexcitation data are usually already included in the input.

7.4.6 MINIMIZATION RUN - INITIAL STAGE

```
OP,TITL  
. .  
OP,GOSI  
LEVE  
. .  
ME  
. .  
EXPT  
. .  
CONT  
FMI,  
PRT,  
4,0  
. .  
0,0  
. .  
END,  
  
OP,YIEL  
. .  
OP,MINI  
. .
```

OP,EXIT

Input: TAPE4,TAPE7,TAPE9

Output: TAPE11,TAPE12

Comments: In this example it is assumed that the q-parameter map (TAPE7) has been generated during a previous run. OP,MAP can be executed before OP,MINI in the same run in which case TAPE7 should not be attached as an input file, but will appear as an output file instead. The PRT, entry 4,0 switches off the time-consuming calculation of the sensitivity map and is recommended during the initial stage of the minimization. To further speed up the fitting procedure one can also use the CONT switch FMI, if the printout of the comparison of the fitted and experimental data is not crucial. Usually one needs this table only periodically, so it is recommended to generate it separately when needed, by setting a high value of CHILIM in MINI command to inhibit actual minimization. This procedure is also more reliable, since it refreshes the normalization constants.

7.4.7 MINIMIZATION - FINAL STAGE

OP,TITL

.

OP,GOSI

LEVE

.

ME

.

EXPT

.

CONT

CRF,

SEL,

.

END,

OP,YIEL

.

OP,REST

.

OP,MINI

.

OP,EXIT

Input: TAPE11,TAPE12,TAPE4,TAPE7,TAPE9

Output: TAPE11,TAPE12,TAPE18

Comments: The CONT switch SEL, in conjunction with the default setting of the print parameter 4 (i.e. -2) causes the generation of an output file TAPE18, containing the information used by the code SELECT to create the correlation matrix, subsequently used during the error calculation. OP,REST causes GOSIA to use the values of the matrix elements stored on TAPE12 instead of those given in

the ME input. The internal correction factors file TAPE11 may be updated if the TEST criterion is fulfilled.

7.4.8 SELECT - CORRELATION MATRIX GENERATION

No user-given input is required to run SELECT. The only files needed are:

Input: TAPE18, created by GOSIA as TAPE18, as described above.

Output: TAPE10, containing the correlation matrix.

7.4.9 DIAGONAL ERROR CALCULATION

```
OP,TITL
.
OP,GOSI
LEVE
.
.
ME
.
.
EXPT
.
.
CONT
CRF,
.
.
END,

OP,YIEL
.
.
OP,REST
.
.
OP,ERRO
0,MS,MEND,0,0,RMAX
OP,EXIT
```

Input: TAPE11,TAPE12,TAPE4,TAPE7,TAPE9

Output: TAPE15

Comments: This example assumes the first diagonal error calculation, so IREP=0 and TAPE15 is not attached as an input file. To resume the diagonal error calculation the input to OP,ERRO should be modified as follows:

```
OP,ERRO
0,MS,MEND,1,0,RMAX
```

and the file TAPE15 should be attached as an input file. TAPE15 will be updated and overwritten. It is also assumed that the internal correction factors (TAPE11) and the current set of matrix elements (TAPE12) are those generated by the last OP,MINI run.

7.4.10 CALCULATION OF THE CORRELATED ERRORS

```
OP,TITL
.
OP,GOSI
LEVE
.
ME
.
EXPT
.
CONT
CRF,
SMR,
.
END,

OP,YIEL
.
OP,REST
.
OP,ERRO
1,MS,MEND,1,0,RMAX
OP,EXIT
```

Input: TAPE11,TAPE12,TAPE4,TAPE7,TAPE9,TAPE15,TAPE18

Output: TAPE3,TAPE15,TAPE17 if sets of matrix elements yielding better values of χ^2 were found during the run.

Comments: The above example assumes that the file for the sum-rules code SIGMA (TAPE3) is to be created and that the correlation matrix (TAPE18) is to be used during the error calculation. If more than one run is necessary to perform the full error calculation one should modify the input to OP,ERRO as follows to resume the job:

OP,ERRO
1,MS,MEND,2,0,RMAX

and attach TAPE3 as an input file. TAPE3 will be updated and overwritten by the current job.

7.4.11 6-j SYMBOLS TABLE

OP,TITL

.

OP,SIXJ
OP,EXIT

Input: None

Output: TAPE14

Comments: OP,SIXJ can be inserted anywhere in the command sequence, in which case the input files required by the preceding options must be attached.

8 SIMULTANEOUS COULOMB EXCITATION: PROGRAM GOSIA2

GOSIA2 is a special version of GOSIA that is intended to handle both target and projectile excitation simultaneously. This avoids introducing free parameters (normalization constants) which is important when only a very limited number of experimental data results from the experiment, like in case using radioactive beams and when the Rutherford scattering cross section is not measured simultaneously to provide a normalization. As an extreme case one can imagine the situation in which only the lowest transition is observed, then there are at least two parameters; the matrix element and the normalization constant. Simultaneous inclusion of the lines originating from the second partner and possibly known spectroscopic data makes it possible to achieve a unique solution. The problem of arbitrary normalization constants does not exist in case of multiple COULEX, where both the number of fitted matrix elements and the number of experimental data is large enough to neglect the impact of introducing few more parameters fitted by regular GOSIA.

GOSIA2 requires two parallel inputs describing both collision partners. It was chosen to keep separate inputs rather than merging them to form a single one to preserve maximum compatibility with the regular GOSIA input. One can switch to GOSIA by deleting only three input records. Using GOSIA relieves some restriction imposed by GOSIA2 when the use of GOSIA is justified. At the stage of fitting matrix elements GOSIA2 will switch between the two inputs. This results in the necessity of observing some conventions imposed by the GOSIA2 logic. The most important one is that experiments in both inputs and experimental data sets should be ordered parallel, i.e. experiment $\#n$ in the first input should be the same as experiment $\#n$ in the second. Then the common normalization constant will be found by the code. All geometric factors are included in the calculations without arbitrary renormalization. In the best case the experiments should be coupled together, like in GOSIA (although this is not required). In this situation there is only one constant remaining, reflecting “flux” or the total number of particles irradiating the target. An example of such organization of inputs is given below.

GOSIA2, as with GOSIA, has two main modes. The first is the Coulomb Excitation calculation which is designated by the OP,COUL section. The other is the experimental fit which is designated by OP,GOSI. Both of these options are input to GOSIA2 in the same manner as one would with GOSIA. The process for running the two functions is different.

To run the OP,COUL calculation the input files must be created using the guidelines described in the manual, I shall refer to the projectile and target input files as input1.inp and input2.inp respectively. It is important to note that each file requires a separate execution when calculating the gamma-ray yields. To execute each file type the following:

```
gosia2 < input1.inp
```

The output will then be written according to the designated output file in OP,FILE. The same line is used to execute the target file for target excitation, making sure to replace input1.inp with input2.inp.

To run the OP,GOSI portion of GOSIA2 the process is slightly more complicated. As with GOSIA each file must be run three separate times for the fit to be executed, once with OP,CORR, once with OP,MAP and once with OP,MINI. Once the inputs are prepared the execution is done as follows. First run each file, projectile and target, with OP,CORR using,

```
gosia2 < input1.inp
```

```
gosia2 < input2.inp
```

A file should be written with the corrected yields for both the projectile and target. Where the files are located will depend on whether or not there was a specific designation for the output in OP,FILE. Next each file should be run with OP,MAP. The execution is the same as before. Finally the projectile file should be run with OP,MINI. Again, the execution is the same as before.

GOSIA2 has been upgraded in parallel with GOSIA to maintain uniformity of both codes.

An example of inputs is intended to reflect a typical MINIBALL experiment. Note that actual numbers are not real (e.g. level schemes are not, so krypton is not really krypton, carbon is not really carbon etc. The aim of the inputs is to demonstrate their structure. The inputs illustrate the situation of “Kr” beam scattered on “C” target. Particle detectors form the ring in such a way that only “C” particles can be detected, “Kr” going through a central hole. The GOSIA2 commands are in bold, the non-bold comments should not be entered into the input file..

8.1 INPUT INSTRUCTIONS

Important – to avoid confusion execute one executable option at a time. The only exceptions are the sequences OP,REST+OP,MINI and OP,INTG+OP,CORR

1 Input identifier –associates this input with a filename (see below). Remove for GOSIA compatibility

OP, FILE Option to name the files which will be used. Not all of them is needed in every step, but the list below is complete, thus it is convenient to keep it full

22, 3, 1 22 is GOSIA(2) unit number (TAPE in the manual), 3 defines status=unknown, while 1=old, 2=new. Third entry means „formatted”.

kr88.out Output filename.

25, 3, 1 Unit 25 corresponds to input identifier 1. Remove for GOSIA compatibility. Start GOSIA2 with GOSIA2 < kr88.inp, then the code will switch between inputs itself.

kr88.inp The name of this input.

26, 3, 1 Same as above for C12 input.

c12.inp

14, 3, 1

dum.14 Usually internal, as defined in GOSIA manual.

17, 3, 1

dum.17 As above.

15, 3, 1 Used for error estimation, otherwise internal.

dum.15 As above.

kr88.me Current set of matrix elements in Kr. Written by OP,MINI, read by OP,REST

32, 3, 1

c12.me As above for C.

9, 3, 1

det.inp Gamma detectors file crated by OP,GDET. Requested by options involving calculation of gamma yields. Assumed to be the same for Kr and C (detector setup is identical).

11, 3, 2

crf.dat Internal, unformatted to save space. Updated by GOSIA2 for Kr and C.

3, 3, 1

kr88.org Here „uncorrected”, yields reside. See below.

27, 3, 1

c12.map A map of parameters for fast approximation for C. Required for OP,MINI and OP,ERRO. Created by OP,MAP.

7, 3, 1

kr88.map As above for Kr.

4, 3, 1

kr88.cor Kr corrected yields file. See OP,CORR.

18, 3, 1

dum.18 Internal.

23, 3, 1

kr88.raw Used by OP,RAW (OP,RAW is optional).

33, 3, 1

kr88.smr Sum-rules file for quadrupole sum-rules code SIGMA. Created by OP,ERRO if CONT switch SMR, was set.

13, 3, 1

cnor.dat Normalization constants file used by OP,MINI and OP,ERRO.

0, 0, 0 End of file definitions

OP, TITL

Projectile excitation of Kr88 Optional, causes the user-given title to be reprinted in the output

Here the definition of the problem starts. The only executable option which can be run at this point is OP,SIXJ if one wants to create a Wigner 6-j file, needed by SIGMA code. It will be written on unit 14 and GOSIA(2) will stop. Resulting file 14 should be renamed and kept for further use.

OP, GOSI Tells the code that fitting of the matrix elements is foreseen. Alternatively OP,COUL can be used if only the excitation part is of interest. OP,COUL simplifies the input of matrix elements. OP,GOSI requires the following suboptions:

LEVE Level scheme of the nucleus.

1, 1, 0, 0 Here four levels are defined. First entry is a user-given level index

2, 1, 2, .7 that the code will refer to in the output. Ground state must be given *index* = 1,

3, 1, 4, 1.5 the rest is arbitrary. Here there are four levels defined. Second entry

4, 1, 2, 1.2 is parity +1 or -1. The third one is spin, while the fourth is level energy in MeV.

0, 0, 0, 0 Four zeros ends input

ME Definition of starting matrix elements.

2, 0, 0, 0, 0 Multipolarity; 2 means *E2*.

1, 2, .8, .01, 2 Matrix elements-initial state index (as defined by LEVE), final state index, value (eb),

1, 4, .1, -1, 1 lower and upper limits the matrix element is allowed to change during fitting

2, 2, -.5, -1, 1 and error estimation. Note that ME's appear in odometric order by indices,

2, 3, 1., .01, 2 i.e. final increases first, initial second

2, 4, .2, -1, 1

3, 3, -.7, -2, 2

3, 4, .2, -1, 1

4, 4, .2, -1, 1

7, 0, 0, 0, 0 *E2* exhausted, now *M1*. First entry= 6 + *M* multipolarity (1 and 2 allowed).

2, 4, .5, -2, 2

0, 0, 0, 0, 0 First entry= 0 means that ME setup is complete

EXPT Definition of experiments at mean values of scattering angle and energy

2, 36, 88 Two experiments, Z,A of investigated nucleus

-6, 12, 194, -4, 3, 1, 0, 0, 360, 0, 1 First experiment $-Z$ of uninvestigated nucleus (minus appended means projectile excitation, i.e. Kr is projectile). *A* of uninvestigated nucleus. Bombarding energy (MeV) Projectile scattering angle(deg). Appended minus sign tells that actually target was detected. Number of magnetic substates from the starting *m* of the ground state to be used in the calculation using the full COULEX formalism, number of magnetic substates to be included in the fast approximation (0 or 1). Particle detector axial symmetry flag, 0 means axial symmetry, ϕ range of particle detector, redundant for axial symmetry. Kinematics flag -0 means larger CMS solution if projectile is heavier than target, 1 otherwise. Coupling of experiment normalizations, for the first experiment it is coupled to itself.

-6, 12, 194, -6.4, 3, 1, 0, 0, 360, 0, 1 As above, differs by scattering angle. Last entry specifies common normalization with experiment 1 (see OP,YIEL).

CONT As in GOSIA. Some print defaults changed, so to custom-make your input use PRT,

END, END, concludes CONT, End must be followed by a blank line. Empty record is the end of OP,GOSI input.

Before OP,YIEL, OP,GDET must be executed only once to create a file (Unit9). Remove the OP,GDET sequence after executing OP,GDET.

Assuming that all gamma detectors are physically identical one inserts:

OP, GDET

1 One physical detector (geometry)

.0001, 3.5, 10, 10 Radius of inactive core (historical), radius of the crystal, length of the crystal, distance from target to the detector face -all in cm.

0, 0, 0, 0, 0, 0, 0 Thicknesses of Al,C,Fe,Cu,Ag/Cd/sn, Ta and Pb absorbers in front of the detector. Here no absorbers are specified.

OP, EXIT End of execution, the remainder of the input ignored.

Note that the Coulex amplitudes and level populations can be calculated using:

OP, STAR

OP, EXIT

The gamma-yields related portion of the input starts:

OP, YIEL

- 0** Correction for in-flight decay changing the geometry of gamma detectors. 0 means no correction, 1 tells the code to apply it.
- 5, 2** Number of energy meshpoints and multiplicities to define internal conversion coefficients for Kr.
- .05, .1, .4, .8, 1.** Energy meshpoints (MeV)
- 2** E2
- 1, 1, 1, 1, 1** ICC's for E2 (here of course not real)
- 7** M1
- 1, 1, 1, 1, 1** As above
- 2, -2** Number of gamma detectors for each experiment. Here two detectors are defined. Minus sign appended to the second entry signifies that gamma detector setup is identical to this defined for previous experiment (common situation)
- 1, 1** Definition of the „physical” detectors as they appear in OP,GDET. There we assumed that all detectors are physically identical and we defined only one, so for experiment 1 both detectors are the same, as well as for experiment 2.
- 5, 90** θ angles of the gamma detectors
- 0, 0** ϕ angles of the gamma detectors

In the case of a non-identical detector setup the above sequence should be defined for each experiment.

- 2, 1** Normalization transition (level #2 to level#1). Used only for printout and simulation of experimental yields by OP,POIN.
- 2** Number of data sets, usually equal to the number of detectors unless clusters were formed by OP,RAW. Given for experiment 1, experiment 2 assumed to have identical setup.
- 1000, 1000** Upper limits of the transition intensities relative to the normalization transition for both detectors. If exceeded for the transitions not given as observed the contribution to least-squares function is added. Here this feature is practically switched off.
- 1, 1** Relative normalization constants of gamma detectors. The values should be the same for efficiency-corrected spectra or if OP,RAW is used.
- 4** Defines the file experimental „corrected” yields reside on. See also OP,POIN.
- 0, 0** Numbers and weights of available spectroscopic data – branching ratios,
- 0, 0** lifetimes, mixing ratios and known matrix elements.
- 0, 0** First 0 means no data available, otherwise the input is like in GOSIA.
- 0, 0**

OP, POIN

- 0, 0** or 1,limit, Optional, 0,0 – calculation of „point” yields just for printout. 1,limit causes additionally creation of the simulated experimental yields file containing all transitions of intensities exceeding the value of limit with respect to the normalization transition specified in OP,YIEL. This file will be written on unit 4. When executing OP,POIN the unit selector in OP,YIEL (in this example =4 should be set to 0.)

- OP, INTG** Performs integration over target thickness and particle detectors ranges

3, 5, 190, 194, 17.8, 28 Number of energy and theta meshpoints, energy range, theta range of detected particle, in this case target.

190, 192, 194 Energy meshpoints

-3, -3.5, -4., -4.5, -5. Projectile scattering angle meshpoints (appended minus sign when target was actually detected)

3, 5, 190, 194, 28, 32.8 Number of energy and theta meshpoints, etc. for experimnt 2..

190, 192, 194

-5., -5.7, -6.4, -7.1, -7.71 As above, for experiment 2.

3 Number of meshpoints to define dE/dx

190, 192, 194 Meshpoints

10, 10, 10 dE/dx values

20, 20 Number of subdivisions for numerical integration

0 Use the same dE/dx table for experiment 2

20, 20 Number of subdivisions for experiment 2.

In the present case input to OP,INTG is very simple – we defined axially symmetric ring detectors, so it is not necessary to define theta-phi dependence to reproduce arbitrary shape. Also the geometry is identical for both experiments. This corresponds to usual MINIBALL situation. OP,INTG offers the full description of an experiment, not only-as OP,POIN does-limited to mean values of bombarding energy and scattering angle. Input to OP,INTG is identical to that of GOSIA.

OP, CORR Converts the experimental yields (unit 3) to the values corresponding to „point yields” (unit 4). Corrected yields thus replace „original” yields and are subsequently used in the fitting procedure. Should immediately follow OP,INTG

OP, REST Overwrites the set of matrix elements defined by ME. Should be used when re-running the code.

1, .5 Matrix element #1 set to .5 by hand. Of course remove this when running fitting again, otherwise once again the value will be reset.

0, 0 Ends the input.

A sequence

OP, REST

0, 0

means read the matrix elements as stored with no hand-made changes

OP, MINI

2100, 5, .0001, .0001, 1.01, 0, 0, 1, 0, 0 Fitting parameters as in GOSIA, but the way GOSIA2 treats fitting is different. GOSIA2, along with fitting the matrix elements fits normalization constants in such a way that the constants are the same for corresponding datasets from both projectile and target excitation. The parameters given here are recommended ones. Before OP,MINI is executed OP,MAP must be executed (only once for each case (projectile or target excitation)).

OP,ERRO Estimation of errors of fitted matrix elements and optionally creation of SIGMA input file.
Executed separately for both target and projectile exactly like in GOSIA.

Parallel input for target – very similar to that of projectile. Below there is a list of options just pointing out what are the differences (easy to guess):

2 —————-input must be labelled 2
OP,FILE ————— change kr88 to c12 where appropriate
22,3,1
c12.out
25,3,1
kr88.inp
26,3,1
c12.inp
14,3,1
dum.14
17,3,1
dum.17
15,3,1
dum.15
12,3,1
kr88.me
32,3,1
c12.me
9,3,1
det.inp
11,3,2
crf.dat
3,3,1
c12.org
27,3,1
c12.map
4,3,1
c12.cor
7,3,1
kr88.map
18,3,1
dum.18
33,3,1
c12.smr
13,3,1
cnor.dat
23,3,1
c12.raw
0,0,0
OP,TITL
Target excited ————— or any other title
OP,GOSI
LEVE ————— level scheme of c12 instead of kr88
1,1,0,0
2,1,2,.8
3,1,4,2.
4,1,2,1.
0,0,0,0
ME —————-c12 matrix elements

2,0,0,0,0
 1,2,.8,.01,2
 1,4,.1,-1,1
 2,2,-.5,-1,1
 2,3,1.,.01,2
 2,4,.2,-1,1
 3,3,-.8,-2,2
 3,4,.2,-1,1
 4,4,.2,-1,1
 7,0,0,0,0
 2,4,.5,-2,2
 0,0,0,0,0
 EXPT —————investigated and uninvestigated nuclei interchanged, target excitation
 2,6,12
 36,88,194,-4,3,1,0,0,360,0,1
 36,88,194,-6.4,3,1,0,0,360,0,1
 CONT
 END,
 OP,YIEL —————internal conversion coefficients for c12, otherwise the same, until...
 0
 5,2
 .05,.1,.4,.8,3.
 2
 .5,.5,.5,.5,.5
 7
 .5,.5,.5,.5,.5
 2,-2
 1,1
 5,90
 0,0
 2,1
 2
 1000,1000
 1,1
 4
 0,0
 1,1 —————spectroscopic data, here lifetime of the first excited state known
 2,1.024,.02
 0,0
 0,0
 Remaining options as in Kr input

9 COULOMB EXCITATION OF ISOMERIC STATES: PROGRAM PAWEL

The code PAWEL is a modification of GOSIA designed to handle those special cases where a fraction of the Coulomb excited nuclei have as an initial state an excited isomeric state rather than the ground state. The only change to the standard GOSIA input is the addition of a first record after EXPT containing one number that is the abundance of the nuclei in the isomer state expressed in %. By convention the isomeric state must be level #2 in the LEVE setup. Otherwise there are no other changes to the standard GOSIA input.

The operation of PAWEL is similar to GOSIA, except that up to the stage of calculating statistical tensors PAWEL performs two passes. For the first pass the initial conditions are set in such a way that at $-\infty$ the excitation amplitude is set to unity for state #1 and to zero for all other states. For the second pass state #1 is replaced by state #2. Then both solutions are merged according to the user-given proportion between the ground and isomeric states. The deexcitation part remains unchanged after merging the statistical tensors, so there is only one calculation. The same applies for the fast approximation.

10 MINIMIZATION BY SIMULATED ANNEALING

R.W. Ibbotson

The problem of minimizing an arbitrary function can be approached computationally using a wide variety of techniques; some approaches are better suited to certain problems than others. A common feature of most of these techniques is that steps are taken iteratively in the variable space which reduce the “cost” function (whatever function is being minimized). For a one-dimensional minimization problem with cost function $C(x)$, a step Δx is chosen so that $C(x + \Delta x) < C(x)$ and repeated steps are taken in x until the value of x for which $C(x)$ is a minimum is found. This approach will be referred to here as “strict minimization”, since the cost function is never allowed to increase as the minimization procedure is executed. This is a logical and efficient approach, but certain problems will not be solved properly by this method. Specifically, if the function being minimized has several local minima, only one of which is the true global minimum of the function, strict minimization will only converge to the global minimum if the starting point is chosen somewhere in the “well” of the global minimum. Any algorithm which only takes steps “downhill” runs the risk of not converging to the global minimum, unless it is started at a point sufficiently close to this global minimum. For example, if a strict minimization procedure is used to find the minimum of the function shown in Figure 13 and the starting point is chosen in region II, the procedure will converge to a value of $x \approx +1.4$ ($C(x) \approx 8.8$), rather than the global minimum value at $x \approx -2.0$ ($C(x) \approx 2.2$). The general location of the global minimum is often known in physics-related problems from a consideration of the physical properties of the system in question. In large Coulomb-excitation problems, however, the fit quality may be sufficiently dependent on certain unknown quantities such as the sign of a static E2 matrix element that an alternative to strict minimization should be considered. The method of Simulated Annealing (SA) is an attempt to overcome this shortcoming of standard minimization techniques by allowing some steps uphill, in a controlled fashion.

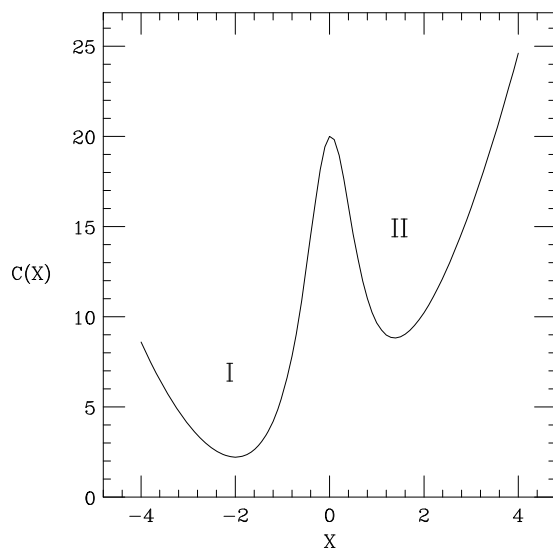


Figure 13: An example of a function which can cause difficulties with strict minimization procedures. A procedure using a starting value of x in region “II” ($x > 0$) will not converge to the global minimum at $x \approx -2.0$.

10.1 The Development of Simulated Annealing

In 1953, Metropolis et al. showed that it is possible to reproduce the thermodynamic properties of a system of particles by what amounts to a Monte-Carlo integration over configuration space [Me53]. The method proposed by Metropolis involves beginning with these particles (or molecules) in a lattice, and choosing new

configurations with a probability $e^{-E/kT}$ (Where E is the energy of the configuration, T is the temperature and k is the Boltzmann constant). These configurations are used in computing statistical properties of the system by averaging the value of such properties in the space of these configurations, and weighting the configurations evenly. In order to accomplish this, new configurations are generated from an initial configuration by considering motions of each particle, and accepting steps for which $\Delta E < 0$ with probability one, and accepting steps for which $\Delta E > 0$ with probability $e^{-\Delta E/kT}$. This method accurately reproduced the equation of state for a two-dimensional system (the ratio PA/nkT as a function of \bar{n} , the average density of particles at the surface of one particle).

The extension of this method to minimization procedures is obvious: since the Boltzmann-like energy weighting reproduces physical thermodynamic properties, it is theoretically possible, by slowly lowering the temperature of the simulated numeric system, to find the global minimum of the system, analogously to the process of annealing of crystals. In the following discussion, the method of Simulated Annealing will be described for problems of one dependent variable only. The adaptation of this method to multi-variable minimization problems will be discussed later.

The Simulated Annealing method in its most general terms is described as follows:

```

Set starting value of temperature T
LOOP For some period of time:
    generate a step  $\Delta x$ 
    calculate change in cost function  $\Delta C(x + \Delta x)$ 
    Calculate probability of accepting a step with  $\Delta C(x + \Delta x)$ :  $G(\Delta C, T)$ 
    accept step ( $x = x + \Delta x$ ) or reject ( $x$  unchanged) based on the value of  $G(\Delta C, T)$ 
After sufficient time/loop executions:
Reduce temperature T
Return to LOOP section above

```

Following the thermodynamic analogy strictly, the probability $G(\Delta C, T)$ is the Boltzmann factor $G = e^{-\Delta C/T}$ where T is now a non-physical parameter in the same units as the cost C. Note that for $\Delta C < 0$, the probability G is defined to be one (downhill steps are always taken, regardless of temperature). At higher temperatures, steps which increase the value of the cost function C are more likely. Since steps are not chosen to produce a maximal decrease in the cost function (as in strict minimization), there is some question of how to determine the direction and magnitude of the steps to be taken. In continuous-variable systems, the steps are usually generated by a random variable with a Gaussian distribution, analogous to the thermal motion of molecules in a gas. The width parameter of the Gaussian motion is controlled by the same temperature which is lowered to provide the annealing.

While the process described above should eventually find the global minimum of the cost function, there are several details which have not yet been addressed. For one, the number of times that the loop is executed (before lowering the temperature) has not been specified. The best method of generating steps (i.e., the magnitude of the step-size) is also not immediately obvious. Finally, the method in which the artificial temperature is lowered has not been specified. These latter two questions are in fact intricately related. We shall therefore first address the methods of step-generation and temperature lowering in the following paragraphs.

The rate at which the temperature is lowered is obviously crucial to finding the global minimum. A too-rapid decrease leads to quenching, which locks the solution into the nearest minimum. The criterion on the cooling schedule may be expressed as follows: any point must be visited "infinitely often in time", which actually implies that a state may be visited at least once in an infinite amount of time. Of course, an infinite amount of time is never available for such an analysis, but at small temperatures the hill-climbing capacity may be assumed to be negligible. It has been shown that [Ge84], for Gaussian motion in the parameters, it is sufficient to lower the temperature logarithmically:

$$T_j = T_0 / \log(1 + j) \tag{1}$$

where T_0 is the initial temperature and j is the step number.

Since the goal of the Simulated Annealing process is not the reproduction of thermodynamic processes, as in Metropolis' work, it is not necessary to use the Gaussian, thermal-like steps described above. Szu and

Hartley [Sz87] have shown that a Cauchy-Lorentz distribution ($p(\Delta x) = \frac{T}{T^2 + \Delta x^2}$) is much more efficient, since the larger probabilities for large jumps allow the possibility of tunneling through barriers. Such a one-dimensional distribution can be produced by $\tan(\pi/2 * (2r - 1))$ (where r is a uniformly distributed random number between 0 and 1). This modification allows a much faster cooling schedule; it is sufficient to lower the temperature as

$$T_j = T_0/j. \quad (2)$$

While the above methods address the question of step-size generation in terms of the generating distribution, the width of this distribution (overall magnitude of the step sizes) has not been addressed. The specification of this magnitude is generally pragmatic: the step-size (width of the distribution) is chosen so that the process spends a “reasonable” amount of time sampling unfavored sections of the parameter space. This may be achieved by adjusting this width so that a certain fraction of the attempted events are not accepted (typically 1/2). Likewise, the number of steps taken before lowering the temperature should be large enough to ensure that the process samples the available section of parameter-space thoroughly. The number which satisfies this is very case-dependent, so no general prescriptions can be given.

The generalization of these methods to multivariate cases introduces several challenges. Firstly, it is not clear whether it is best to perform steps in the variables simultaneously or individually. If the steps are taken simultaneously, there are problems in producing the required distributions, since there is no closed-form method for producing a multi-dimensional Cauchy distribution. It is possible to use a product of one-dimensional Cauchy distributions, however this requires a modification of the cooling schedule. Several other schemes have been suggested to overcome these difficulties (e.g., Very Fast Simulated Reannealing [In89] and Threshold Annealing [Du90]). Many other modifications and new schemes have been proposed over the past decade; the reader interested in further details is directed to e.g., [Mo90, Ki83, Sa91] and references therein.

10.2 Implementation of SA in GOSIA

In addition to the challenges involved in implementing Simulated Annealing (SA) to multi-dimensional problems, several issues inherent in the current Coulomb-excitation technique require special attention in the adaptation of SA techniques. There are three issues which will be discussed in the following sections: (1) since the steps taken in the matrix elements may vary in magnitude, the recalculation of the correction factors must be periodically performed; (2) the different sensitivities of the cost function (χ^2) to the different matrix elements implies that the step sizes for different matrix elements must be independent; (3) due to possible dependencies of these sensitivities on *the portion of the parameter space currently being sampled*, these step-sizes must be periodically re-evaluated. The limits on each matrix element which are set in the ME subsection (described in the GOSIA manual) are obeyed in the annealing process as well.

In the present work, the method of Szu and Hartley has been followed for determining the step size for each matrix element. Steps in the individual matrix elements are generated simultaneously, in order to better account for correlations between matrix elements (i.e., large steps in a certain matrix element may be strongly hindered, unless simultaneous steps in a correlated matrix element are taken) according to a Cauchy-Lorentz distribution. This is achieved by choosing

$$\Delta x_i = \sigma_i \tan\left(\frac{\pi}{2}(2r_i - 1)\right), \quad (3)$$

where r_i is a random number between 0 and 1 and the “width” array σ is an attempt at accounting for the very different sensitivities of the matrix elements. The elements of this width array are initially set proportional to $1/(d\chi^2/dx_i)$, and the widths are monitored and adjusted throughout the annealing procedure. The σ_i are adjusted by recalculating the sensitivities periodically (at a user-specified interval). This re-calculation may be performed in one of two methods: the “forward” calculation and the “forward-backward” calculation. The former method consists of evaluating $d\chi^2/dx_i$ using two values of x_i - the current value, and a step in the “forward” direction $x_i + \Delta x_i$. The latter method involves the calculation of χ^2 at the points $x_i + \Delta x_i$ and $x_i - \Delta x_i$. In both cases only the first derivative (slope) is evaluated. Since the value of χ^2 at the current point is known, the “forward-backward” method involves twice as many χ^2 evaluations, and therefore takes roughly twice the execution time.

The average range covered by each matrix element is also tracked, and the maximum of the two width estimates is used (in order to account for possible inaccuracies in the sensitivities, which are calculated in the fast approximation). An overall scaling factor is applied to the width array (which is otherwise normalized to $\sum \sigma_i^2 = 1$) and this scaling factor is adjusted to maintain a ratio of accepted steps to attempted steps of 1/2. This ensures that the code spends a reasonable fraction of the time sampling unfavored regions.

Since Coulomb-excitation analyses are all somewhat unique, there are several parameters which must be supplied by the user to determine the flow of the program. A basic understanding of the logic of the annealing routine is very helpful for determining the appropriate values of these parameters for a given Coulomb excitation analysis. The structure of the routine is described here, and it is suggested that the user monitor the progress of the procedure regularly.

The core section of the annealing routine is a loop similar to that described above. That is, a sequence:

```

Generate a step (in all matrix elements)
calculate  $\Delta\chi^2$  for this step
calculate probability to accept step  $G(\Delta\chi^2, T)$ 
accept or reject step

```

that is executed a number of times controlled by the input quantities IACC_LIM and ITRY_LIM. If the number of attempted steps exceeds ITRY_LIM or the number of accepted steps exceeds IACC_LIM, the loop will terminate. Upon termination of this “inner” loop, the current statistics are printed to the log file and the width array $\sigma(x_i)$ is re-scaled by an overall factor in order to keep the ratio of attempted to accepted steps as close to 1/2 as possible. Before re-scaling, the sensitivities for each matrix element may be re-calculated on the basis of the input parameter ISENS.

The “inner” loop described above is then re-entered and executed until one of the previously described limits is again reached. The “inner” loop described above is thereby enclosed within an “outer” loop as follows:

```

Execute “inner” loop until termination
print statistics
if isens “outer” loops have been executed, re-calculate sensitivities
    and width array
re-scale width array

```

Once a total of IACC_TOT_LIM steps have been accepted at the current temperature, the program will immediately leave both inner and outer loops, lower the temperature, and begin the above process again. The program will, however, execute this “outer” loop a maximum of OUTERLIM times and then halt execution without lowering the temperature. The OUTERLIM parameter is therefore a maximum value that should not be reached under normal execution. This is assumed to be a number large enough that reaching this value indicates a condition which requires human intervention (for example, if no steps are ever accepted due to an improperly chosen limit).

There is one other condition which will result in the program halting execution. This condition is defined by the “current” χ^2 value dropping below a minimum value CHIOK. The reason for this condition is simple: if the program happens upon a very good fit, there may be little reason to continue the procedure. The user may check the resultant matrix-element values and decide whether the solution is reasonable or not before continuing execution of the program.

Since the SA approach lends itself to long (≈ 1 day) execution times, the implementation of this approach in the Coulomb excitation program GOSIA has been designed to be as fault-tolerant as possible. In the event of a computer crash, the program can usually be re-started with little loss of time. During execution, several auxiliary files are therefore employed for the storage of information necessary for a quick re-start. The current set of matrix elements is written to disk periodically so that in the event of a crash, the calculation may be resumed from the last recorded point. The current width array $\sigma(x_i)$, temperature, and numbers of steps attempted and accepted are also written to disk so that the program can be somewhat system-fault tolerant. The current “best-fit” matrix elements are also tracked and written to disk, so that the user may inspect the quality of the fits. The correction factors (for the “fast” calculation) are also written to disk periodically. These can be corrupted, however, in the case of unexpected program termination (i.e., a crash). The correction factors should therefore always be re-calculated when re-starting GOSIA.

Since the SA approach relies on sampling a large portion of parameter-space, the amount of time required to solve a problem grows very quickly with the dimension of the parameter-space. For this reason, the SA approach currently is most effective when used for smaller problems, or when constrained to a subset of the total parameter-space. The greatest success with this method has been achieved [?] when only a small (≈ 20 matrix element) subset of the parameter-space was “released” for minimization. In this case, after several hundred steps, the annealing approach escaped a physically unreasonable local minimum and found a better minimum that then was reached using the strict minimization methods in GOSIA. The choice of this subset must be made on the basis of physical knowledge of the system, and should of course not exclude variables that are strongly coupled to those which are included.

10.3 Input parameters for OP,ANNL

The annealing routines are used as an alternative to the strict minimization routines which are called with an OP,MINI command. Since the aim of the strict-minimization and Simulated Annealing approaches is in the long run similar (find the set of matrix elements which minimizes the χ^2), the command “OP,ANNL” can be substituted directly for an OP,MINI command with the necessary adjustments in the parameters read from the input file.

The input to OP,ANNL is as follows:

OP,ANNL

NPTL,CONV,CHIOK,TEMP,IMODE,IACC_LIM,ITRY_LIM,OUTERLIM,ISENS,IACC_TOT_LIM

Some of these input parameters are described in detail above. A brief description of the parameters is given below. Note that the SA version of GOSIA contains an additional (optional) input in the CONT subsection of OP,GOSI which is also listed here.

NPTL	Number of temperatures to run
CONV	Convergence criterion: if the sum of the squares of the changes in all matrix elements is less than this value, execution will halt.
CHIOK	If the chisq drops below chiok, the job ends.
TEMP	Starting temperature.
IMODE	IMODE = 10*i+j where i,j are as follows: i=1: forward-only method for sensitivity calculation i=2: forward-backward method for sensitivity calculation j=1: fast approximation is used for χ^2 evaluation j=2: fast approximation is not used for χ^2 evaluation Note: The fast approximation is always used for sensitivity calculations NOTE: Choice of j=2 will SIGNIFICANTLY increase execution time.
IACC_LIM	Acceptance of this many steps ends “inner” loop.
ITRY_LIM	Attempting this many steps ends “inner” loop. NOTE: end of “inner” loop implies that the step sizes are re-calculated before more steps are taken.
OUTERLIM	Maximum number of these “sets” of steps (dictated by iacc_lim and itry_lim) to execute in order to reach iacc_tot_lim accepted steps (for each temp.) If more than innerlim “sets” are required, the job stops.
ISENS	Every “isens” executions of the “outer” loop, the individual step-sizes for each me are recalculated by means of gradients (calculated with fast approximation).
IACC_TOT_LIM	Number of steps to accept before lowering the temperature.

Additional input field for CONT suboption of OP,GOSI:

SFX,
NTOT
I1(1),I2(1),RSIGN(1)

I1(2),I2(2),RSIGN(2)

...

I1(NTOT),I2(NTOT),RSIGN(NTOT)

The specification of SFX allows one to fix the relative signs of pairs of matrix elements. The “SFX,” field must be followed by the total number of pairs to be fixed, and then by the absolute indices of the matrix element pairs (following the same numbering scheme in the non-SA version of GOSIA) and the relative sign. The sign of matrix element number I1(i) is fixed to be RSIGN(i) times the sign of matrix element I2(i). If the sign of I2(i) changes during the minimization, the sign of I1(i) will be changed to keep the relative sign as specified. The program will expect NTOT input fields with I1,I2,RSIGN.

11 LEARNING GOSIA

GOSIA is capable of performing accurate calculations for a wide range of Coulomb excitation experiments. Consequently, precise definitions of the experimental parameters, data and the variables to be fit require careful attention. Chapter 5 of this manual covers the details of each section of the user input (the “input”), while the present chapter will help reduce the time required to install and learn GOSIA. It is strongly advised that the user first learn to use Gosia before using the similar code Gosia2.

Section 1 of this chapter gives compiling instructions.

Section 2 is a description of the basic components of the typical GOSIA input required by the novice user.

Section 3 is a tutorial that introduces the user to the basic operations involved in simulating an experiment and fitting matrix elements to data with the help of flow diagrams.

Section 4 is a second tutorial that demonstrates a fit of 10 adjustable parameters to simulated data. The tutorial guides the user through editing a Gosia input in a text editor to perform each step of the fitting procedure. Understanding this tutorial is aided by the annotated version in Section 5.

Sections 6 and 7 explain important features of a Gosia output file.

Section 8 details the situations in which accuracy problems might arise and describes how they can be avoided.

Lastly, Section 9 gives a brief set of suggestions to help the novice debug syntax errors and physics-related problems.

11.1 Compiling GOSIA 2008

GOSIA 2008 has been updated significantly from previous versions: The code is now explicitly 64-bit and no longer allows the user the option of compiling in 32-bit mode, because of the danger of serious accuracy problems using 32-bit math. Because of these and other changes, GOSIA 2008 is much more portable, and the source is easily compiled to produce an object that gives high-accuracy results. Proper alignment of the common blocks is now handled in the source of GOSIA 2007, so it is no longer necessary for the user to set the alignment for 64-bit accuracy.

We recommend running GOSIA 2008 on a true 64-bit processor using the GNU g77 compiler with the following command:

```
g77 -o gosia gosia.f
```

This will produce a functional object on most modern Unix-like machines. The user may find improvements in speed by using compiler optimization switches. When experimenting with compiler optimization, the accuracy should be tested using the sample inputs and outputs provided on the Gosia website.

11.2 Learning to Write Gosia Inputs

The fastest way to learn to write GOSIA inputs is to begin with one of the sample inputs on the GOSIA website and modify it in stages. The meaning of each line in the sample input can be understood by comparing it with the manual entry for the relevant section (e.g. OP,YIEL or OP,INTG), while Chapter 5 gives a listing of the options that are required for each of the functions of GOSIA. Each function is controlled by an “option” labeled in the input as “OP,XXXX”, where XXXX is a four-letter identifier. The subsections of each option are referred to in this manual as “sub-options,” and have a two- to four-letter identifier. In general, the physical problem is defined in several sections (“options”) of the code in the order that follows, with other sections being optional.

OP,FILE Assigns file names to the input and output files. The OP,FILE entry is optional but recommended, because descriptive file names prevent confusion that can arise from the default names fort.1, fort.2, etc.

OP,TITL The user’s choice of a description of the input.

OP,GOSI This block defines, among other parameters, the nuclear system and a brief description of the experimental situation. (OP,COUL can be used instead, if the user desires only to calculate gamma-ray yields, not to fit matrix elements.)

LEVE This is the level scheme of the nucleus to be studied (either projectile or target).

ME The starting values of the EM matrix elements are given here. The desired coupling of fit parameters and boundaries for the fit are entered if OP,GOSI was specified.

EXPT This sub-option defines the experimental setup briefly, including particle detector geometry and specifications for the point-approximations used to increase the speed of the fit. The mean beam energy (as the beam traverses the target) is specified here, along with the projectile and target species. Up to 50 “experiments” may be specified, where each experiment may be defined as merely a range of projectile scattering angles, or as a truly distinct experiment with a different projectile, target, etc.

CONT A number of accuracy controls are given here. Several other switches in this sub-option allow the user to quickly fix or release matrix elements in the fit. The user may also choose output options in CONT.

END, This entry marks the end of the CONT sub-option and should be followed by a single blank line.

[Blank line]

OP,YIEL This option defines internal conversion coefficients, gamma-ray detector types and angular coverages, normalization of the particle detectors (if necessary), normalization of calculated gamma-ray yields, detector sensitivity (for the calculation of chi-squared). Optionally, a set of lifetime, matrix element, gamma-ray branching ratio and mixing ratio data can be entered and included in the chi-squared fit.

OP,INTG This option defines the particle scattering angle ranges over which the yields are to be integrated for each experiment. This consists of defining the particle detector shape (if necessary), angular limits and meshpoints for the integration. Stopping powers and beam energy ranges effectively define the target thickness here.

The input is generally run several times to perform the fit, with minor changes to the input at each stage, as demonstrated in the tutorials in this chapter. It is recommended that the user begin analysis of real data by running an integration (OP,INTG) based on one of the inputs used in the tutorials. When the physical system is satisfactorily defined (beam, target, level scheme, initial guesses at the matrix elements, beam energies and scattering angles), the integrated yields can be compared to the data. A fit to experimental data can then be accomplished by following the steps that are described in the fitting tutorials.

11.3 Tutorial 1: Gosia basic flow sequence

This tutorial requires the set of files contained in `toyfit.tar` which can be downloaded from the Gosia website <http://www.pas.rochester.edu/~cline/Gosia/index.html>.

This set of demonstration files (`toyfit.tar`) make a up a tutorial on the basic operations that are typically performed to simulate and analyze experimental data. The `toyfit.tar` file contains a sample input, a simulated data set and a set of sample output files, which can be compared to the results in this tutorial. On a Unix-like machine, issue the following command to unpack the tar file in the desired working directory.

```
tar -xvf toyfit.tar
```

The entire demo can be run using Gosia 2007 without any modification to the files. However, in order to learn to run Gosia effectively, it will be necessary to examine the files and compare sections of the input with the corresponding entries in the Gosia manual. A brief overview of relevant sections of the code is given in this tutorial, and the annotated inputs later in this chapter will also help to identify the various “options,” records and fields.

11.3.1 Simulation

The planning of a Coulomb excitation experiment can be aided by simulating the expected yields based on a best guess of the level scheme, including as much previously measured data as possible. This example calculates the expected yields for Coulomb excitation of the *fictionous* nucleus to be investigated, $^{120}_{55}\text{Fi}$. The assumed level scheme for $^{120}_{55}\text{Fi}$ is shown in figure 14. In the planned experiment, a beam of $^{70}_{35}\text{Br}$ will bombard the $^{120}_{55}\text{Fi}$ target. The example Gosia input `simulate.inp` produces simulated cross sections. Refer to the relevant sections of chapter 5 in this manual for each Gosia “option” described below for more detailed descriptions of each record and field. A brief flowchart of the entire simulation procedure is shown in figure 15.

The first Gosia “option” in `simulate.inp` is **OP,FILE**, which assigns a filename chosen by the user to each auxiliary file to be used by Gosia. The files used will depend on the calculation options chosen. In this case, only the input file (`simulate.inp`), the output file (`simulate.out`) and a detector file (`det.gdt`) are assigned. If a needed file is not assigned a name, Gosia will look for or create a file named “fort.[n]”, where n is the fixed file number. It is acceptable to assign names to files that are not being read in a particular step. This means that the user can define all necessary files for the entire process in an early stage, if desired.

OP,TITL allows the user to reprint comments at the header of the output file.

OP,GOSI (Gosia) is executed next. Alternatively, **OP,COUL** (Coulex) could have been used, but **OP,GOSI** is a more flexible version of **OP,COUL** that allows the user to fit matrix elements to data with fewer modifications to the input file. The first “sub-option” in **OP,GOSI** is **LEVE**, which gives the known or predicted level scheme in any convenient order (except that level 1 must be the ground state). The first three excited states in the yrast sequence of the investigated nucleus are known (Figure 14). The 0^+ to 6^+ states are labeled in the example input `simulate.inp` as levels 1—4. Each level is defined on one line by the following quantities: index (beginning with 1), parity (+/- 1), spin, energy (MeV). *Note that comments are not allowed on some lines of the input. Restrict comments to the lines which are commented in the example files.*

The second sub-option of **OP,GOSI** is **ME**, which defines the matrix elements, all E2 in this case. The header 2,0,0,0,0 indicates the beginning of E2 matrix elements, and all relevant E2 reduced matrix elements are then listed with the initial and final indices in “odometer order.” The following quantities describe each matrix element: initial level, final level, matrix element, lower limit, upper limit. The lower and upper limits will be used by Gosia in the fitting tutorial. Setting the lower and upper limits equal (1,1 in the present input) “fixes” the matrix element during a fit. The footer 0,0,0,0,0 terminates the ME input.

The sub-option **EXPT** defines the “logical” experiments to be simulated, in this case only one. A “logical” experiment typically refers to detection of a scattered or recoiling particle over a particular solid angle. The first line of **EXPT**

```
1,55,120
```

tells Gosia that there is one experiment and that the investigated nucleus (for which Coulomb excitation calculations are to be performed) has $Z=55$ and $A=120$. The following line

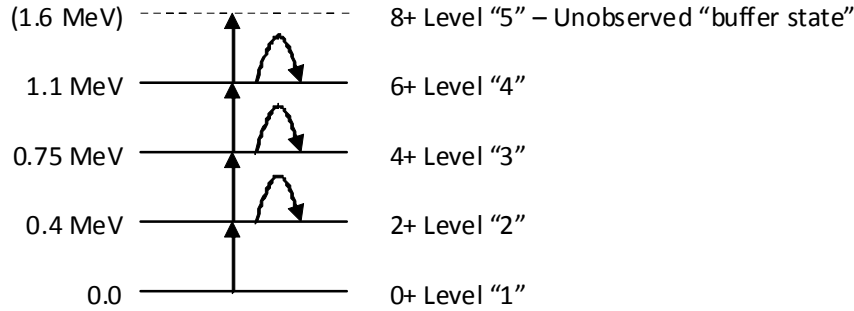


Figure 14: Fictitious level scheme of the nucleus to be investigated in the toyfit.tar demo. Levels are labeled with their energy, spin, and the index used in the Gosia inputs. Arrows represent the E2 matrix elements entered in the Gosia inputs with the consistent phase convention as shown. Three E2 diagonal moments are included. The 8^+ is a "buffer state" required for accurate calculation of the 6^+ state yields. See section 5.13.

35,70,240,70,4,0,0,0,360,1,1

defines the "un-investigated" nucleus ($Z=35$, $A=70$), the mean beam energy in the target (240MeV), the mean laboratory scattering angle (70 degrees polar). The remaining fields define accuracy parameters for the point calculations, symmetry of the detector (azimuthal symmetry in this case), normal or inverse kinematics (irrelevant here) and normalization to other experiments (also irrelevant here).

The **CONT** block is used to set a number of options including fixing/freeing of matrix elements, output options, the use of PIN diodes as particle detectors, etc.

Note that a blank line is required after the flag END,

The 4th option in this input is **OP,YIEL**, which allows the user to define the gamma-ray detector locations, internal conversion coefficients, normalization constants between experiments (irrelevant in this case), tabulated data (branching ratios, lifetimes, mixing ratios and measured matrix elements), etc. The user is referred to section 5.30 (OP,YIEL) for a detailed description. The following are of particular interest to the first time user. (Note that the line numbers will vary with the complexity of the experimental setup.)

Lines 2 - 7: These are the internal conversion data entered by the user from tables, such as those from BRICC.

Lines 9 - 11: This declares that a Ge detector of type "1" in the detector file ("det.gdt" in this case) is positioned at a polar angle of 45 degrees and an azimuthal angle (arbitrary 0) of 90 degrees. Only one Ge detector is defined in this experiment!

NTAP is set to 0, which tells Gosia that no experimental yields are to be read from disk. Obviously, experimental data are not used to simulate yields.

The final option used is **OP,INTG**, which integrates the point calculations over the particle scattering angles and the beam energy range as the projectile traverses the target. If azimuthally symmetric particle detectors are used, the target is "investigated" and the beam particle is detected, as in the present case, the input is relatively simple with the first three lines corresponding to experiment 1. Line 1,

5,5,230,250,60,80

indicates that 5 equally-spaced energy meshpoints and 5 polar scattering angle meshpoints will be provided by the user. The energy range as the beam traverses the target is 250—230 MeV, and the particle detector covers the laboratory scattering angles 60—80 degrees. In the present version of Gosia, the energy range must be calculated by the user from tabulated stopping power data. Line 2 gives the energy meshpoints, and line 3 gives the scattering angle meshpoints, both of which must exceed the integration range.

Lines 4 - 6 give stopping power data for the beam and target combination. (In the present case, the stopping power is about 32 MeV per mg/cm^2 , and the energy range in the target is 20 MeV, so the target thickness is about $2/3 \text{ mg}/\text{cm}^2$.)

Line 7 gives the number of subdivisions in energy and scattering angle to be used for the fast interpolation

between meshpoints. When starting a new calculation it is wise to halve or double the number of subdivisions at least once to make sure that convergence is achieved. Refer to the troubleshooting section in this chapter.

In this example, the Ge detector definitions file `det.gdt` has already been provided. (The fitting tutorial in this section gives an example of how to create a detector file.) In order to produce simulated yields, Gosia only needs to be told to execute the `simulate.inp` input file using the command

```
gosia < simulate.inp
```

The following output should be generated

```
OPENED simulate.out
IO-num = 22 UNKNOWN FORMATTED
etc
```

When the system prompt is returned, an output file `simulate.out` will be present. Among other data, the simulated, integrated yields appear at the end of the input. The yield output looks like the following.

```
INTEGRATED RUTHERFORD CROSS SECTION=.9472E+03 FOR EXP. 1
INTEGRATED YIELDS
EXPERIMENT 1 DETECTOR 1
ENERGY RANGE 230.000--- 250.000 MEV SCATTERING ANGLE RANGE 60.000--- 80.000 DEG
NI NF II IF YIELD NORMALIZED YIELD
5 4 8.0 6.0 0.12033E-08 0.12681E-09
4 3 6.0 4.0 0.14781E-04 0.15576E-05
3 2 4.0 2.0 0.64335E-01 0.67797E-02
2 1 2.0 0.0 0.94893E+01 0.10000E+01
***** END OF EXECUTION *****
```

First, the Rutherford cross section is given, integrated over the target thickness as well as the solid angle, in $mb \bullet mg/cm^2$. To obtain the usual Rutherford cross section, it is necessary to divide this number by the target thickness, giving

$\sigma_R = (0.9472E + 03mb \bullet mg/cm^2)/(0.62mg/cm^2) = 1528mb$. The cross section for measuring the gamma-ray transition from state 2 to state 1 in a perfect (blackbody) detector can be obtained from the final line of output. In the YIELD column, Gosia gives a differential cross section, which is integrated over the particle detector solid angle and the energy range in the target, but not over the Ge detector solid angle. In the present example, this quantity is $d\sigma/d\Omega_\gamma = (0.94893E + 01)mb \bullet (mg/cm^2)(1/sr)$. The `det.gdt` file that came with `simulate.inp` represents a Ge detector of 5 cm diameter placed with its face 15 cm from the target position. Hence, it subtends a solid angle of $0.087sr$. (Refer to the second demo on fitting matrix elements for an example that shows how to define a Ge detector.) The absolute cross section for scattering of the beam into the particle detector and emission of the 2^+ to 0^+ γ -ray into the Ge detector is then $\sigma_{p\gamma} = 0.94893E + 01mb \bullet (mg/cm^2)(1/sr) \times 0.087sr \div 0.62mg/cm^2 = 1.33mb$. Note that this is not a point calculation of the mean cross section at the mean beam energy, but rather, it is integrated over the energy range of the beam in the target. Refer to section 5.12.5 of this manual to convert this cross section to absolute counts.

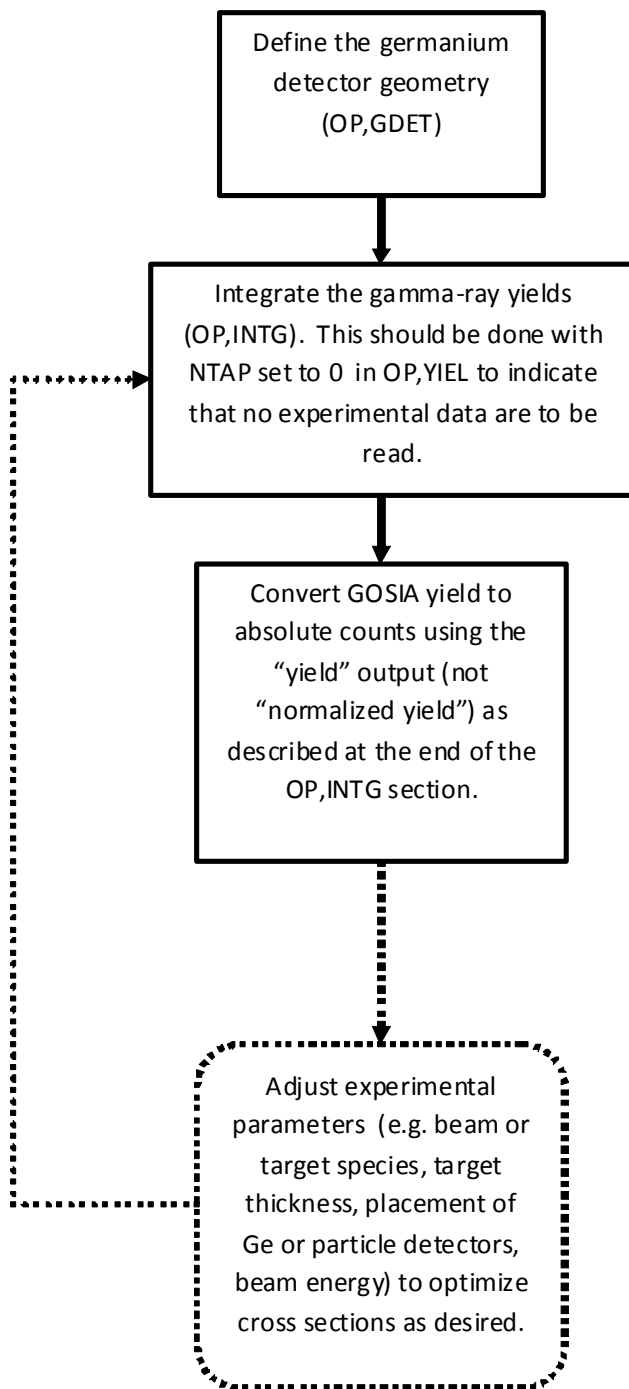


Figure 15: Gosia simulation flow diagram

11.3.2 Fitting Matrix Elements to Gamma-Ray Yield Data

This section describes the use of a series of sample inputs to fit matrix elements to experimental data. The simplest possible case is examined: fitting one parameter (two $E2$ reduced matrix elements coupled as one parameter) to a few experimental gamma-ray yields (from the lowest 4 excited states in a fictitious nucleus). The level scheme is the same as the one in the previous demonstration, that is Fig 13, but in this case, matrix elements 3 and 5 will be adjusted to find the chi-squared minimum in the calculated yields.

This “toy” problem can be used as a model for the basic procedure used to analyze real data, even though a real problem might involve more sophistication, such as, axially asymmetric particle detectors (of arbitrary shape), data from user-defined Ge detector “clusters,” choices regarding the normalization of one data subset to another, data from multiple beam and target combinations, data from unresolved doublets, inverse scattering kinematics, etc. A flowchart of the general procedure to define the germanium detector(s), fit matrix elements to the data and estimate the errors in the fitted matrix elements is given in Fig 16 plus 17.

The demonstration is run using a set of inputs and related files in the `toyfit.tar` archive on the Gosia website. Each step of the demonstration is run with a different `*.inp` file. In practice it is probably better to use the same input file for all or most steps to prevent accidental inconsistencies between steps. The files should be modified for each step in a text editor such as `emacs` or `vi`, paying attention to delimiters, spacing and capitalization. The second fitting demonstration (section 11.4) uses this method of editing one input file between steps and fits more matrix elements. However, the present demonstration can be run without any modification to each input file. Each step in the procedure is executed by typing

```
gosia < *.inp
```

At each step, the relevant portion of the input is described, but the novice user should refer to the manual entry in Chapter 5 for complete details of the records and fields required for a particular Gosia option, e.g. `OP,GOSI` or `OP,INTG` etc. This demonstration includes two iterations of the fitting procedure to make sure that the correction factors for the point approximations used in the fit were sufficiently accurate at the starting point in the chi-squared surface (steps 5 - 7).

A set of simulated gamma-ray yield data is provided for the user in the file `ge-data.yld`. In practice, this file would be typed by the user according to the format in section 5.31.

1. Define the Ge detector(s) (1-make-detector.inp)

In Gosia, detectors are considered to be “physically different” if they have different geometry (crystal length, crystal radius, etc.), if they are placed at different distances from the target position, or if they are fitted with different absorbers. Two identical Ge detectors placed at different distances from the target would need to be defined separately, but two identical detectors that only differ by their angular position in space (and their efficiencies) should be defined as the same “type.” In this demonstration, one detector type is defined and named type “1.”

Refer to the file “1-make-detector.inp”. In `OP,FILE` the three necessary files for `OP,GDET` are defined. The general output will be written to `1-make-detector.out`, but the coefficients for the angular attenuation (Sections 5.10 and 2.2.3) will be written to “`det.gdt`” for use by Gosia in steps 2 - 10.

`OP,GDET` has three lines. The first line is the detector type, 1. The second line `0.1,2.5,10.,15.`

defines a Ge crystal with an inactive core of radius 0.1 cm, outer radius of 2.5 cm and length 10. cm, placed 15. cm from the target. The angular position(s) in space of all detectors of this type will be defined in the next step.

To execute the input, issue the command

```
gosia < 1-make-detector.inp
```

The output file `1-make-detector.out` contains verbose output, some of which is selected by the user in the sub-option `PRT` of `CONT`. Error messages will also be written to file 22 (`*.out` in this demonstration). The Ge detector file `det.gdt` is created with the following records.

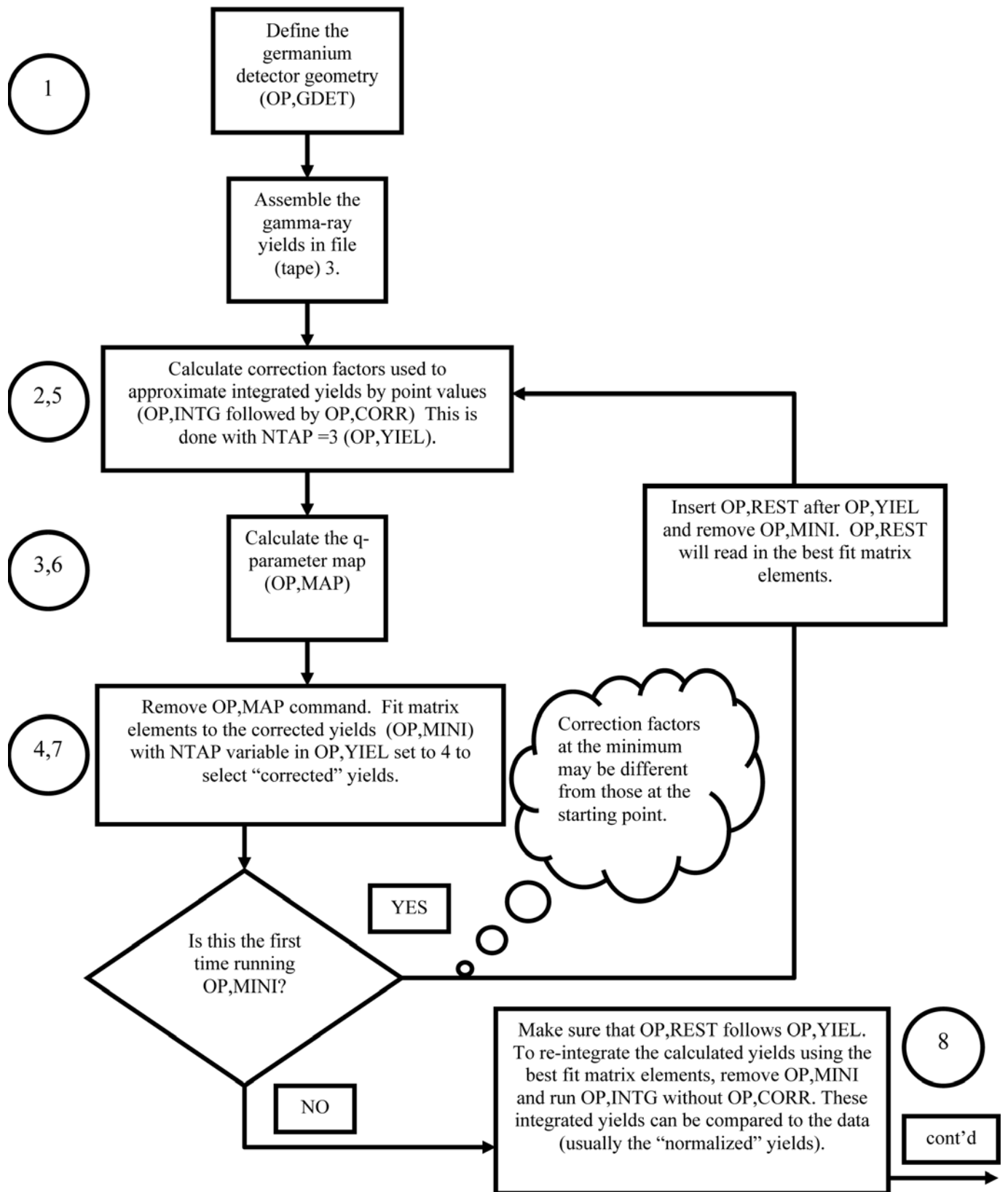


Figure 16: Flow diagram for Gosia matrix element fitting procedure, [part A]

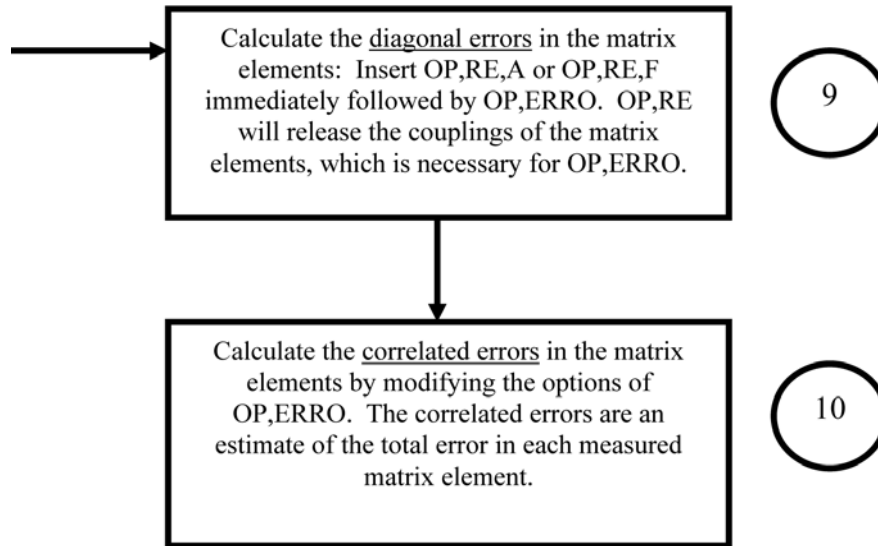


Figure 17: Flow diagram for Gosia fitting procedure, [part B]

```

1
15.
0.0500000007
0.994781568 0.021136071 0.993235058
0.9844016 0.0211650254 0.979796558
0.968973081 0.0212087755 0.959865727
0.948663497 0.0212677132 0.933710572
0.933477038 0.0213739219 0.914365642
0.89432871 0.0214334683 0.864204804
0.86088619 0.0215418701 0.821776765
0.823719839 0.0216686757 0.774954141

```

In subsequent steps the detector will be referred to as type “1” (line 1). The second line is the distance from the target, and the third line is the energy offset E_0 of equation 4.15. The remaining lines are the values C_1, C_2 and Q_k of equations 4.15 and 2.66 for each order $k = 1..8$.

Now attaching the file det.gdt to an input (OP,FILE) will allow Gosia to find the angular attenuation factors when detector type “1” is called.

2. Calculate the Correction Factors for the Point Approximation (2-make-correction-factors.inp)

Now a set of correction factors needs to be calculated so that Gosia can use a point approximation for the scattering angle range of the particle detector to speed up the fit process. The input used is nearly identical to the one described in the first demo (simulate.inp). Refer to section 11.3.1 for a description. One difference is that OP,CORR is added just after OP,INTG. OP,CORR takes no arguments, but tells Gosia to compare the yields it has just integrated to the corresponding point calculations and use the quotient as a correction factor.

Notice that NTAP is labeled in the input file under OP,YIEL. In this step NTAP is set to 3, the file number of ge-data.yld, which contains the experimental yields. (The file number for γ -ray yield data is not open to the user’s choice. It must always be 3.) The experimental yields in the file ge-data.yld are read by Gosia because NTAP=3, and these yields are “corrected” to be consistent with the point approximation. The results are then written to file 4, firstfit.cor, which has a similar format to ge-data.yld. In the steps that follow, these corrected yields will be read by Gosia and compared to the calculated yields to calculate the chi-squared statistic.

To execute this step, issue the command

```
gosia < 2-make-correction-factors.inp
```

3. Generate the q-Parameter Map (3-make-q-parameter-map.inp)

One small change (from the simulation demo) has been made in OP,GOSI in the sub-option ME. Matrix element 5 (for the E2 transition from state 3 to state 4 in figure 14) has been coupled to matrix element 3 (for the E2 transition from state 2 to state 3). This is done by flagging the second field (the index of the final state) with a negative sign and replacing the upper and lower limits with the indices of the “master” matrix element (2,3). This is a useful tactic when there is insufficient data to fit matrix elements individually and the ratio of two matrix elements can be calculated (as in the matrix elements of a rotational band with a constant intrinsic quadrupole moment Q_0).

The “q-parameter” map (Section 4.2) is created by modifying the input as follows. OP,MAP is inserted at the end of OP,YIEL (just before OP,INTG). It takes no arguments and is immediately followed by OP,EXIT. NTAP can be set to 0, since experimental data are not necessary for this step.

Any time the ranges over which matrix elements are allowed to vary are changed, OP,MAP should be run again.

File number 7 is assigned to firstfit.map. After execution of this step, it should contain the q-parameter map appropriate for this fit. Attaching file 7 to the minimization input (step 4) will allow Gosia to read it.

4. Fit the Adjustable Matrix Elements (4-minimize.inp)

In step 4, the variable NTAP in OP,YIEL is set to 4, so that Gosia uses the “corrected yields” to calculate chi-squared.

OP,INTG is not necessary, since the corrected yields will be compared to the point yields at each step of the minimization. OP,MINI is inserted following OP,YIEL. There are a number of user controls (maximum number of iterations, derivative of the matrix element vector, etc.) that define the criteria for convergence and choices of the search method in the parameter space. The best choice will be case-dependent. Refer to section 5.17.

Issue the command

```
gosia < 4-minimize.inp
```

The progress of chi-squared will be sent to standard output until Gosia satisfies the convergence criteria or reaches the maximum number of iterations chosen by the user. The output should look similar to the following.

```
OPENED 4-minimize.out
IO-num = 22 UNKNOWN FORMATTED
OPENED 4-minimize.inp
IO-num = 25 UNKNOWN FORMATTED
OPENED det.gdt
IO-num = 9 UNKNOWN FORMATTED
OPENED firstfit.map
IO-num = 7 UNKNOWN FORMATTED
OPENED firstfit.cor
IO-num = 4 UNKNOWN FORMATTED
OPENED currentbestset.bst
IO-num = 12 UNKNOWN FORMATTED
*** CHISQ= 0.313370E+02 ***
*** CHISQ= 0.204481E+00 ***
```

More details of the progress toward the minimum are given in the *.out file. For instance, if the search hit a limit in one or more matrix elements, this will be reported as a warning to the user that either the range is too narrow, or a matrix element is not sensitive to the data. At the conclusion of the fit, the best set of matrix elements are written to file 12, currentbestset.bst. In the second iteration (steps 5 - 7), Gosia will begin at this new starting point in the parameter space. Steps 5 - 7 are a repeat of steps 2 - 4 with point-correction factors calculated (presumably) closer to the true chi-squared minimum.

5. Re-calculate Correction Factors at the Minimum (5-make-new-correction-factors.inp)

NTAP is set to 3 in this step.

This step is identical to step 2, except that the file 12, `currentbestset.bst`, is attached in `OP,FILE` and `OP,REST` is inserted immediately before `OP,INTG`. In this example, `OP,REST` takes only the arguments 0,0, which tells Gosia to read the position of the previous chi-squared minimum from file 12 without modifying any values.

As in step 2, the corrected yields are written to disk, this time in the file `secondfit.cor`. They will be attached as input in step 7.

6. Generate a New q-Parameter Map (6-make-new-q-parameter-map.inp)

Since the ranges of the matrix elements have not changed in this example, this step is not necessary. However, `OP,MAP` requires little time, and it is good practice to make sure that the q-parameters are correct for the current fit.

7. Fit the Matrix Elements Again from the New Starting Point (7-second-minimization)

This minimization step is identical to the first (step 4), except that `OP,REST` is included, telling Gosia to overwrite the values of the matrix elements in the input with those at the conclusion of the last fit. The fit will resume at this starting point, and with the new correction factors, until the user's convergence criteria are satisfied again.

After issuing the command

```
gosia < 7-second-minimization.inp
```

the output file indicates that the convergence conditions were met at the first step. This indicates that the initial guesses at the matrix elements were close enough to the minimum that the correction factors for the point approximation were valid at the final minimum. If the new minimum were significantly different (if chi-squared improved by $\sim 1/N$, where N is the number of degrees of freedom) then steps 5 - 7 could be repeated again. This is usually not necessary if a reasonable starting point was used.

8. Integrate the Reproduced (Calculated) Yields Using the Final Set of Matrix Elements (8-final-fit-yields.inp)

Typically, at this point, the user would like to see how good the fit is by comparing the calculated yields at the chi-squared minimum to the experimental data. This is done by running an input very similar to `simulate.inp` (in the first demo) with the addition of `OP,REST` immediately before `OP,INTG` and file 12 attached. Issue the command

```
gosia < 8-final-fit-yields.inp
```

Gosia reads the best set of matrix elements from file 12 (`currentbestset.bst`) and integrates the yields. The yields in the output file (22, `8-final-fit-yields.out`) can be compared directly to the experimental data, observing the appropriate normalization. The yields for each experiment are normalized to the chosen transition (NS1, NS2 in `OP,YIEL`) in the column "NORMALIZED YIELD." Absolute counts can be calculated from the "YIELD" data as in section 5.12.5.

9. Estimate the Diagonal Errors (9-diag-error.inp)

The diagonal errors are calculated individually for each matrix element which was varied in the fit. Correlations are not considered in this step, i.e., only one matrix element is freed at a time by Gosia. This is analogous to measuring the width of the minimum at $\chi^2 = \chi_{\min}^2 + 1$ in the parameter space on a plane passing through the minimum parallel to the matrix element's axis.

Notice that `OP,RE,F` (or `OP,RE,A`) must be used to release the couplings between the matrix elements (matrix elements 3 and 5 in this case). Also, it must be placed immediately before `OP,ERRO`.

The `OP,ERRO` option takes 6 arguments. By changing these arguments (and adding appropriate steps to the error calculation), the user can decide which matrix elements to include in the error estimate, activate the sum-rules calculation if desired, etc. In this case, a simple diagonal error will be calculated for each of matrix elements 3 and 5 that were fit. The 6th argument, `RMAX`, is the largest floating point number available on the user's platform. In this case it is set to `1.0E38`, but on many 64-bit systems it will be `1.0E308`. If Gosia reports the error "TOO FAR FROM THE MINIMUM TO CARRY OUT THE ERROR ESTIMATION!" in the output file (22), the user should check that `RMAX` is set correctly.

Issue the command

```
gosia < 9-diag-error.inp
```

Gosia reads the final set of matrix elements of the fit procedure from file 12 and performs the diagonal error calculation. The output file (22) contains the following text:

DIAGONAL ESTIMATED ERRORS

INDEX NI NF ME AND ERRORS

```
 3  2  3  0.31364 ( -0.02737 , 0.02018)..... -8.7 , 6.4 PC
 5  3  4  0.09409 ( -0.00791 , 0.01277)..... -8.4 , 13.6 PC
```

which gives the (lower, upper) diagonal errors. These are also written to file number 15 (errors.dat) for use in the next step—the correlated error calculation.

10. Estimate the Correlated (Total) Errors (10-corr-error.inp)

The diagonal error calculation (step 9) must be run before the correlated error each time correlated errors are calculated. Failing to do so will cause the correlated errors to be poorly estimated.

This input is very similar to the diagonal error input, except that argument 1 (IDF) of OP,ERRO is changed to 1 to select the correlated error and IREP set to 1, which tells Gosia to read the diagonal errors from disk first. Issue the command

```
gosia < 10-corr-error.inp
```

Again, the output file contains a report of the errors. These are the correlated errors—the total errors—which are the widths of projections on each matrix element’s axis of the minimum at the $\chi^2 = \chi_{min}^2 + 1$ level. The output file reports the correlated errors in the same format as the diagonal errors. In this case, the correlated errors are only slightly larger than the diagonal errors.

11.4 Tutorial 2: A Fit to Many Matrix Elements

This tutorial requires the set of files contained in g1demo.tar, which can be downloaded from the GOSIA website:

<http://www.pas.rochester.edu/~cline/Gosia/index.html>

The g1demo.tar file contains a sample input, a simulated data set and a set of sample output files, which can be compared to the results in this tutorial. On a Unix-like machine, issue the following command to unpack the tar file in the desired working directory.

```
tar -xvf g1demo.tar
```

The following five steps will fit 10 matrix elements to the simulated data in the file g1demo.yld and then give calculated yields to compare with the original data. The lines which should be modified or inserted are typed in bold-face. Note that comments are permitted on some lines in the input but not on all lines. It is not recommended that comments be inserted on lines other than the ones shown in this sample input. The GOSIA input file must be formatted correctly with the appropriate delimiters, data types and line breaks as shown. This demonstration input uses the **OP,FILE** option so that it is not necessary to name the input and output files according to the “fort.#” standard or to use symbolic links, etc.

1. Run **OP,GDET** to create the gamma-detector file det.gdt (Gosia unit #9). This should be done by copying the **OP,GDET** sequence at the bottom of the input in a text editor and pasting it just before **OP,YIEL** as follows. (Leave one blank line after “END,.”) The **GDET** command and others can be “stored” at the end of the input after **OP,EXIT**, since execution terminates at the first **OP,EXIT** command.

```
CONT
PRT,0.
1,-1
2,0
```

```

4,0
5,1
11,0
12,0
14,0
16,0
0,0
END,
OP,GDET
1
0.1,2.5,10.,15.
0,0,0,0,0,0
OP,EXIT
OP,YIEL
0
18,1
0.056,0.068,0.082,0.1,0.12,0.15,0.18,0.22,0.26,0.32,0.38,
0.46,0.56,0.68,0.82,1.0,1.2,1.5

```

Run Gosia with the following command.

```
gosia < g1demo.inp
```

This will produce a file named det.gdt with the attenuation factors which describe the gamma-ray detector in the simulated experiment. See section 5.10. The det.gdt file can be compared with the example in g1demo.tar.

Output to the terminal should look like this:

```

OPENED g1demo.out
IO-num = 22          UNKNOWN          FORMATTED
OPENED g1demo.inp
IO-num = 25          UNKNOWN          FORMATTED
OPENED det.gdt
IO-num = 9           UNKNOWN          FORMATTED
(etc.)

```

Additional output at this step, as well as the following steps, will be found in the g1demo.out file (unit 22). The parameters given to OP,GDET should not be changed while running this demo, because changes to the gamma-ray detector setup will introduce inconsistencies with the simulated data in g1demo.yld.

2. Calculate the correction factors for the point approximations (section 5.4).
Remove the OP,GDET sequence inserted in step 1. (Keep one blank line after END,.) No other changes are needed. Issue the same command to run Gosia a second time. (Note that this is running the full integration with OP,CORR inserted after OP,INTG. NTAP is set to 3, which tells Gosia to read the gamma-ray yields from file 3, in this case “g1demo.yld”.)

```
gosia < g1demo.inp
```

This step may take several minutes as GOSIA calculates the Coulomb excitation and gamma-ray yields integrated over the energy and scattering angle ranges specified in OP,INTG. When it is complete, the file g1demo.cor is created (unit #4). If the file g1demo.yld (unit #3) is not found, there will be a fatal error. See section 5.4.

At this point, it is suggested to change NTAP from 3 to 4 so that the corrected yields in the g1demo.cor file will be read instead of the g1demo.yld file in the following steps.

```

1
0.01377
1
.1
0.01237
4          !NTAP
0,0
1,1.0      !lifetime data
3,112.,1.
0,0
0,0
OP,INTG
5,7,634,650,22.000,26.000          !4 deg expts

```

3. Create the q-parameter map (section 4.2) by putting the OP,MAP and OP,EXIT commands in the input just before INTG. The relevant section of the input file will then look like this:

```

1
.1
0.01237
4          !NTAP
0,0
1,1.0      !lifetime data
3,112.,1.
0,0
0,0
OP,MAP
OP,EXIT
OP,INTG
5,7,634,650,22.000,26.000          !4 deg expts

```

Run the code again with the same command at the system prompt. The file g1demo.map (unit #7) will be generated and used in the OP,MINI step below.

4. Run the minimization (section 5.17) by making the following change to the input. Remove OP,MAP and insert the OP,MINI command just before OP,INTG. NTAP should remain set to 4.

```

1
.1
0.01237
4          !NTAP
0,0
1,1.0      !lifetime data
3,112.,1.
0,0
0,0
OP,MINI
2100,100,0.1,.0001,1.01,0,0,1,0,0
OP,EXIT
OP,INTG
5,7,634,650,22.000,26.000          !4 deg expts

```

Issue the command to run Gosia again. The terminal will show the sequence of chi-squared values, which should look similar to this:

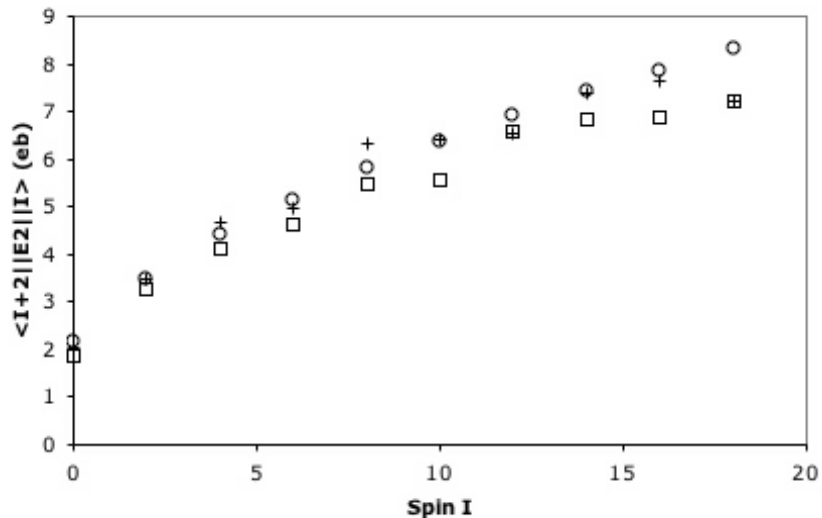


Figure 18: Initial guesses (squares) of transition matrix elements in g1demo.inp and final values (+) compared to the true values used to simulate the data (circles).

```

*** CHISQ= 0.277172E+02 ***
*** CHISQ= 0.965818E+01 ***
*** CHISQ= 0.594594E+01 ***
*** CHISQ= 0.403621E+01 ***
.
.
.
*** CHISQ= 0.100057E+01 ***
*** CHISQ= 0.999197E+00 ***
*** CHISQ= 0.995206E+00 ***
*** CHISQ= 0.984981E+00 ***

```

In this case, the fit converged after 34 steps with chi-squared=0.98. Additional output is given in the g1demo.out file, which can be compared with the example found in g1demo.tar.

The final values of the matrix elements after the fit are compared with the “true” values used to simulate the data in Figure 18. For the assumed data set the multiple-step Coulomb excitation is insensitive to the magnitudes of the lowest transition matrix elements, while the matrix elements for $I=10\dots 14$ agree better with the true values. The calculated yields are not sensitive enough to the matrix element $\langle 20 || E2 || 18 \rangle$ to obtain a fit.

Obviously, the quantity of data in this example is marginally sufficient to fit 10 matrix elements separately and find a unique minimum. Note that only data from a single Ge detector are represented in this fit! It is educational to experiment with the couplings of the matrix elements (e.g. coupling the E2 matrix elements for several states to one intrinsic quadrupole moment), changing the weight and value of the lifetime of state 3, changing the OP,MINI controls, etc. In many cases, a more accurate fit of the matrix elements coupling the lower-spin states can be achieved by fixing the matrix elements for high-spin states (e.g. with the FIX option in the CONT block). Alternatively, new logical experiments and new gamma-ray detectors can be added to the input. If new experiments or detectors are added, it will be necessary to generate new simulated data. This can be done using OP,INTG and inserting the data from the YIELD column into the g1demo.yld file (see section 5.31) or by using OP,POIN (Section 5.18).

A second iteration of steps II to IV will be necessary in some cases, especially if the matrix elements vary greatly in the first fit. (See section 4.2 for details regarding when it is necessary to re-run the map

calculation.) In this case, a copy of the g1demo.bst file (tape 12) which was written by OP,MINI must be kept in the working directory and re-read by inserting OP,REST in the appropriate place in the input, as shown in step 5 below. Note that unit 12 will be overwritten when OP,MINI is run again.

5. Reproduction of the Experimental Yields

Following the minimization, gamma-ray data can be compared to the calculated (expected) values by making the following changes to the input and running one last time.

Remove the OP,MINI command where it was inserted in step IV above, and insert the OP,REST command so that the final values of the matrix elements will be read from the g1demo.bst file. Set NTAP to 0, so that experimental data are not read from a file.

```

1
.1
0.01237
0          !NTAP
0,0
1,1.0          !lifetime data
3,112.,1.
0,0
0,0
OP,REST
0,0
OP,INTG
5,7,634,650,22.000,26.000          !4 deg expts

```

At the bottom of OP,INTG, remove OP,CORR.

```

0
10,10
0
10,10
OP,EXIT

```

The input can now be run with the usual command. Gamma-ray yields will be integrated using the final matrix elements in TAPE 12 (TAPE 2 in older versions of GOSIA) and given in the g1demo.out file. The experimental yields should be compared with these integrated yields, rather than the output given by OP,MINI, since the latter are corrected point calculations and may be normalized on a different scale.

11.5 Annotated GOSIA input g1demo.inp

```
OP, FILE
22, 3, 1
g1demo.out
25, 3, 1
g1demo.inp
9, 3, 1
det.gdt
7, 3, 1
g1demo.map
3, 3, 1
g1demo.yld
4, 3, 1
g1demo.cor
14, 3, 1
```

The OP,FILE “option” names the input and output files that may be read or written by GOSIA while processing the rest of the input.

```
dum.14
17, 3, 1
dum.17
18, 3, 1
dum.18
13, 3, 1
g1cnor.dat
12, 3, 1
g1demo.bst
0, 0, 0
```

One or more OP,TITL records may be entered, each followed by a user comment to be reprinted in the output file.

OP,GOSI (rather than OP,COUL) is chosen in this input, so that a fit can be made to the gamma-ray yield data. OP,COUL allows the user to abbreviate some sections of the input, but does not allow a fit to be performed.

```
OP, TITL
136Xe on 178Hf at 650 MeV
```

```
OP, GOSI
LEVE
1, 1, 0, 0.0
2, 1, 2, 0.09318
3, 1, 4, 0.3066
4, 1, 6, 0.6322
5, 1, 8, 1.059
```

The LEVE “sub-option” defines the states of the nucleus to be investigated.

GOSIA’s index I for the state.

Parity IP: 1= positive, -1= negative.

```
6, 1, 10, 1.571
7, 1, 12, 2.151
8, 1, 14, 2.778
9, 1, 16, 3.436
10, 1, 18, 4.121
11, 1, 20, 4.840
0, 0, 0, 0
```

The spin S.

Energy E of the state in MeV.

The ME sub-option defines the matrix elements and the upper and lower limits over which they may vary during the fit. Matrix elements must be listed in “odometer” order. Refer to sections 5.15 for the OP,COUL format and 5.16 for the OP,GOSI format.

```
ME
2, 0, 0, 0, 0
1, 2, 1.878, 1., 3.
2, -2, -2.245, 1, 2
2, 3, 3.258, 1., 5.
3, -3, -3.106, 2, 3
3, 4, 4.119, 2., 6.
```

$\lambda=2$ indicates the E2 section. It is followed by 4 dummy values “0,0,0,0”.

```

4, -4,      -3.705,   3, 4
4, 5,      4.626,   3., 7.
5, -5,     -4.051,   4, 5
5, 6,      5.478,   4., 8.
6, -6,     -4.725,   5, 6
6, 7,      5.580,   4., 8.
7, -7,     -4.766,   6, 7
7, 8,      6.561,   5., 9.
8, -8,     -5.565,   7, 8
8, 9,      6.816,   5., 9.
9, -9,     -5.753,   8, 9
9, 10,     6.880,   5, 9.
10, -10,   -5.785,   9, 10
10, 11,    7.209,   5., 9.
11, -11,   -6.042,  10, 11
0, 0, 0, 0, 0

```

The initial state (INDEX1=7) and final state (INDEX2=8) are connected by the matrix element ME=6.561 eb.

The matrix element is allowed to vary between R₁=5 eb and R₂=9 eb. Refer to restrictions in section 5.16.

Negative sign on INDEX2 indicates that this matrix element (static moment) is coupled to another--in this case to the matrix element <INDEX2=10 ||E2||INDEX1=9>.

"0,0,0,0,0" terminates ME. Alternatively, matrix elements of other multipolarities could have followed E2.

```

EXPT
27, 72, 178
54, 136, 642, 24.0, 4, 0, 0, 0, 360, 1, 1
54, 136, 642, 28.0, 4, 0, 0, 0, 360, 1, 1
54, 136, 642, 32.0, 4, 0, 0, 0, 360, 1, 1
54, 136, 642, 36.0, 4, 0, 0, 0, 360, 1, 1
54, 136, 642, 40.0, 4, 0, 0, 0, 360, 1, 1
54, 136, 642, 44.0, 4, 0, 0, 0, 360, 1, 1
54, 136, 642, 48.0, 4, 0, 0, 0, 360, 1, 1
54, 136, 642, 51.0, 4, 0, 0, 0, 360, 1, 1
54, 136, 642, 53.0, 4, 0, 0, 0, 360, 1, 1
54, 136, 642, 55.0, 4, 0, 0, 0, 360, 1, 1
54, 136, 642, 57.0, 4, 0, 0, 0, 360, 1, 1
54, 136, 642, 59.0, 4, 0, 0, 0, 360, 1, 1
54, 136, 642, 61.0, 4, 0, 0, 0, 360, 1, 1
54, 136, 642, 63.0, 4, 0, 0, 0, 360, 1, 1
54, 136, 642, 65.0, 4, 0, 0, 0, 360, 1, 1
54, 136, 642, 67.0, 4, 0, 0, 0, 360, 1, 1
54, 136, 642, 69.0, 4, 0, 0, 0, 360, 1, 1
54, 136, 642, 71.0, 4, 0, 0, 0, 360, 1, 1
54, 136, 642, 73.0, 4, 0, 0, 0, 360, 1, 1
54, 136, 642, 75.0, 4, 0, 0, 0, 360, 1, 1
54, 136, 642, 77.0, 4, 0, 0, 0, 360, 1, 1
54, 136, 642, 79.0, 4, 0, 0, 0, 360, 1, 1
54, 136, 642, 81.0, 4, 0, 0, 0, 360, 1, 1
54, 136, 642, 83.0, 4, 0, 0, 0, 360, 1, 1
54, 136, 642, 85.0, 4, 0, 0, 0, 360, 1, 1
54, 136, 642, 87.0, 4, 0, 0, 0, 360, 1, 1
54, 136, 642, 89.0, 4, 0, 0, 0, 360, 1, 1
CONT

```

NEXP=27 logical experiments are defined. The nucleus Hf-178 (Z₁=72, A₁=178) will be investigated.

The collision partner is Xe-136 (Z_n=54, A_n=136). A negative sign on Z_n (e.g. -54) would signify projectile excitation. Here, the positive sign indicates that the Hf-178 target is excited.

The mean laboratory projectile energy E_p (mid-way through the target) is 642 MeV.

The mean *projectile* scattering angle θ_{LAB} is entered, even if the recoiling target nucleus was detected. A minus sign flag (e.g. -65.0) would signify target detection.

Accuracy options M_C and M_A.

Axial symmetry flag IAX and azimuthal limits φ₁ and φ₂ of the particle detector.

"Kinematics" flag IKIN for A_{proj}>A_{targ}

Normalization to experiment LN=1. Requires user-entered normalization constants in OP,YIEL.

EXPT defines the "logical" experiments (section 5.8).

Sub-option CONT allows the user to adjust output options, accuracy controls and other features such as a PIN diode detector option. Refer to section 5.3.

```

PRT, 0.
1, -1
2, 0
4, 0
5, 1

```


.1
0.62633
1
.1
0.41763
1
.1
0.29184
1
.1
0.21134
1
.1
0.15752
1
.1
0.12007
1
.1
0.09889
1
.1
0.08749
1
.1
0.07761
1
.1
0.06908
1
.1
0.06163
1
.1
0.05510
1
.1
0.04936
1
.1
0.04427
1
.1
0.03974
1
.1
0.03573
1
.1
0.03213
1

These three records, NDST, UPL and YNRM, determine the following for experiment #3. There is one data set (usually, but not always equal to the number of gamma detectors entered above). Any *unobserved* yield calculated to be greater than $0.1 \times Y_{5 \rightarrow 4}$ will enter the chi-squared statistic. The normalization constant with respect to experiment #1 is 0.41763. These records continue for each experiment with a positive value of NANG.

```

.1
0.02892
1
.1
0.02603
1
.1
0.02343
1
.1
0.02108
1
.1
0.01896
1
.1
0.01705
1
.1
0.01533
1
.1
0.01377
1
.1
0.01237
3 !NTAP
0,0
1,1.0
3,112.,1.
0,0
0,0
OP,INTG
5,7,634,650,22.000,26.000
634,638,642,646,650
21.,22.,23.,24.,25.,26.,27.
5,4,634,650,26.000,30.000
634,638,642,646,650
25.,27.,29.,31
5,4,634,650,30.000,34.000
634,638,642,646,650
29.,31.,33.,35
5,4,634,650,34.000,38.000
634,638,642,646,650
33.,35.,37.,39
5,4,634,650,38.000,42.000
634,638,642,646,650
37.,39.,41.,43
5,4,634,650,42.000,46.000
634,638,642,646,650
41.,43.,45.,47

```

NTAP=3. Experimental gamma-ray yields data will be read from tape 3 defined as the file g1demo.yld in OP,FILE above. This will be changed to 0 (no data read) or 4 for different operations described in the tutorial in this chapter. (Note that comments such as “!NTAP” are helpful, but not legal on every line. When in doubt, do not use a comment.)

Number (NBRA=0) and weight (WBRA=0) of branching ratio data to be included in chi-squared.
 One experimental lifetime (NL=1) will be included in the chi-squared statistic with weight WL=1.0.

The experimental lifetime of state INDEX=3 is 112(1) ps.

No experimental values of mixing ratios or matrix elements will be entered.

5,7,634,650,22.000,26.000
 634,638,642,646,650
 21.,22.,23.,24.,25.,26.,27.

Integration limits of energy and scattering angle for experiment #1. Because azimuthal symmetry and 360-degree coverage of the particle detector were specified in EXPT (above), only the polar angle information is entered. In the present example, each experiment requires only three lines of input. Other choices of particle-detector geometry may require more.

```

5,4,634,650,46.000,50.000
634,638,642,646,650
45.,47.,49.,51
5,5,634,650,50.000,52.000
634,638,642,646,650
49.,50.,51.,52.,53
5,5,634,650,52.000,54.000
634,638,642,646,650
51.,52.,53.,54.,55
5,5,634,650,54.000,56.000
634,638,642,646,650
53.,54.,55.,56.,57
5,5,634,650,56.000,58.000
634,638,642,646,650
55.,56.,57.,58.,59
5,5,634,650,58.000,60.000
634,638,642,646,650
57.,58.,59.,60.,61
5,5,634,650,60.000,62.000
634,638,642,646,650
59.,60.,61.,62.,63
5,5,634,650,62.000,64.000
634,638,642,646,650
61.,62.,63.,64.,65
5,5,634,650,64.000,66.000
634,638,642,646,650
63.,64.,65.,66.,67
5,5,634,650,66.000,68.000
634,638,642,646,650
65.,66.,67.,68.,69
5,5,634,650,68.000,70.000
634,638,642,646,650
67.,68.,69.,70.,71
5,5,634,650,70.000,72.000
634,638,642,646,650
69.,70.,71.,72.,73
5,5,634,650,72.000,74.000
634,638,642,646,650
71.,72.,73.,74.,75
5,5,634,650,74.000,76.000
634,638,642,646,650
73.,74.,75.,76.,77
5,5,634,650,76.000,78.000
634,638,642,646,650
75.,76.,77.,78.,79
5,5,634,650,78.000,80.000
634,638,642,646,650
77.,78.,79.,80.,81
5,5,634,650,80.000,82.000
634,638,642,646,650
79.,80.,81.,82.,83

```

NE=5 beam-energy meshpoints will be given, followed by NT=5 polar scattering angle meshpoints for the integration.
The beam energy interval $E_{\min}=634$ to $E_{\max}=650$ MeV together with stopping power data below define target thickness.
The (polar) scattering angle range of the <i>detected(!)</i> particle. (The format is different for the circular detector option.)
Energy meshpoints E_1, E_2, \dots for the integration. The range of meshpoints must equal or exceed the beam energy interval.
Polar projectile scattering angle meshpoints $\theta_1, \theta_2, \dots$ for the integration must equal or exceed the scattering angle range of the detected particle. The implicit positive sign of these angles is a flag indicating that the projectile is detected. Note that these are always(!) entered as <i>projectile</i> scattering angles. If the recoiling <i>target</i> nucleus is detected, or the circular detector option is used, refer to section 5.12 for the appropriate format.
Optionally, this record could be set to <code>--5</code> to indicate that the shape of the detector will be defined by the user (section 5.12).

OP,INTG calculates the integrated gamma-ray yields. There are a number of flags and optional records, which can be used to indicate the detected particle, the detector geometry, etc. The example given is for a simple annular particle detector whose data are separated by polar scattering angle into 27 data sets, but more complicated detector shapes can be defined. Refer to section 5.12 for details. When OP,INTG is followed by OP,CORR as in this example, GOSIA writes correction factors to tape 4 (the file "g1demo.cor" as defined above in OP,FILE), which are used for the fast point approximations during the chi-squared fit.
--

5,5,634,650,82.000,84.000
 634,638,642,646,650
 81.,82.,83.,84.,85
 5,5,634,650,84.000,86.000
 634,638,642,646,650
 83.,84.,85.,86.,87
 5,5,634,650,86.000,88.000
 634,638,642,646,650
 85.,86.,87.,88.,89

These entries are repeated for each experiment. This group corresponds to experiment 27.

5,5,634,650,88.000,90.000
 634,638,642,646,650
 87.,88.,89.,90.,91

NP = 4 values of stopping power dE/dx will be entered.

4
 625,635,645,655
 32.395,32.401,32.404,32.404

The beam energies [MeV] of the four stopping powers.

10,10

The stopping power of Xe-136 in Hf-178 is 32.401 MeV/(mg/cm²) at 635 MeV.

0

10,10

Experiment #1 will be integrated using NI₁=10 subdivisions in the beam energy meshpoints and NI₂=10 subdivisions in the scattering angle meshpoints (second). NI₁ and NI₂ must be even. If NT (above) is negative then NI₂ must be negative (and even!) as well, and this line is followed by ϕ intervals (section 5.12).

0

10,10

NP = 0: The stopping power data for experiment# 2 will be taken from the previous experiment (#1).

0

10,10

0

10,10

0

10,10

0

10,10

These records are repeated for all experiments.

0

10,10

0

10,10

0

10,10

0

10,10

0

10,10

0

10,10

0

10,10

0

10,10
0
10,10
0
10,10
0
10,10
0
10,10
0
10,10
0
10,10
0
10,10
0
10,10
0
10,10
0
OP,CORR
OP,EXIT

OP,CORR specifies that the integration will be followed by calculation of the correction factors for the point-approximations used during the chi-squared fit. Refer to section 5.4. In order to use OP,CORR, the value of NTAP (above) must be set to 3, and a set of gamma-ray yield data must be provided by the user in file 3 defined above. Refer to section 5.31.

OP,EXIT terminates the execution. Nothing is read by GOSIA below OP,EXIT.

13	7	8	6.56100	5.00000	9.00000
14	8	8	-5.56500	COUPLED TO 13	
15	8	9	6.81600	5.00000	9.00000
16	9	9	-5.75300	COUPLED TO 15	
17	9	10	6.88000	5.00000	9.00000
18	10	10	-5.78500	COUPLED TO 17	
19	10	11	7.20900	5.00000	9.00000
20	11	11	-6.04200	COUPLED TO 19	

203 EXPERIMENTAL YIELDS 10 MATRIX ELEMENTS TO BE VARIED

LIFETIMES (PSEC)

The experimental lifetime data,
if it is provided by the user.

LEVEL	LIFETIME	ERROR
3	112.00	1.00

LIFETIMES ARE TAKEN WITH WEIGHT 0.100000E+01

*** CHISQ= 0.277172E+02 ***
 *** CHISQ= 0.965818E+01 ***
 *** CHISQ= 0.594594E+01 ***
 *** CHISQ= 0.403621E+01 ***

MATRIX ELEMENT 1 LOCKED!
 *** CHISQ= 0.209903E+01 ***
 *** CHISQ= 0.202990E+01 ***
 *** CHISQ= 0.160540E+01 ***
 *** CHISQ= 0.160194E+01 ***
 *** CHISQ= 0.159863E+01 ***
 *** CHISQ= 0.159805E+01 ***
 *** CHISQ= 0.158588E+01 ***

The progress of chi-squared is printed at each
step. When a matrix element can be locked by
the fit routine, this is reported as well.

MATRIX ELEMENT 9 LOCKED!
 *** CHISQ= 0.156263E+01 ***
 *** CHISQ= 0.153814E+01 ***

MATRIX ELEMENT 17 LOCKED!
 *** CHISQ= 0.153532E+01 ***
 *** CHISQ= 0.153465E+01 ***
 *** CHISQ= 0.153271E+01 ***
 *** CHISQ= 0.153266E+01 ***

MATRIX ELEMENT 15 LOCKED!
 *** CHISQ= 0.143361E+01 ***
 *** CHISQ= 0.138014E+01 ***
 *** CHISQ= 0.136744E+01 ***

MATRIX ELEMENT 7 LOCKED!
 *** CHISQ= 0.135145E+01 ***

```

*** CHISQ= 0.134003E+01 ***
MATRIX ELEMENT 13 LOCKED!
*** CHISQ= 0.133839E+01 ***
*** CHISQ= 0.133774E+01 ***
*** CHISQ= 0.130050E+01 ***
*** CHISQ= 0.128192E+01 ***
*** CHISQ= 0.109960E+01 ***
*** CHISQ= 0.101986E+01 ***
*** CHISQ= 0.101761E+01 ***

MATRIX ELEMENT 5 LOCKED!
*** CHISQ= 0.100682E+01 ***
*** CHISQ= 0.100057E+01 ***

MATRIX ELEMENT 3 LOCKED!
*** CHISQ= 0.999197E+00 ***
*** CHISQ= 0.995206E+00 ***

MATRIX ELEMENT 19 LOCKED!
*** CHISQ= 0.984981E+00 ***
AT STEP 34 CONVERGENCE ACHIEVED ( 0.768053E-07)
*** CHISQ= 0.984981E+00 ***

```

Convergence is reported with the number of steps and the convergence criterion (CONV) in parentheses. Refer to sections 4.5 and 5.17 for details on the minimization procedure.

NORMALIZATION CONSTANTS

DETECTORS (1-32)

```

EXPERIMENT
1 0.35E+03
2 0.22E+03
3 0.15E+03
4 0.10E+03
5 0.75E+02
6 0.56E+02
7 0.43E+02
8 0.35E+02
9 0.31E+02
10 0.28E+02
11 0.25E+02
12 0.22E+02
13 0.20E+02
14 0.18E+02
15 0.16E+02
16 0.14E+02
17 0.13E+02
18 0.11E+02
19 0.10E+02
20 0.92E+01
21 0.83E+01
22 0.75E+01
23 0.67E+01
24 0.61E+01
25 0.54E+01
26 0.49E+01
27 0.44E+01

```

Normalization constants between the experiments, either specified by the user (as in gl demo.inp) or fit by GOSIA, followed by the recommended relative gamma-ray detector efficiencies. Refer to section 4.5.2.

RECOMMENDED RELATIVE GE(LI) EFFICIENCIES

EXPERIMENT	NI	NF
1	0.10E+01	
2	0.10E+01	
3	0.10E+01	
4	0.10E+01	
5	0.10E+01	
6	0.10E+01	
7	0.10E+01	
8	0.10E+01	
9	0.10E+01	
10	0.10E+01	
11	0.10E+01	
12	0.10E+01	
13	0.10E+01	
14	0.10E+01	
15	0.10E+01	
16	0.10E+01	
17	0.10E+01	
18	0.10E+01	
19	0.10E+01	
20	0.10E+01	
21	0.10E+01	
22	0.10E+01	
23	0.10E+01	
24	0.10E+01	
25	0.10E+01	
26	0.10E+01	
27	0.10E+01	

Initial (NI) and final (NF) states of the gamma-decay transition.

CALCULATED AND EXPERIMENTAL YIELDS	EXPERIMENT 1	DETECTOR 1
NI	IF	YCAL
5	8.0	.2884E+00
4	6.0	.3843E+01
3	4.0	.2372E+02
2	2.0	.2082E+02

Initial and final spin of the transition.

CALCULATED AND EXPERIMENTAL YIELDS	EXPERIMENT 2	DETECTOR 1
NI	IF	YCAL
6	10.0	.1007E+01
5	8.0	.9732E+01
4	6.0	.7974E+01
3	4.0	.3017E+01
2	2.0	.1643E+02

CHISQ SUBTOTAL = 0.265775E+01

Gamma-decay yields calculated from final matrix elements at chi-squared minimum (YCAL) and "corrected" experimental yields (YEXP). Note that these are point approximations.

ENERGY (MEV)	YCAL	YEXP	PC. DIFF.	(YE-YC)/SIGMA
0.4268	.2884E+00	.3088E+00	6.6	1.3
0.3256	.3843E+01	.3937E+01	2.4	0.5
0.2134	.2372E+02	.2588E+02	8.4	1.7
0.0932	.2082E+02	.2230E+02	6.6	1.3

CHISQ SUBTOTAL = 0.637868E+01

Percent discrepancy between calculated and experimental yields.

Discrepancy expressed as a fraction of the error in the experimental values.

CALCULATED AND EXPERIMENTAL YIELDS EXPERIMENT 3 DETECTOR 1

NI	NF	II	IF	ENERGY(MEV)	YCAL	YEXP	PC. DIFF.	(YE-YC)/SIGMA
6	5	10.0	8.0	0.5120	.3698E+00	.3562E+00	-3.8	-0.8
5	4	8.0	6.0	0.4268	.2393E+01	.2507E+01	4.5	0.9
4	3	6.0	4.0	0.3256	.1281E+02	.1357E+02	5.6	1.2
3	2	4.0	2.0	0.2134	.3196E+02	.3402E+02	6.0	1.2
2	1	2.0	0.0	0.0932	.1203E+02	.1214E+02	0.9	0.2

CHISQ SUBTOTAL = 0.428679E+01

CALCULATED AND EXPERIMENTAL YIELDS EXPERIMENT 4 DETECTOR 1

NI	NF	II	IF	ENERGY(MEV)	YCAL	YEXP	PC. DIFF.	(YE-YC)/SIGMA
7	6	12.0	10.0	0.5800	.1370E+00	.1303E+00	-5.2	-1.1
6	5	10.0	8.0	0.5120	.9888E+00	.9104E+00	-8.6	-1.7
5	4	8.0	6.0	0.4268	.4513E+01	.4739E+01	4.8	0.9
4	3	6.0	4.0	0.3256	.1652E+02	.1704E+02	3.0	0.6
3	2	4.0	2.0	0.2134	.2907E+02	.3226E+02	9.9	2.1
2	1	2.0	0.0	0.0932	.8517E+01	.8516E+01	0.0	0.0

CHISQ SUBTOTAL = 0.968194E+01

The agreement between the calculated gamma-ray yields and the experimental values (at the chi-squared minimum) is tabulated by logical experiment number (first) and detector number (second). Note that these are the result of point approximations that have been scaled by correction factors to approximate integrated values. The yields should be *integrated* again using the final set of matrix elements in order to make an accurate comparison with the original experimental data and to ensure that the point approximation remains valid at the chi-squared minimum. (In some cases a second iteration of the fit may be required. Refer to the tutorial in this chapter.)

Experiments 4-26 skipped for brevity.

CALCULATED AND EXPERIMENTAL YIELDS EXPERIMENT 27 DETECTOR 1

NI	NF	II	IF	ENERGY(MEV)	YCAL	YEXP	PC. DIFF.	(YE-YC)/SIGMA
10	9	18.0	16.0	0.6850	.1738E+00	.2005E+00	13.3	2.8
9	8	16.0	14.0	0.6580	.4521E+00	.4482E+00	-0.9	-0.2
8	7	14.0	12.0	0.6270	.8240E+00	.8760E+00	5.9	1.3
7	6	12.0	10.0	0.5800	.1071E+01	.1142E+01	6.2	1.3
6	5	10.0	8.0	0.5120	.1283E+01	.1262E+01	-1.7	-0.3
5	4	8.0	6.0	0.4268	.1556E+01	.1562E+01	0.4	0.1
4	3	6.0	4.0	0.3256	.1681E+01	.1735E+01	3.1	0.7
3	2	4.0	2.0	0.2134	.1651E+01	.1616E+01	-2.2	-0.4
2	1	2.0	0.0	0.0932	.4006E+00	.3747E+00	-6.9	-1.3

CHISQ SUBTOTAL = 0.138775E+02

CALCULATED LIFETIMES

LEVEL	LIFETIME (PSEC)	EXP	ERROR
2	0.2498E+04		
3	0.1106E+03	0.1120E+03	0.1000E+01
4	0.1258E+02		
5	0.3907E+01		
6	0.1207E+01		
7	0.7453E+00		
8	0.5660E+00		
9	0.3999E+00		
10	0.3405E+00		
11	0.3344E+00		

Calculated and experimental (if applicable) values of the mean lifetimes. The weight of lifetime data in the chi-squared calculation is specified in the input by the user.

MATRIX ELEMENTS

MULTIPOLARITY=2

INDEX	NF	NS	ME	PC CHANGE	RED.	TRANS.	PROB.
1	1	2	2.01846	7.47911	0.81483		
2	2	2	-2.41291	7.47911	*****		
3	2	3	3.49426	7.25159	1.35665		
4	3	3	-3.33123	7.25159	*****		
5	3	4	4.66743	13.31462	1.67576		
6	4	4	-4.19831	13.31462	*****		
7	4	5	4.94613	6.92022	1.43907		
8	5	5	-4.33134	6.92022	*****		
9	5	6	6.30875	15.16524	1.89525		
10	6	6	-5.44156	15.16524	*****		
11	6	7	6.42859	15.20767	1.65307		
12	7	7	-5.49080	15.20767	*****		
13	7	8	6.54653	-0.22057	1.47783		
14	8	8	-5.55273	-0.22057	*****		
15	8	9	7.36836	8.10387	1.64523		
16	9	9	-6.21922	8.10387	*****		
17	9	10	7.65017	11.19432	1.58176		
18	10	10	-6.43259	11.19432	*****		
19	10	11	7.20253	-0.08980	1.26528		
20	11	11	-6.03657	-0.08980	*****		

***** END OF EXECUTION *****

Final values of the matrix elements at the chi-squared minimum. Matrix elements [B(E2), B(M1), etc.] are expressed in the appropriate powers of e,barns and μN .

Reduced transition probabilities.

Percent change from the initial to final values of ME.

Values of the matrix elements at the chi-squared minimum.

Initial (NF) and final (NS) states of the matrix element in the direction given in the input file.

11.7 Annotated excerpt from a Coulomb excitation yield calculation (OP,INTG)

The output of OP,INTG is a set of gamma-ray yields integrated over the user-defined ranges of beam energy and particle scattering angle. The essential features which differentiate it from the output of OP,MINI (above) are identified below.

INTEGRATED RUTHERFORD CROSS SECTION=.1328E+05 FOR EXP. 1

The Rutherford cross section is integrated over energy and particle scattering angle and given in units of $\text{mb}\times\text{mg}/\text{cm}^2$. In this case if the target thickness is $0.5 \text{ mg}/\text{cm}^2$, then $\sigma_R = 0.1328\text{E}+05 / 0.5 = 2.66\text{E}+04 \text{ mb}$.

		INTEGRATED YIELDS			
EXPERIMENT	DETECTOR	ENERGY RANGE	SCATTERING ANGLE RANGE	YIELD	NORMALIZED YIELD
1	1	31.200---	20.100---	35.700 MEV	49.500 DEG
NI	NF	II	IF	YIELD	NORMALIZED YIELD
6	3	6.0	4.0	0.53645E-08	0.11322E-07
5	3	4.0	4.0	0.75301E-08	0.15893E-07
5	4	4.0	2.0	0.69686E-12	0.14708E-11
4	1	2.0	0.0	0.26156E-05	0.55204E-05
4	2	2.0	2.0	0.25518E-05	0.53858E-05
3	2	4.0	2.0	0.40693E-04	0.85887E-04
2	1	2.0	0.0	0.47380E+00	0.10000E+01

EXPERIMENT 1 DETECTOR 2
 ENERGY RANGE 31.200--- 35.700 MEV SCATTERING ANGLE RANGE 20.100--- 49.500 DEG

NI	NF	II	IF	YIELD	NORMALIZED YIELD
6	3	6.0	4.0	0.53645E-08	0.11322E-07
5	3	4.0	4.0	0.75301E-08	0.15893E-07
5	4	4.0	2.0	0.69686E-12	0.14708E-11
4	1	2.0	0.0	0.26156E-05	0.55204E-05
4	2	2.0	2.0	0.25518E-05	0.53858E-05
3	2	4.0	2.0	0.40693E-04	0.85887E-04
2	1	2.0	0.0	0.47380E+00	0.10000E+01

The last column lists the yields normalized to the transition chosen by the user in the input file, in this case transition 2→1.

The absolute gamma-ray yield is expressed in units of $\text{mb} \times \text{mg}/\text{cm}^2/\text{sr}$. For example, if the target thickness is $0.5 \text{ mg}/\text{cm}^2$ and the Ge detector subtends 0.06 sr solid angle, the integrated cross section would be
 $\sigma = 0.4738 \times 0.06 / 0.5 = 0.057 \text{ mb}$
 for transition 2→1. Refer to section 5.12.5 for the conversion to total counts.

11.8 Accuracy and speed of calculations

This section discusses accuracy in the integration of gamma-ray yields. Integration accuracy affects calculated yields as well as minimization (through the correction factors calculated by OP,INTG and OP,CORR). Accuracy in the chi-squared minimization process is discussed in detail in chapter 4.

While the integrated yields do not present convergence issues in the majority of calculations, even with default accuracy settings, special attention should be given to the following:

1. High transition energies (>2 MeV in one step). In these cases (and in any case where speed is not a problem), it is recommended that the INT option in the CONT (control) block be used to set IS=1000 for maximum accuracy. In addition, note that the use of very fine integration meshpoints (OP,INTG) may introduce convergence problems with high transition energies.
2. Experiments involving light ($A < 50$) ions or small forward scattering angles may also require setting IS=1000 in the INT control.
3. In general, using an excessive number of meshpoints in the OP,INTG step may cause convergence problems. The following are useful starting points for choosing integration meshpoints:
 - a. beam energy meshpoints spaced at approximately 0.5 MeV intervals
 - b. scattering angle meshpoints spaced at approximately 5 degrees
 - c. approximately 10 subdivisions in energy and scattering angle

Meshpoints will need to be spaced more closely for far forward scattering.

4. Use equal intervals between meshpoints since unequal intervals may cause the Lagrange interpolation to fail.

Accuracy problems that directly affect the minimization (fitting) could cause a failure to converge at a chi-squared minimum (although this is not the only possible cause) or termination of the fit at a false minimum. The accuracy of the minimum can easily be tested by comparing the experimental data to the integrated yields at the minimum.

The integrated yields calculated by GOSIA typically converge for a wide range of chosen meshpoints (energy and scattering angle) and their subdivisions (NI1 and NI2) in OP,INTG. For far forward scattering and light ions ($A < 50$), or for an unnecessarily large number of energy and angle subdivisions, GOSIA may occasionally fail to converge in the OP,INTG step. To find accuracy problems in the integrated yields, we highly recommend the following tests.

1. Use the INT switch to set IS=1000 for each experiment in the CONT (control) block. (This option is described in section 5.3 of the gosia manual. Refer also to section 4.1 regarding the Adams-Moulton method. Be sure to include a decimal point after INT,#. or the option will not operate properly.) Setting IS=1000 will increase the calculation time, but on most modern systems the decrease in speed is not significant. Calculations for forward-scattered light ions that produce unphysically large yields may be improved by this setting.
2. To quickly ensure that the meshpoints for scattering angle and/or energy are chosen suitably, the integrated yields can be recalculated with increased and decreased numbers of subdivisions to ensure that the Lagrange interpolation is not oscillating. The integrated yields should be stable with changes in the number of subdivisions. For sensitive situations, choose the number of meshpoints in the region where the yields converge.

11.9 Troubleshooting GOSIA inputs

When making changes to the input, the following guidelines will help the user avoid introducing inconsistencies. Refer to the relevant sections of the manual for details on the input format.

- When the level scheme (LEVE) or matrix elements (ME) are changed, the following items should be checked. The transition energies and multiplicities defined in LEVE and ME require internal conversion coefficients in OP,YIEL which cover the range of transition energies for each multiplicity introduced in ME. Note that the level energies are entered in MeV, not keV.
- Changes that affect the kinematics (projectile or target species, beam energy, target thickness, scattering angle ranges, etc.) should be checked for consistency in the EXPT, OP,YIEL and OP,INTG sections. Pay special attention to the selection of the detected particle and whether the projectile scattering or target recoil angles are being specified in each section, as well as the accompanying kinematic flags (minus signs). Target thickness is specified indirectly through a range of beam energy and stopping power data. Stopping powers may need to be updated when the beam energy range is changed, or when the beam or target species is modified.
- If one experiment (EXPT) is normalized to another, relative particle-detector normalization constants must be entered in OP,YIEL. Inaccuracies in these normalizations will not affect the yield integration (OP,INTG), but they will cause problems in finding the true chi-squared minimum (OP,MINI).

The safest approach to avoid introducing errors is to make changes to the input in the smallest possible increments, running the code frequently to check for problems. The following troubleshooting notes may be helpful.

- Pay special attention to commas and periods; interchanging one for the other causes errors that are difficult to spot.
- Check the auxiliary files created by GOSIA. Occasionally, an overflow will result in “INF” (infinity) or “NaN” (not a number) being written into a file such as TAPE 4 (the correction factor file). This may cause problems later, when GOSIA re-reads the file.
- GOSIA will tolerate comments on some lines in the input (after the required fields), but not on others. Putting comments on the wrong line could cause read errors. Refer to the examples in the sample inputs. When in doubt, do not insert a comment.
- If an error occurs when GOSIA reads the input file, it may be helpful to insert OP,EXIT (to halt execution) immediately before another “OP,” command in the input and run it again to determine which section contains the problem.
- Many integers that are entered in the input file (and in TAPE 3, experimental gamma-ray yields) determine the number of records and fields to follow, or the number of corresponding records in a later section. Errors are frequently caused by inconsistencies in these numbers and may be indicated by messages such as “UNRECOGNIZED SUBOPTION,” or Fortran read errors. If errors are suspected to be caused by a mismatch in the number of records and can not be found by a cursory inspection, it is often helpful to check each line of the input, comparing it to the corresponding manual entry.

The following is an example of the above type of error. The execution terminates with this error:

```
invalid integer: read unexpected character
apparent state: unit 5 (unnamed)
last format: list io
lately reading sequential formatted external I
Abort
```

This is a Fortran (system) error that is not trapped by GOSIA, so the location of the problem is not specified. Running the input again with OP,EXIT inserted immediately after OP,YIEL to halt the execution results in the same error, but inserting OP,EXIT just before OP,YIEL prevents the error. Hence, the error is somehow related to OP,YIEL. The beginning of OP,YIEL looks like this:

```
OP ,YIEL
0
```

```

18,1
0.056,0.068,0.082,0.1,0.12,0.15,0.18,0.22,0.26,0.32,0.38,
0.46,0.56,0.68,0.82,1.0,1.2,1.5
2
41.7,17.6,7.97,3.58,1.78,0.785,0.415,0.212,0.124,0.0660,0.04,
0.0241,0.0148,0.00939,0.00623,0.00413,0.00288,0.00188
1,1
1
45
90

```

The EXPT section defines 3 experiments:

```

EXPT
3,72,178
54,136,642,24.0,4,0,0,0,360,1,1
54,136,642,42.0,4,0,0,0,360,1,1
54,136,642,60.0,4,0,0,0,360,1,1

```

However, line 8 in OP,YIEL “1,1” contains only 2 values of NANG(I), but the entry for NANG(I) In section 5.30 of this manual states that NANG(I) needs to be entered once for each experiment. Line 8 needs to be corrected; in this case a third value should be added to specify the number of gamma-ray detectors for the third experiment. The rest of OP,YIEL should be checked for similar omissions. Stubborn errors can be found most efficiently by checking line-by-line against the required format in the manual.

12 GAMMA DETECTION EFFICIENCY CODE: GREMLIN

Alexander Kavka
University of Rochester

The FORTRAN program **GREMLIN** (“**G**amma-**R**ay **E**fficiency **M**easurement and **L**ine **I**ntensity calculation”) was developed at Rochester in 1987 by Alexander Kavka. The purpose is to simplify the routine procedure of γ -ray detector efficiency calibration and detection efficiency correction of measured peak areas for deexcitation γ -ray yields following Coulomb excitation.

GREMLIN can perform two separate tasks:

1) Least-squares fit of a γ -ray detection efficiency-calibration function to a set of peak areas from γ -ray calibration spectra.

2) Calculation of detection-efficiency corrected γ -ray intensities from peak areas, using the fitted efficiency function for the Doppler shift corrected γ -ray energy.

The functional form of the dependence of detection efficiency on γ -ray energy is factored into terms that separately account for γ -ray absorption, high and low energy dependence, and electronic thresholds in order to obtain well-behaved functions that do not exhibit pathological behaviour such as at K-edges.

GREMLIN is an essential component of the GOSIA suite of Coulomb excitation analysis codes and can be used in either of two modes. One approach is to use GREMLIN to correct the raw peak areas of the observed deexcitation γ -rays to account for the γ -ray detector efficiency at the appropriate Doppler-shifted energy. These corrected yields then are input as the data to be fit by GOSIA. The second approach is to use the GOSIA option OP,RAW which allows input to GOSIA of the raw, i.e. not detector efficiency corrected, γ -ray yields. The parameters for the γ -ray detection efficiency function, as determined by the GREMLIN least-squares fit, are used by OP,RAW to detector-efficiency correct the raw yields input to GOSIA.

The code GREMLIN is interactive, and its prompts and questions are hopefully sufficient to guide the user. Therefore, this memo provides no real input instructions, with one exception: it describes the structure of the input files containing the calibration points.

12.1 Option 1: EFFICIENCY CALIBRATION

1.1 Input of calibration points

A maximum of 500 calibration points can be entered, grouped in up to 9 independently normalized data sets. Typically, these will originate from runs with different calibration sources, but there can just as well be several sets from the same source. If there is more than one data set, the code will automatically fit normalization parameters.

GREMLIN will ask for calibration points for each data set separately. For each set the input can be from a disk file or from the keyboard, and consists of one record for each calibration line. A record looks as follows:

$$E, \quad I, \quad \Delta I, \quad A, \quad \Delta A$$

where E is the γ -ray energy, $I \pm \Delta I$ the tabulated relative intensity, and $A \pm \Delta A$ the measured peak area. Note that two data sets cannot be in one file.

However, the input is simplified in the case of ^{152}Eu or ^{182}Ta sources, because the energies and intensities of major ^{152}Eu and ^{182}Ta transitions are stored in DATA statements in the program. These values were taken from R.A. Meyer: *Multigamma-Ray Calibration Sources* (Lawrence Livermore Laboratory 1978). The record format is then

$$A, \quad \Delta A$$

If keyboard input was chosen, the code will display each tabulated energy and intensity and ask for the area and error. In an input file, the ^{152}Eu or ^{182}Ta lines must be given according to the following table:

line number	¹⁵² Eu (keV)	¹⁸² Ta (keV)
1	121.783	31.737
2	244.692	65.722
3	295.939	67.750
4	344.276	84.680
5	367.789	100.106
6	411.115	113.673
7	443.967	116.421
8	488.661	152.430
9	564.021	156.390
10	586.294	179.397
11	688.678	198.350
12	778.903	222.108
13	867.388	229.322
14	964.131	264.078
15	1005.279	927.983
16	1085.914	1001.696
17	1112.116	1113.414
18	1212.950	1121.299
19	1299.124	1157.505
20	1408.011	1189.051
21	1528.115	1221.406
22		1231.019
23		1257.421
24		1273.735
25		1289.158

Any unobserved line that is to be excluded from the fit must be entered as $A = \Delta A = 0$, at the keyboard as well as in a file. Data for other sources than ¹⁵²Eu and ¹⁸²Ta easily can be added to the code in the future, should the need arise. Similarly it is trivial to include additional ¹⁵²Eu and ¹⁸²Ta lines in the lists.

1.2 Experimental and theoretical efficiency

For each calibration line GREMLIN calculates the relative efficiency and root-mean-square error:

$$\varepsilon = \frac{A}{I} \quad \Delta\varepsilon = \varepsilon \sqrt{\left(\frac{\Delta A}{A}\right)^2 + \left(\frac{\Delta I}{I}\right)^2}$$

and makes a transformation to the variables which are then internally used for the fit, i.e.

$$x \equiv \log \frac{E}{E_0} \quad y \equiv \log \varepsilon \quad \Delta y = \frac{\Delta\varepsilon}{\varepsilon}$$

The logarithms are of base e and $E_0 = 50$ keV.

The functional form used by GREMLIN is factored into four functions that separately account for γ -ray absorption, higher energy, lower energy detection efficiencies, and electronic thresholds in order to obtain well-behaved functions that do not exhibit pathological behaviour such as at K-edges etc. That is, the functional form of the detection efficiency used is

$$\varepsilon(E) = A(E)P(E; a_1 \dots a_n)F(E; f)W(E; b, c)$$

with the parameters $a_1 \dots a_n$, f , b , and c to be determined. The separate terms are discussed below.

1.3 Attenuation factor

$$A(E) = \exp \left[- \sum_{i=1}^m \mu_i(E) d_i \right]$$

$A(E)$ stands for the absorption in layers of m different materials placed in front of the detector, μ_i and d_i being the linear attenuation coefficient and the thickness of the i th material, respectively.

The absorber materials that GREMLIN takes into account are C, Al, Si, Fe, Cu, Cd, Sn, Ta, and Pb. The thicknesses (in cm) are given by the user from the keyboard. DATA statements in the code contain the attenuation coefficient of each material for 20 gamma energies ranging from 30 to 4000 keV. Interpolation is done by means of cubic spline curves. Two of the energy meshpoints were chosen to be 67.416 and 88.004 keV, which are the K-edges of Ta and Pb respectively, and for each of those elements GREMLIN maintains two spline curves, below and above the edge. All other absorption edges for these nine elements lie below 30 keV.

The variables actually used for the spline curves are $\log \frac{E}{E_0}$ and $\log \frac{\mu}{\mu_0}$ ($\mu_0 = 1\text{cm}^{-1}$), since the points are more evenly spaced in the log-log plane.

The attenuation coefficients were calculated from total cross-sections σ given in E. Storm, H. I. Israel, Nuclear Data Tables **A7** (1970) 565, according to

$$\mu[\text{cm}^{-1}] = \frac{\rho N_A \sigma}{M} = 0.602205 \frac{\rho[\text{g}/\text{cm}^3] \sigma[\text{barn}]}{M[\text{g}/\text{mol}]}$$

where ρ is the density, N_A Avogadro's number, and M the atomic weight.

1.4 Polynomial factor

The polynomial factor, degree $n \leq 3$,

$$P(E; a_1 \dots a_n) = \exp \left[\sum_{k=0}^n a_k \left(\log \frac{E}{E_0} \right)^k \right]$$

is a simple representation of the basic decrease of the efficiency with increasing γ energy. The word ‘‘polynomial’’ refers, of course, to $\log \epsilon$ as function of $\log E$.

The degree n is chosen by the user. GREMLIN finds good initial values for the parameters a_k by fitting a pure n th-degree polynomial in the region above 250 keV, where $P(E)$ can be expected to dominate.

1.5 Functions describing the low-energy slope

An inverse-power factor, with arbitrary $N > 0$, and $f < 0$,

$$P(E; a_1 \dots a_n) = \exp \left[f \left(\log \frac{E}{E_0} \right)^{-N} \right]$$

and a ‘‘Woods-Saxon’’-type factor, with b and $c > 0$,

$$W(E; b, c) = \frac{1}{1 + \exp \frac{b-E}{c}}$$

are optional, and are unlikely to be used simultaneously, although the code allows that both be used simultaneously. Each represents the low-energy slope of the efficiency curve. Whereas F is just an *ad hoc* mathematical function, W attempts to model the effect of a discriminator threshold in the pulse-handling electronics.

When F was used, good results were obtained with e.g. $N = 5$, but the value of N does not seem to very crucial. An initial value for the parameter f is found by simply sampling the value of x^2 throughout a range of f . The range and stepsize are given by the user, but if the code finds the optimum value at an endpoint of the range, it requests a new range and tries again.

Initial values (in keV) for the parameters b and c , in the ‘‘Woods-Saxon’’ case, are given by the user. They are easy to estimate, b being the threshold and c a measure of the ‘‘rise time’’ of this step function.

1.6 Normalization between data sets

In case of more than one data set, initial normalization factors are chosen in the following way: A linear function

$$y^{(j)} = a_0^{(j)} + a_1^{(j)} x$$

is fitted to every data set in the region $E > 250$ keV (j labels the data sets). The efficiency values in data set $\#j$ are then rescaled by replacing y with $y + a_0^{(1)} - a_0^{(j)}$. This is done before determining initial values for the other parameters.

During the main fit, each normalization parameter is corrected after every iteration by a simple χ^2 scan throughout a range of its value. The scan does not have to be iterated, since there is no correlation between the normalization factors.

1.7 The main fit

When all parameters have been given starting values, the full function is fitted to the calibration points by an interactive matrix inversion method (the same that is used for peak-shape fitting in SILVIA). After every iteration (and renormalization, in case of more than one data set) the program displays the χ^2 and the new parameter values and the user decides whether to continue or stop. Convergence is usually rapid thanks to good initial values – often only 2 or 3 iterations of the main fit are necessary.

When the fit is stopped, GREMLIN reports the best (not necessarily the latest) χ^2 , the corresponding fitted parameters with errors and correlation matrix and a table showing values of the fitted function in comparison with the measure efficiencies. Three optional output files can be written on disk at this moment:

- 1) A text file showing the results of the fit in the same way as on the screen.
- 2) An input file for TOPDRAWER that can generate a log-log plot of the calibration points and the fitted curve on the laser printer. The user can specify a header text and a different point plot symbols for each data set.
- 3) A storage file containing the fitted parameter values, information about the functional form used, and absorber thicknesses. This file is read by GREMLIN's Option 2 to calculate γ -ray intensities.

12.2 Option 2: INTENSITY CALCULATION

In this option, the program reads a storage file written by Option 1, and then can re-create the fitted function $\varepsilon(E)$. It also asks the user to specify the kinematics of the experiment (masses of projectile and target; bombarding energy; mass and direction θ, ϕ of radiating ejectile) as well as the angular position $\theta_\gamma, \phi_\gamma$ of the γ detector, so that the efficiencies can be calculated for the actually detected (Doppler-shifted) γ energies.

The shifted energy is

$$E' = \frac{E}{1 - \frac{\nu}{c} \cos \alpha}$$

where the velocity ν is calculated from the kinematics and α is the angle between the γ -ray and the radiating nucleus.

$$\cos \alpha = \sin \theta \sin \theta_\gamma \cos(\phi - \phi_\gamma) + \cos \theta \cos \theta_\gamma$$

The user now types a series of transition energies E and peak areas $A \pm \Delta A$, and GREMLIN returns the corresponding relative intensities

$$I = \frac{A}{\varepsilon(E')}$$

and errors ΔI . The errors are calculated from

$$\left(\frac{\Delta I}{I}\right)^2 = \left(\frac{\Delta A}{A}\right)^2 + \left(\frac{\Delta \varepsilon}{\varepsilon}\right)^2$$

where the efficiency error is estimated using the correlation matrix C that results from the fit:

$$(\Delta\varepsilon)^2 = \sum_{j=1}^p \sum_{k=1}^p \frac{\partial\varepsilon}{\partial\alpha_j} \frac{\partial\varepsilon}{\partial\alpha_k} C_{ij}$$

$\alpha_j (j = 1 \dots p)$ represents all the parameters of the fit.

The derivatives with respect to the parameters have simple analytical expressions:

$$\begin{aligned} \frac{\partial\varepsilon}{\partial\alpha_j} &= \varepsilon(E') \left(\log \frac{E'}{E_0} \right)^j & \frac{\partial\varepsilon}{\partial f} &= \varepsilon(E') \left(\log \frac{E'}{E_0} \right)^{-N} \\ \frac{\partial\varepsilon}{\partial b} &= -\frac{\varepsilon(E')}{c(1 + \exp \frac{E'-b}{c})} & \frac{\partial\varepsilon}{\partial c} &= \frac{E' - b}{c} \frac{\partial\varepsilon}{\partial b} \end{aligned}$$

13 GOSIA 2008 RELEASE NOTES

These notes include updates as of May 29, 2008.

The original GOSIA code was developed in 1980 by T. Czosnyka, D. Cline and C.Y. Wu at the University of Rochester. In the years since, several other versions of the code have been developed: GOSIA2 and PAWEL by T. Czosnyka, and ANNL by R. Ibbotson. These Release Notes are for the 2008 version of GOSIA. GOSIA2 is being upgraded in parallel with GOSIA and thus most of these release notes also apply to GOSIA2. These release notes do not necessarily apply to PAWEL or ANNL.

The coding of the GOSIA suite of codes was maintained by Tomasz Czosnyka from 1980 until his untimely death in 2006. Since 2007 Nigel Warr has upgraded the coding of GOSIA and GOSIA2.

Responsibility for the management and development of the Gosia suite of codes was assumed by the Steering Committee of the Gosia Users Group in April 2008.

The Gosia Steering Committee comprises:

Douglas Cline, (University of Rochester)
Adam Hayes, (University of Rochester)
Pawel Napiorkowski, (Warsaw University)
Nigel Warr, (University of Cologne)

Valuable contributions to GOSIA were made by the following people.

L. Hasselgren (Uppsala)
R. Ibbotson (Rochester)
A.E. Kavka (Uppsala and Rochester)
B. Kotlinski (Warsaw and Rochester)
J. Srebrny (Warsaw)
Eh. Vogt (München and Rochester)

References and Credits

T. Czosnyka, D. Cline and C. Y. Wu, Bull. Am. Phys. Soc. 28, 745 (1983).

University of Rochester internal laboratory report UR/NSRL 308/1986

Some concepts used were taken from the 1978 Winther, de Boer code COULEX and from the deexcitation code CEGRY developed by Cline and coworkers at Rochester. However, the parts taken from both codes are in most cases completely rewritten, so the similarity of variable and routine names may be misleading.

Resources

GOSIA is now being maintained by the newly formed Gosia Users Group Steering Committee. It is recommended that users check the GOSIA website periodically for important updates to the code and the manual, as well as sample input and output files and other information. Chapter 11 of this manual provides novice users with instructions, tutorials, etc.

<http://www.pas.rochester.edu/~cline/Gosia/index.html>

If you need additional information, please contact:

Prof. Douglas Cline
Department of Physics and Astronomy
University of Rochester
Rochester, NY 14627, U.S.A. Phone (585)275-4934
Cline@pas.rochester.edu
<http://www.pas.rochester.edu/~cline/>

Compiling GOSIA

GOSIA 2008 compiles on most 64-bit systems with GNU g77, using the default compiler settings. Previous versions of the Gosia code did not explicitly specify 64-bit precision and were intended to be compiled by the user at the highest machine precision available. The current availability of 64-bit machines and the accuracy

problems which may arise when relying on 32-bit precision led to the decision to make this code explicitly 64-bit. Modifying the code to run with 32-bit precision is discouraged.

13.1 Chronology of Major Changes to GOSIA1: 2007 - present

20080630

- Reordering of all variable declarations so variables in common blocks are together.
- Increased size of arrays for levels from 75 to 100.
- Change in many format statements to accommodate 100 levels (I2 -> I3).
- Increased size of arrays for substates from 600 to 1200.
- Restructure function EFFIX to allow more flexible selection of efficiency calibration type.
- Added Radware efficiency calibration (Pawel J. Napiorkowski).
- Added EFF, option to CONT to make it easier to select efficiency method.
- Bugfix in gremlin efficiency method: a sign was wrong in Woods-Saxon term.
- Bugfix in initialisation of conversion coefficients for interpolation method (only part of array was initialized).
 - Add CONTINUE statements to prevent GOTO the ENDDO of a loop. This is deprecated and will be removed in future.
 - Call either LAGRAN or SPLNER to do interpolation according to ISPL variable.
 - Approximation in TRINT if Arg is very large (then ratio is one) as in Pawel.
 - Replaced OPEN(NAME=xxx) with OPEN(FILE=xxx) as the former is an extension to the language, while the latter is standard.
 - Bugfix in BRICC: we need the absolute value of the difference in energy levels not the signed difference.
 - Use JZB to indicate which unit to read from as in gosia2.
 - Use IUNIT3 to indicate which unit is TAPE3 as in gosia2.
 - Use irix variable to select units 7 and 12 as in gosia2.
 - Add dummy variable Op2 to ANGULA as in gosia2.
 - In OPENF we refuse to open units 25 and 26 unless reading from unit 5 as in gosia2 (however, gosia always reads from unit 5, so this does nothing).
 - Bugfix for dimension of bten, which should have been 1600 and was different in different places.
 - Use DCMLPX instead of CMLPX for portability.
 - Use DIMAG instead of IMAG for portability.
 - Reorder DATA statement in NEWCNV for portability.
 - Use LAGRAN for interpolation if there are less than three data points even if ISPL = 1.

20080519

- Add spline support (Pawel J. Napiorkowski).
- Add new version of CONV which can lookup internal conversion coefficients from a table, which must have all the necessary energies (no interpolation).
- Add OP,BRIC to use BrIcc database to generate conversion coefficient table for new version of CONV.

20080508

- Increased size of arrays for matrix elements from 500 to 1500. N.B. we are still limited to 999 matrix elements because 1000 is used as a flag.
- Added OP,SELE.

20080507

- Correct inaccurate constants in SEQ.
- Replaced constant 10 with NLIFT in loop (this was a bug).
- Initialized some variables explicitly to remove compiler warnings.
- Increased AKAVKA dimensions from 8 to 9 to prepare for merge of Pawel Napiorkowski's efficiency code.

- Added ISPL variable in CCC common to prepare for merge of Pawel Napiorkowski's spline code and SPL, option in CONT.
- Restructured a repeated IF with the same condition to use IF/THEN.

20080418

- Increased dimensions of arrays fiex1, wpi in GOSIA.
- Increased dimensions of XV, YV, ZV, DSG and DSE in GOSIA.
- Moved OP,EXIT code to end of GOSIA (as in gosia2).
- Limited ABS(NI2) rather than NI2 to 50 in GOSIA.
- Fixed call to MIN so both parameters have same precision in GOSIA.
- Remove unused variables u and v in ALLOC.
- Changed format of normalisation coefficients write in CEGRY.
- Changed dimensions of X, Y, w and arh in LAGRAN.
- Changed dimensions of XV, YV, ZV, DSG and DSE in TAPMA.
- Changed dimensions of Wpi in COORD.
- Changed dimensions of XV, YV, ZV, DSG and DSE in COORD.
- Changed dimensions of XV, YV, ZV, DSG and DSE in KONTUR.
- Added Leuven efficiency calibration in EFFIX (as in gosia2).

20080328

- Put back warnings in CEGRY which was removed by mistake.
- Fix typo misspelling "WARNING" in CEGRY.

20080229

- Limit NI2 to 50 in GOSIA.

20070726

- Reorder initialisation so it is similar to gosia2 in GOSIA.
- Remove spurious attempt to provoke floating point exception in ALLOC.
- Remove superfluous ELSE in WTHREJ.
- Move some format statements in PRELM.

20070721

- Fix initialisation of CNOR from 1 to 75 not 1 to 50 in GOSIA.
- Make both parameters of SIGN have same precision in FXIS1.

20070709

- Restucture IF statement in GOSIA.
- Add explicit STOP statement to ALLOC.
- Move duplicated lines out of IF/ELSE in MINI.
- Make both parameters of SIGN have same precision in FXIS2.
- Run spag.
- Convert to double precision.
- Reorder common LCZP.
- Reorder common CAUX0.
- Reorder common COEX.
- Reorder common KIN.
- Reorder common CCC.
- Reorder common ME2D.
- Declare all variables explicitly.
- Add PROGRAM statement to GOSIA.
- Replace ALOG with LOG.
- Replace ALOG10 with LOG10.
- Replace AMIN1 with MIN.

- Replace MIN0 with MIN.
- Replace AMAX1 with MAX.
- Replace MAX0 with MAX.
- Replace IABS with ABS.
- Replace FLOAT with REAL.
- Replace IFIX with INT.
- Add SAVE statement in DJMM.

13.2 Chronology of Major Changes to GOSIA2: 2007 - present

20080630 (synchronized with gosia1)

- Reordering of all variable declarations so variables in common blocks are together.
- Increased size of arrays for levels from 75 to 100.
- Change in many format statements to accomodate 100 levels (I2 -> I3).
- Increased size of arrays for substates from 600 to 1200.
- Restructure function EFFIX to allow more flexible selection of efficiency calibration type.
- Added Radware efficiency calibration (Pawel J. Napiorkowski).
- Added EFF, option to CONT to make it easier to select efficiency method.
- Bugfix in gremlin efficiency method: a sign was wrong in Woods-Saxon term.
- Bugfix in initialisation of conversion coefficients for interpolation method (only part of array was initialized).
- Add CONTINUE statements to prevent GOTO the ENDDO of a loop. This is deprecated and will be removed in future.
- Call either LAGRAN or SPLNER to do interpolation according to ISPL variable.
- Approximation in TRINT if Arg is very large (then ratio is one) as in Pawel.
- Replaced OPEN(NAME=xxx) with OPEN(FILE=xxx) as the former is an extension to the language, while the latter is standard.
- Bugfix in BRICC: we need the absolute value of the difference in energy levels not the signed difference.
- Bugfix for dimension of bten, which should have been 1600 and was different in different places.
- Use DCMLPX instead of CMLPX for portability.
- Use DIMAG instead of IMAG for portability.
- Reorder DATA statement in NEWCNV for portability.
- Use LAGRAN for interpolation if less than three data points even if ISPL = 1

20080519 (synchronized with gosia1)

- Add spline support (Pawel J. Napiorkowski)
- Add CONT option SPL,
- Add OP,SELE
- Add OP,BRIC
- Add new method of reading conversion coefficients
- Replaced constant 10 with NLIFT in loop (this was a bug)
- Correct inaccurate constants in SEQ
- Initialized some variables explicitly to remove compiler warnings
- Increased AKAVKA dimensions from 8 to 9 to prepare for merge of Pawel Napiorkowski's efficiency code
- Added ISPL variable in CCC common to prepare for merge of Pawel Napiorkowski's spline code and SPL, option in CONT
- Restructured a repeated IF with the same condition to use IF/THEN 20080418
- Change default printing options to match gosia1
- Split CINIT into CINIT (same as gosia1) and CINIT2 (new for gosia2)

20080417

- STOP if NI2 > 50
- Increase flex1 and wpi dimensions

- Increase arrays in VLIN

20080414

- Save DJM in DJMM
- Replace IFIX with INT
- Replace FLOAT with REAL
- Replace IABS with ABS
- Replace MAX0 with MAX
- Replace AMAX1 with MAX
- Replace MIN0 with MIN
- Replace AMIN1 with MIN
- Replace ALOG10 with LOG10
- Replace ALOG with LOG
- Remove unused common blocks in main routine
- Add PROGRAM statement at start
- Run spag
- Reorder common blocks ME2D, CCC, KIN, COEX, CAUX0, LCZP
- Convert to REAL*8 and COMPLEX*16
- Fix precision of constants
- Restructure IF in MINI
- Add IUNIT3 to SWITCH common block
- Replace unit 33 with variable IUNIT33
- Change some IF logic to match gosia1
- Store matrix elements so that percentage change works

20080412

- Import pristine version of gosia2 from Rochester

13.3 Chronology of Major Changes to GOSIA: 1980 - 2006

(June 2006, T. Czosnyka) - The array size for the internal conversion coefficients has been increased to 50. This allows the user to enter more ICC values near discontinuities (i.e., electron binding energies) where several closely spaced values are needed for an accurate interpolation. Refer to OP,YIEL in this manual.

(Nov 2000, T. Czosnyka) - A Jaeri efficiency calibration has been added for the Ge detector data.

(2000) - A FITEFF Ge efficiency calibration has been added with credit to P. Olbratowski, P. Napierkowski.

(July 1997, T. Czosnyka) - Known matrix elements of all multiplicities may now be entered as data in OP,YIEL. Note that this necessitates adding the multipole order LAMBDA as the first field in the new input format,

LAMBDA, NS1, NS2, ME, DME

where LAMBDA=7 and 8 represent M1 and M2, respectively.

(September 1996, T. Czosnyka) - The PIN diode particle detector option has been added. See the entry for “PIN,X.” under the sub-option CONT in this manual.

(May 1995, T. Czosnyka) - A collective model matrix element generator “OP,THEO” was added.

(April 1991, T. Czosnyka) - The OP,RAW function has been added. OP,RAW handles non-efficiency-corrected gamma-ray yield data and allows the definition of Ge detector “clusters.” Up to 20 clusters can be defined. This effectively increases the number of physical Ge detectors to 200, while the number of data sets (i.e. single detectors + detector clusters) is still limited to 32.

(April 1991, T. Czosnyka) - Output is now written on unit 22 to avoid mixing it with system messages on some systems.

(November 1990, T. Czosnyka) - The level scheme data arrays have been increased to the following sizes:

Levels	75
Gamma-ray yields	32 x 1500
Magnetic substates	600
Matrix elements	500

(April 1990, T. Czosnyka) - The dominant multipolarity switch formerly set in the “ME” sub-option (Section 5.15) is now ignored by the code and does not need to be set. Full Q-maps are now calculated for electric multipole orders E1 through E4 (Chapter 2). The electric matrix elements up to multipole order E6 may be entered and fit. The Xi and Zeta function ranges are now calculated for each multipolarity individually (Chapter 2).

(1990, Eh. Vogt, T. Czosnyka) - OP,FILE has been added (Section 5.9), giving the user the option of specifying descriptive names of the input and output files in the GOSIA input, rather than using the Fortran default names fort.1, fort.2, etc.

(March 1989, T. Czosnyka) - The code has been updated to allow input of gamma-ray yield data from 32 Ge detectors. [As of the 2007 version, this means a total of 32 x 1500 data points.]

(1980, T. Czosnyka, D. Cline, C.Y. Wu) - Original version.

14 GOSIA MANUAL: RECENT UPDATES

14 April 2009:

- 1) Many editorial corrections to manual
- 2) Expanded description of relativistic transformation of the angular distribution,
- 3) Elucidated the adiabaticity limitations of the present version of Gosia.

30 June 2008:

- 1) Includes increase in size of arrays.
- 2) restructure of EFFIX to allow more flexible selection of efficiency calibration type.
- 3) Addition of Radware efficiency calibration
- 4) Allow caling of LAGRAN or SPLNER to perform interpolation

12 June 2008:

- 1) Added a section on kinematics,
- 2) several editorial corrections to improve presentation.

20 May 2008:

- 1) Listed all members of the Gosia Users Steering Committee and their institutions.
- 2) Added a dedication page to Tomasz Czosnyka,
- 3) Expanded chapter 11 by addition af another tutorial and corrected some errors.

16 May 2008:

- 1) Added section 2.2.4 on the calculation of internal conversion coefficients including addition of E0 conversion.
- 2) Corrected a comment at end of OP,RE regarding requiring it to immediately precede OP,ERRO or OP,MIN

5 May 2008:

- 1) Updated the Introduction to separate the introduction from the history and manual description.
- 2) Added section 2.2.4 "Sources of Systematic Error".
- 3) Corrected input descriptions to correspond to the current version of Gosia.
- 4) Added a description of the output from OP,GDET.
- 5) Replaced chapter 11 Learning Gosia, by a new version that includes more sample inputs and corresponding outputs.

2 April 2008:

Updated the Manual to correct an error in OP,INTG to reflect the fact that the maximum dimension of NI2 is 50, not 100. Also revised the Introduction and Release Notes chapters of the manual plus corrected typing errors in CONT and the Rotational Invariants chapter 6.

8 Oct 2007:

Chapter 11 in the Gosia Manual changed to include a tutorial and instructions for compiling and using GOSIA. Release Notes added to manual as chapter 13. Some minor editorial changes made to the GOSIA Manual. Posted the latest 2007 version of GOSIA code plus the accuracy-speed-test.tar and g1demo.tar input/output files used by the GOSIA tutorial described in chapter 11.

30 Aug 2007:

Updated the manual description of how to evaluate absolute counts using OP,POIN or OP,INTG

20 Aug 2007:

Upgraded the GOSIA Manual to include the code GREMLIN

July-Aug 2007:

Nigel Warr upgraded the coding of GOSIA, and GOSIA2 which were tested by Adam Hayes.

26 Feb 2007:

Updated the manual regarding accuracy problems associated with large adiabaticity. Added a chapter 11 on accuracy, speed and compiling options.

25 Feb 2007:

To facilitate new installations a new test input with associated output file and read me file were created that illustrate the accuracy, speed and compiling options for GOSIA.

20 Feb 2007:

Corrected error in input instructions for ME in OP. YIEL.

6 Dec 2006:

Corrected typing errors in OP: MINI input

24 Aug 2006:

Added Drew Whitbeck comments to manual on input for GOSIA2.

25 June 2006

Made corrections to eq 3.15 and 3.16 in manual

13 June 2006:

Corrected ICC description in OP,YIEL to include use of four point interpolation and increase in number of ICC energies to 50.

9 June 2006:

1) ICC description in OP.YIEL revised with warning about how to handle ICC at energies near the K,L edges.

2) Inserted the PIN diode option in CONT and OP.INTG.

3) Added a very short comment about PAWEL.

30 May 2006: New version of GOSIA Manual:

1) Includes GOSIA2 for handling simultaneous Coulex of radioactive beams.

2) All equations and chapter numbers in manual incremented by one

3) Corrected figure 2.1 to coord B

4) Added description of Ibbotson annealing code approach to minimization

5) Added comments to aid in calculating total cross sections to OP.INTG

6) Update OP.YIEL to include 1997 update allowing input of matrix elements for all multipolarities.

7) Added description of OP,THEO to calculate rotational mode E2 matrix elements

References

- [ABR53] A. Abragam, R.V. Pound - Phys. Rev. 92:943 (1953)
- [ABR72] M. Abramowitz, I. Stegun (eds.) - Handbook of Mathematical Functions, National Bureau of Standards, Washington (1972)
- [ALD56] K. Alder, A. Bohr, T. Huus, B. Mottelson, A. Winther - Rev. Mod. Phys. 28:432 (1956)
- [ALD66] K. Alder, A. Winther - Coulomb Excitation, Academic, New York, (1966)
- [ALD75] K. Alder, A. Winther - Electromagnetic Excitation, Theory of Coulomb Excitation with Heavy Ions, North Holland, Amsterdam, (1975)
- [BOE84] J. de Boer, Treatise on Heavy-Ion Science, Vol. 1, Plenum Press, 1984, p293
- [BOH69] A. Bohr, B. Mottelson - Nuclear Structure, Benjamin, New York, (1969)
- [BOS77] F. Bosch, H. Spehl - Z. Phys. A280:329 (1977)
- [BRE77] R. Brenn, H. Spehl, A. Weckherlin, H. Doubt, G. Van Middelkoop - Z. Phys. A281:219 (1977)
- [CHU56] E.L. Church and J. Weneser, Phys. Rev. 103 (1956) 1035
- [CLI69a] D. Cline, H.S. Gertzman, H.E. Gove, P.M.S. Lesser, J.J. Schwartz, Nucl. Phys. A133 (1969) 445
- [CLI69b] D. Cline - Bull. Am. Phys. Soc. 14:726 (1969)
- [CLI72] D. Cline, C. Flaum - Proc. Int. Conf. on Nucl. Struct. Studies using Electron Scatt. and Photoreaction, Sendai 1972, K. Shoda and H. Ui (eds.), Tohoku Univ. (1972)
- [CLI73] D. Cline, Journ. Phys. Soc. of Japan, 34 (1973) 377
- [CLI74] D. Cline, P.M.S. Lesser, C. Towsley; unpublished
- [CLI86] D. Cline - Ann. Rev. Nucl. Part. Sci. 36:683 (1986)
- [CZO83] T. Czosnyka, D. Cline, C.Y. Wu - Bull. Am. Phys. Soc. 28:745 (1983)
- [Du90] G. Dueck, T. Scheuer, *J. Comp. Phys.* 90 (1990) 161.
- [FRA65] H. Frauenfelder, R. Steffen - in Alpha-, Beta and Gamma Spectroscopy, K. Siegbahn (ed), North Holland, Amsterdam, (1965)
- [Ge84] S. Geman and D. Geman, *IEEE Trans. Patt. Anan. Mach. Int.* PAM1-6 (1984) 721.
- [GER70a] H.S. Gertzman, D. Cline, H.E. Gove, P.M.S. Lesser, J.J. Schwartz, Nucl. Phys. A151 (1970) 273
- [GER70b] H.S. Gertzman, D. Cline, H.E. Gove, P.M.S. Lesser, Nucl. Phys. A151 (1970) 282
- [GOL77] G. Goldring, private communication
- [GRE84] H. Grein, H. Emling, J. Stachel - GSI Rep. GSI-84-1 (1984)
- [HAS80] L. Hasselgren and D. Cline; Proceeding of the International Conference on Interacting Bose-Fermi Systems in Nuclei, Ed. F. Iachello, Plenum Press (1981) p.59
- [HAY07] A.B. Hayes, D. Cline, K.J. Moody, C.y. Wu, et al, Laser Physics 17 (2007) 745
- [IBB95] R.W. Ibbotson, Ph.D. Thesis, University of Rochester, 1995.
- [In89] L. Ingber, *Math.. Comput. Modelling* 12 (1989) 967.
- [KAV90] A. E. Kavka, Ph.D. Thesis, University of Uppsala, 1990

- [KIB08] T. Kibédi, T.W. Burrows, M.B. Trzhaskovskaya, P.M. Davidson, C.W. Nestor, Nucl. Instr. Meth. A589 (2008) 202
- [Ki83] S. Kirkpatrick, C. D. Gelatt Jr. and M. P. Vecchi, *Science* 220 p 671 (1983).
- [KOT84] B. Kotlinski, Ph.D. Thesis, University of Rochester, 1984
- [KRA70] K. Krane, R. Steffen - Phys. Rev. C2:724 (1970)
- [KRA72] K. Krane - Nucl. Instr. Meth. 98:205 (1972)
- [LEE81] P.A. lee, P.H. Citrin, P. Eisenberger, B.M. Kinkaid, Rev. Mod. Phys. 53 (1981) 769
- [LEL78] A. Lell, Diplomarbeit, Sektion Physik, Universität München (1978)
- [LES70] P.M.S. lesser, D. Cline, J.D. Purvis, Nucl. Phys. A151 (1970) 257
- [LES72] P.M.S. Lesser, D. Cline, P. Goode, R. Horoshko, Nucl. Phys. 28 (1972) 368
- [LES71] P.M.S. Lesser - PhD Thesis, Univ. of Rochester (1971)
- [MA78] M.H. Macfarlane, S.C. Pieper, Argonne Nat. Lab. Report, ANL-76-11 Rev. 1 (1978)
- [Me53] N. Metropolis, A.W. Rosenbluth, M.N. Rosenbluth, A.H. Teller, E. Teller, *J. Chem. Phys.* 21 (1953) 1087.
- [Mo90] P. Moscato and J.F. Fontanari, *Phys. Lett.* A146 (1990) 204.
- [NIK68] V.S. Nikolayev, I.S. Dmitriev - Phys. Lett. 28A:277 (1968)
- [PRE92] W.R. Press, S.A. Teukolsky, W.T. Vetterling, B.P. Flannery, "Numerical Recipes in Fortran", Cambridge University Press, 1992
- [RH80] M. Rhodes-Brown, M.H. Macfarlane, S.C. Pieper, Phys. Rev C21 (1980) 2417
- [ROT59] M. Rotenberg, R. Bivins, N. Metropolis, J. Wooten - The 3j and 6j Symbols, The Technology Press, Cambridge, Mass. (1959)
- [Sa91] *Algorithmica* 6 (1991) 295. (Special Edition on Simulated Annealing edited by A. Sangiovanni-Vincentelli)
- [SIM97] M.W. Simon, D. Cline, C.Y. Wu, R. Gray, R. Teng, C. Long; Nuclear Instruments and Methods, A452 (2000) 205
- [STA82] J. Stachel, N. Kaffrell, E. Grosse, H. Emling, H. Folger, R. Kulesa, D. Schwalm, Nucl. Phys. A383 (1982) 429
- [Sz87] H. Szu and R. Hartley, *Phys. Lett.* A122 (1987) 157.
- [TOL79] L.D. Tolsma, Phys. Rev. C20 (1979) 592
- [TOW72] C. Towsley, D. Cline, R. Horoshko, Phys. Rev. Letts. 28 (1972) 368
- [TOW73] C. Towsley, D. Cline, R. Horoshko, Nucl. Phys. A204 (1973) 574
- [TOW75] C. Towsley, D. Cline, R. Horoshko, Nucl. Phys. A250 (1975) 381
- [VAR86] B. Varnestig, A. Backlin, C. Fahlander, A. Kavka, T. Lenke, L.E. Svensson - Nucl. Instr. Meth. A248:419 (1986)
- [WIN65] A. Winther and J. de Boer, 1965, A Computer Program for Multiple Coulomb Excitation, California Institute of Technology, Technical Report, reprinted in [ALD66]
- [WU83] C-Y Wu, Ph.D. Thesis, University of Rochester, 1983

- [WU89] C-Y. Wu, D. Cline, E.G. Vogt, W.J. Kernan, T. Czosnyka, A.E. Kavka, R.M. Diamond, Phys. Rev. C40 (1989) R3
- [WU91] C-Y. Wu, D. Cline, E.G. Vogt, W.J. Kernan, T. Czosnyka, A.E. Kavka, B. Kotlinski, R.M. Diamond, Nucl. Phys. A533 (1991) 369
- [WU96] C-Y. Wu, D. Cline T. Czosnyka, A. Backlin, C. Baktash, R.M. Diamond, G.D. Dracoulis, L. Hasselgren, H. Kluge, B. Kotlinski, J.R. Leigh, J.O. Newton, W.R. Phillips, S.H. Sie, J. Srebrny, F.G.S. Stephens, Nucl. Phys. A607 (1996) 178